



# รายงานวิจัยฉบับสมบูรณ์

โครงการกระบวนการตีพอลิเมอร์เซชันไคติน/ไคโตซาน  
ด้วยเทคนิคพลาสมาในสารละลาย

โดย

รองศาสตราจารย์ ดร. รัตนา รุจิรวนิช

กุมภาพันธ์ 2561

สัญญาเลขที่ BRG5480008

## รายงานวิจัยฉบับสมบูรณ์

โครงการกระบวนการตีพอลิเมอร์เซชันไคติน/ไคโตซาน

ด้วยเทคนิคพลาสมาในสารละลาย

โดย

รองศาสตราจารย์ ดร. รัตนา รุจิรวนิช

วิทยาลัยปิโตรเลียมและปิโตรเคมี

จุฬาลงกรณ์มหาวิทยาลัย

สนับสนุนโดยสำนักงานกองทุนสนับสนุนการวิจัย (สกว.)

(ความเห็นในรายงานนี้เป็นของผู้วิจัย สกว.ไม่จำเป็นต้องเห็นด้วยเสมอไป)

## Contents

	Page
Executive Summary	ii
Depolymerization of chitosan-metal complexes via solution plasma technique	1
Enhanced degradation of chitosan by applying plasma treatment in combination with oxidizing agents for potential use as an anticancer agent	28
Degradation of chitosan hydrogel dispersing in dilute carboxylic acids by solution plasma and evaluation of anticancer activity of degraded products	57
Facile preparation of chitooligosaccharides by degradation of chitosan powder dispersed in dilute salt solutions via electrical discharge plasma and their cytotoxicity evaluation against cancer cell lines and normal cells	109
<b>Appendix A</b>	153
Carbohydrate Polymers 102 (2014) 504-512.	
<b>Appendix B</b>	163
Carbohydrate Polymers 102 (2014) 504-512.	
<b>Appendix C</b>	175
Japanese Journal of Applied Physics, 57(1), Article Number: 0102B5. DOI: 10.7567/JJAP.57.0102B5.	

## Executive Summary

Biopolymers, especially polysaccharides like chitin and chitosan, possess some inherent molecular weight-dependent biological properties. In order to gain those benefits of biopolymers, the development on degradation processes that not only can effectively reduce molecular weight of a biopolymer but also can achieve both economic feasibility and environmental concerns is of important. Electrical discharge plasma in a liquid phase by using a bipolar-pulsed power supply is an emerging green technology that can generate highly reactive species like hydroxyl radical ( $\text{OH}\cdot$ ) and hydrogen radical ( $\text{H}\cdot$ ) by creating an electric field between a pair of electrodes which are submerging in an aqueous solution. In this study, degradation of chitin and chitosan by applying the electrical discharge of plasma in a liquid phase, so called “solution plasma”, was investigated aiming to achieve the reduction of chemical wastes, high production yield of the water-soluble degraded products, fast degradation rate and the reduction of the overall production cost. Moreover, cytotoxicity against cancer cell lines, e.g. human uterine cervix cancer cell line (HeLa cells), human breast adenocarcinoma cell line (MCF-7 cells) and human lung cancer cell Line (H460 cells) of the obtained water-soluble degraded products, which were classified as chitooligosaccharides based on their molecular weights, was evaluated. The values of selectivity index of the as-prepared chitooligosaccharides toward cancer cells and normal cells were reported. Furthermore, the induction of apoptosis in the cancer cell line by the as-prepared chitooligosaccharides was also examined. This is a studied model that may be applied to reduce molecular weights of other biopolymers in order to attain the advantages of their biological properties, especially for biomedical purposes.



# Depolymerization of chitosan-metal complexes via solution plasma technique

Orathai Pornsunthorntawe<sup>a</sup>, Chaiyapruk Katepetch<sup>a</sup>,  
Chutima Vanichvattanadecha<sup>a</sup>, Nagahiro Saito<sup>b</sup>, Ratana Rujiravanit<sup>a,c,\*</sup>

<sup>a</sup>*The Petroleum and Petrochemical College, Chulalongkorn University,  
Bangkok 10330, Thailand*

<sup>b</sup>*Department of Molecular Design and Engineering, Graduate School of  
Engineering, Nagoya University, Nagoya 464-8603, Japan*

<sup>c</sup>*Center of Excellence on Petrochemical and Materials Technology,  
Chulalongkorn University, Bangkok 10330, Thailand*

## Abstract

Chitosan-metal complexes were depolymerized under acidic condition by using solution plasma system. Four different types of metal ions which are Ag<sup>+</sup>, Zn<sup>2+</sup>, Cu<sup>2+</sup>, and Fe<sup>3+</sup> ions were added into chitosan solution at a metal-to-chitosan molar ratio of 1:8. The depolymerization rate was found to be affected by the types of metal ions forming complexes with chitosan. The complexation of chitosan with Cu<sup>2+</sup> or Fe<sup>3+</sup> ions strongly promoted the depolymerization rate of chitosan by solution plasma treatment. However, chitosan-Ag<sup>+</sup> and chitosan-Zn<sup>2+</sup> complexes exhibited no change in the depolymerization rate in comparison with chitosan. After plasma treatment of chitosan-metal complexes, the depolymerized chitosan products were separated into water-insoluble and water-soluble fractions. The yield of the water-soluble fraction containing low-molecular-weight chitosan as high as nearly 57 % was obtained for the depolymerization of chitosan-Fe<sup>3+</sup> complex at the plasma treatment time of 180 min.

**Keywords:** Chitosan; Solution plasma; Metal complexation; Chitosan oligomers

## 1. Introduction

Regarding to chitin and chitosan, several researches have already been studied to prepare low molecular weight of chitosan and their oligomers which reported to possess distinguished biological activities such as antitumor, antifungal, antibacterial activities (Kendra and Hadwiger, 1984, Toda *et al.*, 1987; Qin *et al.*, 2004; Liang *et al.*, 2007, Jeon *et al.*, 2001; Fernandes *et al.*, 2008, Muzzarelli, 2010) and inhibition of the production of metalloproteinases enzyme which can heal the wound and prevent wrinkle formation (Muzzarelli, 2009). Normally, there are three widely used techniques for depolymerization of chitin/chitosan including chemical depolymerization, physical depolymerization, and enzymatic depolymerization. Among these three techniques, the enzymatic methods have received more attention in recent years because they allow regioselective depolymerization of chitin/chitosan under the mildest conditions (Muzzarelli, Stanic, & Ramos, 1999; Harish Prashanth & Tharanathan, 2007). However, the important drawbacks of this technique are that enzyme reaction progresses slowly and low product yield is obtained (Choi, Ahn, Lee, Byun, & Park, 2002). Most commercial enzymes, especially those with high purity, are also expensive (Klaikherd, Jayanta, Boonjawat, Aiba, & Sukwattanasinitt, 2004). In the case of chemical methods, various strong chemical reagents are used for the acid hydrolysis of chitin/chitosan, leading to a difficulty in handling. The generated wastes from these harmful chemicals possibly cause an environmental pollution. Therefore, the development of new technology for depolymerization of chitin/chitosan is of great interest.

Plasma in the liquid phase, known as “solution plasma”, has recently been proposed to be one of the most effective strategies for the depolymerization of biopolymers, such as chitosan (Prasertsung, Damrongsakkul, Terashima, Saito, & Takai 2012) and sodium alginate (Watthanaphanit, & Saito 2013), although most of the early researches focused on the use of the solution plasma, a glow discharge in the liquid phase, to synthesize metal nanoparticles with a narrow particle size distribution without adding reducing agents to the reaction system (Saito, Hieda, & Takai, 2009). At present, the detailed structure of solution plasma is still unclear but it is believed that the emission center of plasma is located in the gas phase surrounded by the liquid phase and an ion sheath is formed near the gas/liquid interface. This solution plasma is able to provide extremely rapid

reactions due to the presence of activated chemical species and radicals under high pressure (Saito, Hieda, & Takai, 2009). Since the solution plasma is generated at a mild condition (the reaction undergoes at room temperature and without using strong chemical reagents) and can be applicable to industrial materials processing, this technique is very beneficial for the depolymerization of biopolymers.

In the present work, the solution plasma was used for the depolymerization of an acidic chitosan solution. Various types of metal ions, including silver ion ( $\text{Ag}^+$ ), zinc ion ( $\text{Zn}^{2+}$ ), copper (II) ion ( $\text{Cu}^{2+}$ ), and ferric ion ( $\text{Fe}^{3+}$ ), were added to the chitosan solution in order to form chitosan-metal complexes since both hydroxyl groups ( $-\text{OH}$ ) and amine ( $-\text{NH}_2$ ) groups on the skeleton of chitosan are good ligands to coordinate with the metal ions. Coordination with the metal ions should result in weakening of the covalent bonds near the coordinating site and cause weak points on the chitosan chain, as a consequence, promoting the depolymerization reaction. A viscometric method and a liquid chromatography were used to investigate the depolymerization process of chitosan. Any changes in the chemical structures and the crystallinity of the depolymerized products were characterized by using Fourier transform infrared (FTIR) spectroscopy and wide angle X-ray diffraction (WAXD) analysis, respectively. Molecular mass and degree of polymerization (DP) of the depolymerized chitosan were revealed with the use of mass spectrometry (MS).

## 2. Experimental

### 2.1 Materials

Chitosan was prepared from the shells of *Metapenaeus dobsoni* shrimp, kindly provided by Surapon Foods Public Co., Ltd. (Thailand). Acetonitrile ( $\text{CH}_3\text{CN}$ ), glacial acetic acid ( $\text{CH}_3\text{COOH}$ ), hydrochloric acid ( $\text{HCl}$ ), and sodium hydroxide ( $\text{NaOH}$ ) pellets were purchased from RCI Labscan Limited (Thailand). A 50 % (w/v)  $\text{NaOH}$  solution was supplied by Chemical Enterprise Co., Ltd. (Thailand). Silver nitrate ( $\text{AgNO}_3$ ) was purchased from Fisher Scientific (UK). Zinc nitrate hexahydrate ( $\text{Zn}(\text{NO}_3)_2 \cdot 6\text{H}_2\text{O}$ ) and copper (II) sulfate pentahydrate ( $\text{CuSO}_4 \cdot 5\text{H}_2\text{O}$ ) were provided by Ajax Finechem Pty Ltd. (Australia). Ferric chloride hexahydrate ( $\text{FeCl}_3 \cdot 6\text{H}_2\text{O}$ ), D-glucosamine hydrochloride ( $\text{GlcN} \cdot \text{HCl}$ ) used as a standard in a high performance liquid chromatography (HPLC), and high-

purity distilled water used as a solvent in the MS analysis were supplied by Sigma-Aldrich (USA). Sodium borohydride ( $\text{NaBH}_4$ ) was obtained from Carlo Erba Reagenti (Italy).

## 2.2 Preparation of chitosan from shrimp shells

*M. dobsoni* shrimp shells were cleaned and dried under sunlight before grinding into small pieces. The ground shrimp shells were immersed in a 1 M HCl solution for 2 days with an occasional stirring and were washed with distilled water until neutral. The demineralized shrimp shell chips were soaked in a 4 % (w/v) NaOH solution at 80 °C for 4 h, followed by an excessive wash with distilled water. The deproteinized product, or chitin, was subsequently deacetylated by heating in a 50 % (w/v) NaOH solution containing 0.5 wt.%  $\text{NaBH}_4$  in an autoclave at 110 °C for 75 min. After deacetylation, the chitosan flakes were washed with distilled water until neutral and were dried at 60 °C. The deacetylation step was carried out two times to obtain chitosan with a high degree of deacetylation (%DD) of 90 %, as determined by the FTIR technique following the method of Baxter, Zivanovic, & Weiss (2005). A solid-to-liquid ratio used in the decalcification step, the deproteinization step, and the deacetylation step was fixed constant at 1:10.

## 2.3 Solution plasma experiment

An aqueous solution of chitosan used in the solution plasma experiment was prepared by dissolving chitosan platelets in a 1 % (w/v)  $\text{CH}_3\text{COOH}$  solution at the chitosan concentration of 0.5 % (w/v). In the case of the solution plasma experiment with metal complexation,  $\text{AgNO}_3$ ,  $\text{Zn}(\text{NO}_3)_2$ ,  $\text{Cu}(\text{SO}_4)$ , or  $\text{FeCl}_3$  was dissolved in a 1 % (w/v) acetic acid solution before being added dropwise to the chitosan solution with a constant stirring at the metal-to-chitosan molar ratio of 1:8 at the final chitosan concentration of 0.5 % (w/v). The solution mixture was left at the room temperature (30 °C) for 5 h with a constant stirring. After that, the chitosan solution either with or without complexation with metal ions was poured to the reaction vessel which is a 100-mL beaker connected with two tungsten electrodes with the diameter of 1 mm. The solution plasma system used in this study has been described in the works of Saito, Hieda, & Takai (2009), Pootawang, Saito, & Takai (2011a), and Prasertsung, Damrongsakkul, Terashima, Saito, & Takai (2012). The operation parameters were set constant at the applied voltage of 1.44 kV, the pulse frequency of 15 Hz, the pulse width of 2.0  $\mu\text{S}$ , and

the gap distance of 1 mm. The reaction temperature during plasma treatment was about 80°C. To determine the efficiency of the solution plasma technique in the depolymerization of chitosan, the acid hydrolysis of an aqueous chitosan solution in a 1 % (w/v) CH<sub>3</sub>COOH solution either with or without metal complexation at the reaction temperature of 80 °C was served as a control.

## 2.4 Separation and purification of depolymerized products

An aqueous solution of chitosan sample after the depolymerization via both acid hydrolysis and solution plasma treatment either with or without metal complexation at different reaction times was collected before adjusting the solution pH to about 7 using a 5 M NaOH solution. The neutralized chitosan solution was left overnight at 4 °C for the complete precipitation of the water-insoluble chitosan fraction (Choi, Ahn, Lee, Byun, & Park, 2002). Then, the precipitate was removed by the centrifugation at 8500 rpm at 4 °C for 20 min. The obtained supernatant was further mixed with equal volume of acetone to yield a second precipitate, which should be the water-soluble chitosan fraction (Choi, Ahn, Lee, Byun, & Park, 2002; Prasertsung, Damrongsakkul, Terashima, Saito, & Takai, 2012). The solution mixture was left overnight at 4 °C and the second precipitate was collected by the centrifugation at 8500 rpm at 4 °C for 20 min. After drying at 40 °C overnight, both water-insoluble and water-soluble chitosan fractions were weighed and used to calculate percentages of water-insoluble and water-soluble chitosan fractions as well as total yield percentage as follow:

$$\text{Water-insoluble chitosan (\%)} = (W_i/W_o) \times 100 \quad (1)$$

$$\text{Water-soluble chitosan (\%)} = (W_s/W_o) \times 100 \quad (2)$$

$$\text{Total yield (\%)} = \frac{(W_i + W_s)}{W_o} \times 100 \quad (3)$$

where  $W_i$  is the weight of water-insoluble chitosan fraction after depolymerization,  $W_s$  is the weight of water-soluble chitosan fraction after depolymerization, and  $W_o$  is the initial weight of chitosan in acetic acid solution.

## 2.5 Analytical methods and measurements

To preliminarily study the depolymerization of chitosan, the viscosity of the chitosan solution was measured as a function of the reaction time with the use of a Cannon-Ubbelohde viscometer (Cannon Instrument Co, J758). The viscometer

was filled with a test sample and then equilibrated in water bath at 25 °C. Then, the test solution was passed through the capillary once before measuring the running times at least in triplicate for each test sample. The running times of solvent — a 1 %(w/v) CH<sub>3</sub>COOH solution — and sample solution were used to calculate relative viscosity ( $\eta_{rel}$ ), specific viscosity ( $\eta_{sp}$ ), reduced viscosity ( $\eta_{red}$ ), and inherent viscosity ( $\eta_{inh}$ ) from the following equations:

$$\eta_{rel} = t/t_o \quad (4)$$

$$\eta_{sp} = \eta_{rel} - 1 \quad (5)$$

$$\eta_{red} = \eta_{sp}/C \quad (6)$$

$$\eta_{inh} = (\ln \eta_{rel})/C \quad (7)$$

where  $t$  is the running time of sample solution,  $t_o$  is the running time of solvent, and  $C$  is the concentration of sample solution in g mL<sup>-1</sup>.

After that, viscosity reduction percentage was calculated from the following equation in order to observe the depolymerization of chitosan via acid hydrolysis or solution plasma technique both with and without metal complexation.

$$\text{Viscosity reduction percentage} = (V_t/V_o) \times 100 \quad (8)$$

where  $V_o$  is the viscosity of the initial chitosan solution and  $V_t$  is the viscosity of the depolymerized chitosan solution at the reaction time  $t$ .

The FTIR spectroscopy (Thermo Nicolet Nexus, 670) was used to detect any changes in the chemical structure of chitosan sample after depolymerization via either acid hydrolysis or solution plasma technique. All ATR-FTIR spectra were collected using 64 scans in a wavenumber range of 4000 cm<sup>-1</sup> to 400 cm<sup>-1</sup> at a resolution of 4 cm<sup>-1</sup> with correction for atmospheric carbon dioxide (CO<sub>2</sub>).

The crystalline structure of chitosan both before and after depolymerization was characterized by an X-ray diffractometer (Bruker AXS, D8 advance) operated with the use of Cu K $\alpha$  as an X-ray source. The WAXD analysis was carried out in a continuous mode with a scan speed of 1° min<sup>-1</sup> covering the scanning angle ( $2\theta$ ) from 5° to 80°.

Gel permeation chromatography (GPC) was used to determine any changes in an average molecular weight of chitosan sample at different reaction times. The test chitosan sample was filtered through a nylon 66 membrane with the pore size of 0.45  $\mu$ m (Millipore, USA) before injection into the GPC instrument (Waters, Water 600E) equipped with an refractive index (RI) detector using an ultrahydrogel linear column (molecular weight resolving range of 1.0  $\times$  10<sup>3</sup> Da to

$2.0 \times 10^7$  Da). The eluent used in the GPC analysis was an acetate buffer at pH 4.0 (a mixture of 0.5 M  $\text{CH}_3\text{COOH}$  and 0.5 M sodium acetate,  $\text{CH}_3\text{COONa}$ ). The sample injection volume was 20  $\mu\text{L}$  while the flow rate of the mobile phase was set constant at 0.6  $\text{mL min}^{-1}$ . The GPC analysis was done at the chitosan concentration of 2  $\text{mg/mL}$  and at the temperature of 30  $^\circ\text{C}$ . Pullulans with the molecular weight in the range of  $5.90 \times 10^3$  Da to  $7.08 \times 10^5$  Da were used as standard samples.

The main components in the water-soluble depolymerized chitosan product were further analyzed by using a high performance liquid chromatograph (HPLC) (an Alltech 580 autosampler, an Alltech 626 HPLC pump, and a LiChrospher<sup>®</sup> 100  $\text{NH}_2$  column) with an evaporative light scattering detector (ELSD) (Alltech, 2000ES). The mobile phase solution was isocratic system containing 70%  $\text{CH}_3\text{CN}$  and 30% deionized water. The flow rate of the mobile phase was set constant at 0.8  $\text{mL min}^{-1}$  and the sample injection volume was 50  $\mu\text{L}$ . The ELSD drift tube temperature was 90  $^\circ\text{C}$  while the nebulizer flow rate was 2.2  $\text{L min}^{-1}$ .

Both molecular mass and degree of polymerization (DP) of the extracted water-soluble depolymerized chitosan products (the second precipitate as discussed in section 2.4) was measured by using an electrospray ionization-mass spectrometer (ESI-MS) (Bruker, microTOF II) operated in a positive mode. The test sample was prepared by re-dissolving the extracted water-soluble chitosan fraction in highly purified distilled water at a concentration of 1  $\text{mg mL}^{-1}$  before diluted to  $10^4$  times. The diluted sample solution was injected into the ESI-MS equipment using a syringe at an injection flow rate of 0.8  $\mu\text{L mL}^{-1}$ . The analyzed conditions were set constant at a drying gas temperature of 180  $^\circ\text{C}$ , a drying gas flow rate of 4.0  $\text{L min}^{-1}$ , a nebulizer gas pressure of 0.2 bar, a capillary voltage of 4.5 kV, a skimmer voltage of 30 V. The molecular mass of the test sample was scanned in a mass-to-charge ratio ( $m/z$ ) range of 50 to 5000. All equipment used in the ESI-MS sample preparation was cleaned with  $\text{CH}_3\text{CN}$  before use.

To quantify the amount of the remaining metal ions in the water-soluble depolymerized chitosan fraction, an atomic absorption spectrophotometry (AAS) (Varian, AA280FS) was carried out. The remaining metal percentage was calculated using the following equation:



$$\text{Remaining metal (\%)} = \frac{\text{Remaining metal concentration}}{\text{Initial metal concentration}} \times 100 \quad (9)$$

### 3. Results and discussion

To preliminarily investigate the depolymerization process of the test chitosan sample, the viscosity of the chitosan solution at a concentration of 0.1 mg mL<sup>-1</sup> was measured as a function of reaction time. As shown in **Figure 1**, the solution viscosity slightly decreased with increasing the reaction time when the acid hydrolysis of chitosan without and with metal complexation in a 1 % (w/v) CH<sub>3</sub>COOH solution was performed. On the contrary, when the corresponding chitosan solution was plasma-treated, the solution viscosity rapidly decreased with increasing the reaction time from 0 min to 90 min before beginning to level off at the reaction time longer than 90 min. The results implied that the depolymerization process was enhanced with the use of the solution plasma treatment. In addition, the complexation between chitosan and various types of metal ions was also found to differently affect the depolymerization process. The addition of either Ag<sup>+</sup> or Zn<sup>2+</sup> to the chitosan solution showed a negligible effect on the viscosity reduction since the viscosity reduction profiles of the chitosan solution after complexation with those two metal ions were similar to that in the absence of metal ions. Meanwhile, the viscosity of chitosan solution was found to strongly decrease after the complexation with the added Cu<sup>2+</sup> or Fe<sup>3+</sup>. From **Figure 1**, the viscosity reduction percentage of the chitosan solution after the addition of Cu<sup>2+</sup> in acid hydrolysis without plasma treatment decreased more than that of other metal types and without metal complexation and either Cu<sup>2+</sup> or Fe<sup>3+</sup> under plasma treatment dramatically decreased as the reaction time increased from 0 min to 45 min before remaining constant at the reaction time longer than 45 min. The results suggested that, regardless of the depolymerization methods, i.e. acid hydrolysis and solution plasma treatment, the types of the added metal ions should also play a key role in the depolymerization reaction of chitosan, perhaps due to a difference in the affinities of chitosan towards different kinds of metal ions. The results suggested that the chitosan sample should bind with Cu<sup>2+</sup> and Fe<sup>3+</sup> better than Zn<sup>2+</sup> and Ag<sup>+</sup> (Varma, Deshpande, & Kennedy, 2004), resulting in more decreasing of the molecular weight. Due to the negligible effect of the viscosity reduction of acid hydrolysis and acid hydrolysis with metal complexation, this



present work will further focus on the depolymerization of chitosan-metal complexes via plasma solution in order to obtain the low molecular weight of chitosan products and/or chitosan oligomers compared with the chitosan products obtained from acid hydrolysis and products obtained from solution plasma treatment without metal complexation.

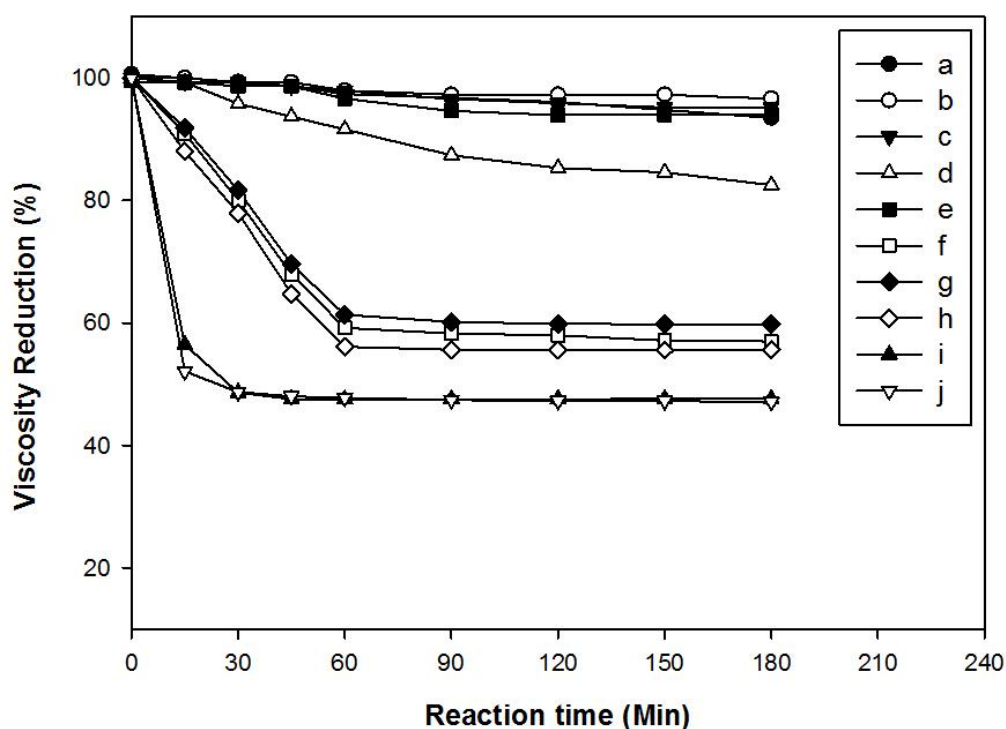


**Figure 1** Changes in relative viscosity of chitosan samples after depolymerization via acid hydrolysis (a) without metal complexation, with complexation with (b)  $\text{Ag}^+$ , (c)  $\text{Zn}^{2+}$ , (d)  $\text{Cu}^{2+}$ , and (e)  $\text{Fe}^{3+}$  and (f) via solution plasma technique without metal complexation and with complexation with (g)  $\text{Ag}^+$ , (h)  $\text{Zn}^{2+}$ , (i)  $\text{Cu}^{2+}$ , and (j)  $\text{Fe}^{3+}$  in a 1 % (w/v)  $\text{CH}_3\text{COOH}$  solution either with or without solution plasma technique at metal-to-chitosan molar ratio of 1:8 as a function of reaction time.

Changes in the color of chitosan solution during acid hydrolysis and solution plasma treatment either with or without metal complexation were also visually observed. The chitosan solution remained colorless and transparent during acid hydrolysis in a 1 % (w/v)  $\text{CH}_3\text{COOH}$  solution over the entire studied reaction time range. On the contrary, when the chitosan solution was plasma-treated either in the presence or absence of metal ions, the color of chitosan solution changed from colorless to pale yellow and then to brown or dark brown as

the reaction time increased from 0 min to 180 min. It was also observed that the color of metal ions could interfere in the color of chitosan solution as well. For examples, the addition of  $\text{Cu}^{2+}$  provided a pale bluish green color to the initial chitosan solution while the added  $\text{Fe}^{3+}$  made the chitosan solution become orangish. Meanwhile, the darkest yellowish to brownish chitosan solution was obtained during the solution plasma treatment after complexation with  $\text{Ag}^+$ . Since the  $\text{Ag}^+$  could be easily reduced after plasma discharge and subsequently formed Ag particles (Pootawang, Saito, & Takai, 2011b), it might be explained that the generated Ag particles in the system should be responsible for the darkest color of the plasma-treated chitosan solution among those obtained from other studied conditions.

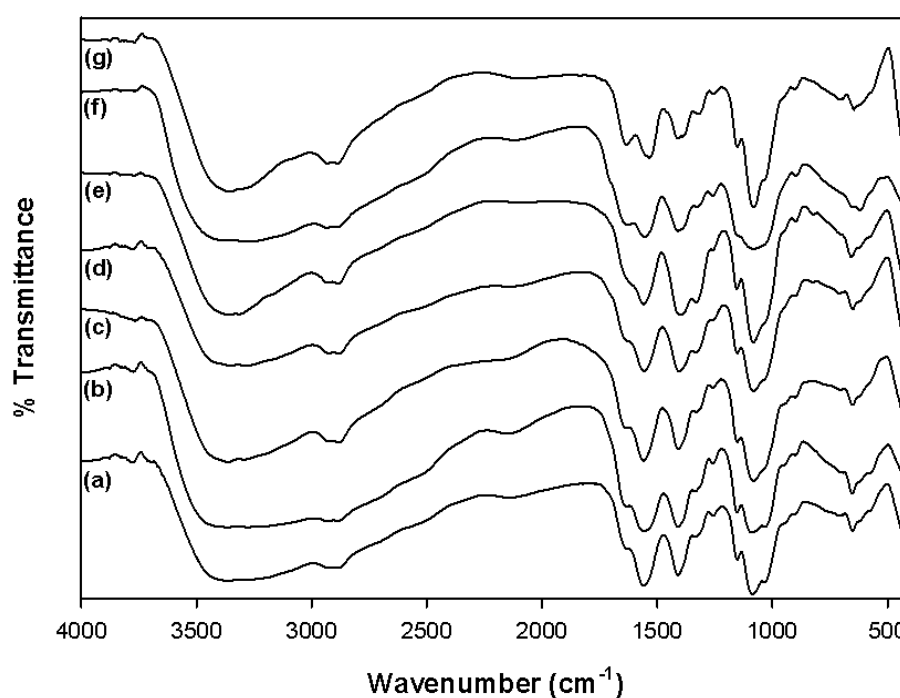


**Figure 2** FTIR spectra of chitosan sample (a) before and after depolymerization via (b) acid hydrolysis and solution plasma technique (c) without metal complexation and with complexation with (d)  $\text{Ag}^+$ , (e)  $\text{Zn}^{2+}$ , (f)  $\text{Cu}^{2+}$ , and (g)  $\text{Fe}^{3+}$  at a metal-to-chitosan molar ratio of 1:8 at a reaction time of 2 h.

The FTIR spectroscopy was used to investigate any changes in the chemical structure of chitosan sample after the depolymerization process. As shown in **Figure 2a**, the FTIR spectrum of the initial chitosan exhibited characteristic peaks located at the wavenumber of about  $3450\text{ cm}^{-1}$ ,  $1650\text{ cm}^{-1}$ ,

and  $1550\text{ cm}^{-1}$ , corresponding to the stretching vibration of hydroxyl group (-OH), amide I (-NH<sub>2</sub>), and amide II (-NH) in the chemical structure of chitosan, respectively (Wang, Du, & Liu, 2004; Chen, Wu, & Zeng, 2005). After depolymerization via acid hydrolysis or solution plasma treatment both with and without metal complexation, these three characteristic peaks of the chitosan structure still appeared in the FTIR spectra of the depolymerized products (see **Figure 2b** to **2g**). Since there was no additional characteristic peaks were observed in the FTIR spectra of the depolymerized products, it was implied that the studied depolymerization techniques — both acid hydrolysis and solution plasma treatment either with or without metal complexation — did not chemically modify the chitosan structure during the depolymerization process. Nevertheless, it was also found that, in the presence of metal ions, the three characteristic peaks in the FTIR spectra of the depolymerized products gradually shift to a lower wavenumber region, implying that both -OH and -NH<sub>2</sub> groups in the chemical structure of chitosan should get involved in complexation with the added metals (see **Figure 2d** to **2g**). **Figure 3** shows possible interaction between chitosan and the added metal ions as well as the proposed depolymerization mechanism of chitosan via metal complexation. Chitosan was able to form a stable complex with the added metal ions via the interaction at the -OH and -NH<sub>2</sub> groups in the chemical structure of chitosan (Wang, Du, & Liu, 2004). As shown in **Figure 3**, the hydroxyl radicals generated by the plasma then reacted with the -NH<sub>2</sub> groups of chitosan, subsequently leading to the breakage of the  $\beta$ -1,4-glycosidic linkage (Prasertsung, Damrongsakkul, Terashima, Saito, & Takai, 2012). The polymeric chain scissions at the  $\beta$ -1,4-glycosidic linkage finally decreased the molecular weight of chitosan (Chang, Tai, & Cheng, 2001).

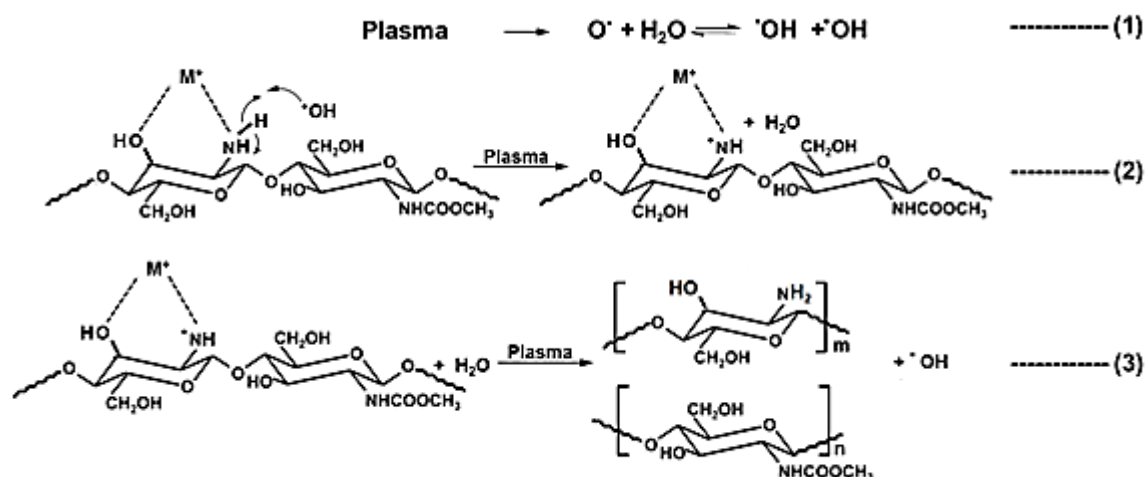


**Figure 3** Possible interactions between metal ions and chitosan during formation of chitosan-metal complexation and proposed depolymerization mechanism.

It has been proposed that the formation of chitosan-metal complex via the interaction at the -OH and -NH<sub>2</sub> groups on the skeleton of chitosan could lead to a weakened bond near the coordinating site, consequently providing weak points on the chitosan chain for the depolymerization (Yin, Zhang, Lin, Feng, Yu, & Zhang, 2004). Since the polymeric chain of chitosan in the complex was broken easier than that of chitosan itself, the depolymerization of chitosan could be enhanced after metal complexation (Yin, Zhang, Lin, Feng, Yu, & Zhang, 2004). Furthermore, the added metal ions were also found to be capable of affecting some reaction during the depolymerization of chitosan, especially in the oxidative depolymerization. In the work of Yin, Zhang, Lin, Feng, Yu, & Zhang (2004), it was suggested that the added Cu<sup>2+</sup> in the chitosan solution did not only form the complex with chitosan but also catalyze the decomposition of hydrogen peroxide (H<sub>2</sub>O<sub>2</sub>) in the system which act as an initiator of the depolymerization reaction. In addition, the chitosan-metal complex exhibited a lower crystallinity than the chitosan itself, resulting in a better accessibility to reactants and a better reactivity (Yin, Zhang, Lin, Feng, Yu, & Zhang, 2004).

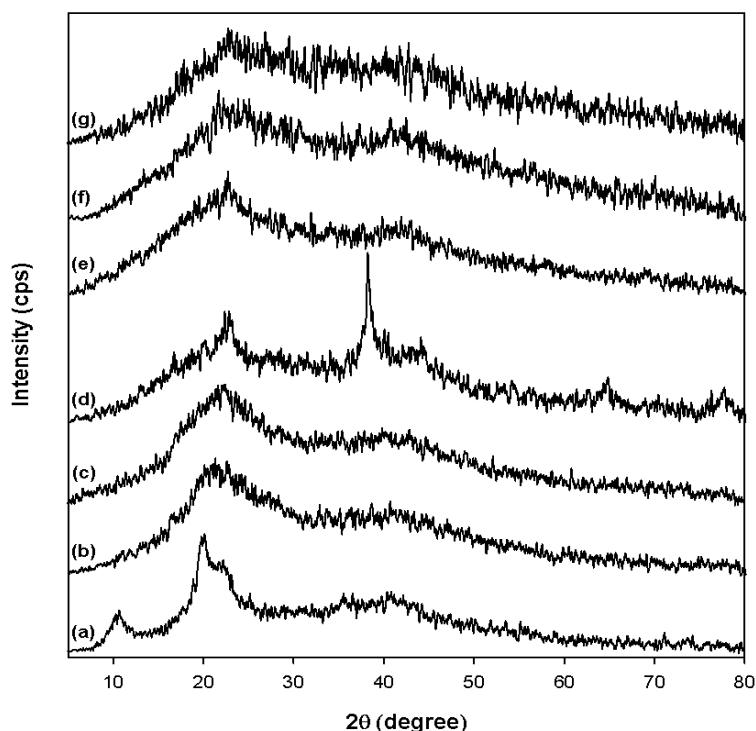


**Figure 4** WAXD patterns of chitosan sample (a) before and after depolymerization via (b) acid hydrolysis and solution plasma technique (c) without metal complexation and with complexation with (d)  $\text{Ag}^+$ , (e)  $\text{Zn}^{2+}$ , (f)  $\text{Cu}^{2+}$ , and (g)  $\text{Fe}^{3+}$  at a metal-to-chitosan molar ratio of 1:8 at a reaction time of 2 h.

**Figure 4** shows the WAXD patterns of chitosan as well as depolymerized chitosan products after acid hydrolysis and solution plasma treatment either with or without metal complexation. Before the depolymerization process (see **Figure 4a**), the WAXD pattern exhibited two major characteristic diffraction peaks at  $2\theta$  equal to  $10^\circ$  and  $20^\circ$ , corresponding to semi-crystalline structure of chitosan (Wang, Du, & Liu, 2004; Yue, Yao, & Wei, 2009; Kisku & Swain, 2012; Kumar, & Koh, 2012). After the depolymerization via either acid hydrolysis or solution plasma technique, the diffraction peak located at  $2\theta$  equal to  $10^\circ$  disappeared while that located at  $2\theta$  equal to  $20^\circ$  became broader (see **Figures 4b** to **4c**), suggesting that the crystalline region of the chitosan sample should be disrupted during the depolymerization. When the solution plasma treatment was applied in a combination with metal complexation, the diffraction peak at  $2\theta$  equal to  $10^\circ$  in the WAXD patterns of the depolymerized chitosan products still disappeared but that at  $2\theta$  equal to  $20^\circ$  was much broader with a much lower peak intensity, especially those after complexation with  $\text{Cu}^{2+}$  and  $\text{Fe}^{3+}$  (see **Figures 4d** to **4f**). The results

implied that the solution plasma treatment of the chitosan-metal complexes could disrupt the crystalline structure of chitosan sample more than the acid hydrolysis and the solution plasma treatment without metal complexation. Interestingly, it was also observed that, after the chitosan-Ag<sup>+</sup> complex was plasma-treated, the WAXD patterns of the depolymerized product also showed the sharp and intense characteristic diffraction peaks of Ag particles at 2θ equal to about 40°, 45°, 65°, and 78°, corresponding to (111), (200), (220), and (311) planes of the Ag crystals, respectively (Mandal, Arumugam, Pasricha, & Sastry, 2005; Pootawang, Saito, & Takai, 2011b; Shameli, Ahmad, Jazayeri, Sedaghat, Shabanzadeh, Jahangirian, Mahdavi, & Abdollahi, 2012). Therefore, the results of the WAXD analysis also confirmed the formation of Ag particles in the system during the solution plasma treatment of chitosan solution after complexation with Ag<sup>+</sup>.

**Table 1** shows changes in weight average molecular weight ( $\overline{M}_w$ ) and polydispersity index (PDI) of chitosan sample during depolymerization via acid hydrolysis and solution plasma treatment either with or without metal complexation as a function of reaction time. From the GPC analysis, the molecular weight of the initial chitosan was found to be in the range of 10<sup>5</sup> Da to 10<sup>6</sup> Da. As shown in **Table 1**, after acid hydrolysis in a 1 % (w/v) CH<sub>3</sub>COOH solution for 180 min, the molecular weight of chitosan sample slightly decreased from its initial value to be in the range of 10<sup>4</sup> Da to 10<sup>5</sup> Da. On the contrary, when the solution plasma treatment was applied for the depolymerization, the molecular weight of chitosan strongly reduced to around 10<sup>3</sup> Da to 10<sup>4</sup> Da. As a result, the depolymerized products obtained from the solution plasma treatment could be identified as LMWC (molecular weight in the range of 5 kDa to 20 kDa) (Harish Prashanth & Tharanathan, 2007). Our finding agrees well with the work of Prasertsung, Damrongsakkul, Terashima, Saito, & Takai (2012), who reported that the solution plasma technique was a potential method for the preparation of LMWC via the depolymerization of chitosan.

**Table 1** Weight average molecular weight ( $\overline{M}_w$ ) and polydispersity index (PDI) of chitosan sample after depolymerization via acid hydrolysis and solution plasma technique in a 1 % (w/v) CH<sub>3</sub>COOH solution without metal complexation and with complexation with Ag<sup>+</sup>, Zn<sup>2+</sup>, Cu<sup>2+</sup>, and Fe<sup>3+</sup> at a metal-to-chitosan molar ratio of 1:8 at different reaction time intervals.

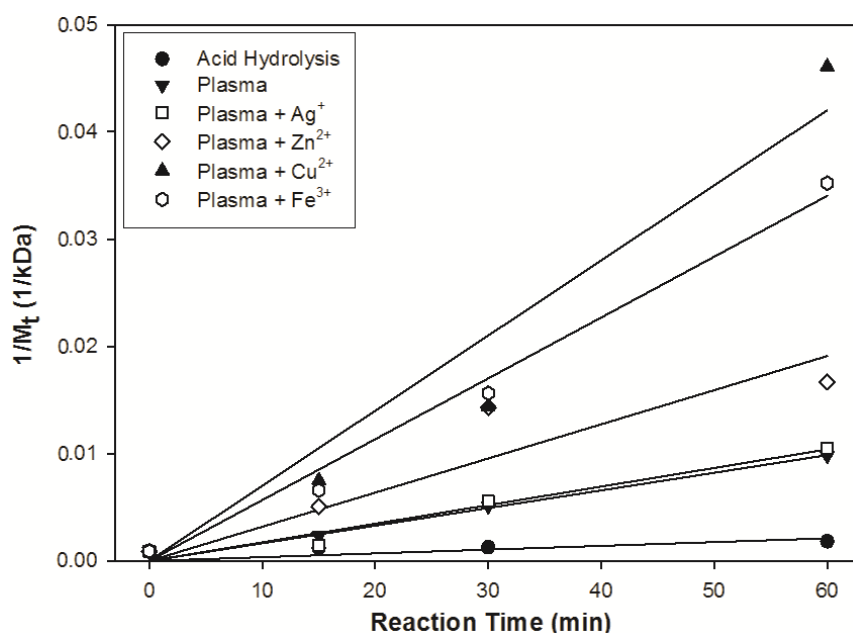
Reaction Time (min)	Molecular Weight (Da)/PDI					
	Acid Hydrolysis	Solution Plasma	Solution Plasma with Metal Complexation			
			Ag <sup>+</sup>	Zn <sup>2+</sup>	Cu <sup>2+</sup>	Fe <sup>3+</sup>
<b>0</b>	$1.1 \times 10^{6,a}$ (4.1) <sup>b</sup>	$1.1 \times 10^6$ (4.1)	$1.1 \times 10^6$ (4.1)	$1.1 \times 10^6$ (4.1)	$1.1 \times 10^6$ (4.1)	$1.1 \times 10^6$ (4.1)
<b>15</b>	$8.3 \times 10^5$ (5.0)	$4.3 \times 10^5$ (5.4)	$7.1 \times 10^5$ (5.3)	$2.0 \times 10^5$ (3.3)	$1.3 \times 10^5$ (3.2)	$1.5 \times 10^5$ (4.1)
<b>30</b>	$7.9 \times 10^5$ (4.3)	$2.0 \times 10^5$ (5.3)	$1.8 \times 10^5$ (4.9)	$7.0 \times 10^4$ (3.3)	$7.0 \times 10^4$ (3.0)	$6.4 \times 10^4$ (4.1)
<b>60</b>	$5.5 \times 10^5$ (6.2)	$1.0 \times 10^5$ (4.4)	$9.5 \times 10^4$ (4.1)	$6.0 \times 10^4$ (3.6)	$2.2 \times 10^4$ (2.1)	$2.9 \times 10^4$ (3.6)
<b>120</b>	$6.4 \times 10^5$ (5.0)	$4.8 \times 10^4$ (5.7)	$1.6 \times 10^5$ (10.5)	$2.6 \times 10^4$ (3.9)	$6.2 \times 10^3$ (2.4)	$1.4 \times 10^4$ (2.9)
<b>180</b>	$2.3 \times 10^5$ (2.6)	$1.8 \times 10^4$ (3.7)	$1.4 \times 10^4$ (3.2)	$1.0 \times 10^4$ (2.7)	$1.9 \times 10^3$ (1.4)	$3.6 \times 10^4$ (21.8)

<sup>a</sup>Reported values are  $\overline{M}_w$  of chitosan sample after depolymerization.

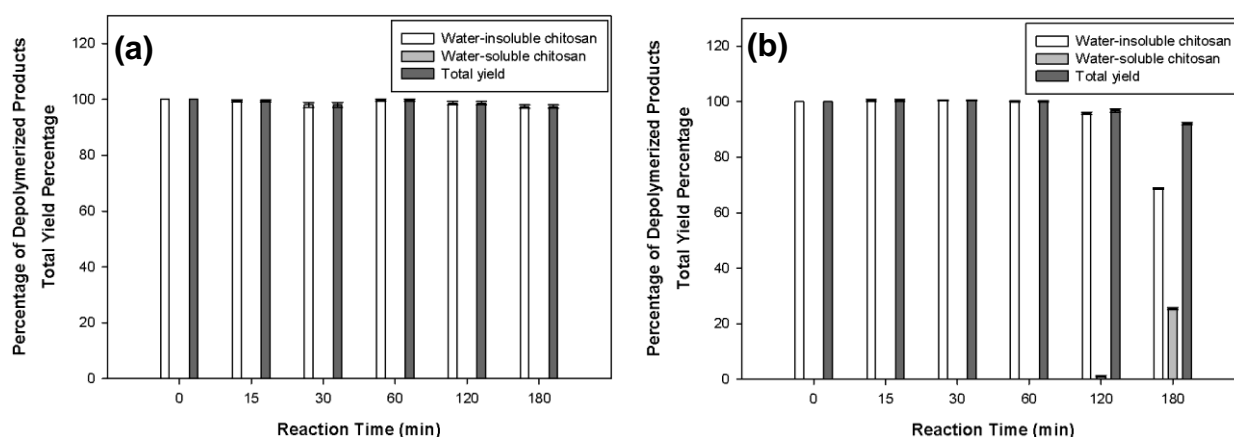
<sup>b</sup>Reported values in parentheses indicate PDI of chitosan sample after depolymerization.

The results of the GPC analysis further revealed that the addition of either Ag<sup>+</sup> or Zn<sup>2+</sup> to the chitosan solution slightly affected the depolymerization reaction because the molecular weight of the obtained products was not much different from that of the solution plasma treatment without metal complexation (see **Table 1**). Nevertheless, as the Cu<sup>2+</sup> or Fe<sup>3+</sup> was added to the chitosan solution, the depolymerization reaction was found to be dramatically enhanced. As shown in **Table 1**, the weight average of molecular weight of the depolymerized chitosan products was measured to be about 10<sup>3</sup> Da for the chitosan-Cu<sup>2+</sup> complex, which was considered to be in the range of chitosan oligimers (molecular weight less than 5 kDa) (Harish Prashanth & Tharanathan, 2007). A stronger promoting effect of the added Cu<sup>2+</sup> or Fe<sup>3+</sup> on the depolymerization reaction of chitosan should be caused not only by a greater affinity of chitosan towards these two metal ions but also by the catalytic activities of both ions on the decomposition of H<sub>2</sub>O<sub>2</sub> as a fenton reaction (Tanioka, *et al.*, 1996; Chang, Tai, & Cheng, 2001) generated in the system during the plasma discharge (Yin, Zhang, Lin, Feng, Yu, & Zhang, 2004; Bláha, Riesová, Zedník, Anžlovar, Žigon, & Vohlídal, 2011; Pootawang, Saito, & Takai, 2011b; Prasertsung, Damrongsakkul, Terashima, Saito, &

Takai,2012). Therefore, a catalyzed decomposition reaction of  $H_2O_2$  might also be responsible for the lowering of the molecular weight of the depolymerized products.



**Figure 5** Linear relationship between inverse of molecular weight ( $1/M_t$ ) and degradation time (t) at initial stage of depolymerization of chitosan sample after acid hydrolysis and solution plasma treatment either without metal complexation or with complexation with  $Ag^+$ ,  $Zn^{2+}$ ,  $Cu^{2+}$ , and  $Fe^{3+}$  at a metal-to-chitosan molar ratio of 1:8 at different reaction time intervals.





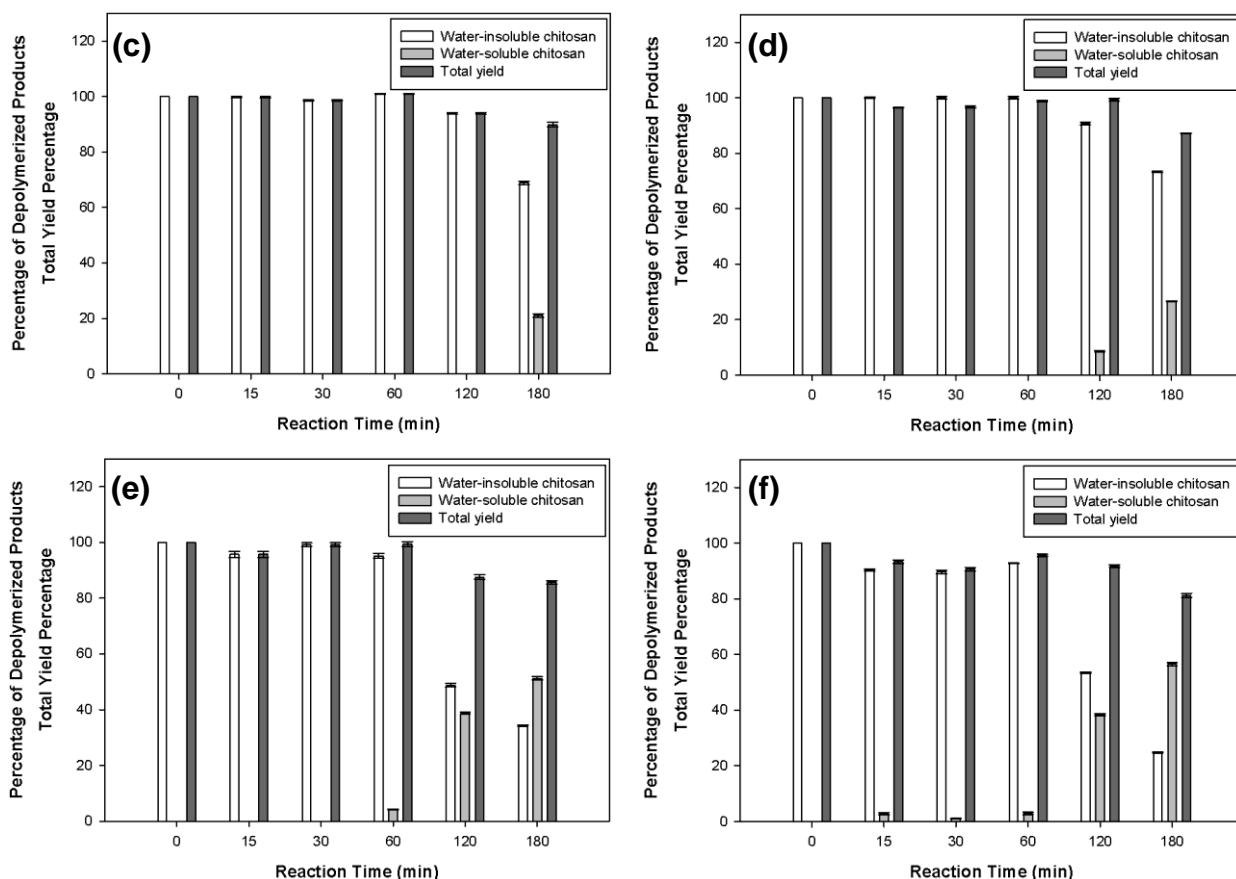


**Figure 6** Percentages of water-insoluble chitosan, water-soluble chitosan, and total yield of depolymerized products obtained from (a) acid hydrolysis and solution plasma treatment of chitosan in a 1 % (w/v)  $CH_3COOH$  solution (c) without metal complexation and with complexation with (d)  $Ag^+$ , (e)  $Zn^{2+}$ , (f)  $Cu^{2+}$ , and (g)  $Fe^{3+}$  at a metal-to-chitosan molar ratio of 1:8 at different reaction time intervals.

Depolymerization kinetic was analyzed based on the relationship between  $\overline{M}_w$  of the chitosan sample and reaction time as follow:

$$1/M_t = 1/M_0 + kt/M = 1/M_0 + k't \quad (10)$$

where  $M_t$  is  $\overline{M}_w$  of the chitosan sample at the reaction time (t),  $M_0$  is an initial  $\overline{M}_w$  of the chitosan sample, M is molecular weight of the chitosan monomer, k ( $\text{min}^{-1}$ ) or  $k'$  ( $\text{mol g}^{-1} \text{min}^{-1}$ ) is the depolymerization rate constant, and t is reaction time (Chang, Tai, & Cheng, 2001). **Figure 5** shows a linear relationship between an inverse of the chitosan molecular weight and reaction time at an initial stage of depolymerization (reaction time between 0 min to 60 min). The k value of the depolymerization of chitosan via the acid hydrolysis route was found to be  $2.42 \times 10^{-3} \text{ min}^{-1}$  while that of the solution plasma treatment without metal complexation

was one order of magnitude higher (or about  $2.42 \times 10^{-2} \text{ min}^{-1}$ ). After complexation with  $\text{Ag}^+$ ,  $\text{Zn}^{2+}$ ,  $\text{Cu}^{2+}$ , and  $\text{Fe}^{3+}$ , the  $k$  value was calculated to be  $2.47 \times 10^{-2} \text{ min}^{-1}$ ,  $4.83 \times 10^{-2} \text{ min}^{-1}$ ,  $1.10 \times 10^{-4} \text{ min}^{-1}$ , and  $8.83 \times 10^{-2} \text{ min}^{-1}$ , respectively. Based on the calculated  $k$ , the order of the depolymerization reaction of chitosan sample was found to be  $\text{Cu}^{2+}$  ( $1.10 \times 10^{-1} \text{ min}^{-1}$ )  $\sim$   $\text{Fe}^{3+}$  ( $8.83 \times 10^{-2} \text{ min}^{-1}$ )  $\gg \gg$   $\text{Zn}^{2+}$  ( $4.83 \times 10^{-2} \text{ min}^{-1}$ )  $\sim$   $\text{Ag}^+$  ( $2.47 \times 10^{-2} \text{ min}^{-1}$ )  $\sim$  solution plasma without metal complexation ( $2.42 \times 10^{-2} \text{ min}^{-1}$ )  $\gg \gg$  acid hydrolysis ( $2.42 \times 10^{-3} \text{ min}^{-1}$ )  $\sim$  acid hydrolysis with metal complexation (data not shown). Hence, our finding implies that the solution plasma treatment with metal complexation, especially with  $\text{Cu}^{2+}$  and  $\text{Fe}^{3+}$ , is an effective way for the depolymerization of chitosan. Moreover, it was also found that the calculated  $k$  of the chitosan depolymerization by the solution plasma treatment with metal complexation in this present work was much higher than those reported in the literature. For example, based on the work of Ilyina, Tikhonov, Albulov, & Varlamov (2000), the  $k$  value of the enzymatic depolymerization of chitosan was in the range of  $10^{-5}$  to  $10^{-4} \text{ min}^{-1}$  (approximately 2-3 orders of magnitude lower than that of our results). In another study (Chang, Tai, & Cheng, 2001), the  $k$  value of the chitosan depolymerization in the presence of  $\text{H}_2\text{O}_2$  was reported to be in the range of  $4.2 \times 10^{-4} \text{ min}^{-1}$  to  $7.1 \times 10^{-4} \text{ min}^{-1}$ .

To further investigate the potential use of the solution plasma treatment for the depolymerization of chitosan, the depolymerized products — water-insoluble or water-soluble — were subsequently separated from the chitosan solution at different reaction times. **Figure 6** shows percentages of water-insoluble and water-soluble fractions as well as total yield percentages as a function of reaction time. At any studied reaction time, it was obvious that a majority of the depolymerized chitosan product obtained from the conventional acid hydrolysis route was water-insoluble. The result implied that the acid-depolymerized chitosan products should still possess too high molecular weight to be dissolved in an aqueous solution at neutral pH. On the contrary, the depolymerized chitosan products obtained from the solution plasma treatment either with or without metal complexation were found to contain both water-insoluble and water-soluble fractions as the reaction time increased to be longer than 120 min. As shown in **Figure 6**, the highest water-soluble chitosan fraction of 57 % was obtained when the solution plasma treatment in combination with  $\text{Fe}^{3+}$  complexation was used for the

depolymerization at the reaction time of 180 min (which was comparable to that obtained from the solution plasma treatment in combination with  $\text{Cu}^{2+}$  complexation at the same reaction time — of approximately 51 %). Again, it was also observed that the addition of  $\text{Ag}^+$  and  $\text{Zn}^{2+}$  to the chitosan solution slightly enhanced the depolymerization process since the percentages of water-insoluble and water-soluble depolymerized chitosan fractions were similar to those obtained from the solution plasma treatment in the absence of metal complexation. Therefore, the order of the efficiency in the depolymerization of chitosan sample was found to be  $\text{Cu}^{2+} \sim \text{Fe}^{3+} \gg \text{Zn}^{2+} \sim \text{Ag}^+ \sim$  solution plasma without metal complexation  $\gg$  acid hydrolysis. This finding is also consistent with the calculated rate constant of depolymerization reaction of the chitosan sample. According to the literatures (Choi, Ahn, Lee, Byun, & Park, 2002; Prasertsung, Damrongsakkul, Terashima, Saito, & Takai, 2012), the water-soluble depolymerized chitosan fraction was expected to be the chitosan oligomers.

The HPLC-ELSD technique was subsequently used in order to analyze the components in the water-soluble depolymerized chitosan products. Obviously, the HPLC-ELSD chromatogram (figure not shown) of the commercial GlcN showed the main peak at the retention time of around 6.9 min. This GlcN peak at the same retention time was also observed in the HPLC-ELSD chromatograms of all test water-soluble depolymerized chitosan products. However, another peak was found in the HPLC-ELSD chromatograms of the water-soluble fractions at a longer retention time of around 7.9 min. This should be mostly likely corresponded to the presence of chitosan oligomers in the test samples.

To verify the presence of chitosan oligomers in the water-soluble depolymerized chitosan products, the ESI-MS analysis was carried out. In the present study, since the MS analysis was operated in the positive ESI mode, positively charged molecules were observed. **Figure 7** shows ESI-MS spectra of water-soluble depolymerized chitosan products obtained from the solution plasma treatment either without or with metal complexation. It was observed that all ESI-MS spectra showed three dominant peaks located at the  $m/z$  ratio of around 381, 425, and 543, which should be the most likely relate to the cluster ions of GlcN monomer  $[2(\text{GlcN}) + \text{Na}^+]$ , the  $\text{CH}_3\text{CN}$  adduct of dimer containing one GlcN unit and one GlcNAc unit  $[\text{GlcN-GlcNAc} + \text{CH}_3\text{CN} + \text{H}^+]$ , and the proton adduct of

trimer containing two GlcN units and one GlcNAc unit  $[2(\text{GlcN})\text{-GlcNAc} + \text{H}^+]$ . Thus, the ESI-MS results indicated that the water-soluble depolymerized chitosan products were composed of GlcN monomer as well as chitosan oligomers with DP in the range of 2 to 3.

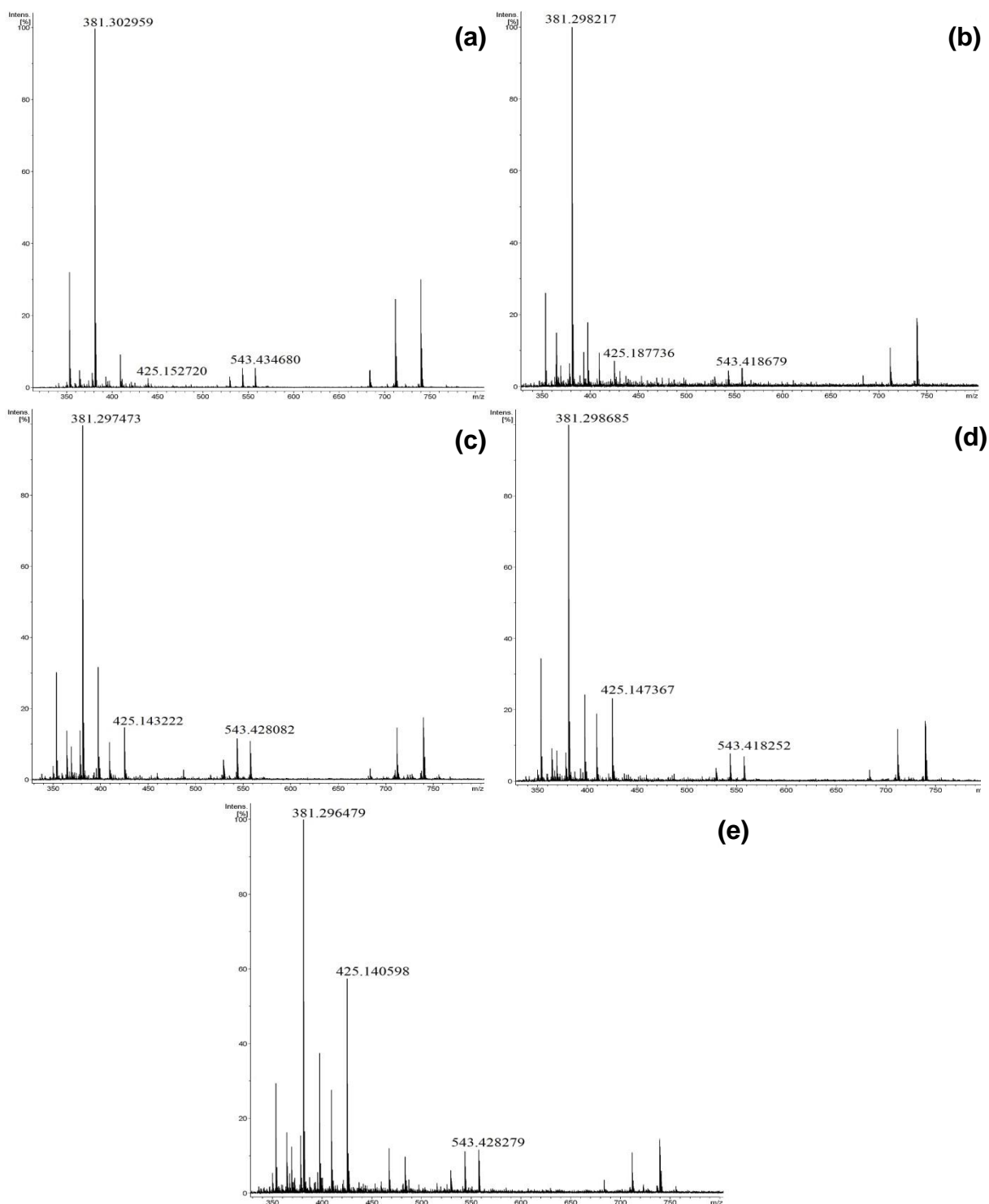


**Figure 7** ESI-MS spectra of water-soluble depolymerized chitosan products obtained from solution plasma technique (a) without metal complexation and with

complexation with (b)  $\text{Ag}^+$ , (c)  $\text{Zn}^{2+}$ , (d)  $\text{Cu}^{2+}$ , and (e)  $\text{Fe}^{3+}$  at a metal-to-chitosan molar ratio of 1:8 at a reaction time of 180 min. All spectra were detected at three main peaks which are  $m/z$  around 381 [ $2(\text{GlcN}) + \text{Na}^+$ ], 425 [ $\text{GlcN-GlcNAc} + \text{CH}_3\text{CN} + \text{H}^+$ ] and 543 [ $2(\text{GlcN})\text{-GlcNAc} + \text{H}^+$ ].

The AAS analysis was also carried out in order to quantify the amount of the added metals remaining in the water-soluble depolymerized chitosan fraction since the remaining metals possibly further affect the end-use of the chitosan oligomers product. The AAS results indicated that all added metals remaining in the water-soluble depolymerized chitosan products obtained from solution plasma treatment after complexation with  $\text{Ag}^+$ ,  $\text{Zn}^{2+}$ ,  $\text{Cu}^{2+}$ , and  $\text{Fe}^{3+}$  were very low in ppm-scale as  $6.87 \pm 0.03$  ppm ( $1.16 \pm 0.01$  %),  $38.99 \pm 0.25$  ppm ( $3.75 \pm 0.02$  %),  $8.07 \pm 0.03$  ppm ( $0.93 \pm 0.00$ %) and  $0.35 \pm 0.01$  ppm ( $0.04 \pm 0.00$  %), respectively implying that most of the added metals were removed during the separation and purification step.

#### 4. Conclusion

Compared to the conventional acid hydrolysis, chitosan was found to be depolymerized much more effectively with the use of the solution plasma treatment. The depolymerization of chitosan via the solution plasma technique could be further enhanced after the complexation of chitosan with metal ions. However, the types of metal ions added to the chitosan solution also played a crucial role in the depolymerization process due to a difference in the affinities of chitosan towards different kinds of metal ions. Not only glucosamine but also the low molecular weight of the depolymerized chitosan products of about  $10^3$  Da, which is in the range of chitosan oligomers, was achieved when the solution plasma was applied in a combination with the complexation with either  $\text{Cu}^{2+}$  or  $\text{Fe}^{3+}$ . To be summarized, the solution plasma technique in combination with chitosan-metal complexation can be potentially used for a large-scale production of both LMWC and chitosan oligomers with high polymerization rate and high yield of water-soluble depolymerized products.

## Acknowledgements

The Ratchadapiseksomphot Endowment Fund, Chulalongkorn University, was acknowledged for providing the postdoctoral fellowship to OP and CV while the Dutsadi Phiphat Scholarship, Chulalongkorn University, was acknowledged for providing the Ph.D. scholarship to CK. This work was financially supported by the Thailand Research Fund (TRF) for the contract number BRG5480008. The authors would like to thank Surapon Foods Public Co., Ltd. (Thailand) for providing the shrimp shells used in the preparation of chitosan.

## References

- Baxter, S., Zivanovic, S., & Weiss, J. (2005). Molecular weight and degree of acetylation of high-intensity ultrasonicated chitosan. *Food Hydrocolloids*, 19, 821-830.
- Bláha, M., Riesová, M., Zedník, J., Anžlovar, A., Žigon, M., & Vohlídal, J. (2011). Polyaniline synthesis with iron(III) chloride–hydrogen peroxide catalyst system: reaction course and polymer structure study. *Synthetic Metals*, 161, 1217-1225.
- Cabrera, J.C., & Cutsem, P.V. (2005). Preparation of chitooligosaccharides with degree of polymerization higher than 6 by acid or enzymatic degradation of chitosan, *Biochemical Engineering Journal*, 25, 165-172.
- Chang, K.L.B., Tai, M.C., & Cheng, F. H. (2001). Kinetics and products of the degradation of chitosan by hydrogen peroxide, *Journal of Agricultural and Food Chemistry*, 49, 4845–4851.
- Chen, S., Wu, G., & Zeng, H. (2005). Preparation of high antimicrobial activity thiourea chitosan-Ag<sup>+</sup> complex. *Carbohydrate Polymers*, 60, 33-38.
- Choi, W.S., Ahn, K.J., Lee, D.W., Byun, M.W., & Park, H.J. (2002). Preparation of chitosan oligomers by irradiation. *Polymer Degradation and Stability*, 78, 533-538.
- Fernandes, J.C., Tavaría, F.K., Soares, J.C., Ramos, Ó.S., Monteiro, M.J., Pintado, M.E. & Malcata, F.X., (2008). Antimicrobial effects of chitosans and chitooligosaccharides, upon *Staphylococcus aureus* and *Escherichia coli*, in food model systems. *Food Microbiology*, 25, 922-928.

- Harish Prashanth, K.V., & Tharanathan, R.N. (2007). Chitin/chitosan: modifications and their unlimited application potential — an overview. *Trends in Food Science & Technology*, 18, 117-131.
- Jeon, Y.-J., Park, P.-J. & Kim, S.-K. (2001). Antimicrobial effect of chitooligosaccharides produced by bioreactor. *Carbohydrate Polymers*, 44, 71–76.
- Liang, T.-W., Chen, Y.-J., Yen, Y.-H. & Wang, S.-L., (2007). The antitumor activity of the hydrolysates of chitinous materials hydrolyzed by crude enzyme from *Bacillus amyloliquefaciens* V656. *Process Biochemistry* , 42, 527-534.
- Ilyina, A. V., Tikhonov, V. E., Albulov, A. I., & Varlamov, V. P. (2000). Enzymic preparation of acid-free-water-soluble chitosan. *Process Biochemistry*, 35, 563-568.
- Kendra, D.F. & Hadwiger. L.A., (1984). Characterization of the smallest chitosan oligomer that is maximally antifungal to *Fusarium solani* and elicits pisatin formation in *Pisum sativum*. *Experimental Mycology*, 8, 276-281.
- Kisku, S.K., & Swain, S.K. (2012). Synthesis and characterization of chitosan/boron nitride composites. *Journal of the American Ceramic Society, in press*.
- Klaikherd, A., Jayanta, M.L.S., Boonjawat, J., Aiba, S., & Sukwattanasinitt, M. (2004). Depolymerization of  $\beta$ -chitin to mono- and disaccharides by the serum fraction from the para rubber tree, *Hevea brasiliensis*. *Carbohydrate Research*, 339, 2799-2804.
- Kumar, S., & Koh J. (2012). Physiochemical, optical and biological activity of chitosan-chromone derivative for biomedical applications. *International Journal of Molecular Sciences*, 13, 6102-6116.
- Lii, C.Y., Liao, C.D., Stobinski, L., & Tomasik, P. (2002). Behaviour of granular starches in low-pressure glow plasma. *Carbohydrate Polymers.*, 49, 499-507.
- Mandal, S., Arumugam, S.K., Pasricha, R., & Sastry, M. (2005). Silver nanoparticles of variable morphology synthesized in aqueous foams as novel templates. *Bulletin of Materials Science*, 28, 503-510.

- Muzzarelli, R.A.A., Stanic, V. & Ramos, V. (1999). Enzymatic depolymerization of chitins and chitosans. In *Methods in Biotechnology: Carbohydrate Biotechnology Protocols*, C. Bucke, ed., Humana Press, Totowa.
- Muzzarelli, R.A.A. (2009). Chitins and chitosans for the repair of wounded skin, nerve, cartilage and bone. *Carbohydrate Polymers*, 76, 167-182.
- Muzzarelli, R. A. A. (2010). Enhanced biochemical efficacy of oligomeric and partially depolymerized chitosans. In F. Columbus (Ed.), *Chitosan: Manufacture, properties and usages*. Hauppauge NY, USA: Nova Publication.
- Pootawang, P., Saito, N., Takai, O. (2011a). Solution plasma for template removal in mesoporous silica: pH and discharge time varying characteristics. *Thin Solid Films*, 519, 7030-7035.
- Pootawang, P., Saito, N., Takai, O. (2011b). Ag nanoparticles incorporation in mesoporous silica synthesized by solution plasma and their catalysis for oleic acid hydrogenation. *Materials Letters*, 65, 1037-1040.
- Prasertsung, I., Damrongsakkul, S., Terashima, C., Saito, N., & Takai, O. (2012). Preparation of low molecular weight of chitosan using solution plasma system. *Carbohydrate Polymers*, 87, 2745-2749.
- Qin, C., Zhou, B., Zeng, L., Zhang, Z., Liu, Y., Du, Y. & Xiao, L., (2004). The physicochemical properties and antitumor activity of cellulase-treated chitosan. *Food Chemistry*, 84, 107-115.
- Saito, N., Hieda, J., & Takai, O. (2009). Synthesis process of gold nanoparticles in solution plasma. *Thin Solid Films*, 518, 912-917.
- Shameli, K., Ahmad, M.B., Jazayeri, S.D., Sedaghat, S., Shabanzadeh, P., Jahangirian, H., Mahdavi, M., & Abdollahi Y. (2012). Synthesis and characterization of polyethylene glycol mediated silver nanoparticles by the green method. *International Journal of Molecular Sciences*, 13, 6639-6650.
- Tanioka, S., Matsui, Y., Irie, T., Tanigawa, T., Tanaka, Y., Shibata, H., Sawa, Y. & Kono, Y. (1996). Oxidative depolymerization of Chitosan by Hydroxyl Radical. *Bioscience Biotechnology and Biochemistry*, 60, 2001-2004.



- Varum, K.M., Ottoy, M.H., & Smidsrod, O. (2001). Acid hydrolysis of chitosans. *Carbohydrate Polymers*, 46, 89-98.
- Varma, A.J., Deshpande, S.V., & Kennedy, J.F. (2004) Metal complexation by chitosan and its derivatives: a review. *Carbohydrate Polymers*, 55, 77-93.
- Wang, X., Du, Y., & Liu, H. (2004). Preparation, characterization, and antimicrobial activity of chitosan-Zn complex. *Carbohydrate Polymers*, 56, 21-26.
- Watthanaphanit, A., & Saito, N. (2013). Effect of polymer concentration on the depolymerization of sodium alginate by the solution plasma process. *Polymer Degradation and Stability*, 98, 1072-1080.
- Yin, X., Zhang, X., Lin, Q., Feng, Y., Yu, X., & Zhang, Q. (2004). Metal-coordinating controlled oxidative degradation of chitosan and antioxidant activity of chitosan-metal complex. *ARKIVOC*, ix, 66-78.
- Yue, W., Yao, P., & Wei, Y. (2009). Influence of ultraviolet-irradiated oxygen on depolymerization of chitosan. *Polymer Degradation and Stability*, 94, 851-858.

## Table caption

**Table 1** Weight average molecular weight ( $\overline{M}_w$ ) and polydispersity index (PDI) of chitosan sample after depolymerization via acid hydrolysis and solution plasma technique without metal complexation and with complexation with  $\text{Ag}^+$ ,  $\text{Zn}^{2+}$ ,  $\text{Cu}^{2+}$ , and  $\text{Fe}^{3+}$  at a metal-to-chitosan molar ratio of 1:8 at different reaction time intervals.

## Figure captions

**Figure 1** Changes in Relative viscosity of chitosan-metal complexed samples after depolymerization via acid hydrolysis (a) without metal complexation, with complexation with (b)  $\text{Ag}^+$ , (c)  $\text{Zn}^{2+}$ , (d)  $\text{Cu}^{2+}$ , and (e)  $\text{Fe}^{3+}$  and via solution plasma technique (f) without metal complexation and with complexation with (g)  $\text{Ag}^+$ , (h)  $\text{Zn}^{2+}$ , (i)  $\text{Cu}^{2+}$ , and (j)  $\text{Fe}^{3+}$  in a 1 % (w/v)  $\text{CH}_3\text{COOH}$  solution at metal-to-chitosan molar ratio of 1:8 as a function of reaction time.

**Figure 2** FTIR spectra of chitosan sample (a) before and after depolymerization via (b) acid hydrolysis and solution plasma technique (c) without metal complexation and with complexation with (d)  $\text{Ag}^+$ , (e)  $\text{Zn}^{2+}$ , (f)  $\text{Cu}^{2+}$ , and (g)  $\text{Fe}^{3+}$  at a metal-to-chitosan molar ratio of 1:8 at a reaction time of 2 h.

**Figure 3** Possible interactions between metal ions and chitosan during formation of chitosan-metal complexation and proposed depolymerization mechanism.

**Figure 4** WAXD patterns of chitosan sample (a) before and after depolymerization via (b) acid hydrolysis and solution plasma technique (c) without metal complexation and with complexation with (d)  $\text{Ag}^+$ , (e)  $\text{Zn}^{2+}$ , (f)  $\text{Cu}^{2+}$ , and (g)  $\text{Fe}^{3+}$  at a metal-to-chitosan molar ratio of 1:8 at a reaction time of 2 h.

**Figure 5** Linear relationship between inverse of molecular weight ( $1/M_t$ ) and degradation time (t) at initial stage of depolymerization of chitosan sample after acid hydrolysis and solution plasma treatment either without metal complexation or with complexation with  $\text{Ag}^+$ ,  $\text{Zn}^{2+}$ ,  $\text{Cu}^{2+}$ ,

and  $\text{Fe}^{3+}$  at a metal-to-chitosan molar ratio of 1:8 at different reaction time intervals.

**Figure 6** Percentages of water-insoluble chitosan, water-soluble chitosan, and total yield of depolymerized products obtained from (a) acid hydrolysis and solution plasma treatment (c) without metal complexation and with complexation with (d)  $\text{Ag}^+$ , (e)  $\text{Zn}^{2+}$ , (f)  $\text{Cu}^{2+}$ , and (g)  $\text{Fe}^{3+}$  at a metal-to-chitosan molar ratio of 1:8 at different reaction time intervals.

**Figure 7** ESI-MS spectra of water-soluble depolymerized chitosan products obtained from solution plasma technique (a) without metal complexation and with complexation with (b)  $\text{Ag}^+$ , (c)  $\text{Zn}^{2+}$ , (d)  $\text{Cu}^{2+}$ , and (e)  $\text{Fe}^{3+}$  at a metal-to-chitosan molar ratio of 1:8 at a reaction time of 180 min. All spectra were detected at three main peaks which are  $m/z$  around 381 [ $2(\text{GlcN}) + \text{Na}^+$ ], 425 [ $\text{GlcN-GlcNAc} + \text{CH}_3\text{CN} + \text{H}^+$ ] and 543 [ $2(\text{GlcN})\text{-GlcNAc} + \text{H}^+$ ].

# Enhanced degradation of chitosan by applying plasma treatment in combination with oxidizing agents for potential use as an anticancer agent

Chayanaphat Chokradjaroen<sup>a</sup>, Ratana Rujiravanit<sup>a,b,c\*</sup>, Anyarat Watthanaphanit<sup>d</sup>, Sewan Theeramunkong<sup>e</sup>, Nagahiro Saito<sup>f</sup>, Kazuko Yamashita<sup>g</sup>, Ryuichi Arakawa<sup>g</sup>

<sup>a</sup>*The Petroleum and Petrochemical College, Chulalongkorn University, Bangkok 10330, Thailand*

<sup>b</sup>*Center of Excellence on Petrochemical and Materials Technology, Chulalongkorn University, Bangkok 10330, Thailand*

<sup>c</sup>*NU-PPC Plasma Chemical Technology Laboratory, Chulalongkorn University, Bangkok 10330, Thailand*

<sup>d</sup>*Department of Chemistry, Faculty of Science, Mahidol University, Bangkok 10400, Thailand*

<sup>e</sup>*Faculty of Pharmacy, Thammasat University, Pathumthani 12120, Thailand*

<sup>f</sup>*Department of Materials, Physics and Energy Engineering, Graduate School of Engineering, Nagoya University, Nagoya 464-8603, Japan*

<sup>g</sup>*Department of Chemistry and Materials Engineering, Faculty of Chemistry, Materials and Bioengineering, Kansai University, Osaka 564-8680, Japan*

## Abstract

Solution plasma (SP) treatment in combination with oxidizing agents, *i.e.*, hydrogen peroxide (H<sub>2</sub>O<sub>2</sub>), potassium persulfate (K<sub>2</sub>S<sub>2</sub>O<sub>8</sub>) and sodium nitrite (NaNO<sub>2</sub>) were adopted to chitosan degradation in order to achieve fast degradation rate, low chemicals used and high yield of low-molecular-weight chitosan and chitoooligosaccharide (COS). Among the studied oxidizing agents, H<sub>2</sub>O<sub>2</sub> was found to be the best choice in terms of appreciable molecular weight reduction without major change in chemical structure of the degraded products of chitosan. By the combination with SP treatment, dilute solution of H<sub>2</sub>O<sub>2</sub> (4 – 60 mM) was required for effective degradation of chitosan. The combination of SP treatment and dilute solution of H<sub>2</sub>O<sub>2</sub> (60 mM) resulted in the great reduction of molecular weight of chitosan and water-soluble chitosan was obtained as a major product. The

resulting water-soluble chitosan was precipitated to obtain COS. An inhibitory effect against cervical cancer cell line (HeLa cells) of COS was also examined.

**Keywords:** chitosan, degradation, plasma treatment, oxidizing agent, chitooligosaccharide

---

\*Corresponding author. Tel: +66 2 218 4132; Fax: +66 2 215 4459

*E-mail address:* ratana.r@chula.ac.th (R. Rujiravanit)

## 1. Introduction

Chitosan is a deacetylated form of chitin which can be found in some crustaceans such as shrimp and crab. Chitosan consists of 2-deoxy-2-amino-D-glucopyranose (GlcN) and 2-deoxy-2-acetamido-D-glucopyranose (GlcNAc) units that are linked together with  $\beta$ -(1,4) glycosidic bonds. A native chitosan usually has a high molecular weight with ubiquitous hydrogen bonds leading to low solubility of chitosan powder and high viscosity of chitosan solution. Degradation of chitosan to obtain low-molecular-weight chitosan (LMWC) and chitooligosaccharide (COS) can solve the problems originated from its high molecular weight. Moreover, LMWC and COS exhibit some incredible biological functions, especially antitumor and anticancer activities (Harish Prashanth & Tharanathan, 2005; Zheng & Zhu, 2003). Harish Prashanth and Tharanathan (2005) have reported that COS with the molecular weight of 0.4 to 1.2 kDa showed *in vitro* and *in vivo* inhibitory effect on human hepatocellular carcinoma cells (HepG2 cells) proliferation and lung cancer metastasis. Shen et al. (2009) also evaluated and suggested about a potential anti-tumor growth and anti-metastatic potency of COS with molecular weight of 23.99 kDa against HepG2 cells and Lewis lung carcinoma cells (LLC cells). COS having degree of polymerization (DP) from 3 to 9 or molecular weight of 0.5 to 1.5 kDa was found to induce an apoptosis in human hepatocellular carcinoma cells (SMMC-7721 cells) (Xu et al., 2008).

Degradation of chitosan by using strong acids for preparing LMWC and COS is widely used in both industries and research works due to the cost effectiveness and simple processing (Vårum, Ottøy & Smidsrød, 2001). However, the hazardous chemical usage may lead to chemical contamination in the final products and cause environmental pollution. Alternatively, enzymatic methods have received more attention in recent years

because of the potential of region-selective degradation of chitin and chitosan under mild conditions (Cabrera & Van Cutsem, 2005; Harish Prashanth & Tharanathan, 2007). Although, enzymatic method gives a good yield of oligomers being composed of 2 to 8 monomers, it exhibits slow progress in molecular weight reduction (Mourya, Inamdar & Choudhari, 2011). In addition, production of LMWC and COS can also be achieved by the oxidative degradation using oxidizing agents, such as  $O_3$ ,  $HNO_2$  and  $H_2O_2$  (Allan & Peyron, 1995; Chang, Tai & Cheng, 2001; Yue, Yao & Wei, 2009). In general, oxidizing agents are attractive for not only chemical decomposition of organic compounds (De Laat & Gallard, 1999; Venkatadri & Peters, 1993), but also chemical degradation of polymers (Liu et al., 2014; Moad et al., 2015) including chitosan. Most oxidizing agents can generate highly reactive species which are capable of attacking many organic compounds and polymers with high rate constants (Chang, Tai & Cheng, 2001; Méndez-Díaz et al., 2010; Tian et al., 2004). Moreover, using oxidizing agents in polymer degradation is highly versatile, since other physical methods can be applied together with an oxidizing agent in order to enhance effectiveness of the reactions.

Chitosan degradation by applying physical methods using energy impact such as microwave (Li et al., 2012), ultraviolet (Yue, Yao & Wei, 2009), ultra-sonication (Savitri et al., 2014), gamma-ray (Wasikiewicz et al., 2005) and plasma has been widely reported. These methods have been considered as effective tools for the degradation reaction because of the ability to provide a rapid reaction with less chemicals used. However, the studies in the past have shown that degradation of chitosan by employing energy impact alone is less effective than that using energy impact in combination with other methods. Some researchers investigated the combination of energy impact method with oxidative degradation aiming to increase radical intensity in the systems. For example,  $^{60}Co$   $\gamma$ -rays together with  $H_2O_2$  was applied to degrade chitosan (El-Sawy et al., 2010; Kang et al., 2007). Microwave irradiation in combination with  $H_2O_2$  was another example used for the degradation of chitosan (Li et al., 2012). Accordingly, it has been suggested that the combined methods are more effective than the individual methods for effective degradation of chitosan (El-Sawy et al., 2010; Kang et al., 2007). Although, there were numerous degradation methods studied in the past, the attempt to acquire novel effective methods is still a challenge focusing on for better production of LMWC and COS together with an environmental concern.

Solution plasma (SP), one of the newly invented non-thermal plasma, is a plasma discharge generated between two electrodes immersed under a liquid phase by providing

high voltage electricity to the electrodes. When plasma is generated, molecules surrounding the electrodes are collided by electrons coming out from the electrodes, resulting in the formation of highly active species (*e.g.*  $\bullet\text{H}$ ,  $\bullet\text{O}$ ,  $\bullet\text{OH}$ ,  $\text{H}^-$ , and  $\text{O}^-$ ), high energy electrons and UV radiation (Baroch et al., 2008; Bratescu et al., 2011). Therefore, SP is a powerful tool to provide extremely rapid reactions (Potocký, Saito & Takai, 2009). The previous researches have focused on using SP for the synthesis of noble metal nanoparticles (Bratescu et al., 2011; Jin et al., 2014; Saito, Hieda & Takai, 2009), the decomposition of some organic compounds in waste water (Baroch et al., 2008) and the removal of polymeric template in mesoporous silica (Pootawang, Saito & Takai, 2011). In recent years, several studies have adopted the use of SP for synthesis and modification of carbon nanoparticles (Ishizaki et al., 2014; Panomsuwan, Saito & Ishizaki, 2016). The SP technology also has potential as an alternative method for biopolymer degradation, because SP generates radicals such as  $\bullet\text{OH}$  that can promote the degradation of polymer chains such as chitosan (Prasertsung, Damrongsakkul & Saito, 2013; Prasertsung et al., 2012) and sodium alginate (Watthanaphanit & Saito, 2013). Even though, the SP treatment alone could facilitate the degradation of chitosan, the improvement of degradation rate and production yield of LMWC and COS by applying the SP treatment is still of great challenge. It has been expected that when the SP treatment has been used together with oxidizing agents, highly active species will be intensively produced by the both systems, resulting in synergetic effect on degradation of chitosan.

In this study, the degradation of chitosan by the combination of the SP treatment and oxidizing agents including  $\text{H}_2\text{O}_2$ ,  $\text{NaNO}_2$  and  $\text{K}_2\text{S}_2\text{O}_8$  at very low concentrations of oxidizing agents (4–60 mM) were carried out. The effects of plasma treatment time, initial concentrations of chitosan and oxidizing agents on molecular weight reduction of chitosan were evaluated. In addition, anticancer activity against HeLa cells of the obtained COS was also examined in comparison with normal cells.

## 2. Experimental

### 2.1. Materials

Shells of *Metapenaeus dobsoni* shrimp, provided by Surapon Foods Public Co., Ltd. (Thailand), were used to prepare chitosan by following a procedure described by Pornsunthorntawee et al. (2014). A 50% (w/v) NaOH solution was purchased from the Chemical Enterprise Co., Ltd. (Thailand). Glacial acetic acid ( $\text{CH}_3\text{COOH}$ , 99.9%),

hydrochloric acid (HCl, 37.0%), hydrogen peroxide ( $\text{H}_2\text{O}_2$ , >30.0%) and sodium hydroxide (NaOH, 97.0%) pellets were obtained from RCI Labscan Ltd. (Thailand). Potassium persulfate ( $\text{K}_2\text{S}_2\text{O}_8$ , 99.5%) and sodium nitrite ( $\text{NaNO}_2$ , 99.0%) were supplied by Sigma–Aldrich (USA). Sodium borohydride ( $\text{NaBH}_4$ ) was obtained from Carlo Erba Reagenti (Italy). All chemicals were reagent grade and used without further purification.

## 2.2. Degradation of chitosan

Chitosan solution was prepared in 40 mL of 0.1 M acetic acid. The solution of each oxidizing agent was separately prepared to achieve a desired concentration in 40 mL of 0.1 M acetic acid solution. Then, the two solutions were poured into a 100 mL SP glass reactor equipped with 1 mm-diameter tungsten electrodes (purity 99.9%, Nilaco Corp., Japan) and mixed by stirring for 5 min prior to the discharge of plasma. A schematic of the experimental set-up of the SP reactor is shown in **Fig. 1**. The plasma discharge occurred at the tip of the tungsten electrodes that were connecting to a high-frequency bipolar pulsed DC power supply (Kurita-Nagoya MPS-06K06C, Kurita Co. Ltd., Japan). The electrodes were submerged in the reaction solution and the distance between the electrodes was adjusted to be 0.5 mm. The operating condition of SP treatment was fixed at the frequency, voltage and pulse width of 15 kHz, 1.6 kV and 2  $\mu\text{s}$ , respectively. A magnetic stirrer was used in order to provide the uniformity of the solution inside the reactor.



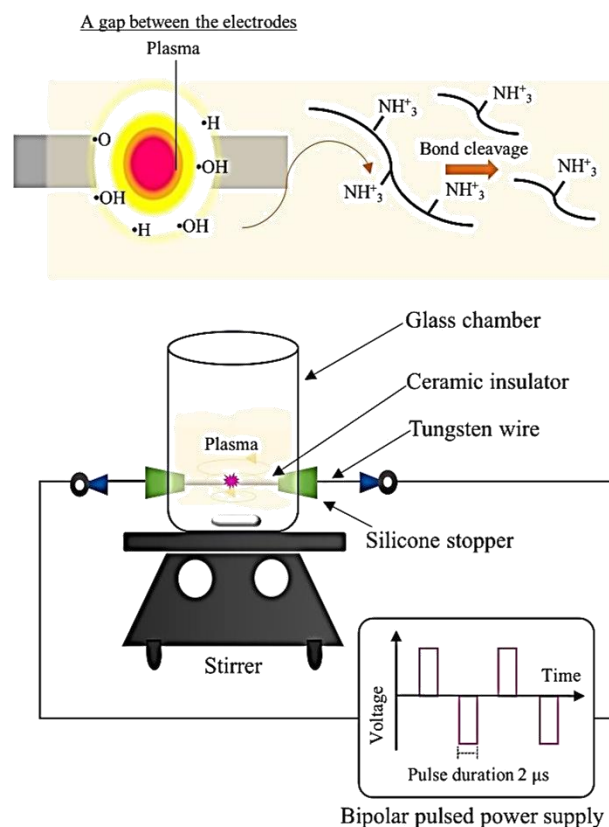


**Fig. 1** Experimental set-up of solution plasma equipment.

### 2.3. Separation and purification of plasma-treated chitosan

The plasma-treated chitosan solution was neutralized by the addition of 2 M NaOH solution and kept at 4°C overnight for complete precipitation (Pornsunthorntawee et al., 2014). After that, the precipitate was collected as a water-insoluble fraction. The supernatant was concentrated by a rotary evaporator under vacuum to a final volume of 10 mL (8 times concentrated). The concentrated solution was then added to a twice-volume acetone, followed by keeping at 4 °C overnight and the precipitate was collected as a water-soluble fraction. Each fractions was collected by centrifugation at 10,000 rpm for 30 min and washed twice with the same ratio of acetone-water mixture. Finally, the precipitated products were dried in a vacuum oven at ambient temperature for 4 h. The water-insoluble and water-soluble fractions were weighed and calculated by the following equations:

$$\text{Percentage of insoluble-chitosan fraction} = 100 \times W_i/W_0 \quad (1)$$

$$\text{Percentage of soluble-chitosan fraction} = 100 \times W_s/W_0 \quad (2)$$

$$\text{Percentage of total yield} = 100 \times (W_i + W_s)/W_0 \quad (3)$$

where  $W_0$  is the initial dry weight of chitosan and  $W_i$  and  $W_s$  are the dry weight of water-insoluble fraction and water-soluble fraction, respectively.

#### 2.4. Fractionation of chitooligosaccharides by adding water-ethanol mixture solution

This method was modified from the previous works (Cabrera & Van Cutsem, 2005; Lin & Lin, 2003). After neutralization and removal of water-insoluble chitosan, ethanol, which had a volume equal to a concentrated solution of water-soluble chitosan, was gradually poured into the solution. The first precipitate, labeled as 1:1 (volumetric ratio of sample solution to the added ethanol) fraction, was then collected by centrifugation. After that, the additional ethanol was added into a supernatant, which left from the above process, to obtain 1:3 fraction and the second precipitate was collected. The same procedure was repeated to prepare the 1:5 fraction. After adding ethanol, all samples were kept at 4 °C overnight for complete precipitation. The precipitates were washed with their corresponding water-ethanol mixture solution for three times and then dissolved in deionized water prior to freeze drying. Finally, freeze-dried products were kept in dehumidifier for further characterization.

#### 2.5 Characterization

The change in viscosity of chitosan solution as a function of the plasma treatment time was measured by Cannon-Ubbelohde viscometer (J758, Cannon Instrument Co., USA). A 0.1 M  $\text{CH}_3\text{COOH}$  solution was used as a solvent for measuring the running time of the solvent ( $t_0$ ). A sample of the plasma-treated chitosan solution was poured into the viscometer immersed in a water bath at a controlled temperature of 25 °C and the running time of the sample ( $t_s$ ) was measured repeatedly for at least three times. Then, the relative viscosity ( $\eta_r$ ) was calculated according to the following equation (4):

$$\eta_r = t_s / t_0 \quad (4)$$

And the percentage of the relative viscosity reduction,  $\eta_r(\%)$ , was further calculated by using the following equation:

$$\eta_r(\%) = 100 \times (\eta_{r,t} / \eta_{r,0}) \quad (5)$$

where  $\eta_{r,0}$  is the viscosity of the chitosan solution before plasma treatment and  $\eta_{r,t}$  is the viscosity of the plasma-treated chitosan solution at reaction time  $t$ .

The weight-average molecular weight ( $M_w$ ) and polydispersity index (PDI) of chitosan during the degradation by applying SP treatment were determined by GPC (CTO-10A, Shimadzu, Japan) was equipped with a refractive index (RI) detector. The ultra-

hydrogel linear column (Water 600E, Waters, USA) was connected with the guard column in series. An acetate buffer at pH 4.0 which consists of 0.5 N CH<sub>3</sub>COOH and 0.5 N sodium acetate (CH<sub>3</sub>COONa) was used as mobile phase. A 40 µL of chitosan solution in the acetate buffer was filtrated through a syringe filter containing a 0.45 µm-pore sized nylon 66 membrane (Vertical Chromatography Co., Ltd., Thailand) before injection. The operating flow rate and temperature were set at 0.6 mL·min<sup>-1</sup> and 40 °C, respectively. Pullulans with the molecular weight range of 1.32×10<sup>3</sup> to 8.05×10<sup>5</sup> Da were used as standard samples.

The change of chemical structure was investigated by FT-IR (Nicolet iS5, Thermo Fisher Scientific, USA) using 64 scans in the range of 4000–600 cm<sup>-1</sup> at a resolution of 4 cm<sup>-1</sup> with a correction for atmospheric carbon dioxide (CO<sub>2</sub>). A 500-MHz NMR (AVANCE III, Bruker, Bruker Corp., Germany) was also used. Samples were dissolved in CD<sub>3</sub>COOD/D<sub>2</sub>O at a concentration of 10–30 mg·mL<sup>-1</sup>. Degree of deacetylation (DD) is calculated by equations (6)-(7) according to previously reported methods (Kasaai et al., 1999; Sabnis & Block, 1997).

For FT-IR,

$$D = 97.67 - \{26.486 \times (A_{1655}/A_{3450})\} \quad (6)$$

where A corresponds to the absorbance of the respective bands.

For <sup>1</sup>H-NMR,

$$DD = 100 \times \{1 - (I_{\text{at } 2 \text{ ppm}}/3) / I_{\text{at } 3 \text{ ppm}}\} \quad (7)$$

where I corresponds to the integral of the respective bands.

The crystalline structure of chitosan before and after degradation was observed by using an XRD (SmartLab, Rigaku, Japan) with Cu Kα radiation in a continuous mode with a scan rate of 5° min<sup>-1</sup>.

An ESI(+)-MS (Exactive Orbitrap, Thermo Fisher Scientific, USA) was employed in an infusion mode with a flow rate of approximately 10 µL·min<sup>-1</sup> for mass spectrometry analysis of the COS product. Sheath, auxiliary and sweep gases were N<sub>2</sub> gas set at 10, 1, and 1 psi, respectively. Spray voltage was 4.2 kV. Capillary temperature and voltage were 200 °C and 10 V. Tube lens voltage was 180–250 V. Skimmer voltage was 13 V.

## 2.6 Biological Assay

### 2.6.1 Cell culture

HeLa cells (Human uterine cervix cancer cell line) and MRC-5 cells (Homo sapiens lung normal cell line) were cultured by using Dulbecco's Modified Eagle Medium (DMEM) high glucose with *L*-glutamine and sodium pyruvate (Biowest, France), and Eagle's Minimum Essential Medium (EMEM) with sodium bicarbonate, non-essential amino acids, *L*-glutamine, and sodium pyruvate (Corning Inc., USA), respectively. Both media were supplemented with 10% fetal bovine serum (Biowest, France), 100 U·mL<sup>-1</sup> Penicillin and 100 µg·mL<sup>-1</sup> Streptomycin (Gibco, Life Technologies Inc., USA) prior to culturing in a humidified incubator (37 °C, 5% CO<sub>2</sub>).

### 2.6.2 Cytotoxicity assay

The chitosan samples were tested *in vitro* by using MTT assay. Cells were seeded into 96-well microliter plates (1×10<sup>4</sup> cells/well). After 24 h, cells were treated with different concentrations of 1.44-kDa COS sample, diluted with sterile water to make the desired final concentration (0.1 to 40 mg·mL<sup>-1</sup>). Then, the COS-treated cells were incubated in an incubator at 37 °C and 5% CO<sub>2</sub> for 24 h. After incubation, medium was replaced with PBS (phosphate buffer saline) solution containing 0.05% w/v of MTT (3-(4,5-dimethylthiazol-2-yl)-2,5-diphenyltetrazolium bromide) solution and further incubated for 3 h. The solution were then discarded and DMSO was added to dissolve the formed formazan crystals and the absorbance (A) of each well was measured at 570 nm using a microplate reader (Varioskan™ Flash Multimode Reader, Thermo Fisher Scientific, USA). Doxorubicin was used as positive control. All experiments were performed in triplicate and repeated for five experiments. The cell viability was expressed as a percentage relative to the untreated control cells as following:

$$\text{Cell viability (\%)} = 100 \times | (A_{\text{treated}} - A_{\text{blank}}) / (A_{\text{untreated}} - A_{\text{blank}}) | \quad (8)$$

After the percentage of cell viability was calculated and plotted, then the mean growth-inhibitory concentration (*IC*<sub>50</sub>) value was determined.

## 3. Results and discussion

### 3.1. Degradation of chitosan by applying SP treatment in combination with different oxidizing agents

As shown in **Fig. 2A**, the change in viscosity of the chitosan solution was measured as a function of reaction time as a preliminary study on the degradation of chitosan. The

chitosan solution with the addition of each oxidizing agent at a concentration of 4 mM was subjected to either SP treatment or conventional heat treatment at a temperature of 75 °C which was the maximum temperature of the chitosan solutions measured during the SP treatment. The viscosity of chitosan solution slightly decreased during the heat treatment at 75 °C for 60 min. On the contrary, SP treatment resulted in dramatically decreasing of viscosity of the chitosan solution under the corresponding condition. The reduction of viscosity of chitosan solution reflected the cleavage of chitosan chains (Choi et al., 2002). This evidence indicated that the SP treatment could greatly promote the degradation of chitosan and possibly lead to the production of COS (Pornsunthornatavee et al., 2014). The viscosity of chitosan solution dramatically decreased within the first 30 min of the SP treatment, followed by gradually reducing until the SP treatment time of 60 min. This might be explained in terms of crystalline structure of chitosan which could be investigated by the XRD. The XRD result was shown in supplementary data (see Fig. A1). Chitosan is a semicrystalline polymer containing both amorphous and crystalline regions. In general, amorphous structure is more susceptible to degradation than crystalline structure (Tian et al., 2004). At the beginning of the SP treatment, the amorphous region was firstly degraded and would eventually dissolve in the reaction medium, whereas the crystalline region still remained intact. However, the crystalline region in the chitosan was subsequently destroyed with further degradation and turned into amorphous structure before peeling off to the reaction medium (Kang et al., 2007; Tian et al., 2004). Accordingly, the presence of crystalline structure of chitosan was a plausible cause that retards the decrement of viscosity of chitosan solution (Prasertsung et al., 2012). Besides, it was found that the addition of the oxidizing agents enhanced the degradation reaction of chitosan in all studied conditions. After the SP treatment, the viscosity of chitosan solution with the addition of either  $K_2S_2O_8$  or  $NaNO_2$  sharply decreased over 80%, while viscosity of chitosan solution obtained from the corresponding condition with the addition of  $H_2O_2$  reduced by 70%. The addition of either  $K_2S_2O_8$  or  $NaNO_2$  resulted in the similar viscosity reduction profiles regardless of the degradation methods. Degradation of chitosan by the SP treatment in the presence of  $H_2O_2$  led to more rapid reduction in viscosity of chitosan solution than that obtained under the corresponding condition using heat treatment.

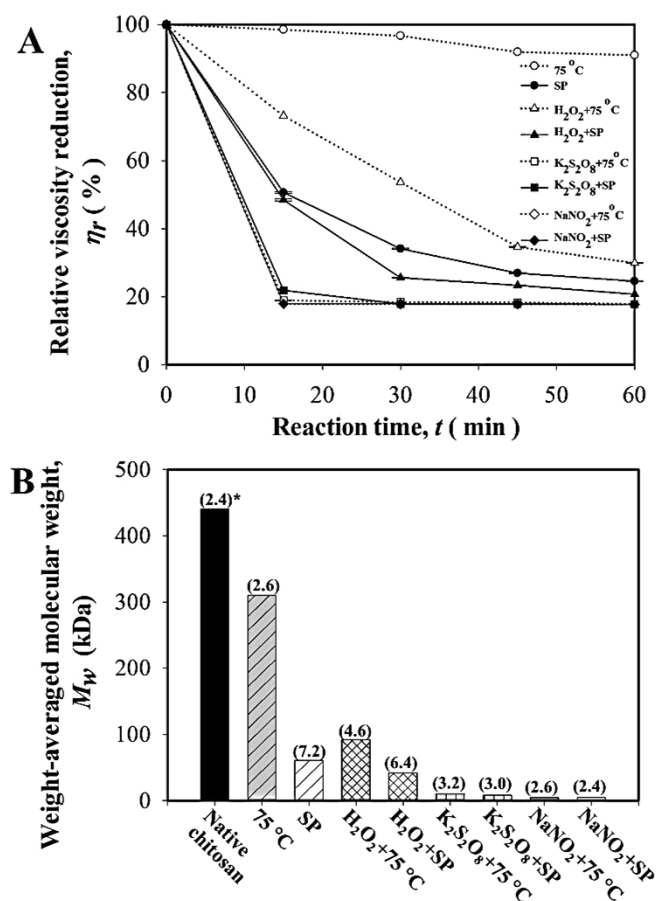


**Fig. 2 (A)** Reduction of relative viscosity as a function of the reaction time and **(B)**  $M_w$  and PDI of chitosan solutions containing 0.5% chitosan in 0.1 M CH<sub>3</sub>COOH after 60 min of degradation via either the conventional heat treatment at 75 °C or SP treatment with and without oxidizing agents at a concentration of 4 mM (Note: \* refers to PDI).

A comparison on  $M_w$  of the degraded chitosan obtained by the heat treatment and the SP treatment at the reaction time of 60 min with and without the addition of oxidizing agents at the concentration of 4 mM is shown in **Fig. 2B**. The tendency on the reduction of  $M_w$  of chitosan after degradation by heat treatment and SP treatment was in good agreement with the result that was determined by the viscosity measurement of chitosan solution that is shown in **Fig. 2A**. Without the addition of oxidizing agent, the SP treatment could reduce  $M_w$  of chitosan more effective than the heat treatment at the same temperature. Moreover, it was found that the use of oxidizing agents in combination with heat treatment and SP treatment could enhance the degradation reaction of chitosan. Nevertheless, in case of NaNO<sub>2</sub>, the SP treatment and the heat treatment gave the degraded products having about the same  $M_w$ . It has been reported that in an acid-nitrite system, nitrosating species could be formed at the room temperature or even lower, resulting in

degradation of chitosan (Mao et al., 2004). In case of  $K_2S_2O_8$ , the SP treatment had a slightly higher performance than the heat treatment in the aspect of giving lower  $M_w$  of the degraded chitosan. According to the literature,  $K_2S_2O_8$  was thermally dissociated at 75 °C to form anionic radicals which would further attack chitosan chains, resulting in cleavage of  $\beta$ -1,4 glycosidic bond and eventually chitosan degradation (Harish Prashanth & Tharanathan, 2005; Hsu, Don & Chiu, 2002).

**Fig. 3** shows the percentages of water-insoluble and water-soluble fraction as well as the percentage of total yield of the degraded chitosan as a function of reaction time. Water-soluble chitosan was referred to chitosan having molecular weight less than 10 kDa (Lee et al., 2001). The results in all studied conditions revealed that the longer reaction time proceeded, the higher amount of water-soluble chitosan was obtained. According to the percentages of the total yield, loss of chitosan sample after the degradation by the SP treatment alone was relatively low, while the SP treatment in combination with oxidizing agents led to more loss of chitosan sample. The SP treatment with the addition of  $H_2O_2$  resulted in losing 4.5% of chitosan sample. Degradation of chitosan by the SP treatment in the presence of either  $NaNO_2$  or  $K_2S_2O_8$  led to much more loss of the chitosan, that were 24% and 32%, respectively. The severe reaction occurring by the addition of  $NaNO_2$  and  $K_2S_2O_8$  may cause the formation of by-products, which were unable to recover by the collecting method in this work, such as 2,5-anhydro-D-mannitol and 5-hydroxymethylfurfural (HMF) (Tømmerraas et al., 2001). However, the addition of each oxidizing agent could lead to the increasing of the amount of water-soluble chitosan after the SP treatment, compared to that obtained from using the SP treatment alone. At the plasma treatment time of 60 min, the addition of either  $K_2S_2O_8$  or  $NaNO_2$  achieved approximately 70% of the water-soluble chitosan, while the water-soluble chitosan obtained from the corresponding condition with the addition of  $H_2O_2$  was 66% and the SP treatment alone gave 50%. This result is consistent with the viscosity reduction of the plasma-treated chitosan solution in the presence of oxidizing agents.

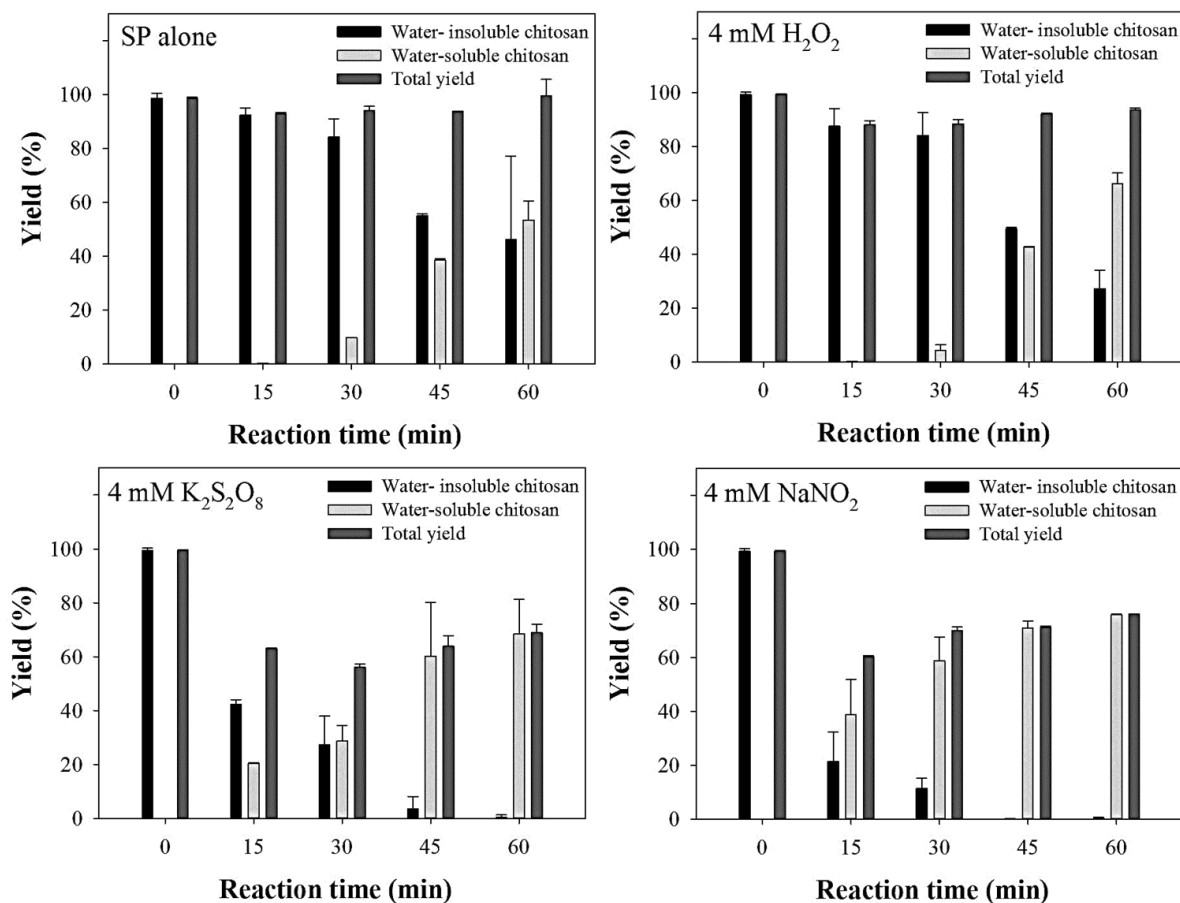


**Fig. 3** Percentages of water-insoluble and water-soluble fractions, and total yield of degraded chitosan using the SP treatment alone and the SP treatment in combination with oxidizing agents at a concentration of 4 mM.

FT-IR analysis was carried out to evaluate degree of deacetylation (DD) and chemical structures of native chitosan and the degraded chitosan. The results are shown in **Fig.4A**. The characteristic peaks of native chitosan and the degraded chitosan obtained by the SP treatment with and without oxidizing agents appeared at the wavenumbers of 3450, 1650, 1550 and 1074  $\text{cm}^{-1}$  corresponding to  $-\text{OH}$  stretching, amide I  $\text{C}=\text{O}$  bending, amide II  $\text{N}-\text{H}$  bending and  $\text{C}-\text{O}-\text{C}$ , respectively (Ifuku et al., 2012; Kang et al., 2007; Ostrowska-Czubenko & Gierszewska-Drużyńska, 2009; Qin et al., 2006). The native chitosan had the DD of 91.5%, whereas the degraded chitosan obtained from the SP treatment alone had the DD of 87.8%. The DD of degraded chitosan obtained from the combination of the SP treatment with  $\text{H}_2\text{O}_2$ ,  $\text{K}_2\text{S}_2\text{O}_8$  and  $\text{NaNO}_2$  were 87.5%, 85.6% and 77.2%, respectively. The results suggested that the SP treatment with and without oxidizing agents could induce



scission of some side chains at the amino group of chitosan resulting in the reduction of DD of the degraded chitosan.

The chemical structures of chitosan before and after degradation by applying the SP treatment in combination with different oxidizing agents were further investigated by  $^1\text{H}$ -NMR as shown in **Fig 4B**. Native chitosan showed a singlet at 3.0 ppm and multiplets at 3.2–4.3 ppm, corresponding to the ring methane protons, together with a singlet at approximately 1.90 ppm, which refers to N-acetyl glucosamine units (Tian et al., 2004). Regardless of type of oxidizing agents, the  $^1\text{H}$ -NMR spectra of the degraded chitosan had similar pattern to that of native chitosan. The DD was also calculated from the NMR results. The DD of the native chitosan was equal to 92%, while the DD of the degraded chitosan obtained by the SP treatment in combination with  $\text{H}_2\text{O}_2$ ,  $\text{K}_2\text{S}_2\text{O}_8$  and  $\text{NaNO}_2$  were equal to 80%, 83% and 74%, respectively. Moreover, the NMR spectrum of the degraded chitosan obtained from the SP treatment in combination with  $\text{NaNO}_2$  had minimal signals appearing at 4.5, 6.5 and 7.3 ppm which could be assigned to HMF (Vigier et al., 2012). According to the literature, the severe degradation of chitosan by using nitrous acid could lead to the change of the chemical structure of chitosan to 2,5-anhydro-D-mannitol and 5-hydroxymethylfurfural (HMF) (Tømmerraas et al., 2001; Sánchez et al., 2017).

Even though  $\text{H}_2\text{O}_2$  may not be as powerful oxidizing agent as  $\text{K}_2\text{S}_2\text{O}_8$  and  $\text{NaNO}_2$ , the yield of the water-soluble chitosan and the total yield of degraded chitosan were acceptable and the loss of degraded chitosan in case of  $\text{H}_2\text{O}_2$  was less than that obtained from the addition of either  $\text{K}_2\text{S}_2\text{O}_8$  or  $\text{NaNO}_2$ .  $\text{H}_2\text{O}_2$  was easy to handle, cheap and environmentally friendly oxidant (Qin et al., 2002; Shen et al., 2010). Moreover,  $\text{H}_2\text{O}_2$  could degrade chitosan with less side reaction than  $\text{K}_2\text{S}_2\text{O}_8$  and  $\text{NaNO}_2$ . As mentioned, the severe degradation of chitosan by the addition of  $\text{NaNO}_2$  could result in the change of the chemical structure of chitosan to 2, 5-anhydro-D-mannitol or HMF. In case of degradation of chitosan by using  $\text{K}_2\text{S}_2\text{O}_8$ , it has been reported that anionic persulfate free radicals which generated from  $\text{K}_2\text{S}_2\text{O}_8$  could attack at the cationic amino group of chitosan and form crosslinking via electrostatic attraction (Prashanth & Tharanathan, 2006). Therefore,  $\text{H}_2\text{O}_2$  was considered as a good choice of oxidizing agent for enhancing the degradation of chitosan by using the SP treatment.

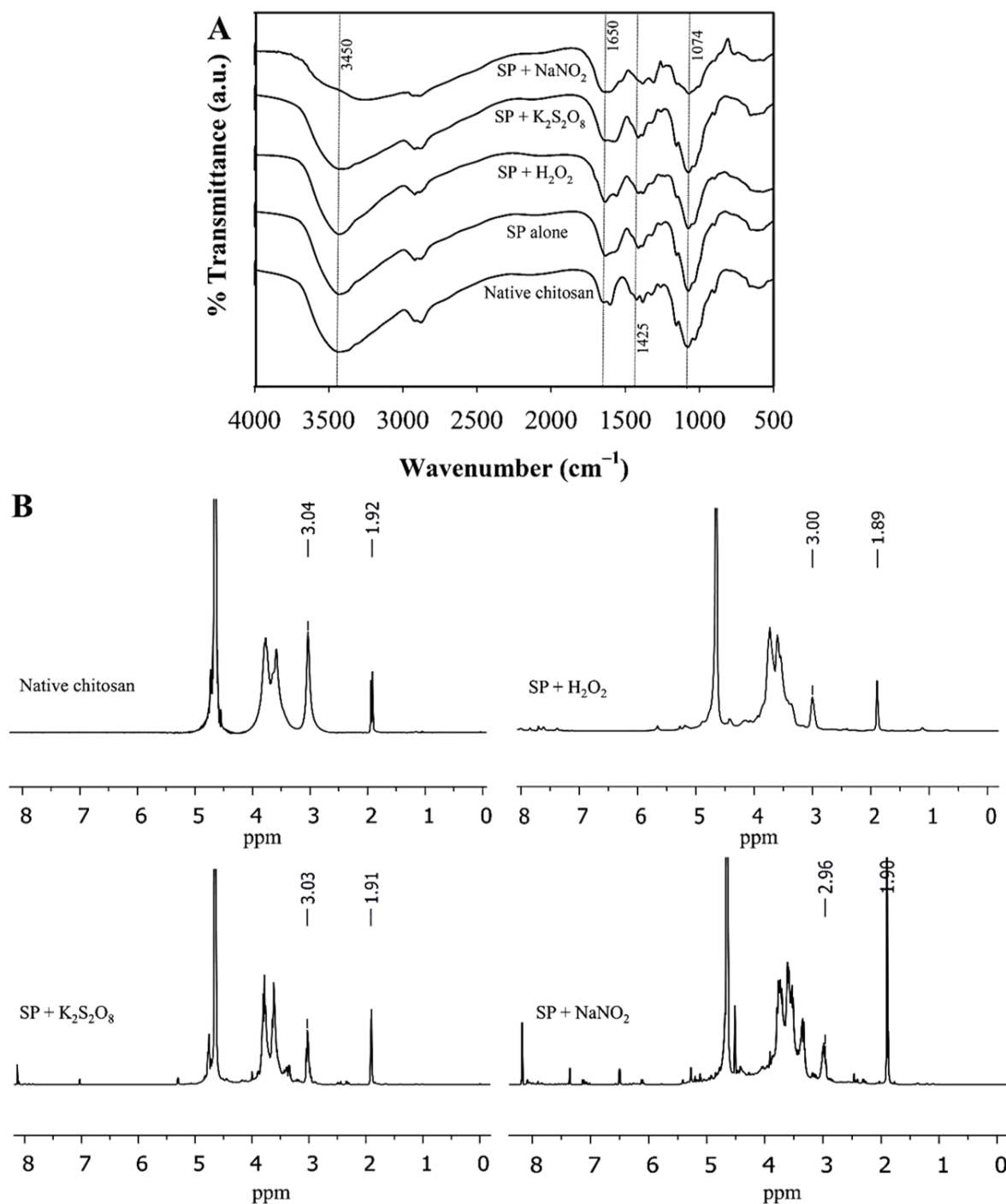
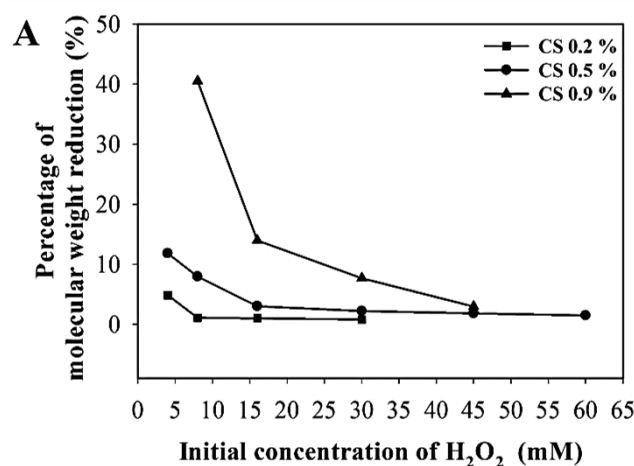


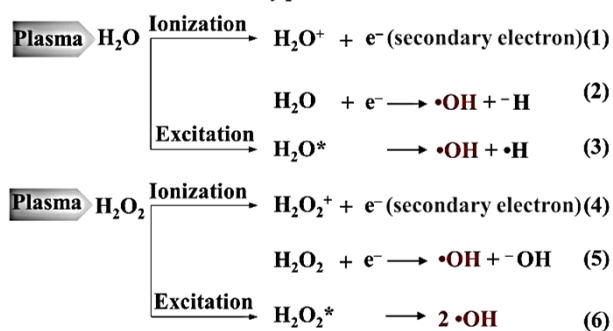
**Fig. 4** (A) FT-IR spectra and (B)  $^1\text{H}$ -NMR spectra of the native chitosan and degraded chitosan obtained by degradation of chitosan at a concentration of 0.5 % by the SP treatment in combination with  $\text{H}_2\text{O}_2$ ,  $\text{K}_2\text{S}_2\text{O}_8$  and  $\text{NaNO}_2$  at a concentration of 4 mM for 60 min.

The factors influencing the degradation of chitosan by the combination of SP treatment and  $\text{H}_2\text{O}_2$ , such as the initial concentration of chitosan and  $\text{H}_2\text{O}_2$ , were investigated. **Fig. 5A** depicts the effect of the initial concentrations of chitosan and  $\text{H}_2\text{O}_2$

on the changes in the  $M_w$  of chitosan after the degradation by SP treatment for 60 min. This evidence implied that the susceptibility to degradation of chitosan was correlated to the initial concentration of the polymer. According to the literature, chitosan chains normally expand in an acidic aqueous solution, because of the protonation reaction of amino group at the C2 position that lead to an electrostatic repulsion (Mao et al., 2004). Therefore, at low concentration, the chitosan chains are in the expanded conformation and can freely move in the solution, causing an easy access of the free radicals such as  $\bullet\text{OH}$  to the polymer chains. On the contrary, the increment of initial concentration of chitosan solution leads to a progressive entanglement between the polymer chains. As a result of less mobility, some intermolecular interactions between polymer chains become stronger and the accessible chain segments may be limited while the distribution of  $\bullet\text{OH}$  in solution can be obstructed, leading to the reduction of the degradability of the polymer chains. On the other hand, the increment of the amount of  $\text{H}_2\text{O}_2$  could increase the chitosan degradation, because of the production of more  $\bullet\text{OH}$ . The increasing of  $\bullet\text{OH}$  content in the system would increase an opportunity of  $\bullet\text{OH}$  to react with the chitosan chains.



**B Ionization and excitation by plasma:**



**Degradation of chitosan in acidic solution:**

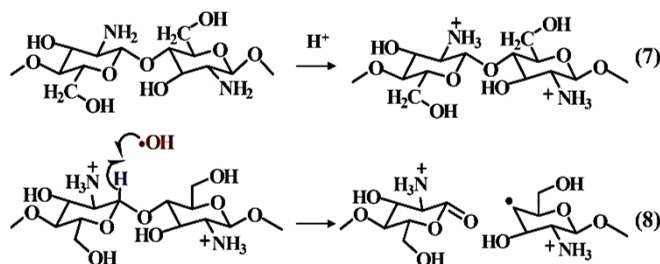


**Fig. 5 (A)**  $M_w$  of chitosan measured by GPC after 60 min of the SP treatment with the addition of various H<sub>2</sub>O<sub>2</sub> concentrations as a function of initial chitosan concentrations of 0.2% , 0.5% and 0.9% in 0.1 M CH<sub>3</sub>COOH. **(B)** Possible mechanism for the degradation of chitosan by applying the combination of the SP treatment and H<sub>2</sub>O<sub>2</sub>.

The degradation mechanism of chitosan by applying the SP treatment in combination with H<sub>2</sub>O<sub>2</sub> was proposed (**Fig. 5B**). In the reaction solution, there were four types of molecules including H<sub>2</sub>O, H<sub>2</sub>O<sub>2</sub>, CH<sub>3</sub>COOH and chitosan. The major component in the system was H<sub>2</sub>O molecules. When the plasma was discharged in the solution, excitation and ionization of H<sub>2</sub>O molecules occurred. Electrons, that were emitted as a result of ionization (*secondary electrons*) (**Fig. 5B (1)**), collided with the surrounding H<sub>2</sub>O

molecules. The ionization and excitation of H<sub>2</sub>O molecules can further produce more •OH (**Fig. 5B (2, 3)**) which is important for the degradation of chitosan (Kang et al., 2007; Qin, Du & Xiao, 2002). The addition of H<sub>2</sub>O<sub>2</sub> could promote the chitosan degradation because H<sub>2</sub>O<sub>2</sub> itself dissociates to form •OH as shown in **Fig. 5B (4–6)** (Chang, Tai & Cheng, 2001). This phenomenon helps to increase the •OH concentration in the system. The possible mechanism for the degradation of chitosan in the presence of •OH has been proposed. In general, amino groups of chitosan are protonated by H<sup>+</sup> dissociated from CH<sub>3</sub>COOH in water. The structure of chitosan in CH<sub>3</sub>COOH solution carries positive charge as displayed in **Fig. 5B (7)**. The •OH attacks at the C-1 carbon and transferred the radical to the C-1 carbon by subtracting the hydrogen from it, resulting in the breaking down of the chitosan chain at β-1,4 glycosidic linkage (Chang, Tai & Cheng, 2001; Tian et al., 2004). The scission of the β-1,4 glycosidic linkage causes the reduction of chitosan molecular weight (Kang et al., 2007). Besides, chitosan molecule itself can also possibly be collided by electron generated by the SP treatment, leading to the scission at β-1,4 glycosidic linkages.

The kinetics of degradation reaction were evaluated by a linear relationship of reversed molecular weight ( $1/M_w$ ) as a function of reaction time ( $t$ ), according to the previous reports (Chang, Tai & Cheng, 2001; Pornsunthorntawe et al., 2014; Wasikiewicz et al., 2005). The rate constant ( $k$ ) was calculated by the following equation:

$$1/M_t = (1/M_0) + (kt/M) = (1/M_0) + k't \quad (9)$$

where  $M_t$  is  $M_w$  of the sample at reaction time  $t$ ,  $M_0$  is the initial  $M_w$  of the sample,  $M$  is the molecular weight of the monomer,  $k$  (min<sup>-1</sup>) or  $k'$  (mol g<sup>-1</sup> min<sup>-1</sup>) is the rate constant, and  $t$  is the reaction time (min). The  $k$  values of chitosan degradation by the combination of SP treatment and H<sub>2</sub>O<sub>2</sub> were calculated and compared to other methods that have been reported in some previous works, as shown in **Table 1**. To the best of our knowledge it was found that according to the rate constants, the degradation rate of chitosan by the SP treatment in combination with the dilute concentration of H<sub>2</sub>O<sub>2</sub> at 60 mM was found to be faster than the degradation rate of chitosan by most physical methods reported in the literature.

The relationships between initial concentration of chitosan ( $c_0$ ) and  $k$  were also evaluated for the determination of the order of reaction,  $n$ . The relationship of  $k$  and  $c_0$  can be described as  $k \propto c_0^{-n}$ . For zeroth-order reaction ( $n = 0$ ),  $k$  is proportional to  $c_0^{-1}$ . For a first-order reaction ( $n = 1$ ),  $k$  is independent of  $c_0$ . For a second-order reaction ( $n = 2$ ),  $k$  is

proportional to  $c_0$  (Cai et al., 2011; Tayal, Kelly & Khan, 1999). The obtained  $k$  values were plotted against  $c_0$  and the initial concentration of  $H_2O_2$  as shown in supplementary data Fig. A3. The  $k$  values were inversely proportional to  $c_0$ , which implied the zeroth-order reaction. The result indicated that the increasing of chitosan concentration did not increase the number of bond cleavages in the polymer chains under the investigated condition. Similar kinetic behavior was observed for the degradation of chitosan by an electrochemical process (Cai et al., 2011). Furthermore, the  $k$  values were found to be proportional to the concentration of  $H_2O_2$ . The result suggested that the higher concentration of  $H_2O_2$  led to the better degradation of chitosan under the studied condition.

**Table 1** Comparison of rate constants obtained in this study with some previous works.

Methods	[chitosan], %(w/v)	[H <sub>2</sub> O <sub>2</sub> ], mM	$k \times 10^{-2}$ , min <sup>-1</sup>	Ref.
SP	0.2	4	7.20	This study
	0.5	4	2.46	
	0.9	4	0.54	
	0.5	8	3.70	
	0.5	16	8.05	
	0.5	30	14.49	
	0.5	45	19.64	
	0.5	60	19.96	
SP	1.0	–	4.83	(Prasertsung et al., 2012)
SP + Fe <sup>3+</sup> complex	0.5	–	8.83	(Pornsunthorntawee et al., 2014)
Heating at 80°C	0.5	447	0.71	(Chang et al., 2001)
γ-irradiation	5.0	420	7.95	(Hien et al., 2012)

### 3.2. Fractionation of chitooligosaccharides by adding ethanol/water mixture solution

The degraded chitosan was separated into various fractions having different molecular weights by precipitation using water–ethanol mixture solution. A degraded chitosan fraction with  $M_w$  of 12.03 kDa, which was assigned as COS1, could be precipitated by the mixture solution at the water-to-ethanol ratio of 1:1. The lower- $M_w$  degraded chitosan fraction with  $M_w$  of 4.92 kDa and 1.44 kDa, which were assigned as COS2 and COS3, were precipitated by the mixture solution having water-to-ethanol ratios of 1:3 and 1:5, respectively. The precipitated products were freeze-dried to determine the production yield and re-dissolved to evaluate their solubility in water. The production yield of COS1, which could rarely dissolve in water, was found to be 5% whereas those of COS2 and COS3 were 32% and 23%, respectively. COS2 could mostly dissolve in water, while COS3 was able to completely dissolve in water. More details were given in supplementary data (Table A1).

In this study, the completely water-soluble chitosan fraction, COS3, was used for evaluation of anticancer activity. Therefore, the mass of COS3 was further characterized by ESI-MS as shown in **Fig. 6A**. The COS3 having the degree of polymerization (DP) ranging from 2 to 9 was composed of fully deacetylated sequences as well as mono- and di-acetylated COS. The details on the assigned ion composition of ESI-MS spectra of COS exhibit in the supplementary data (see Fig. A4 and Table A2). The fully deacetylated sequences were dominant with percent abundance equal to 77%, while mono- and di-acetylated COS possessed percent abundance equal to 22% and 1%, respectively. The chemical structure of the COS3 product was also evaluated by  $^1\text{H}$ -NMR and liquid-state  $^{13}\text{C}$ -NMR as shown in **Fig. 6B**. Chemical structures of the monomeric units in COS3 were not altered from those of chitosan during the degradation and fractionation processes. In addition, the DD of COS3 was calculated to be 80%.

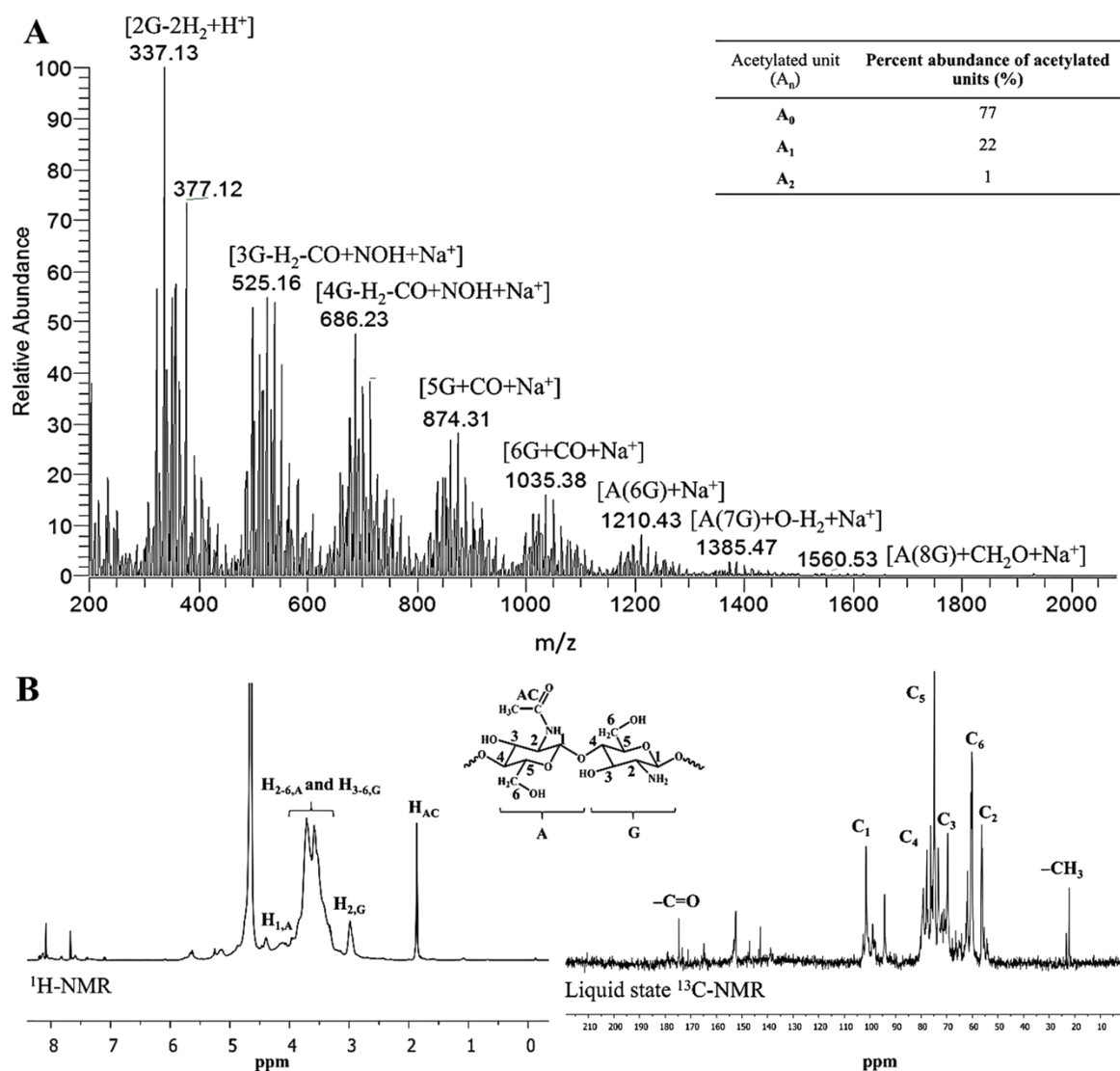


**Fig.6** (A) ESI-MS spectrum of 1.44-kDa chitosan fraction (COS3). “G” refers to D-glucosamine unit ( $m = 161.06$  Da), “A” refers to N-acetyl-D-glucosamine unit ( $m = 203.07$  Da) and “n” refers to the number of acetylated unit found in COS3. (B) <sup>1</sup>H-NMR and liquid-state <sup>13</sup>C-NMR spectra of 1.44-kDa chitosan fraction (COS3) obtained by precipitation using water-ethanol mixture solution at the ratio of water-to-ethanol of 1:5.

### 3.3. Evaluation of anticancer activity

To evaluate the inhibitory effect of COS3 having  $M_w$  of 1.44 kDa on the cell proliferation of HeLa cells, different concentrations of the COS3 ranging from 1 to 40  $\text{mg}\cdot\text{mL}^{-1}$  were added to the wells containing the cancer cells. **Fig. 7A** shows the morphology of HeLa cells before and after being treated with different concentrations of COS3. HeLa cells normally have rhomboid–tetrahedral shape as reported by Martínez-Ramos et al. (2005). After 24 h of the treatment, the wells without the addition of the COS3 exhibited the rapid increasing of the number of cells, while the cells that were



treated with the COS3 at a concentration of  $15 \text{ mg}\cdot\text{mL}^{-1}$  grew in a slower manner. The morphology of HeLa cells gradually changed with the increasing of COS3 concentrations and completely changed to abnormal shapes when the concentration of the COS3 reached  $40 \text{ mg}\cdot\text{mL}^{-1}$ . Furthermore, the percentage of cell viability was measured by comparing the values of absorbance at  $\lambda = 570 \text{ nm}$  of the COS3-treated cells and the control. As shown in **Fig. 7B**, the number of survival cells gradually decreased as the increasing of the loaded amounts of COS3. The COS3 concentration that inhibited 50% of the cell proliferation ( $IC_{50}$ ) was approximately  $13.5 \text{ mg}\cdot\text{mL}^{-1}$ . Moreover, the cell viability of normal cells (MRC-5 cells) was also examined by the corresponding concentration of COS3.  $IC_{50}$  for MRC-5 was approximately  $20.7 \text{ mg}\cdot\text{mL}^{-1}$ . A selectivity index ( $SI$ ), which is determined by the  $IC_{50}$  ratio of a compound tested against cancer cells and normal cells, refers to the differential cytotoxic activity of the tested compound against cancer and normal cells (Badisa et al., 2009). The  $SI$  of COS3 in this study was approximately 1.5 which indicated a slightly higher selectivity for cytotoxic activity against HeLa cells than MRC-5 cells. As a result, COS3, that was the chitooligosaccharide with the  $M_w$  of 1.44 kDa and DD of 80%, showed a potential to be an anticancer agent, even though the  $SI$  was not significantly higher than that of normal cell. Nevertheless, COS3 can be used as a starting material for further modification aiming for higher degree of cytotoxic selectivity for cancer cells. As one possible strategy, COS may be chemically modified by etherification with glycidyl trimethylammonium chloride (GTMAC) in order to obtain quaternized COS which become a stronger positively charged molecule and may exhibit a better selectivity to cancer cells over normal cells comparing to native COS (Huang et al., 2006). Therefore, the further chemical modification of COS3 is another step to acquire a potent anticancer agent with higher selectivity to cancer cells.

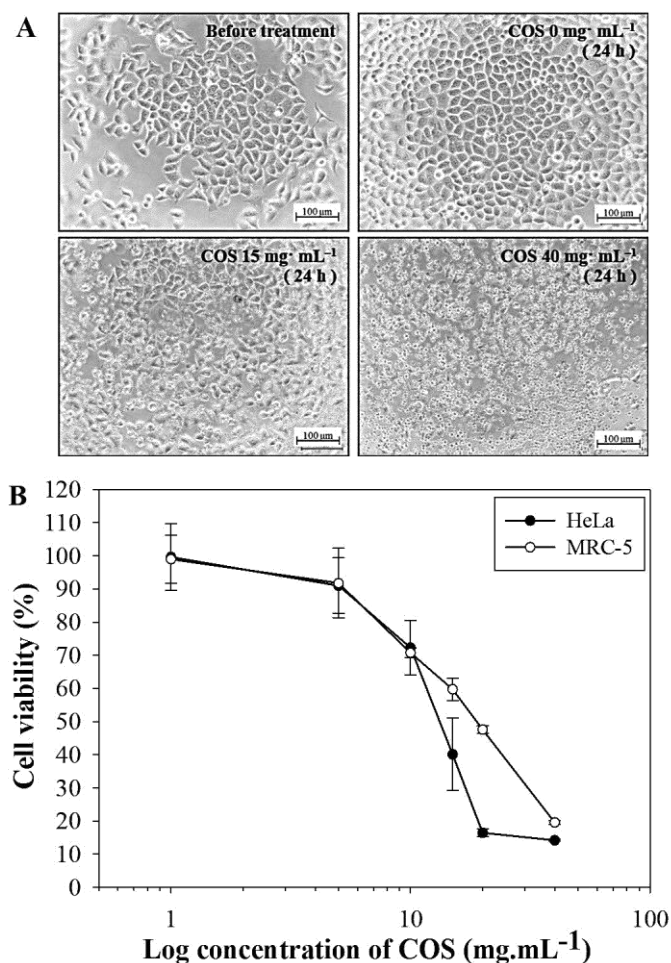


**Fig. 7 (A)** Microscopic images ( $\times 20$ ) of Hela cells before and after the treatment with COS3 having molecular weight of 1.44 kDa for 24 h and **(B)** the effect of concentrations of COS3 on cell viability of cancer cells (HeLa cells) and normal cells (MRC-5 cells), determined by the MTT assay. Values are mean  $\pm$  SD of 15 determinations from 5 separated experiments ( $n = 3$  for each experiment).

#### 4. Conclusion

The SP treatment alone could effectively reduce  $M_w$  of chitosan and could achieve as high as 86% of molecular weight reduction which was higher than that obtained by the conventional heat treatment for approximately 3 times under the corresponding condition. The combination of the SP treatment and  $H_2O_2$  resulted in much more reduction of molecular weight of chitosan without causing any changes to the chemical structure of the degraded products of chitosan. The SP treatment of chitosan solution in presence of a very low concentration of  $H_2O_2$  (60 mM) produced a high yield of the water-soluble chitosan that consisted of LMWC and COS. After fractionation of the degraded products of

chitosan, the COS having DP up to 9 could be produced with relatively high production yield of approximately 23% within 1 h. Moreover, the obtained COS showed the inhibitory effect on the proliferation of HeLa cancer cells. It might be concluded that the SP treatment is an effective tool for the production of water-soluble chitosan via the degradation reaction. Especially, when the SP treatment was used together with a small amount of the oxidizing agent like  $\text{H}_2\text{O}_2$ , a considerable yield of COS with DP up to 9 was generated at a comparable fast reaction rate. The combination of the SP treatment and  $\text{H}_2\text{O}_2$  is a promising green technology for a mass production of COS.

## **5. Acknowledgement**

CC would like to acknowledge the Thailand Research Fund (TRF) for providing her a Royal Golden Jubilee Ph.D. Scholarship (RGJ-Ph.D.: Grant number PHD/0179/2556). This work was financially supported by the Thailand Research Fund (TRF) under the contract number BRG5480008. The authors thank Surapon Foods Public Co., Ltd. (Thailand) for providing the shrimp shells and the NU-PPC Plasma Chemical Technology Laboratory at Chulalongkorn University (Thailand) for providing the use of solution plasma equipment. All facilities for biological tests were supported by Drug Discovery and Development center at Thammasat University (Thailand).

## References

- Allan, G. G., & Peyron, M. (1995). Molecular weight manipulation of chitosan I: kinetics of depolymerization by nitrous acid. *Carbohydrate Research*, 277(2), 257-272.
- Badisa, R. B., Darling-Reed, S. F., Joseph, P., Cooperwood, J. S., Latinwo, L. M., & Goodman, C. B. (2009). Selective cytotoxic activities of two novel synthetic drugs on human breast carcinoma MCF-7 cells. *Anticancer research*, 29(8), 2993-2996.
- Baroch, P., Anita, V., Saito, N., & Takai, O. (2008). Bipolar pulsed electrical discharge for decomposition of organic compounds in water. *Journal of Electrostatics*, 66(5-6), 294-299.
- Bratescu, M. A., Cho, S.-P., Takai, O., & Saito, N. (2011). Size-controlled gold nanoparticles synthesized in solution plasma. *The Journal of Physical Chemistry C*, 115(50), 24569-24576.
- Cabrera, J. C., & Van Cutsem, P. (2005). Preparation of chitooligosaccharides with degree of polymerization higher than 6 by acid or enzymatic degradation of chitosan. *Biochemical Engineering Journal*, 25(2), 165-172.
- Cai, Q., Gu, Z., Fu, T., Liu, Y., Song, H., & Li, F. (2011). Kinetic study of chitosan degradation by an electrochemical process. *Polymer bulletin*, 67(4), 571-582.
- Chang, K. L. B., Tai, M.-C., & Cheng, F.-H. (2001). Kinetics and products of the degradation of chitosan by hydrogen peroxide. *Journal of Agricultural and Food Chemistry*, 49(10), 4845-4851.
- Choi, W.-S., Ahn, K.-J., Lee, D.-W., Byun, M.-W., & Park, H.-J. (2002). Preparation of chitosan oligomers by irradiation. *Polymer Degradation and Stability*, 78(3), 533-538.
- De Laat, J., & Gallard, H. (1999). Catalytic decomposition of hydrogen peroxide by Fe (III) in homogeneous aqueous solution: mechanism and kinetic modeling. *Environmental Science & Technology*, 33(16), 2726-2732.
- El-Sawy, N. M., Abd El-Rehim, H. A., Elbarbary, A. M., & Hegazy, E.-S. A. (2010). Radiation-induced degradation of chitosan for possible use as a growth promoter in agricultural purposes. *Carbohydrate Polymers*, 79(3), 555-562.
- Harish Prashanth, K. V., & Tharanathan, R. N. (2005). Depolymerized products of chitosan as potent inhibitors of tumor-induced angiogenesis. *Biochimica et Biophysica Acta (BBA) - General Subjects*, 1722(1), 22-29.

- Harish Prashanth, K. V., & Tharanathan, R. N. (2007). Chitin/chitosan: modifications and their unlimited application potential—an overview. *Trends in Food Science & Technology*, 18(3), 117-131.
- Hien, N. Q., Phu, D. V., Duy, N. N., & Lan, N. T. K. (2012). Degradation of chitosan in solution by gamma irradiation in the presence of hydrogen peroxide. *Carbohydrate Polymers*, 87(1), 935-938.
- Hsu, S.-C., Don, T.-M., & Chiu, W.-Y. (2002). Free radical degradation of chitosan with potassium persulfate. *Polymer Degradation and Stability*, 75(1), 73-83.
- Huang, R., Mendis, E., Rajapakse, N., & Kim, S.-K. (2006). Strong electronic charge as an important factor for anticancer activity of chitooligosaccharides (COS). *Life Sciences*, 78(20), 2399-2408.
- Ifuku, S., Wada, M., Morimoto, M., & Saimoto, H. (2012). A short synthesis of highly soluble chemoselective chitosan derivatives via “click chemistry”. *Carbohydrate Polymers*, 90(2), 1182-1186.
- Ishizaki, T., Chiba, S., Kaneko, Y., & Panomsuwan, G. (2014). Electrocatalytic activity for the oxygen reduction reaction of oxygen-containing nanocarbon synthesized by solution plasma. *Journal of Materials Chemistry A*, 2(27), 10589-10598.
- Jin, S.-H., Kim, S.-M., Lee, S.-Y., & Kim, J.-W. (2014). Synthesis and characterization of silver nanoparticles using a solution plasma process. *Journal of Nanoscience and Nanotechnology*, 14(10), 8094-8097.
- Kang, B., Dai, Y.-D., Zhang, H.-Q., & Chen, D. (2007). Synergetic degradation of chitosan with gamma radiation and hydrogen peroxide. *Polymer Degradation and Stability*, 92(3), 359-362.
- Kasaai, M. R., Arul, J., Chin, S. L., & Charlet, G. (1999). The use of intense femtosecond laser pulses for the fragmentation of chitosan. *Journal of Photochemistry and Photobiology A: Chemistry*, 120(3), 201-205.
- Lee, M., Nah, J.-W., Kwon, Y., Koh, J.J., Ko, K.S., Kim, S.W. (2001). Water-Soluble and Low Molecular Weight Chitosan-Based Plasmid DNA Delivery. *Pharmaceutical Research*, 18(4), 427-431.
- Li, K., Xing, R., Liu, S., Qin, Y., Meng, X., & Li, P. (2012). Microwave-assisted degradation of chitosan for a possible use in inhibiting crop pathogenic fungi. *International Journal of Biological Macromolecules*, 51(5), 767-773.

- Lin, C.-W., & Lin, J.-C. (2003). Characterization and blood coagulation evaluation of the water-soluble chitooligosaccharides prepared by a facile fractionation Method. *Biomacromolecules*, 4(6), 1691-1697.
- Liu, X., Jiang, Y., He, H., & Ping, W. (2014). Hydrogen peroxide-induced degradation of type I collagen fibers of tilapia skin. *Food Structure*, 2(1–2), 41-48.
- Mao, S., Shuai, X., Unger, F., Simon, M., Bi, D., & Kissel, T. (2004). The depolymerization of chitosan: effects on physicochemical and biological properties. *International Journal of Pharmaceutics*, 281(1–2), 45-54.
- Martínez-Ramos, I., Maya-Mendoza, A., Gariglio, P., & Aranda-Anzaldo, A. (2005). A global but stable change in HeLa cell morphology induces reorganization of DNA structural loop domains within the cell nucleus. *Journal of Cellular Biochemistry*, 96(1), 79-88.
- Méndez-Díaz, J., Sánchez-Polo, M., Rivera-Utrilla, J., Canonica, S., & von Gunten, U. (2010). Advanced oxidation of the surfactant SDBS by means of hydroxyl and sulphate radicals. *Chemical Engineering Journal*, 163(3), 300-306.
- Moad, G., Dagley, I. J., Habsuda, J., Garvey, C. J., Li, G., Nichols, L., Simon, G. P., & Nobile, M. R. (2015). Aqueous hydrogen peroxide-induced degradation of polyolefins: A greener process for controlled-rheology polypropylene. *Polymer Degradation and Stability*, 117, 97-108.
- Mourya, V. K., Inamdar, N. N., & Choudhari, Y. M. (2011). Chitooligosaccharides: synthesis, characterization and applications. *Polymer Science Series A*, 53(7), 583-612.
- Ostrowska-Czubenko, J., & Gierszewska-Drużyńska, M. (2009). Effect of ionic crosslinking on the water state in hydrogel chitosan membranes. *Carbohydrate Polymers*, 77(3), 590-598.
- Panomsuwan, G., Saito, N., & Ishizaki, T. (2016). Electrocatalytic oxygen reduction on nitrogen-doped carbon nanoparticles derived from cyano-aromatic molecules via solution plasma process. *Carbon*, 98, 411-420.
- Pootawang, P., Saito, N., & Takai, O. (2011). Solution plasma for template removal in mesoporous silica: pH and discharge time varying characteristics. *Thin Solid Films*, 519(20), 7030-7035.
- Pornsunthorntawee, O., Katepetch, C., Vanichvattanadecha, C., Saito, N., & Rujiravanit, R. (2014). Depolymerization of chitosan–metal complexes via a solution plasma technique. *Carbohydrate Polymers*, 102, 504-512.

- Potocký, Š., Saito, N., & Takai, O. (2009). Needle electrode erosion in water plasma discharge. *Thin Solid Films*, 518(3), 918-923.
- Prasertsung, I., Damrongsakkul, S., & Saito, N. (2013). Degradation of  $\beta$ -chitosan by solution plasma process (SPP). *Polymer Degradation and Stability*, 98(10), 2089-2093.
- Prasertsung, I., Damrongsakkul, S., Terashima, C., Saito, N., & Takai, O. (2012). Preparation of low molecular weight chitosan using solution plasma system. *Carbohydrate Polymers*, 87(4), 2745-2749.
- Prashanth, K. V. H., & Tharanathan, R. N. (2006). Crosslinked chitosan—preparation and characterization. *Carbohydrate Research*, 341(1), 169-173.
- Qin, C., Li, H., Xiao, Q., Liu, Y., Zhu, J., & Du, Y. (2006). Water-solubility of chitosan and its antimicrobial activity. *Carbohydrate Polymers*, 63(3), 367-374.
- Qin, C. Q., Du, Y. M., & Xiao, L. (2002). Effect of hydrogen peroxide treatment on the molecular weight and structure of chitosan. *Polymer Degradation and Stability*, 76(2), 211-218.
- Sabnis, S., & Block, L. H. (1997). Improved infrared spectroscopic method for the analysis of degree of N-deacetylation of chitosan. *Polymer Bulletin*, 39(1), 67-71.
- Saito, N., Hieda, J., & Takai, O. (2009). Synthesis process of gold nanoparticles in solution plasma. *Thin Solid Films*, 518(3), 912-917.
- Sánchez, Á., Mengíbar, M., Rivera-Rodríguez, G., Moerchbacher, B., Acosta, N., & Heras, A. (2017). The effect of preparation processes on the physicochemical characteristics and antibacterial activity of chitooligosaccharides. *Carbohydrate Polymers*, 157, 251-257.
- Savitri, E., Juliastuti, S. R., Handaratri, A., Sumarno, & Roesyadi, A. (2014). Degradation of chitosan by sonication in very-low-concentration acetic acid. *Polymer Degradation and Stability*, 110, 344-352.
- Shao, J., Yang, Y., & Zhong, Q. (2003). Studies on preparation of oligoglucosamine by oxidative degradation under microwave irradiation. *Polymer Degradation and Stability*, 82(3), 395-398.
- Shen, C., Song, S., Zang, L., Kang, X., Wen, Y., Liu, W., & Fu, L. (2010). Efficient removal of dyes in water using chitosan microsphere supported cobalt (II) tetrasulfophthalocyanine with  $H_2O_2$ . *Journal of Hazardous Materials*, 177(1-3), 560-566.



- Shen, K.-T., Chen, M.-H., Chan, H.-Y., Jeng, J.-H., & Wang, Y.-J. (2009). Inhibitory effects of chitooligosaccharides on tumor growth and metastasis. *Food and Chemical Toxicology*, 47(8), 1864-1871.
- Tayal, A., Kelly, R. M., & Khan, S. A. (1999). Rheology and molecular weight changes during enzymatic degradation of a water-soluble polymer. *Macromolecules*, 32(2), 294-300.
- Tian, F., Liu, Y., Hu, K., & Zhao, B. (2004). Study of the depolymerization behavior of chitosan by hydrogen peroxide. *Carbohydrate Polymers*, 57(1), 31-37.
- Tømmeraas, K., Vårum, K. M., Christensen, B. E., & Smidsrød, O. (2001). Preparation and characterisation of oligosaccharides produced by nitrous acid depolymerisation of chitosans. *Carbohydrate Research*, 333(2), 137-144.
- Vårum, K. M., Ottøy, M. H., & Smidsrød, O. (2001). Acid hydrolysis of chitosans. *Carbohydrate Polymers*, 46(1), 89-98.
- Venkatadri, R., & Peters, R. W. (1993). Chemical oxidation technologies: ultraviolet light/hydrogen peroxide, Fenton's reagent, and titanium dioxide-assisted photocatalysis. *Hazardous Waste and Hazardous Materials*, 10(2), 107-149.
- Vigier, K. D. O., Benguerba, A., Barrault, J., & Jerome, F. (2012). Conversion of fructose and inulin to 5-hydroxymethylfurfural in sustainable betaine hydrochloride-based media. *Green Chemistry*, 14(2), 285-289.
- Wasikiewicz, J. M., Yoshii, F., Nagasawa, N., Wach, R. A., & Mitomo, H. (2005). Degradation of chitosan and sodium alginate by gamma radiation, sonochemical and ultraviolet methods. *Radiation Physics and Chemistry*, 73(5), 287-295.
- Watthanaphanit, A., & Saito, N. (2013). Effect of polymer concentration on the depolymerization of sodium alginate by the solution plasma process. *Polymer Degradation and Stability*, 98(5), 1072-1080.
- Xu, Q., Dou, J., Wei, P., Tan, C., Yun, X., Wu, Y., Bai, X., Ma, X., & Du, Y. (2008). Chitooligosaccharides induce apoptosis of human hepatocellular carcinoma cells via up-regulation of Bax. *Carbohydrate Polymers*, 71(4), 509-514.
- Yue, W., Yao, P., & Wei, Y. (2009). Influence of ultraviolet-irradiated oxygen on depolymerization of chitosan. *Polymer Degradation and Stability*, 94(5), 851-858.
- Zheng, L.-Y., & Zhu, J.-F. (2003). Study on antimicrobial activity of chitosan with different molecular weights. *Carbohydrate Polymers*, 54(4), 527-530.



# **Degradation of chitosan hydrogel dispersing in dilute carboxylic acids by solution plasma and evaluation of anticancer activity of degraded products**

Chayanaphat Chokradjaroen<sup>1</sup>, Ratana Rujiravanit<sup>1,2\*</sup>, Sewan Theeramunkong<sup>3</sup> and Nagahiro Saito<sup>4</sup>

<sup>1</sup>*The Petroleum and Petrochemical College, Chulalongkorn University, Bangkok 10330, Thailand*

<sup>2</sup>*Center of Excellence on Petrochemical and Materials Technology, Chulalongkorn University, Bangkok 10330, Thailand*

<sup>3</sup>*Faculty of Pharmacy, Thammasat University, Pathumthani 12120, Thailand*

<sup>4</sup>*Department of Materials, Physics and Energy Engineering, Graduate School of Engineering, Nagoya University, Nagoya, Japan*

\*E-mail: ratana.r@chula.ac.th

## **Abstract:**

Chitosan is a polysaccharide that has been extensively studied in the field of biomedicine, especially its water-soluble degraded products called “chitooligosaccharides (COS)”. In this study, the COS was produced by degradation of chitosan hydrogel dispersing in a dilute solution (i.e. 1.55 mM) of various kinds of carboxylic acids using non-thermal plasma technology called “solution plasma (SP)”. The degradation rates of chitosan were influenced by the types of carboxylic acids, depending on the interaction between chitosan and each carboxylic acid. After SP treatment, the water-soluble degraded products containing COS, could be easily separated from the water-insoluble residue of chitosan hydrogel by centrifugation. The production yields of the COS were mostly higher than 55%. Furthermore, the obtained COS products were evaluated for their inhibitory effect as well as selectivity against human lung cancer cells (H460) and human lung normal cells (MRC-5).

## 1. Introduction

Biopolymer is a polymer produced by living organisms such as an animal, plant, fungus and bacterium<sup>1, 2)</sup>. It contains monomeric units that are covalently bonded together to form polymeric chain structures. In general, there are four main types of biopolymers according to their monomeric units. The four main classes of biopolymers include polynucleotides (RNA and DNA), polypeptides, polysaccharides and other biopolymers such as natural rubber and lignin. Polynucleotides are consisting of nucleotide monomers, while polypeptides are the polymers of amino acids. Polysaccharides have monosaccharides as repeating units that linked together through glycosidic bonds<sup>3, 4)</sup>. For other biopolymers, natural rubber is a polymer of isoprene, and lignin is a network structure of phenolic polymer. Recently, polysaccharides have drawn much attention as an interest in the use of natural products is being devoted. Due to their biocompatibility and biodegradability, their uses for eco-commodities, food supplements, cosmetics, and especially biomedical application have been growing during the past decade<sup>5)</sup>. There are numerous types of polysaccharides which have different sources and types of monomeric unit. For example, cellulose, which is the most abundant polysaccharides found in plants, is composed of glucose units.  $\beta$ -glucan and starch also contain glucose as their monomeric unit.  $\beta$ -glucan can be found in fungal and certain bacterial cell walls whereas starch is the major component in cereal grains. Alginate and fucoidan exist in seaweed. Alginate is composed of mannuronic and guluronic acid units while fucoidan consists of L-fucose with sulfate ester groups. In addition, chitin, that has two monomeric units of D-glucosamine and N-acetyl-D-glucosamine, is found in shells of crustacean, cuticle of insect and cell wall of fungi. Moreover, numerous studies have been reported on the diverse biological properties of polysaccharides, which depend on their molecular weight

(MW) as shown in **Table I**, including anti-inflammatory, antimutagenic, antioxidative, immune regulatory, anti-HIV, anticoagulant and antitumor/cancer.

**Table I** Polysaccharides and their biological properties

Polysaccharides	MW (kDa)	Biological actions	Ref.
$\beta$ -glucan from <i>Saccharomyces cerevisiae</i>	-	Increasing of interferon- $\gamma$ and nitric oxide level leading to a resistance to primary influenza virus	6)
$\beta$ -glucan from <i>Flammulina velutipes</i>	28, 268	Anticancer activity against cancer cells including A549 and BGC-823 cells	7)
$\beta$ -glucan from barley	-	Desmutagenic and bio-antimutagenic activity	8)
Fucoidan from <i>Lessonia vadosa</i>	320, 32	Higher anticoagulant activity as increasing of MW	9)
Porphyran from <i>Porphyra haitanensis</i>	30, 7, 6	Higher antioxidant activities as decreasing of MW	10)
Sodium alginate	250–320	Inhibition of pancreatic lipase as potential treatment for obesity	11)
Alginate	0.35–0.75	Inhibition of lipid oxidation	12)
Alginate from <i>Sargassum fusiforme</i>	-	<i>In vitro</i> anti-tumor activity against Bel7402 and SMMC7721 cells	13)
Fuccoidan	-	Inhibition of colony formation of SK-MEL-28 and DLD-1 cancer cells	14)
Chitosan (Chitin derivative)	1–3	Inhibition of protein oxidation	15)
Chitin	0.2–0.6	Inhibition of myeloperoxidase (MPO) activity in human myeloid cells	16)
Chitosan	1–22	Antibacterial effects for gram- negative	17)

(Chitin derivative)		bacteria	
Chitosan	< 5	Increment of calcium absorption	18)
(Chitin derivative)			
D-glucan from <i>Strongylocentrotus nudus</i> eggs		Inhibition of H22 tumor growth by enhancing the host	19)

---

Chitosan is a polysaccharide which attracts much interest from both academic and industrial sections. Chitosan is a chitin derivative which contains D-glucosamine as major monomeric units randomly connected with N-acetyl-D-glucosamine units by  $\beta$ -(1 $\rightarrow$ 4) linkages<sup>20)</sup>. Their chemical structures are shown in **Fig. 1**. Chitosan consists of several reactive functional groups including hydroxyl groups at the C3 and C6 positions and an amino or acetamido group at the C2 position<sup>21)</sup>. These amino groups causing positively charged character of chitosan are the main reason that makes chitosan different from other polysaccharides which have neutral or negatively charged character. The positively charged nature of chitosan correlates to its metal chelation, flocculation, as well as biological properties<sup>21)</sup>. Therefore, chitosan has been investigated in several applications, especially in biomedical field such as drug and gene delivery<sup>22, 23)</sup>, tissue engineering (scaffolds)<sup>24)</sup>, wound dressings<sup>25, 26)</sup> and biosensors<sup>27)</sup>.

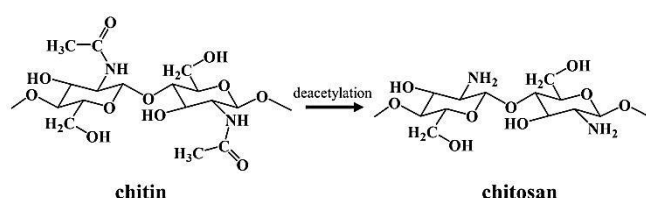


**Fig. 1** Chemical structures of chitin and chitosan.

Unfortunately, native chitosan generally has high molecular weight together with intense intra- and intermolecular hydrogen bonds due to the abundance of hydroxyl groups, resulting in its insolubility in water and poor solubility in most organic solvents<sup>28)</sup>. Thereafter, many studies relating to chitosan have focused on a soluble form of chitosan like chitooligosaccharides (COS) which, moreover, broadens the biological properties of chitosan. Biological properties of both chitosan and COS according to previous studies are summarized in **Table II**.

**Table II** Biological properties of chitosan and chitooligosaccharide (COS)

Biological properties	MW (kDa)	Possible actions	Ref.
Antioxidant activity and free radical scavenger	2.1	Inhibition of linoleic acid peroxidation.	<sup>29)</sup>
	1–3	Scavenging effect on hydroxyl radical, superoxide radical, alkyl radical, and 1,1-diphenyl-2-picrylhydrazyl (DPPH) radical.	<sup>30)</sup>
Antiallergy activity	1–3	Inhibitory effects on degranulation and cytokine generation of mast cells, RBL-2H3 cells.	<sup>31)</sup>
Antitumor and anticancer activity	1.3	Antitumor activity on sarcoma 180 (S180) tumor cells in the mice.	<sup>32)</sup>
	1.3	Higher inhibitory effect on the growth of Ehrlich ascites tumor (EAT) cells than low molecular weight chitosan with MW of ~ 37 kDa.	<sup>33)</sup>
Antimicrobial activity	28–1671	Antibacterial effects for gram-positive bacteria.	<sup>17)</sup>
	1–22	Antibacterial activity for gram-negative bacteria.	
Calcium absorption	< 5	Inhibition of the formation of insoluble calcium salts leading to higher absorption.	<sup>18)</sup>

Hypocholesterolemic effect	High	Reduction of plasma triglyceride, total cholesterol and low-density-lipoprotein cholesterol levels.	34)
Anti-inflammatory	5–10	Anti-inflammatory effect due to the inhibition activity of lipopolysaccharides-stimulated production of PGE2, TNF- $\alpha$ and IL-6, as well as the expression of iNOS, COX-2, TNF-a, and IL-6.	35)

Cancer is one of the major causes of death worldwide<sup>36)</sup>. The current treatment of cancer, such as radiation therapy and chemotherapy, still causes high risks of harming normal cells and lead to long-term and short-term side effects to patients<sup>37, 38)</sup>. Therefore, many researchers have made an attempt to find new ways of cancer treatment with minimizing a negative effect to healthy cells such as using natural products. The COS is one of the natural products that have been widely studied and showed the potential as an alternative choice for the treatment of cancer. **Table III** reveals the examples relating to the anticancer activity of COS.

**Table III** Chitooligosaccharides (COS) with anticancer activities

Samples	MW (kDa)	Cell lines	Possible actions	Ref.
COS	1	HL-60	Induction of apoptosis	39)
Modified COS	6–7	HeLa, Hep3B, SW480	Inhibition of cell growth by inducing necrosis	40)
COS	1.3	HeLa	Inhibition of cell growth	41)
COS	1.5–5.5	S180	Inhibition of the growth of solid tumor	42)
COS and glucosamine	0.16–0.8	HepG2, HeLa	Anti-proliferation of the cell	43)

The COS can be prepared by degradation of chitosan. The degradation has been used to produce low-molecular-weight products of not only chitosan but also other polysaccharides leading to the improvement of water solubility and bioabsorbability in order to exert the biological effects. In general, there are three main methods applied for the degradation of chitosan including chemical degradation<sup>44-46)</sup>, enzymatic degradation<sup>47-49)</sup> and physical degradation<sup>50, 51)</sup>. Degradation by using strong chemicals has been widely used in industrial scale, but the use of high amount of chemicals leads to difficulty to handle the generated wastes and may cause environmental pollution<sup>52)</sup>. Using enzymes to degrade chitosan draws much attention, because it was found to be able to region-selectively degrade chitosan under mild condition<sup>53)</sup>. However, high-quality enzymes and operating setup are expensive, while the production yield has been reported to be relatively low<sup>20)</sup>. Recently, physical methods by applying energy impact, such as microwave<sup>54-57)</sup>, ultraviolet<sup>58)</sup>, ultra-sonication<sup>59, 60)</sup>, gamma-ray<sup>50)</sup> and plasma<sup>61)</sup>, have been extensively studied, because they can enhance the degradation of chitosan with low chemical required.

Non-thermal plasma discharge under liquid phase, so called “solution plasma (SP)”, is one of energy-impact methods that has been recently utilized as a tool for the degradation of polysaccharides such as chitosan<sup>52, 62, 63)</sup> and alginate<sup>64)</sup>. The term SP was proposed by Takai<sup>65)</sup>. In the early researches, SP was used for the synthesis of noble metal nanoparticles<sup>66, 67)</sup> and the decomposition of organic compounds in water treatment<sup>68)</sup>. SP has an ability to produce highly active species such as hydroxyl radical ( $\bullet\text{OH}$ ), hydroperoxyl radical ( $\bullet\text{HO}_2$ ), free electron ( $e^-$ ), superoxide anion ( $\text{O}_2^-$ ), and atomic oxygen anion ( $\text{O}^-$ ) under atmospheric pressure and room temperature<sup>52, 69)</sup>. These radicals play an important role in the enhancement of the degradation of polymers. For instance, in the degradation of chitosan to produce the high-valued product of COS by the SP treatment, it

has been reported that the plasma-induced  $\bullet\text{OH}$  attacked the chitosan chain and caused the scission at a glycosidic bond<sup>52)</sup>. Moreover, the SP treatment could significantly provide high rate of degradation which was one order of magnitude higher than the conventional heating method for the corresponding chitosan solution<sup>52)</sup>.

Since COS is a high-valued natural product possessing potential anticancer activity, its production processes, including not only degradation process but also separation and purification, are highly concerned. Currently, the production of COS still uses a lot of chemicals and needs complicated separation and purification systems. For example, it has been reported that the degradation of chitosan by 35% HCl was effectively conducted within 30 mins to produce COS with degree of polymerization (DP) of 8, but owing to the use of strong acid, the further neutralization by NaOH as well as the separation and purification to remove contaminants were required<sup>48)</sup>. Even though, the physical methods such as microwave and SP treatment have been claimed as the green degradation methods of chitosan, chitosan still have to be dissolved in acetic acid solution with concentration of approximately 1–2 M in order to obtain chitosan solution prior to the degradation<sup>41, 52, 55, 62, 63)</sup>. Degradation of chitosan solution usually lead to some difficulty of separating COS from the high-molecular-weight chitosan. It is because they are dissolved together in the solution. Therefore, the heterogeneous degradation of chitosan in an undissolved form, like chitosan hydrogel, probably lead to ease of separation of the COS products from the high-molecular-weight chitosan. Hydrogel is generally defined as a hydrophilic polymer with capability of holding a large amount of water within its three-dimensional network structure<sup>70)</sup>. In this study, COS was produced by applying plasma technology in order to reduce the chemical used in the degradation reaction. Furthermore, simple separation and purification processes to attain COS could be accomplished by conducting a heterogeneous degradation of chitosan hydrogel dispersing in dilute acid solution. The chitosan hydrogel



was prepared by the re-precipitation method which resulted in the reduction of crystallinity of chitosan<sup>71</sup>). Moreover, various carboxylic acids were added to the suspension of chitosan hydrogel in order to examine the influences of distinct carboxylic acids, other than acetic acids, which have never been reported before on degradation of chitosan. Finally, the obtained COS products were evaluated for their anticancer activity as well as selectivity against cancer and normal cells.

## 2. Experimental methods

### 2.1 Materials

Chitosan was obtained from the deacetylation of chitin which was prepared from the shells of *Metapenaeus dobsoni* shrimp, provided by Surapon Foods Public Co., Ltd. (Thailand). Glacial acetic acid ( $\text{CH}_3\text{COOH}$ , 99.9%), hydrochloric acid ( $\text{HCl}$ , 37.0%), sodium chloride ( $\text{NaCl}$ , 99.0%) and sodium hydroxide ( $\text{NaOH}$ , 97.0%) pellets were purchased from RCI Labscan Ltd. (Thailand). A 50% (w/v)  $\text{NaOH}$  solution was supplied by the Chemical Enterprise Co., Ltd. (Thailand). Oxalic acid dihydrate ( $(\text{COOH})_2 \cdot 2\text{H}_2\text{O}$ , 98.0%) and succinic acid ( $\text{C}_2\text{H}_4(\text{COOH})_2$ , 99.5%) were purchased from Ajax Finechem Pty Ltd. (USA). Malonic acid ( $\text{CH}_2(\text{COOH})_2$ , 99.0%) glutaric acid ( $\text{C}_3\text{H}_6(\text{COOH})_2$ , 99.0%), adipic acid ( $\text{C}_4\text{H}_8(\text{COOH})_2$ , 99.0%), pimelic acid ( $\text{C}_5\text{H}_{10}(\text{COOH})_2$ , 98.0%) and azelaic acid ( $\text{C}_7\text{H}_{14}(\text{COOH})_2$ , 98.0%) were supplied by Sigma-Aldrich (USA). Critic acid ( $\text{C}_3\text{H}_5\text{O}(\text{COOH})_3$ , 99.5–102.0%) was purchased from Loba Chemie Pvt. Ltd. (India). Sodium borohydride ( $\text{NaBH}_4$ ) and potassium bromide ( $\text{KBr}$ ) were obtained from Carlo Erba Reagenti (Italy) and Wako (Japan), respectively.

### 2.2. Preparation of chitosan hydrogel from the shrimp shell

*Metapenaeus dobsoni* shrimp shells were washed and dried under sunlight before grinding into small flakes. The flakes of dried shrimp shell were demineralized by soaking

in a 1 M HCl solution for 24 h. The demineralization step to remove calcium carbonate in shrimp shells was repeated by adding a fresh 1 M HCl solution and soaking for another 24 h before the flakes were removed and washed with distilled water until neutral. Subsequently, the demineralized shrimp shell flakes were deproteinized by immersing in a 4% (w/v) NaOH solution at 80 °C with well-stirring for 4 h. The flakes were filtrated and washed with distilled water until the eluent reached a pH of 7.0. Then the deproteinized product, known as chitin, was obtained. A 50% (w/v) NaOH solution containing 0.5% (w/v) NaBH<sub>4</sub> was added into the chitin flakes before the suspension was heated in an autoclave at 110 °C for 75 min. After filtration, the solid fraction from the deacetylation process was washed with distilled water until pH became neutral. The deacetylation process was repeated twice to achieve a required value of degree of deacetylation (%DD) of chitosan (i.e., 90%), which was calculated by using an equation of Sabnis and Block <sup>72</sup>). A solid-to-liquid ratio used in the above-mentioned processes was 1:10. After washing in each process, water in the product was removed by drying in an oven at 60 °C before continuing to further steps or usages.

Chitosan solution was prepared by dissolving chitosan flake (2 g) into 200 ml of 2% (v/v) acetic acid solution. The obtained chitosan solution was then poured dropwise into 400 mL of 5% (w/v) NaOH solution with vigorous stirring <sup>71</sup>). The gel-like precipitate was dialyzed against distilled water in a dialysis tube with a molecular weight cut off of 12,132 Da (Sigma-Aldrich, USA) until neutral to attain chitosan hydrogel.

### **2.3. Degradation of chitosan hydrogel**

A suspension of chitosan hydrogel for degradation by the SP treatment was prepared by adding 6 g of chitosan hydrogel (having dry weight of ~0.2 g) to the SP reactor and then 50 ml of dilute acid solution was added into the suspension with an acid-to-chitosan molar ratio of 1:8 or equivalent to 1.55 mM. The suspension was stirred at room temperature (30

°C) for 5 min. The SP reactor was made of a glass beaker having two tungsten electrodes (purity 99.9%, Nilaco Corp., Japan) with a diameter of 1 mm inserted in it. The SP system used in this study has been described in previous works<sup>63, 65, 69)</sup> and is schematically shown in **Fig. 2**. The operating parameters including voltage, pulse frequency, pulse width, and electrode distance were 1.6 kV, 23 kHz, 2  $\mu$ s, and 0.75 mm, respectively. The reaction temperature during the plasma treatment was approximately 60–80 °C.

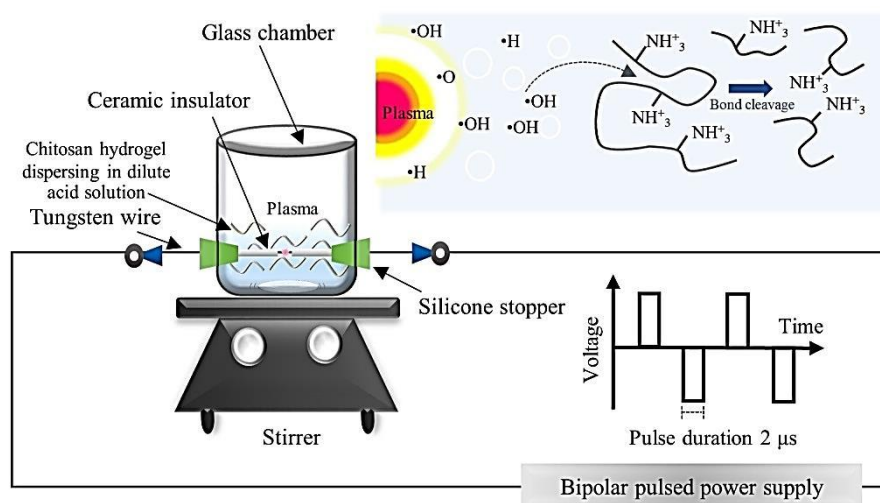


**Fig. 2** Schematic diagram of solution plasma (SP) setup.

#### 2.4. Separation of water-soluble degraded products

After the degradation of chitosan hydrogel by the SP treatment, the suspension was centrifuged to collect the remaining solid residue assigned as “solid fraction”, which was water-insoluble chitosan that was then dried in an oven at 60 °C. The supernatant was further freeze-dried and assigned as “solution fraction” which should contain water-soluble COS. All fractions were weighed and the percentage of yield of each fraction was calculated using the following equation:

$$\text{Yield (\%)} = W_i/W_0 \times 100 \quad (1)$$

where  $W_0$  is the initial dry weight of chitosan in the system and  $W_i$  is the dry weight of the degraded chitosan fraction while  $i$  refers to either solid fraction or solution fraction.

## 2.5. Characterization

The crystallinity of native chitosan and chitosan hydrogel before and after the SP treatment were characterized by using a wide angle X-ray diffraction (WAXD) analyzer (SmartLab, Rigaku, Japan) operated in a continuous mode with a scan speed of  $5^{\circ} \text{ min}^{-1}$  and scattering angle ( $2\theta$ ) from  $5^{\circ}$  to  $60^{\circ}$ , using  $\text{Cu K}\alpha$  as an X-ray source.

Morphology of chitosan flake and dried chitosan hydrogel were examined by using field emission scanning electron microscope (FE-SEM) (JEOL-JSM-7610F, JOEL Ltd, Japan).

The changes in the average molecular weight and the molecular weight distribution of chitosan during the degradation via the SP treatment were determined by gel permeation chromatography (GPC) (CTO-10A, Shimadzu, Japan) equipped with a refractive index (RI) detector. The ultrahydrogel linear column (Water 600E, Waters, USA) for separation of molecular weight in the range of  $1.0 \times 10^3 - 2.0 \times 10^7$  Da was connected in series with a guard column equipped in an oven at the operating temperature of  $40^{\circ} \text{C}$ . The mobile phase was a 0.5 M acetate buffer solution at pH 4.0 and the flow rate was set at  $0.6 \text{ mL} \cdot \text{min}^{-1}$ . The injection volume of a sample was  $40 \text{ }\mu\text{L}$  comprising of  $3 \text{ mg} \cdot \text{mL}^{-1}$  chitosan in the acetate buffer solution. Pullulans with molecular weight in the range of  $2.17 \times 10^3$  to  $8.05 \times 10^5$  Da were used as standard samples.

The investigation on any changes in the chemical structures of chitosan after the degradation via the SP treatment was carried out by using Fourier transform infrared (FT-IR) spectrometer (Nicolet iS5, Thermo Fisher Scientific, USA). FT-IR spectra with wavenumber from  $4000$  to  $400 \text{ cm}^{-1}$  was taken on KBr pellets at a resolution of  $4 \text{ cm}^{-1}$  using 64 scans with the correction for atmospheric carbon dioxide ( $\text{CO}_2$ ).

## 2.7 Biological Assay

### 2.7.1 Cell culture

H460 cells (Human lung cancer cell line) and MRC-5 cells (Human lung normal cell line) were cultured by using Roswell Park Memorial Institute (RPMI) 1640 Medium with L-glutamine (Biowest, France), and Eagle's Minimum Essential Medium (EMEM) with sodium bicarbonate, non-essential amino acids, L-glutamine, and sodium pyruvate (Corning Inc., USA), respectively. Before the cell cultivation, both media were supplemented with 10% fetal bovine serum (Biowest, France), 100 U·mL<sup>-1</sup> penicillin and 100 µg·mL<sup>-1</sup> streptomycin (Gibco, Life Technologies Inc., USA). The cells were incubated in a 5% CO<sub>2</sub> humidified incubator at 37 °C.

### 2.7.2 Cytotoxicity assay

A test on *in vitro* cytotoxicity of the chitosan sample was performed by MTT assay against both cancer and normal cells. Firstly, cells were seeded into 96-well microliter plates (1x10<sup>4</sup> cells/well) and incubated in a 5% CO<sub>2</sub> humidified incubator at 37 °C for 24 h. After that, different concentrations of chitosan samples, diluted with sterile water, were added into the wells to make the desired final concentration (0.1 to 5 mg·mL<sup>-1</sup>) and further incubated in an incubator at 37 °C and 5% CO<sub>2</sub>. After 24-h incubation, medium was discarded and replaced with PBS (phosphate buffer saline) solution containing 0.05% w/v of MTT (3-(4,5-dimethylthiazol -2-yl)-2,5-diphenyltetrazolium bromide) solution with further incubation for 3 h. Then the solution was discarded and DMSO was added to dissolve the formed formazan crystals and the absorbance (A) of each well was measured at 570 nm using a microplate reader (Varioskan™ Flash Multimode Reader, Thermo Fisher Scientific, USA). The cell viability was calculated according to the following equation:

$$\text{Cell viability (\%)} = 100 \times |(A_{\text{treated}} - A_{\text{blank}}) / (A_{\text{untreated}} - A_{\text{blank}})| \quad (2)$$

The percentage of cell viability was plotted versus the concentration of the COS sample to determine the mean growth-inhibitory concentration ( $IC_{50}$ ) value. All experiments were repeated for five times. Doxorubicin was used as positive control.

### 3. Results and discussion

#### 3.1 Degradation of chitosan hydrogel

A comparison on morphology of native chitosan flake and freeze-dried chitosan hydrogel was investigated by using FE-SEM and the SEM images are shown in **Fig. 3 (a)**. The SEM image revealed that chitosan flake was composed of well-packed multi-layered sheets. After dissolving chitosan flake in the acetic acid solution, followed by re-precipitating in the NaOH solution to form chitosan hydrogel, intra- and intermolecular hydrogen bonding interactions within the structure of native chitosan were disrupted during dissolution and the regeneration of chitosan hydrogel resulted in the loss of the former well-packed multi-layered structure, leading to the more amorphous region in chitosan hydrogel compared with native chitosan <sup>73)</sup>.

Moreover, the change in crystalline structure of native chitosan and chitosan hydrogel was examined by WAXD analysis, as shown in **Fig 3 (b)**. The WAXD spectrum of native chitosan showed that the main characteristic peaks of native chitosan appeared at  $2\theta = 9.8^\circ$  and  $19.9^\circ$ . As reported in the previous works <sup>74, 75)</sup>, the reflection of  $2\theta$  at around  $9 - 10.5^\circ$  indicated that chitosan had a hydrate polymorph. In the hydrate tendon crystal, the chain conformation appeared as a 2-fold helix stabilized by hydrogen bonds (O3---O5) with the orientation of O6. The hydrogen bonds also occurred between adjacent chains (via N2---O6) to form a sheet structure. These sheets stacked together in a parallel fashion. There were water molecules that bounded between these sheets as water-bridges, resulting in the stabilization of sheet structure<sup>75)</sup>. Upon the transformation of native chitosan to hydrogel, the crystalline structure in native chitosan was changed. The WAXD result of chitosan

hydrogel exhibited obviously broader peaks at  $2\theta = 9.8^\circ$ . The characteristic peak at  $2\theta = 19.9^\circ$  disappeared, while two new broad peaks at  $2\theta = 28.1^\circ$  and  $35.0^\circ$  could be observed. The WAXD result suggested that the crystalline structure of native chitosan was destroyed. The peaks of  $2\theta$  at  $28.1^\circ$  and  $35.0^\circ$  indicated the formation of chitosan acetate salt as reported by Modrzejewska et al.<sup>76)</sup>. According to these evidences, the chitosan hydrogel had lower crystallinity compared with native chitosan and should be more susceptible to degradation by the SP treatment.

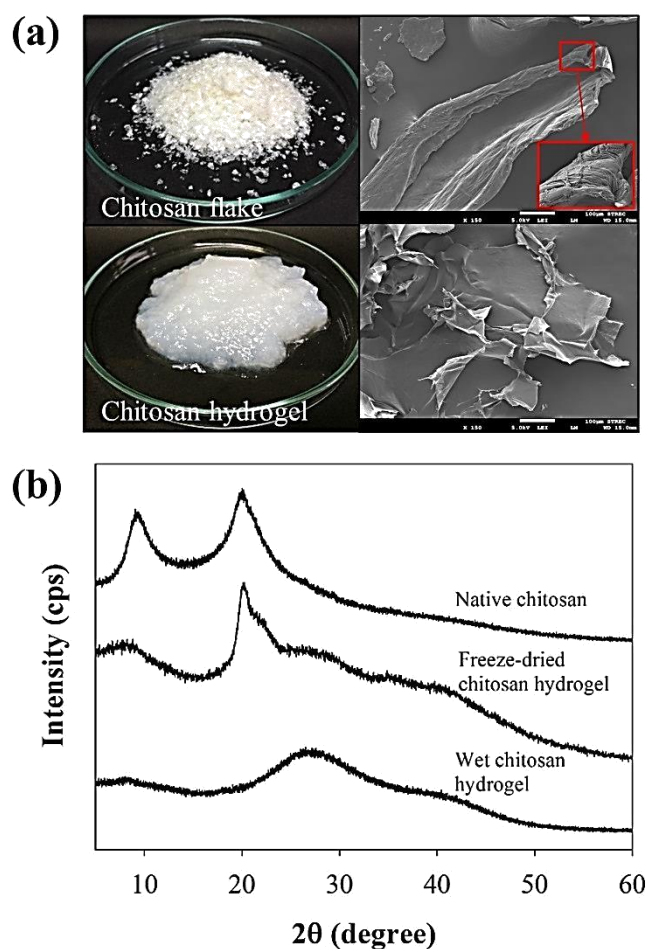


**Fig. 3** (a) FE-SEM images and (b) WAXD spectra of native chitosan, freeze-fried and wet chitosan hydrogel samples.

The degradation of chitosan hydrogel dispersing in the dilute acetic acid by applying the SP treatment and the conventional heat treatment were conducted under corresponding conditions. The chitosan hydrogel was found to disperse well in the dilute acetic acid

solutions. It was found that the weight-average molecular weight ( $M_w$ ) of chitosan hydrogel after SP treatment dramatically decreased, while the reduction of  $M_w$  of chitosan hydrogel by the conventional heating treatment slightly occurred, as shown in **Table IV**. Furthermore, when the degradation of chitosan hydrogel dispersing in the dilute acetic acid by the SP treatment was performed in comparison with the degradation of chitosan solution dissolved in 1 M acetic acid by SP treatment, which have been studied in some previous works<sup>52, 62, 63</sup>). It was found that the  $M_w$  of both types of chitosan samples were greatly reduced after the SP treatment. From GPC measurement, the degradation of chitosan hydrogel dispersing in the dilute acetic acid by applying the SP treatment for 60 min could reduce the  $M_w$  of chitosan for approximately 98%. On the other hand, the  $M_w$  of chitosan in the chitosan solution was decreased for 95% under the corresponding condition. Therefore, it might be concluded that chitosan hydrogel dispersing in the dilute acetic acid was readily degraded by the SP treatment. Moreover, it also indicated that the SP treatment is an effective tool for promoting the degradation of chitosan to produce chitooligosaccharides (COS), even though only a dilute organic acid solution presents in the reaction.

**Table IV** Weight-average molecular weight ( $M_w$ ) and polydispersity index (PDI) of chitosan solution at a concentration of 0.2% dissolving in 1 and 2 M acetic acid solutions and chitosan hydrogel at a solid content of 0.2% (dry weight) dispersing in 1.55 mM acetic acid solution after the degradation via conventional heat treatment and SP treatment at different reaction time intervals, according to the results in this study in comparison with the previous works

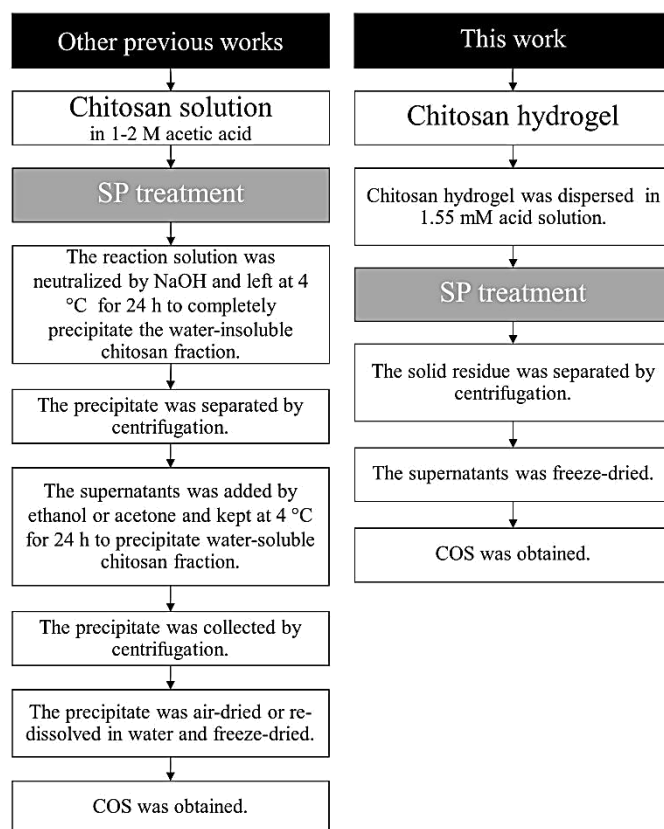


SP treatment time	Weight-average molecular weight (Da)/PDI				
	Heat 75 °C		SP		
	Chitosan hydrogel in 1.55 mM acetic acid solutions	Chitosan in 1 M acetic acid	Chitosan in 2 M acetic acid <sup>a</sup>	Chitosan in 1 M acetic acid <sup>b</sup>	
0 min	4.4×10 <sup>5</sup> (2.35)	4.4×10 <sup>5</sup> (2.35)	4.4×10 <sup>5</sup> (2.35)	1.1×10 <sup>6</sup> (4.10)	2.1×10 <sup>5</sup> (4.10)
15 min	-	7.3×10 <sup>4</sup> (4.20)	-	4.3×10 <sup>5</sup> (5.40)	-
30 min	4.2×10 <sup>5</sup> (4.35)	2.2×10 <sup>4</sup> (3.35)	1.1×10 <sup>5</sup> (5.21)	2.0×10 <sup>5</sup> (5.30)	6.2×10 <sup>4</sup> (2.70)
45 min	-	1.1×10 <sup>4</sup> (2.74)	-	-	-
60 min	4.0×10 <sup>5</sup> (4.24)	6.6×10 <sup>3</sup> (2.35)	2.1×10 <sup>4</sup> (5.42)	1.0×10 <sup>5</sup> (2.35)	5.6×10 <sup>4</sup> (2.70)

Note: <sup>a</sup>Pornsunthorntawee et al.<sup>52)</sup>, <sup>b</sup>Prasertsung et al.<sup>63)</sup>

**Figure 4** shows the flow charts for a comparison on the experimental procedures for degradation of chitosan solution and chitosan hydrogel to produce COS by SP treatment employed in this study and other previous works<sup>41, 52)</sup>. At a high concentration of acetic acid (pH ≈ 4.0), chitosan can dissolve well, because most NH<sub>2</sub> groups at the C2 position in the structure of chitosan are protonated by protons from dissociation of acetic acid and become soluble under an acidic environment<sup>59)</sup>. However, at a very low concentration (pH

≈ 6.5) of acetic acid, only a small number of  $\text{NH}_2$  groups in chitosan will be protonated due to the lack of protons and; consequently, the chitosan hydrogel still remain as a suspension in the dilute acetic acid solution. Accordingly, the water-soluble degraded product of COS that obtained from the SP treatment of the chitosan hydrogel dispersing in the dilute acetic acid could be easily separated from the remaining solid fractions by using simple centrifugation. The COS dissolving in the solution was collected as a supernatant, while the solid fraction that contained a water-insoluble, high-molecular-weight chitosan was separated as a precipitate after centrifugation. On the other hand, the degraded product from the degradation of the chitosan solution in the presence of high concentration of acetic acid by the SP treatment required the neutralization by using NaOH in order to separate the water-insoluble, high-molecular-weight chitosan from the water-soluble, low-molecular-weight product that contained COS. Furthermore, the addition of a non-solvent like ethanol and acetone was necessary for separation of the COS products from the solution as precipitate. According to the flow charts in Figure 4, the production of COS from chitosan hydrogel was more simple and less time-consuming than that obtained from chitosan solution.

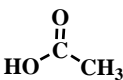
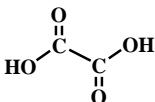
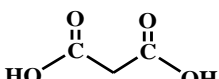
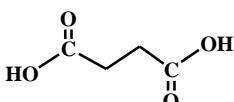
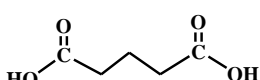
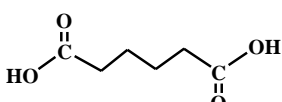


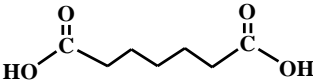
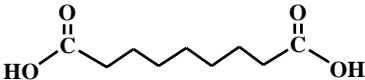
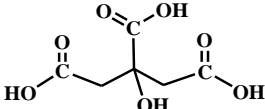
**Fig. 4 A comparison on the experimental procedures for degradation of chitosan solution and chitosan hydrogel to produce COS by SP treatment.**

In addition to acetic acid, various types of other carboxylic acids, as shown in **Table V**, were also used to disperse chitosan hydrogel in order to study their influence on the degradation of chitosan hydrogel by applying the SP treatment. According to GPC analysis, the results on molecular weight reduction as a function of the SP treatment time were shown in **Table VI**. The  $M_w$  of the original chitosan hydrogel before the SP treatment was  $4.4 \times 10^5$  Da. The  $M_w$  was found to reduce for all types of carboxylic acids with the increasing of the SP treatment time. For the addition of oxalic acid and adipic acid, the dramatic reduction of the  $M_w$  was observed and the scales of molecular weight reduction were comparable to that obtained from acetic acid. The  $M_w$  of the degraded products obtained from the systems containing acetic acid, oxalic acid and adipic acid were approximately  $6 \times 10^3$  Da after 60 min of the SP treatment. It was expected that the

degraded products would contain COS having  $M_w$  less than 5 kDa<sup>53</sup>), as a major component. In the systems with the addition of malonic acid, succinic acid, glutaric acid and pimelic acid, the SP treatment could reduce the  $M_w$  of the chitosan hydrogel from  $4.4 \times 10^5$  Da to the range of  $7.2 \times 10^3 - 1.2 \times 10^4$  Da, while by the addition of azelaic acid and citric acid, the  $M_w$  of the degraded chitosan was equal to approximately  $2 \times 10^4$  Da after the SP treatment for 60 min.

**Table V** Chemical structures, acid dissociation constants, the number of carboxylic groups and the number of methylene groups on the backbone of the carboxylic acids used in this study

Acids	Chemical structures	pKa*	Number of carboxylic groups	Number of $-\text{CH}_2-$ groups on backbone
Acetic acid		4.76	1	-
Oxalic acid		1.23, 4.19	2	0
Malonic acid		2.83, 5.76	2	1
Succinic acid		4.19, 5.48	2	2
Glutaric acid		4.34, 5.42	2	3
Adipic acid		4.42, 5.41	2	4

Pimelic acid		4.48, 5.42	2	5
Azelaic acid		4.55, 5.41	2	7
Citric acid		3.09, 4.75, 5.41	3	-

Note: \* Jencks and Regenstein<sup>77)</sup>

**Table VI** Weight average molecular weight ( $M_w$ ) and polydispersity index (PDI) of chitosan hydrogel at a solid content of 0.2% (dry weight) dispersing in various carboxylic acid solutions with a concentration of 1.55 mM after degradation via SP treatment at different reaction time intervals

SP treatment time	Molecular weight (Da)/PDI								
	Acetic acid	Oxalic acid	Malonic acid	Succinic acid	Glutaric acid	Adipic acid	Pimelic acid	Azelaic acid	Citric acid
0 min	4.4×10 <sup>5</sup> (2.35)	4.4×10 <sup>5</sup> (2.35)	4.4×10 <sup>5</sup> (2.35)	4.4×10 <sup>5</sup> (2.35)	4.4×10 <sup>5</sup> (2.35)	4.4×10 <sup>5</sup> (2.35)	4.4×10 <sup>5</sup> (2.35)	4.4×10 <sup>5</sup> (2.35)	4.4×10 <sup>5</sup> (2.35)
15 min	7.3×10 <sup>4</sup> (4.20)	7.4×10 <sup>4</sup> (4.95)	1.2×10 <sup>5</sup> (5.64)	9.9×10 <sup>4</sup> (4.97)	8.7×10 <sup>4</sup> (5.82)	7.3×10 <sup>4</sup> (4.20)	1.1×10 <sup>5</sup> (7.50)	1.4×10 <sup>5</sup> (6.06)	1.8×10 <sup>5</sup> (3.76)
30 min	2.2×10 <sup>4</sup> (3.35)	2.5×10 <sup>4</sup> (3.67)	4.0×10 <sup>4</sup> (4.55)	4.1×10 <sup>4</sup> (4.50)	3.2×10 <sup>4</sup> (4.92)	2.2×10 <sup>4</sup> (3.35)	4.0×10 <sup>4</sup> (5.34)	5.8×10 <sup>4</sup> (6.72)	1.2×10 <sup>5</sup> (5.48)
45 min	1.1×10 <sup>4</sup> (2.74)	9.3×10 <sup>3</sup> (2.59)	1.9×10 <sup>4</sup> (3.68)	1.7×10 <sup>4</sup> (3.46)	1.2×10 <sup>4</sup> (3.13)	1.1×10 <sup>4</sup> (2.74)	2.0×10 <sup>4</sup> (4.03)	2.4×10 <sup>4</sup> (4.73)	5.4×10 <sup>4</sup> (4.20)
60 min	6.6×10 <sup>3</sup> (2.35)	5.6×10 <sup>3</sup> (2.22)	1.1×10 <sup>4</sup> (3.00)	8.2×10 <sup>3</sup> (2.62)	7.2×10 <sup>3</sup> (2.65)	6.6×10 <sup>3</sup> (2.35)	1.2×10 <sup>4</sup> (3.58)	1.7×10 <sup>4</sup> (4.75)	2.5×10 <sup>4</sup> (3.68)

The rate constant of the degradation reaction of chitosan hydrogel was analyzed based on a linear relationship of reversed molecular weight ( $1/M_w$ ) and reaction time ( $t$ ), according to the previous reports<sup>52, 78)</sup>, as shown below:

$$1/M_t = (1/M_0) + (kt/M) = (1/M_0) + k't \quad (2)$$

where  $M_t$  is  $M_w$  of the sample at reaction time ( $t$ ),  $M_0$  is the initial  $M_w$  of the sample,  $M$  is the molecular weight of the monomer,  $k$  ( $\text{min}^{-1}$ ) or  $k'$  ( $\text{mol g}^{-1} \text{min}^{-1}$ ) is the rate constant, and  $t$  is the reaction time. The  $k$  values are shown in **Table 7**. The  $k$  value obtained by the system with the addition of oxalic acid was equal to  $3.67 \times 10^{-4} \text{ min}^{-1}$  which was slightly higher than that of acetic acid ( $k = 3.48 \times 10^{-4} \text{ min}^{-1}$ ). Meanwhile, the addition of the other dicarboxylic acids led to the lower  $k$  values than that obtained by the system with the addition of acetic acid. The obtained  $k$  values for the systems using dicarboxylic acids were ranging from  $1.36 \times 10^{-4} \text{ min}^{-1}$  to  $3.67 \times 10^{-4} \text{ min}^{-1}$  which seemed to be varied depending on the number of methylene groups on the backbone. For tricarboxylic acid like citric acid, the  $k$  value was the lowest among all the studied carboxylic acids. Nevertheless, the  $k$  values which were obtained in this study, from the degradation of chitosan hydrogel dispersing in dilute carboxylic acids by applying the SP plasma treatment, were comparable to those obtained from the degradation of chitosan solution by using concentrated  $\text{H}_2\text{O}_2$  or using other energy impacts with the  $k$  values ranging from  $10^{-4} \text{ min}^{-1}$  to  $10^{-2} \text{ min}^{-1}$ <sup>55, 62, 78, 79)</sup>.

For further investigation, the chemical structures of chitosan hydrogel before and after degradation by applying the SP treatment in the presence of various types of dilute carboxylic acids were examined by using FT-IR, and the FT-IR results are shown in **Fig. 5**. The absorption peaks of chitosan hydrogel before the SP treatment at the wavenumber of approximately  $3450 \text{ cm}^{-1}$  were assigned to the N–H and hydrogen bonded O–H stretching vibration and the peaks at the wavenumbers of  $1650 \text{ cm}^{-1}$  and  $1600 \text{ cm}^{-1}$  are referred to

C=O stretch of amide bond and N–H bending vibrations of secondary amide, respectively<sup>20, 32, 80, 81</sup>). The peaks at around 1420 cm<sup>-1</sup> and 1375 cm<sup>-1</sup> are attributed to –CH<sub>2</sub>– bending with orientation of the primary hydroxyl group in the polysaccharides and methyl group<sup>82, 83</sup>). The peak at 1070 cm<sup>-1</sup> was assigned to the stretching of C–O–C<sup>20</sup>). According to FT-IR results, the overall chemical structures of the degraded chitosan hydrogel dispersing in various dilute carboxylic acids did not change after the SP treatment. For the degraded chitosan hydrogel obtained from the system with the addition of acetic acid, the strong absorption at 1650 cm<sup>-1</sup> was observed. It might indicate to the ionic interaction between the protonated amino groups (–NH<sub>3</sub><sup>+</sup>) of chitosan and carboxylate anion (–COO<sup>-</sup>) of the carboxylic acid<sup>84</sup>). Normally, protons (H<sup>+</sup>) from the dissociation of acetic acid (CH<sub>3</sub>COOH) can protonate amino groups (–NH<sub>2</sub>) of chitosan to form ammonium group –NH<sub>3</sub><sup>+</sup><sup>73</sup>). Then, acetate anion (CH<sub>3</sub>COO<sup>-</sup>) which has relatively small size and low steric hindrance should be able to penetrate into the structure of chitosan and form ionic interaction with –NH<sub>3</sub><sup>+</sup>. After that, these interactions could lead to an electrostatic repulsion between chitosan chains<sup>41</sup>). Consequently, the structure of chitosan may freely expand and distribute in the solution, as demonstrated in **Fig. 7 (a)**, leading to an increasing of probability that radicals generated by plasma discharge could penetrate to the β-(1,4)–glycosidic linkage of chitosan and greatly promote the *M<sub>w</sub>* reduction of chitosan hydrogel. For the addition of oxalic acid, the FT-IR spectra of the degraded product showed that the absorption at 1650 cm<sup>-1</sup> became sharp and stronger than that of the degraded product obtained from the system with the addition of acetic acid. In case of oxalic acid which is a dicarboxylic acid with no methylene group, it was reported that its dissociation could be influenced by the phenomena called “mesomeric effect”<sup>85</sup>). The mesomeric effect could lead to the formation of intramolecular hydrogen bonding between the firstly-dissociated carboxylic group and the OH part of the undissociated group in another oxalic acid which bears a partial positive charge. Similar to acetic acid, oxalic acid

could interact with chitosan, but the interaction might be a bit stronger, leading to the slightly higher rate of degradation than that of acetic acid. Meanwhile, the FT-IR spectra of the degraded product from the system with the addition of other dicarboxylic acids and tricarboxylic acid exhibited the characteristic peak at  $1600\text{ cm}^{-1}$  which slightly shifted to lower wavenumbers and the absorption at  $1650\text{ cm}^{-1}$  became obvious but had lower intensity than that obtained by the addition of oxalic acid. According to *pKa* values in **Table 5**, all dicarboxylic acids and tricarboxylic acid are able to dissociate in the water and can lead to the protonation of  $\text{-NH}_2$  in chitosan, similar to acetic acid and oxalic acid. The result might indicate that there were the ionic interactions between the  $\text{-NH}_3^+$  groups of chitosan and  $\text{-COO}^-$  groups of the carboxylic acids. However, since dicarboxylic acid and tricarboxylic acid contain two and three groups of  $\text{-COO}^-$ , respectively, they could form ionic crosslinking or complexation with some adjacent chitosan chains as reported in some previous studies<sup>86-88</sup>). These ionic crosslinking or complexation might be the reason for the slower  $M_w$  reduction of chitosan hydrogel. Moreover, since the ionic crosslinking could lead to not only intra- but also intermolecular interaction depending on the number of methylene groups in the structures of dicarboxylic acid and tricarboxylic acid<sup>89</sup>). This phenomenon might be the reason for the result that the addition of different dicarboxylic acids led to the different rate of the degradation of chitosan.



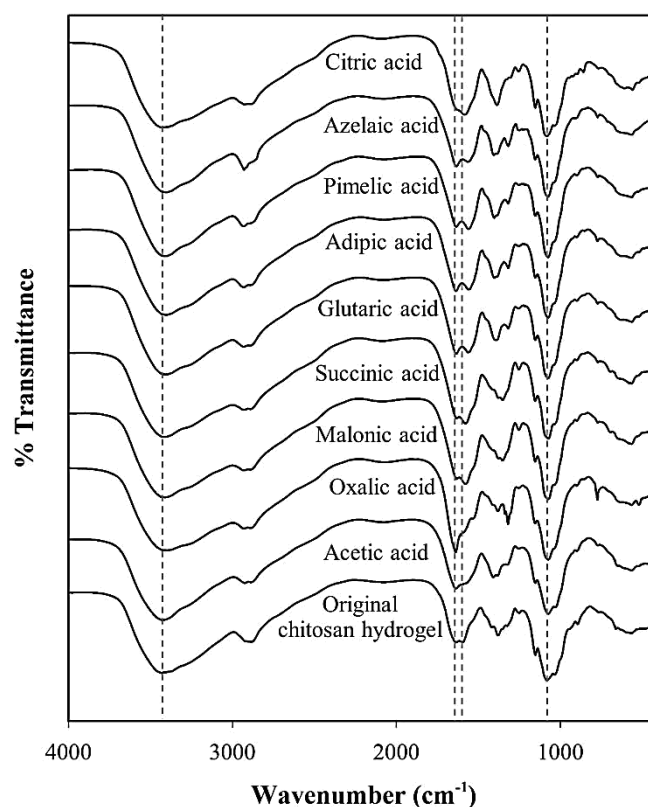


**Fig. 5** FT-IR spectra of the chitosan hydrogel before the SP treatment and the degraded chitosan hydrogel dispersing in various carboxylic acid solutions at a concentration of 1.55 mM after applying the SP treatment for 60 min.

**Figure 6** shows the WAXD patterns of chitosan hydrogel before the SP treatment and the degraded chitosan hydrogel after applying the SP treatment in the presence of various types of carboxylic acid solutions at a concentration of 1.55 mM. The presence of acetic acid during the SP treatment resulted in the degraded product with amorphous structure and in case of oxalic acid very low-intensity of the peaks at  $2\theta = 19.6^\circ$  and  $22.2^\circ$  was observed. It might be implied that the destruction of the crystalline structure of chitosan was facilitated by the presence of acetic acid and oxalic acid during the SP treatment. Meanwhile, the addition of other dicarboxylic acids and tricarboxylic acid gave the peaks with relatively stronger intensity at  $2\theta = 19.6^\circ$  and  $22.2^\circ$ . According to the previous study, the broad peak at around  $2\theta = 19^\circ$  and  $22^\circ$  might be ascribed to the diffraction of the plane

of the crystal region in the chitosan carboxylate<sup>90</sup>). The chitosan carboxylate was induced by the formation of ionic interactions between the  $\text{-NH}_3^+$  groups of chitosan and  $\text{-COO}^-$  groups of the carboxylic acid. In case of the dicarboxylic acids and tricarboxylic acid, they could form ionic crosslinking or complexation with some adjacent chitosan chains, leading to stabilization of the crystal structure of chitosan and, consequently, these two peaks could be obviously observed. Especially, the relatively high crystallinity of the degraded chitosan products from the systems with the addition of azelaic acid and citric acid was an evidence that indicated the formation of some extent of crosslinking within the structure of degraded chitosan. Therefore, the WAXD results was consistent with the FT-IR results and could be also used to explain the reason that the different rates of degradation were obtained when the chitosan hydrogel dispersing in the different carboxylic acids was degraded by the SP treatment.

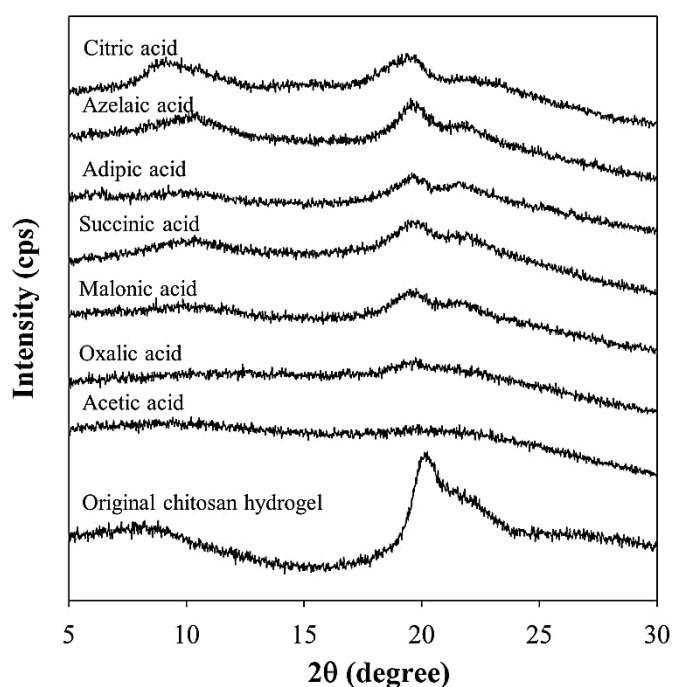


**Fig. 6** WAXD spectra of the hitosan hydrogel before the SP treatment and the degraded chitosan hydrogel dispersing in various carboxylic acid solutions at a concentration of 1.55 mM after applying the SP treatment for 60 min.

A schematic drawing of a possible degradation mechanism of chitosan hydrogel dispersing in various carboxylic acid solutions by applying the SP treatment was proposed in **Fig. 7 (b)**. The reaction solution containing only molecules of H<sub>2</sub>O, carboxylic acids and chitosan was subjected to the SP treatment. The major component in the system was H<sub>2</sub>O molecules. The plasma discharge can result in excitation and ionization of H<sub>2</sub>O molecules<sup>91</sup>). Electrons are emitted as a result of ionization (*i.e.* H<sub>2</sub>O → H<sub>2</sub>O<sup>+</sup> + e<sup>-</sup>) and then continuously collide with the surrounding H<sub>2</sub>O molecules (*i.e.* e<sup>-</sup> + H<sub>2</sub>O → •OH + <sup>-</sup>H) to produce radicals. In addition, the excitation of H<sub>2</sub>O molecules also directly lead to the formation of radicals (*i.e.* H<sub>2</sub>O\* → •OH + •H). Both ionization and excitation of H<sub>2</sub>O molecules by the SP treatment rapidly produce •OH which is necessary for the degradation of chitosan<sup>83, 92</sup>). The generated •OH could attack at the C1 position and transferred the radical to the C1 and subtracted the hydrogen from it causing the chain scission of the chitosan at β-1,4 glycosidic linkage which have been reported in the previous studies<sup>52, 78, 83</sup>). The breakdown of the β-(1,4) glycosidic linkage leads to the reduction of molecular weight of chitosan<sup>83</sup>). Moreover, the electron from the plasma discharge can also directly collide to chitosan, leading to the chain scission.

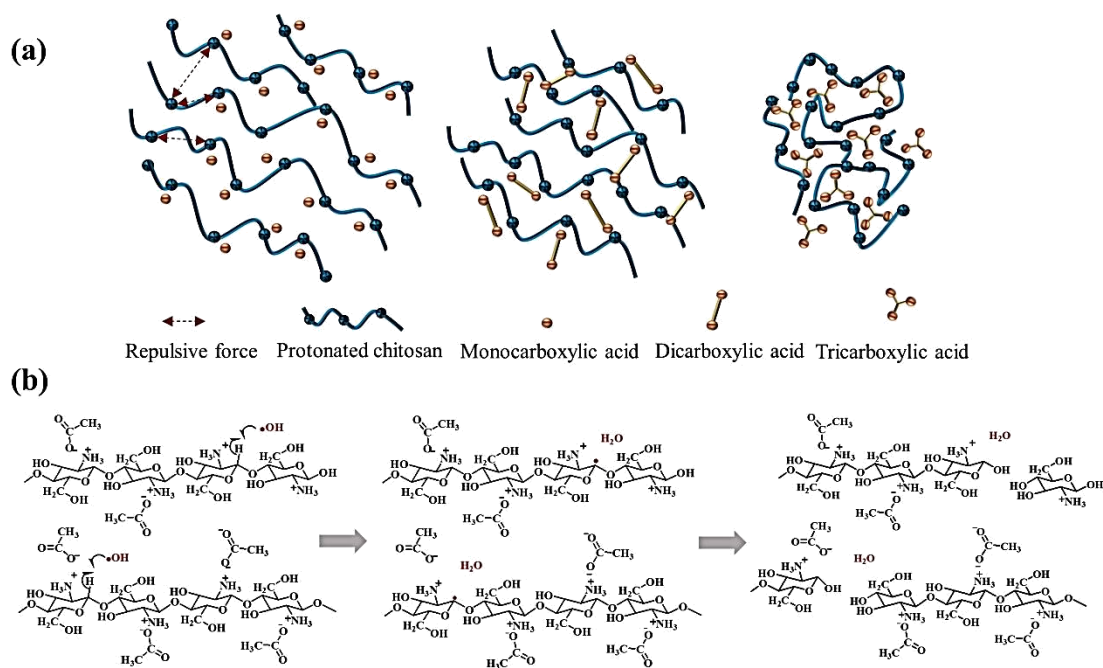


**Fig. 7 (a)** Possible ionic interaction and ionic crosslink between chitosan hydrogel and different types of carboxylic acids including monocarboxylic acid, dicarboxylic acid and tricarboxylic acid. **(b)** Possible degradation mechanism of chitosan hydrogel dispersing in dilute acid solution by the SP treatment.

The degraded chitosan hydrogel obtained by the SP treatment in the presence of various dilute carboxylic acids for 60 min was centrifuged in order to separate the degraded products into water-soluble and water-insoluble degraded products.. The solid precipitate consisted of water-insoluble chitosan, while the supernatant contained the water-soluble COS. The further purification after the centrifugation was unnecessary, because the very low concentration of carboxylic acids was used in the reaction. Moreover, carboxylic acids that are generally found in many natural products are safe for being used . in food and drug production<sup>93</sup>). After centrifugation, in most cases of the studied carboxylic acids, the production yield of water-soluble COS was in the range of 50 – 70% with the exception of azelaic acid and citric acid that the production yields of water-soluble COS were 40% and less than 5%, respectively. For further investigation on molecular weight

reduction, the weight-average molecular weight ( $M_w$ ), number-average molecular weight ( $M_n$ ) and PDI of the water-soluble COS were determined by GPC as shown in **Table 7**. Based on the  $M_n$ , the major oligosaccharides in the water-soluble COS could be estimated for each carboxylic acid as shown in **Table 8**. Degradations of chitosan hydrogel dispersing in the dilute solution of citric acid could produce COS with the major oligosaccharide of 10-mers, while the addition of acetic acid, oxalic acid and adipic acid resulted in the COS containing mainly of 12-mers. The addition of malonic acid, glutaric acid and azelaic acid could give the major oligosaccharides of 13-mers and the COS with the major oligosaccharide of 14-mers could be produce by the addition of succinic acid and pimelic acid. Therefore, it could be concluded that the degradation of chitosan hydrogel dispersing in the dilute solution of various carboxylic acids by applying the SP treatment could produce the COS with degree of polymerization (DP) ranging from 10 to 14, which are difficult to be produced by the enzymatic degradation<sup>20</sup>. Besides, since the carboxylate anions were still remained in the degraded products, they should form ionic interaction with the COS leading to the formation of the COS-carboxylates.

**Table VII** Rate constants ( $k$ ) of the degradation reactions of chitosan hydrogel at a solid content of 0.2% (dry weight) dispersing in 1.55 mM carboxylic acid solutions by the SP treatment and production yield of water-soluble COS produced by the degradation of chitosan hydrogel dispersing in various carboxylic acids at a concentration of 1.55 mM by applying the SP treatment as well as their weight-average molecular weight ( $M_w$ ), number-average molecular weight ( $M_n$ ) and polydispersity index (PDI)

Acids	$k \times 10^{-4} (\text{min}^{-1})$	Yield of liquid fraction (%)	Molecular weight (Da) /PDI		
			$M_n$	$M_w$	PDI
Acetic acid	$3.48 \pm 0.05$	$68.3 \pm 2.36$	1861	2969	1.59
Oxalic acid	$3.67 \pm 0.20$	$60.3 \pm 6.85$	1944	3344	1.72
Malonic acid	$2.37 \pm 0.26$	$53.3 \pm 7.17$	2053	3482	1.69
Succinic acid	$2.39 \pm 0.08$	$60.9 \pm 4.71$	2321	4484	1.93
Glutaric acid	$3.09 \pm 0.01$	$63.1 \pm 3.12$	2181	4033	1.84
Adipic acid	$2.75 \pm 0.02$	$60.3 \pm 3.54$	2008	3395	1.69
Pimelic acid	$1.80 \pm 0.04$	$64.1 \pm 6.56$	2216	4032	1.81
Azelaic acid	$1.36 \pm 0.03$	$40.0 \pm 2.04$	2133	4515	1.93
Citric acid	$0.75 \pm 0.02$	$2.5 \pm 0.21$	1538	2330	1.51

**Table VIII** Possible major oligosaccharides in the water-soluble COS-carboxylate samples with the evaluation of their anticancer activity

COS samples	Possible major oligosaccharide	Evaluation of anticancer activity		
		IC <sub>50</sub> * (mg·mL <sup>-1</sup> )		SI**
		H460	MRC-5	
COS-acetate	12	2.9	5.0	1.72
COS-oxalate	12	2.6	3.7	1.42
COS-malonate	13	2.0	4.5	2.25
COS-succinate	14	1.6	5.0	3.13
COS-glutarate	13	2.2	4.0	1.81
COS-adipate	12	2.0	2.4	1.20
COS-pimelate	14	1.6	3.5	2.19
COS-azalate	13	2.4	3.7	1.54
COS-citrate	10	-	-	-
COS***	13	5.0	6.5	1.30

Note: \*IC<sub>50</sub> is the concentration required to kill 50% of the cell population.

\*\*SI is the selectivity index (SI = IC<sub>50</sub> of tested compound in a normal cell line/IC<sub>50</sub> of the same tested compound in cancer cell line)<sup>94, 95)</sup>

\*\*\*COS was obtained by the precipitation, of the degraded chitosan solution in 1 M acetic acid after the SP treatment under the corresponding condition.

### 3.2 Evaluation of anticancer activity

To evaluate the anticancer activity and to determine the concentrations of the COS-carboxylate samples which could kill 50% of the cell population ( $IC_{50}$ ), H460 and MRC-5 were used as representatives of cancer cell line and normal cell line, respectively. The COS-carboxylate samples were added to testing wells to make the final concentrations ranging from 1 to 5  $mg \cdot mL^{-1}$ . **Table 8** shows  $IC_{50}$  of the COS-carboxylate and the normal COS samples against cancer cells (H460) and normal cells (MRC-5). The normal COS was obtained by following the protocol as reported in the previous work<sup>41)</sup>, using the SP treatment of chitosan solution. For a comparison between the COS-carboxylate and the COS,  $IC_{50}$  values of all COS-carboxylate samples against cancer cells were twice lower than that of the normal COS. It suggested that the presence of carboxylate in the structure of the COS could enhance the anticancer activity. Among the studied COS-carboxylate samples, it was found that the COS-carboxylate samples with the majority of 14-mers which obtained from the degradation of chitosan hydrogel dispersing succinic acid and pimelic acid exhibited the best inhibitory effect on the growth of H460 cells ( $IC_{50}$  equaled to 1.6  $mg \cdot mL^{-1}$ ). For cytotoxicity against MRC-5 cells, the COS-acetate and COS-succinate samples had the highest value of  $IC_{50}$  at 5  $mg \cdot mL^{-1}$ . Moreover, a selectivity index (SI) of the COS-carboxylate and the COS samples could be determined by the  $IC_{50}$  ratio of a compound tested against cancer cells and normal cells. SI implies the differential cytotoxic activity of the tested sample against cancer and normal cells<sup>94)</sup>. Therefore, the high value of SI indicates a higher selectivity for cytotoxic activity against H460 cells than MRC-5 cells. Among the studied COS-carboxylate samples, the SI of the COS-succinate had the highest value of 3.1. COS-succinate was also found to have the better selectivity to cancer cells than COS. Since the last decade, succinate has been extensively studied for the treatment of cancer, because it was found to be a key metabolic factor in the cancer-immune and may lead to cancer immunotherapies<sup>96)</sup>. Previous studies reported that vitamin



E succinate showed the inhibitory effect on cancer cells and tumor<sup>97, 98)</sup>. Therefore, the combination of COS and succinate, which possessed the better selectivity against cancer cells, could be recommended for further development as a potential anticancer agent. In addition, according to **Table 9**, the cell viability obtained for COS-succinate was comparable to that of COS prepared by the enzymatic degradation. According to these evidence, it was proved the SP treatment can be used to reduce molecular weight of chitosan in order to obtain COS without changing the biological property like anticancer activity which naturally belongs to COS.

**Table IX** Anticancer activity of COS and COS derivatives prepared by different methods.

COS and COS derivatives	Preparation Methods	Cell lines	Cell viability (%)			SI*	Ref.
			At~0.5 mg·mL <sup>-1</sup>	At~1.5 mg·mL <sup>-1</sup>	At~15 mg·mL <sup>-1</sup>		
COS (DP1–5)	enzymatic	HeLa	48	-	-	-	43)
COS (DP3–9)	enzymatic	SMMC-7721	80	65	-	-	99)
COS (DP2–9)	SP	HeLa	-	95	45	1.5	41)
		MRC-5**	-	100	70		
COS-succinate (DP~14)	SP	H460	80	50	-	3.1	This work
		MRC-5**	89	75	-		

Note: \*SI is the selectivity index (SI = IC<sub>50</sub> of tested compound in a normal cell line/IC<sub>50</sub> of the same tested compound in cancer cell line)<sup>94, 95)</sup>

\*\* Normal cell line

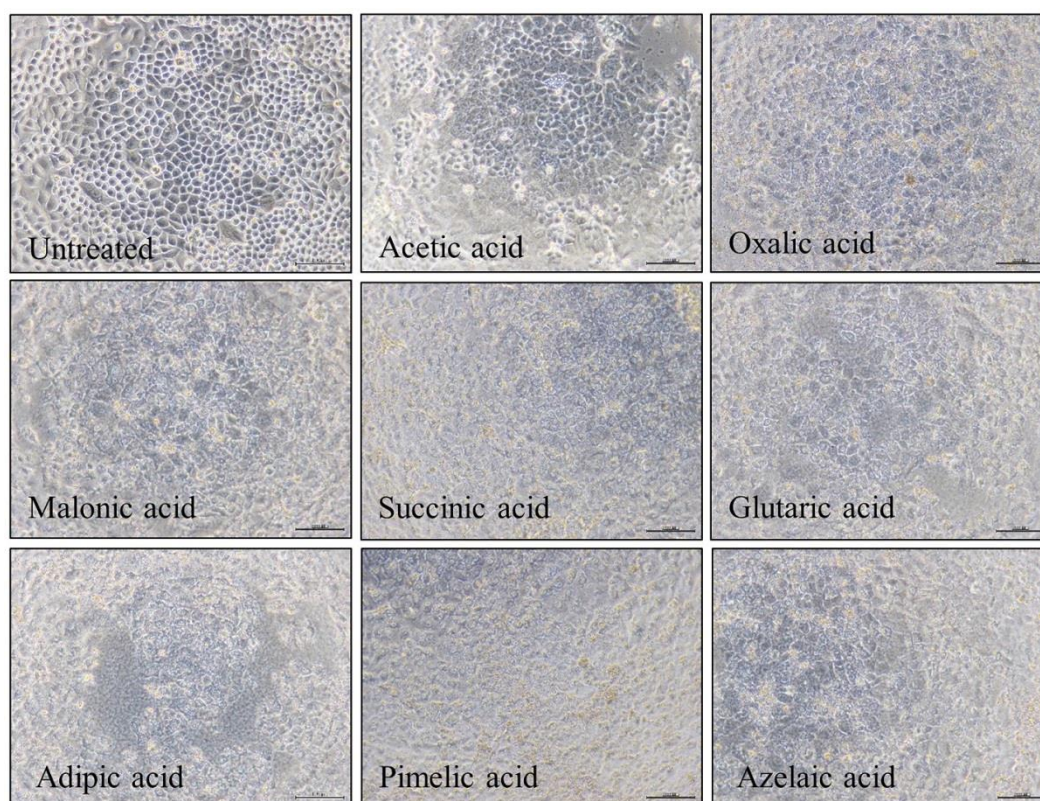


**Fig. 8** Microscopic images ( $\times 20$ ) of H460 cells before and after the 24-hour treatment with water-soluble COS obtained from the degradation of chitosan hydrogel dispersing in various types of dilute carboxylic acid solutions by the SP treatment.

In addition, the morphology of H460 cells untreated and treated with the COS-carboxylate samples at a concentration of  $5 \text{ mg} \cdot \text{mL}^{-1}$  was shown in **Fig. 8**. After 24 h of the treatment without the addition of COS sample, the control cells showed a dense confluence of monolayer cells with typical growth patterns and had smooth, flattened morphology with normal nuclei. The cells after the treatment with COS samples exhibited the change of the morphology to abnormal shapes. The breakage of cell membrane was widely observed.

## 4. Conclusions

Chitosan hydrogel was found to be a suitable form of chitosan to produce water-soluble COS via a heterogeneous degradation reaction by using solution plasma treatment. As a result of the further disruption of the crystalline structure of chitosan hydrogel, the molecular weight reduction of chitosan hydrogel was enhanced by the presence of a small amount of carboxylic acids, especially acetic acid and oxalic acid, during the degradation of chitosan hydrogel under the discharge of plasma. Since a dilute concentration of carboxylic acids was used and chitosan hydrogel still remained as an undissolved hydrogel, the separation process to remove water-soluble degraded products containing COS from the remaining chitosan hydrogel could be simply achieved by centrifugation. Due to the application of simple processes with less chemical use, the production cost of COS can be significantly reduced. Although the addition of carboxylic acids to the suspension of chitosan hydrogel results in the formation of COS-carboxylate products, the presence of succinate anion in COS could enhance the inhibitory effect towards the cancer cells, resulting in the higher value of selectivity index. This study proposed a novel, simple process to produce COS having anticancer activity. The proposed process not only gives a high production yield of COS but also can reduce the production cost of COS.

## Acknowledgments

CC would like to express thankfulness to the Thailand Research Fund (TRF) for providing her a Royal Golden Jubilee Ph.D. Scholarship (RGJ-Ph.D.: Grant number PHD/0179/2556). This work was financially supported by the Thailand Research Fund (TRF) under the contract number BRG5480008 and the National Research Funding from the Government of Thailand given to Chulalongkorn University. Moreover, the authors would like acknowledge Surapon Foods Public Co., Ltd. (Thailand) for providing the

shrimp shells and Nagoya university (Japan) for providing solution plasma equipment. In addition, the authors would like to thank Drug Discovery and Development center at Thammasat University (Thailand) for providing all facilities that were used for the biological tests.

## **Appendix**

The plots of the percentage of cell viability versus the concentration of the COS samples obtained from the degradation of chitosan hydrogel dispersing in the dilute solution of various carboxylic acids by the SP treatment were provide in appendix A.

---

## **References**

- 1) I. Armentano, N. Bitinis, E. Fortunati, S. Mattioli, N. Rescignano, R. Verdejo, M.A. Lopez-Manchado and J.M. Kenny, *Progress in Polymer Science*. **38** [10–11], 1720 (2013).
- 2) X. Tang, P. Kumar, S. Alavi and K. Sandeep, *Critical reviews in food science and nutrition*. **52** [5], 426 (2012).
- 3) A.K. Mohanty, M. Misra and L.T. Drzal, *Natural fibers, biopolymers, and biocomposites* (CRC press, 2005) p.
- 4) M.A. Meyers, P.-Y. Chen, A.Y.-M. Lin and Y. Seki, *Progress in Materials Science*. **53** [1], 1 (2008).
- 5) J. Liu, S. Willför and C. Xu, *Bioactive Carbohydrates and Dietary Fibre*. **5** [1], 31 (2015).
- 6) K. Jung, Y. Ha, S.K. Ha, D.U. Han, D.W. Kim, W.K. Moon and C. Chae, *Journal of Veterinary Medicine, Series B*. **51** [2], 72 (2004).
- 7) W. Yang, F. Pei, Y. Shi, L. Zhao, Y. Fang and Q. Hu, *Carbohydrate Polymers*. **88** [2], 474 (2012).
- 8) R.J. Oliveira, L.R. Ribeiro, A.F. da Silva, R. Matuo and M.S. Mantovani, *Toxicology in Vitro*. **20** [7], 1225 (2006).
- 9) N.P. Chandía and B. Matsuhira, *International Journal of Biological Macromolecules*. **42** [3], 235 (2008).
- 10) T. Zhao, Q. Zhang, H. Qi, H. Zhang, X. Niu, Z. Xu and Z. Li, *International Journal of Biological Macromolecules*. **38** [1], 45 (2006).
- 11) D. Houghton, M.D. Wilcox, P.I. Chater, I.A. Brownlee, C.J. Seal and J.P. Pearson, *Food Hydrocolloids*. **49**, 18 (2015).
- 12) M. Falkeborg, L.-Z. Cheong, C. Gianfico, K.M. Sztukiel, K. Kristensen, M. Glasius, X. Xu and Z. Guo, *Food Chemistry*. **164**, 185 (2014).
- 13) Q. Cong, F. Xiao, W. Liao, Q. Dong and K. Ding, *International Journal of Biological Macromolecules*. **69**, 252 (2014).
- 14) S. Ermakova, R. Sokolova, S.-M. Kim, B.-H. Um, V. Isakov and T. Zvyagintseva, *Applied Biochemistry and Biotechnology*. **164** [6], 841 (2011).
- 15) D.-N. Ngo, S.-H. Lee, M.-M. Kim and S.-K. Kim, *Journal of Functional Foods*. **1** [2], 188 (2009).
- 16) D.-N. Ngo, M.-M. Kim and S.-K. Kim, *Carbohydrate Polymers*. **74** [2], 228 (2008).
- 17) H.K. No, N. Young Park, S. Ho Lee and S.P. Meyers, *International Journal of Food Microbiology*. **74** [1–2], 65 (2002).

- 18) W.-K. Jung, S.-H. Moon and S.-K. Kim, *Life Sciences*. **78** [9], 970 (2006).
- 19) M. Wang, H. Wang, Y. Tang, D. Kang, Y. Gao, M. Ke, J. Dou, T. Xi and C. Zhou, *Immunology letters*. **141** [1], 74 (2011).
- 20) V.K. Mourya, N.N. Inamdar and Y.M. Choudhari, *Polym. Sci. Ser. A*. **53** [7], 583 (2011) [in English].
- 21) W. Xia, P. Liu, J. Zhang and J. Chen, *Food Hydrocolloids*. **25** [2], 170 (2011).
- 22) S.A. Agnihotri, N.N. Mallikarjuna and T.M. Aminabhavi, *Journal of controlled release*. **100** [1], 5 (2004).
- 23) X. Zou, X. Zhao and L. Ye, *RSC Advances*. **5** [116], 96230 (2015).
- 24) C. Tangsadthakun, S. Kanokpanont, N. Sanchavanakit, R. Pichyangkura, T. Banaprasert, Y. Tabata and S. Damrongsakkul, *Journal of Biomaterials Science, Polymer Edition*. **18** [2], 147 (2007).
- 25) F.-L. Mi, S.-S. Shyu, Y.-B. Wu, S.-T. Lee, J.-Y. Shyong and R.-N. Huang, *Biomaterials*. **22** [2], 165 (2001).
- 26) R. Jayakumar, M. Prabakaran, P.T. Sudheesh Kumar, S.V. Nair and H. Tamura, *Biotechnology Advances*. **29** [3], 322 (2011).
- 27) X.-L. Luo, J.-J. Xu, Y. Du and H.-Y. Chen, *Analytical Biochemistry*. **334** [2], 284 (2004).
- 28) N.M. El-Sawy, H.A. Abd El-Rehim, A.M. Elbarbary and E.-S.A. Hegazy, *Carbohydrate Polymers*. **79** [3], 555 (2010).
- 29) T. Feng, Y. Du, J. Li, Y. Hu and J.F. Kennedy, *Carbohydrate Polymers*. **73** [1], 126 (2008).
- 30) P.-J. Park, J.-Y. Je and S.-K. Kim, *Journal of Agricultural and Food Chemistry*. **51** [16], 4624 (2003).
- 31) T.-S. Vo, C.-S. Kong and S.-K. Kim, *Carbohydrate Polymers*. **84** [1], 649 (2011).
- 32) C. Qin, Y. Du, L. Xiao, Z. Li and X. Gao, *International Journal of Biological Macromolecules*. **31** [1–3], 111 (2002).
- 33) K.V. Harish Prashanth and R.N. Tharanathan, *Biochimica et Biophysica Acta (BBA) - General Subjects*. **1722** [1], 22 (2005).
- 34) J. Liu, J. Zhang and W. Xia, *Food Chemistry*. **107** [1], 419 (2008).
- 35) S.-H. Lee, M. Senevirathne, C.-B. Ahn, S.-K. Kim and J.-Y. Je, *Bioorganic & Medicinal Chemistry Letters*. **19** [23], 6655 (2009).
- 36) B. Stewart and C.P. Wild, *World*. (2016).

- 37) M.L. Tan, P.F.M. Choong and C.R. Dass, *Journal of Pharmacy and Pharmacology*. **61** [1], 3 (2009).
- 38) C.E. DeSantis, C.C. Lin, A.B. Mariotto, R.L. Siegel, K.D. Stein, J.L. Kramer, R. Alteri, A.S. Robbins and A. Jemal, *CA: A Cancer Journal for Clinicians*. **64** [4], 252 (2014).
- 39) E.-K. Kim, J.-Y. Je, S.-J. Lee, Y.-S. Kim, J.-W. Hwang, S.-H. Sung, S.-H. Moon, B.-T. Jeon, S.-K. Kim, Y.-J. Jeon and P.-J. Park, *Bioorganic & Medicinal Chemistry Letters*. **22** [19], 6136 (2012).
- 40) R. Huang, E. Mendis, N. Rajapakse and S.-K. Kim, *Life Sciences*. **78** [20], 2399 (2006).
- 41) C. Chokradjaroen, R. Rujiravanit, A. Watthanaphanit, S. Theeramunkong, N. Saito, K. Yamashita and R. Arakawa, *Carbohydrate Polymers*. **167**, 1 (2017).
- 42) M.Z. Karagozlu and S.-K. Kim, *Advances in Food and Nutrition Research* (Academic Press, 2014) p. 215.
- 43) C.F. de Assis, L.S. Costa, R.F. Melo-Silveira, R.M. Oliveira, M.G.B. Pagnoncelli, H.A.O. Rocha, G.R. de Macedo and E.S.d. Santos, *World Journal of Microbiology and Biotechnology*. **28** [3], 1097 (2012).
- 44) A. Einbu, H. Grasdalen and K.M. Vårum, *Carbohydrate Research*. **342** [8], 1055 (2007).
- 45) K.M. Vårum, M.H. Ottøy and O. Smidsrød, *Carbohydrate Polymers*. **46** [1], 89 (2001).
- 46) Y.-B. Huang and Y. Fu, *Green Chemistry*. **15** [5], 1095 (2013).
- 47) S.-K. Kim and N. Rajapakse, *Carbohydrate Polymers*. **62** [4], 357 (2005).
- 48) J.C. Cabrera and P. Van Cutsem, *Biochemical Engineering Journal*. **25** [2], 165 (2005).
- 49) G. Li, L. Qi, A. Li, R. Ding and M. Zong, *Macromolecular Symposia*. **216** [1], 165 (2004).
- 50) J.M. Wasikiewicz, F. Yoshii, N. Nagasawa, R.A. Wach and H. Mitomo, *Radiation Physics and Chemistry*. **73** [5], 287 (2005).
- 51) J. Shao, Y. Yang and Q. Zhong, *Polymer Degradation and Stability*. **82** [3], 395 (2003).
- 52) O. Pornsunthorntawe, C. Katepetch, C. Vanichvattanadecha, N. Saito and R. Rujiravanit, *Carbohydrate Polymers*. **102** [0], 504 (2014).

- 53) K.V. Harish Prashanth and R.N. Tharanathan, Trends in Food Science & Technology. **18** [3], 117 (2007).
- 54) J.M. Wasikiewicz and S.G. Yeates, Polymer Degradation and Stability. **98** [4], 863 (2013).
- 55) K. Li, R. Xing, S. Liu, Y. Qin, X. Meng and P. Li, International Journal of Biological Macromolecules. **51** [5], 767 (2012).
- 56) M. Chhatbar, R. Meena, K. Prasad and A.K. Siddhanta, Carbohydrate Polymers. **76** [4], 650 (2009).
- 57) V.L. Budarin, J.H. Clark, B.A. Lanigan, P. Shuttleworth and D.J. Macquarrie, Bioresource Technology. **101** [10], 3776 (2010).
- 58) W. Yue, P. Yao and Y. Wei, Polymer Degradation and Stability. **94** [5], 851 (2009).
- 59) E. Savitri, S.R. Juliastuti, A. Handaratri, Sumarno and A. Roesyadi, Polymer Degradation and Stability. **110** [0], 344 (2014).
- 60) Q. Zou, Y. Pu, Z. Han, N. Fu, S. Li, M. Liu, L. Huang, A. Lu, J. Mo and S. Chen, Carbohydrate Polymers. **90** [1], 447 (2012).
- 61) F. Ma, Z. Wang, H. Zhao and S. Tian, International Journal of Molecular Sciences. **13** [6], 7788 (2012).
- 62) I. Prasertsung, S. Damrongsakkul and N. Saito, Polymer Degradation and Stability. **98** [10], 2089 (2013).
- 63) I. Prasertsung, S. Damrongsakkul, C. Terashima, N. Saito and O. Takai, Carbohydrate Polymers. **87** [4], 2745 (2012).
- 64) A. Watthanaphanit and N. Saito, Polymer Degradation and Stability. **98** [5], 1072 (2013).
- 65) O. Takai, Pure and Applied Chemistry. **80** [9], 2003 (2008).
- 66) N. Saito, J. Hieda and O. Takai, Thin Solid Films. **518** [3], 912 (2009).
- 67) M.A. Bratescu, S.-P. Cho, O. Takai and N. Saito, The Journal of Physical Chemistry C. **115** [50], 24569 (2011).
- 68) P. Baroch, V. Anita, N. Saito and O. Takai, Journal of Electrostatics. **66** [5–6], 294 (2008).
- 69) P. Pootawang, N. Saito and O. Takai, Thin Solid Films. **519** [20], 7030 (2011).
- 70) E.M. Ahmed, Journal of Advanced Research. **6** [2], 105 (2015).
- 71) K. Okano, T. Minagawa, J. Yang, M. Shimojoh and K. Kurita, Polym. Bull. **62** [2], 119 (2009) [in English].
- 72) S. Sabnis and L.H. Block, Polym. Bull. **39** [1], 67 (1997).



- 73) S. Lu, X. Song, D. Cao, Y. Chen and K. Yao, *Journal of Applied Polymer Science*. **91** [6], 3497 (2004).
- 74) K.V. Harish Prashanth, F.S. Kittur and R.N. Tharanathan, *Carbohydrate Polymers*. **50** [1], 27 (2002).
- 75) K. Okuyama, K. Noguchi, T. Miyazawa, T. Yui and K. Ogawa, *Macromolecules*. **30** [19], 5849 (1997).
- 76) Z. Modrzejewska, W. Maniukiewicz and A. Wojtasz-Pająk, (2006).
- 77) W.P. Jencks and J. Regenstein, *Handbook of Biochemistry and Molecular Biology, Fourth Edition* (CRC Press, 2010) p. 595.
- 78) K.L.B. Chang, M.-C. Tai and F.-H. Cheng, *Journal of Agricultural and Food Chemistry*. **49** [10], 4845 (2001).
- 79) N.Q. Hien, D.V. Phu, N.N. Duy and N.T.K. Lan, *Carbohydrate Polymers*. **87** [1], 935 (2012).
- 80) J. Brugnerotto, J. Lizardi, F. Goycoolea, W. Argüelles-Monal, J. Desbrieres and M. Rinaudo, *Polymer*. **42** [8], 3569 (2001).
- 81) S. Sahoo, A. Sasmal, D. Sahoo and P. Nayak, *Journal of Applied Polymer Science*. **118** [6], 3167 (2010).
- 82) A.B. Vishu Kumar, M.C. Varadaraj, R.G. Lalitha and R.N. Tharanathan, *Biochimica et Biophysica Acta (BBA) - General Subjects*. **1670** [2], 137 (2004).
- 83) B. Kang, Y.-d. Dai, H.-q. Zhang and D. Chen, *Polymer Degradation and Stability*. **92** [3], 359 (2007).
- 84) T. Mitra, G. Sailakshmi, A. Gnanamani and A.B. Mandal, *Materials Research*. **16**, 755 (2013).
- 85) F.A. Peter and P. Neta, *The Journal of Physical Chemistry*. **76** [5], 630 (1972).
- 86) M.V. Shamov, S.Y. Bratskaya and V.A. Avramenko, *Journal of Colloid and Interface Science*. **249** [2], 316 (2002).
- 87) B. Martel, M. Weltrowski, D. Ruffin and M. Morcellet, *Journal of Applied Polymer Science*. **83** [7], 1449 (2002).
- 88) A. Watthanaphanit, P. Supaphol, T. Furuike, S. Tokura, H. Tamura and R. Rujiravanit, *Biomacromolecules*. **10** [2], 320 (2009).
- 89) P.-H. Chen, T.-Y. Kuo, F.-H. Liu, Y.-H. Hwang, M.-H. Ho, D.-M. Wang, J.-Y. Lai and H.-J. Hsieh, *Journal of Agricultural and Food Chemistry*. **56** [19], 9015 (2008).
- 90) U. Ubaidulla, R.K. Khar, F.J. Ahmad, Y. Sultana and A.K. Panda, *Journal of Pharmaceutical Sciences*. **96** [11], 3010 (2007).

- 91) S. Le Caër, Water. **3** [1], 235 (2011).
- 92) C. Qin, Y. Du and L. Xiao, Polymer Degradation and Stability. **76** [2], 211 (2002).
- 93) C. Skonberg, J. Olsen, K.G. Madsen, S.H. Hansen and M.P. Grillo, Expert Opinion on Drug Metabolism & Toxicology. **4** [4], 425 (2008).
- 94) R.B. Badisa, S.F. Darling-Reed, P. Joseph, J.S. Cooperwood, L.M. Latinwo and C.B. Goodman, Anticancer research. **29** [8], 2993 (2009).
- 95) R.B. Badisa, L.T. Ayuk-Takem, C.O. Ikediobi and E.H. Walker, Pharmaceutical Biology. **44** [2], 141 (2006).
- 96) S. Jiang and W. Yan, Cancer Letters. **390**, 45 (2017).
- 97) M.P. Malafa and L.T. Neitzel, Journal of Surgical Research. **93** [1], 163 (2000).
- 98) K.T. Barnett, F.D. Fokum and M.P. Malafa, Journal of Surgical Research. **106** [2], 292 (2002).
- 99) Q. Xu, J. Dou, P. Wei, C. Tan, X. Yun, Y. Wu, X. Bai, X. Ma and Y. Du, Carbohydrate Polymers. **71** [4], 509 (2008).

## Appendix A

### Supplementary Data

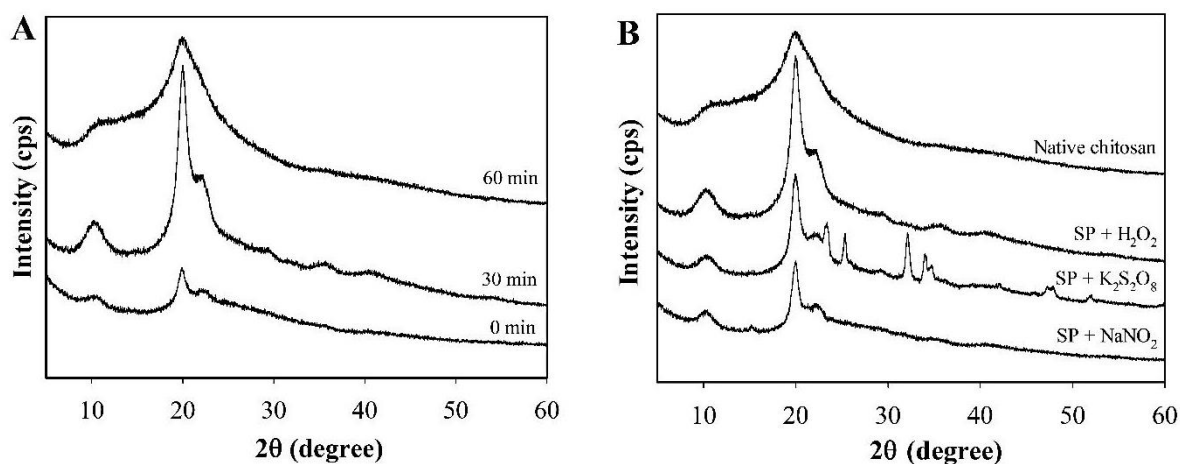


**Fig. A1** XRD patterns of native chitosan and degraded chitosan **(A)** after the SP treatment of 0.5% chitosan solution with the addition of 4 mM  $\text{H}_2\text{O}_2$  at the reaction time of 0, 30 and 60 min and **(B)** after the SP treatment of 0.5% chitosan solution with the addition of different oxidizing agents at a concentration of 4 mM and the reaction time of 30 min.

The XRD patterns of native chitosan and degraded chitosan are shown in **Fig. A1 (A)** and **(B)**. After the SP treatment of chitosan solution for 30 min, the characteristic peaks of chitosan at  $2\theta = 10$  and  $20$  became sharpen. However, at the SP treatment time of 60 min the peaks at  $2\theta = 10$  and  $20$  became broaden. This might be explained that during the first 30 minutes of the SP treatment the amorphous region in chitosan was greatly degraded while the crystalline region still remained, resulting in the sharpen of the characteristic peaks of chitosan in the XRD spectrum. When the SP treatment time was prolonged to be 60 min, the remaining crystalline region of chitosan was destroyed as evidenced by the broadening of the peaks at  $2\theta = 10$  and  $20$  in the XRD result. The XRD patterns of chitosan after the degradation by the solution plasma treatment with the addition of different oxidizing agents are also depicted. The addition of  $\text{NaNO}_2$  showed the least crystallinity, followed by  $\text{K}_2\text{S}_2\text{O}_8$  and  $\text{H}_2\text{O}_2$ . For the addition of  $\text{K}_2\text{S}_2\text{O}_8$ , some sharp minor peaks appeared at  $2\theta = 25.44^\circ$ ,  $34.05^\circ$  and  $47.50^\circ$  which were similar to peaks that appeared in the XRD pattern of  $\text{K}_2\text{S}_2\text{O}_8$  in a previous study (Zhou et al., 2015). Therefore, these peaks may be ascribed to the sulfate anions which had the ionic interaction with chitosan chains.

To determine rate constant ( $k'$ ), plots of  $1/M_t$  versus  $t$  at the initial stage (0 to 30 min) were achieved by varying concentrations of chitosan and  $H_2O_2$  as shown in **Fig. A2**.

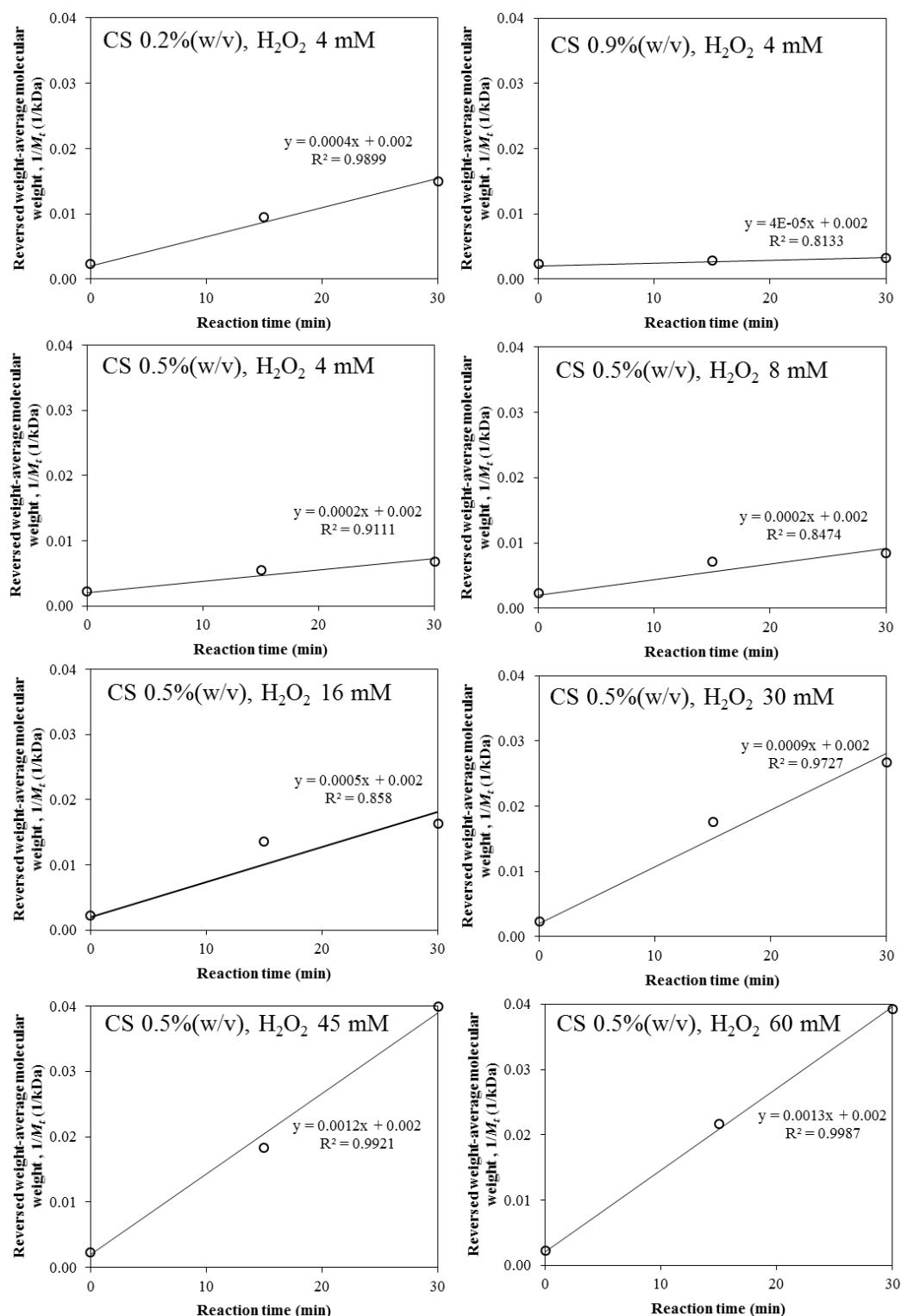


**Fig. A2** Plots of reversed weight-averaged molecular weight ( $1/M_t$ ) and reaction time ( $t$ ) at the initial stage (0 to 30 min) of the chitosan degradation using various concentrations of chitosan and  $H_2O_2$  under the SP treatment.

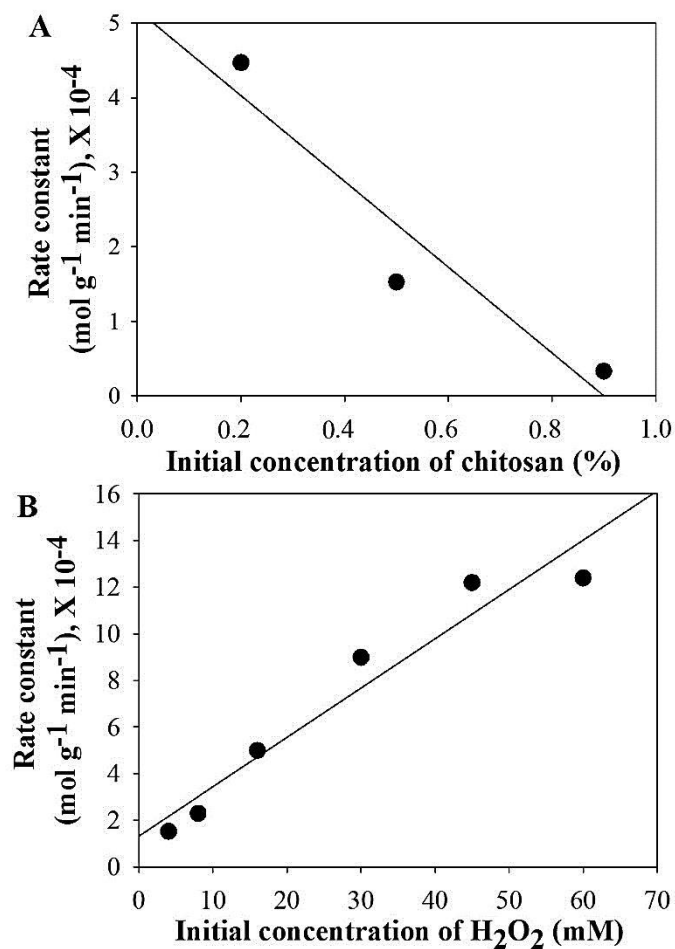


**Fig. A3 (A)** Rate constants as a function of initial chitosan concentrations for the chitosan degradation using the SP treatment with the addition of  $H_2O_2$  at a concentration of 4 mM and **(B)** Rate constants as a function of initial  $H_2O_2$  concentrations using the SP treatment for degradation of chitosan at initial chitosan concentration of 0.5%.

**Table A1** Properties of the degraded chitosan obtained by degradation of chitosan at a concentration of 0.5 % by the SP treatment in combination with H<sub>2</sub>O<sub>2</sub> at a concentration of 60 mM for 60 min and was fractionated by adding water-ethanol mixture solutions having different ratios of water to ethanol.

H <sub>2</sub> O:EtOH	<i>M<sub>w</sub></i> (kDa) {PDI}* <sup>*</sup>	% DD	Water-soluble	Yield (%)
1:1	12.03{2.9}	91.3	Insoluble	5.0 ±0.1
1:3	4.92{3.0}	79.3	Partially soluble	32.5 ±0.5
1:5	1.44{1.4}	80.6	Completely soluble	23.3 ±1.5
<b>Total recovery yield</b>				60.8 ±1.2

\*Determination by GPC measurement.

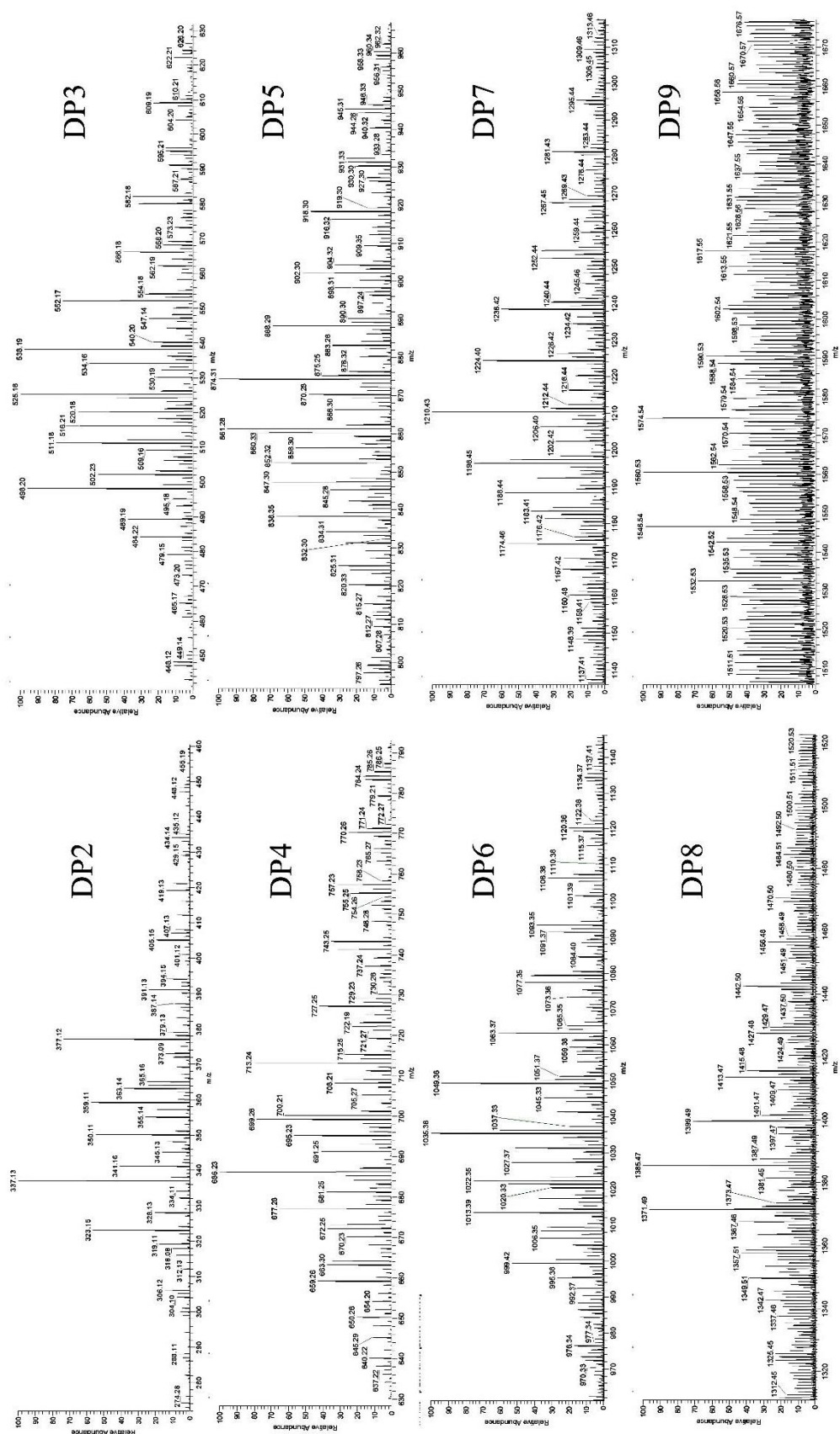


**Table A2** Assigned ion composition found in COS3 fraction having average molecular weight of 1.44 kDa as determined by ESI-MS. “G” refers to D-glucosamine unit (m = 161.06) and “A” refers to N-acetyl-D-glucosamine unit (m = 203.07).

$m/z$	Adduct ion	$M_w$	Attribution	(End)
323.15	H+	322	2G-H <sub>2</sub> O	
337.13	H+	336	2G-2H <sub>2</sub>	
341.16	H+	340	2G	(H <sub>2</sub> O)
350.11	Na+	327	2G-CH <sub>2</sub> O-NH <sub>2</sub>	
355.14	H+	354	2G-H <sub>2</sub> +O	
359.11	Na+	336	2G-2H <sub>2</sub>	
363.14	Na+	340	2G	(H <sub>2</sub> O)
364.09	Na+	341	2G-H <sub>2</sub> -CO+NOH	
365.16	H+	364	AG-H <sub>2</sub> O	
377.12	Na+	354	2G-H <sub>2</sub> +O	
391.13	Na+	368	2G+CO	
405.15	Na+	382	AG	(H <sub>2</sub> O)
419.13	Na+	396	AG-H <sub>2</sub> +O	
421.13	Na+	398	AG+O	
434.14	Na+	411	AG-H <sub>2</sub> +NOH	
435.12	Na+	412	AG+CH <sub>2</sub> O	
448.12	Na+	425	AG-2H <sub>2</sub> +NOH+O	
484.22	H+	481	3G-H <sub>2</sub> O	
498.20	H+	488	3G-2H <sub>2</sub>	
502.23	H+	501	3G	(H <sub>2</sub> O)
511.18	Na+	488	3G-CH <sub>2</sub> O-NH <sub>2</sub>	
516.21	H+	515	3G-H <sub>2</sub> +O	
520.18	Na+	497	3G-2H <sub>2</sub>	
525.16	Na+	502	3G-H <sub>2</sub> -CO+NOH	
538.19	Na+	515	3G-H <sub>2</sub> +O	



552.17	Na+	529	3G+CO	
566.18	Na+	543	A(2G)	(H <sub>2</sub> O)
582.18	Na+	559	A(2G)+O	
595.21	Na+	572	A(2G)-H <sub>2</sub> +NOH	
596.21	Na+	573	A(2G)+CH <sub>2</sub> O	
609.19	Na+	586	A(2G)-2H <sub>2</sub> +NOH+O	
645.29	H+	644	4G-H <sub>2</sub> O	
659.26	H+	658	4G-2H <sub>2</sub>	
663.30	H+	662	4G	(H <sub>2</sub> O)
672.25	Na+	649	4G-CH <sub>2</sub> O-NH <sub>2</sub>	
677.28	H+	676	4G-H <sub>2</sub> +O	
681.25	Na+	658	4G-2H <sub>2</sub>	
686.23	Na+	663	4G-H <sub>2</sub> -CO+NOH	
699.26	Na+	676	4G-H <sub>2</sub> +O	
713.24	Na+	690	4G+CO	
727.25	Na+	704	A(3G)	(H <sub>2</sub> O)
<i>m/z</i>	Adduct ion	<i>M<sub>w</sub></i>	Attribution	(End)
743.25	Na+	720	A(3G)+O	
757.23	Na+	734	A(3G)+CH <sub>2</sub> O	
770.26	Na+	747	A(3G)-2H <sub>2</sub> +NOH+O	
820.33	H+	819	5G-2H <sub>2</sub>	
838.35	H+	837	5G-H <sub>2</sub> +O	
847.30	Na+	824	5G-H <sub>2</sub> -CO+NOH	
860.33	Na+	837	5G-H <sub>2</sub> +O	
861.28	Na+	838	5G+NOH-O	
874.31	Na+	851	5G+CO	
888.29	Na+	865	A(4G)	(H <sub>2</sub> O)
902.30	Na+	879	A(4G)+O-H <sub>2</sub>	

904.32	Na+	881	A(4G)+O	
918.30	Na+	895	A(4G)+CH <sub>2</sub> O	
931.33	Na+	908	A(4G)-2H <sub>2</sub> +NOH+O	
999.42	H+	998	6G-H <sub>2</sub> +O	
1006.35	Na+	983	6G-2H <sub>2</sub> -CO+NOH	
1013.39	H+	1012	6G+CO	
1021.33	Na+	998	6G-H <sub>2</sub> +O	
1022.35	Na+	999	6G+NOH-O	
1035.38	Na+	1012	6G+CO	
1049.36	Na+	1026	A(5G)	(H <sub>2</sub> O)
1063.37	Na+	1040	A(5G)+O-H <sub>2</sub>	
1065.35	Na+	1042	A(5G)+O	
1077.35	Na+	1054	A(5G)+CH <sub>2</sub> O-H <sub>2</sub>	
1079.35	Na+	1056	A(5G)+CH <sub>2</sub> O	
1093.35	Na+	1070	A(5G)-2H <sub>2</sub> +CH <sub>2</sub> O+H <sub>2</sub> O	
1106.38	H+	1083	(2A)(4G)+NOH+3H <sub>2</sub>	
1120.36	Na+	1119	(2A)(4G)+NOH-H <sub>2</sub>	
1134.37	Na+	1111	(2A)(4G)+NOH-2H <sub>2</sub> +O	
1160.48	H+	1159	7G-H <sub>2</sub> +O	
1167.42	Na+	1144	7G-2H <sub>2</sub> -CO+NOH	
1174.48	H+	1173	7G+CO	
1188.44	Na+	1165	7G+H <sub>2</sub> O+H <sub>2</sub>	
1196.45	Na+	1173	7G+CO	
1210.43	Na+	1187	A(6G)	(H <sub>2</sub> O)
1224.40	Na+	1201	A(6G)+O-H <sub>2</sub>	
1226.42	Na+	1203	A(6G)+O	
1238.42	Na+	1215	A(6G)+CH <sub>2</sub> O-H <sub>2</sub>	
1240.44	Na+	1217	A(6G)+CH <sub>2</sub> O	
1252.44	Na+	1229	A(6G)-2H <sub>2</sub> +CH <sub>2</sub> O+O	
1254.44	Na+	1231	A(6G)-2H <sub>2</sub> +CH <sub>2</sub> O+H <sub>2</sub> O	

1267.13	Na+	1244	(2A)(5G)+NOH+3H <sub>2</sub>
1281.43	Na+	1280	(2A)(5G)+NOH-H <sub>2</sub>
1295.00	Na+	1272	(2A)(5G)+CH <sub>2</sub> O+H <sub>2</sub> O-2H <sub>2</sub>

<i>m/z</i>	Adduct ion	<i>M<sub>w</sub></i>	Attribution	(End)
1357.51	Na+	1335	8G+CO	
1371.49	Na+	1348	A(7G)	(H <sub>2</sub> O)
1385.47	Na+	1362	A(7G)+O-H <sub>2</sub>	
1387.49	Na+	1364	A(7G)+O	
1399.49	Na+	1376	A(7G)+CH <sub>2</sub> O-H <sub>2</sub>	
1401.47	Na+	1378	A(7G)+CH <sub>2</sub> O	
1413.47	Na+	1390	A(7G)-2H <sub>2</sub> +CH <sub>2</sub> O+O	
1415.48	Na+	1392	A(7G)-2H <sub>2</sub> +CH <sub>2</sub> O+H <sub>2</sub> O	
1442.50	Na+	1441	(2A)(6G)+NOH-H <sub>2</sub>	
1456.48	Na+	1433	(2A)(6G)+CH <sub>2</sub> O+H <sub>2</sub> O-2H <sub>2</sub>	
1470.50	Na+	1469	(3A)(5G)+NOH-OH	
1532.53	Na+	1510	A(8G)	(H <sub>2</sub> O)
1546.54	Na+	1524	A(8G)+O	
1548.54	Na+	1526	A(8G)+CH <sub>2</sub> O-H <sub>2</sub>	
1560.53	Na+	1538	A(8G)+CH <sub>2</sub> O	
1562.54	Na+	1540	A(8G)-2H <sub>2</sub> +CH <sub>2</sub> O+O	
1574.54	Na+	1552	A(8G)-2H <sub>2</sub> +CH <sub>2</sub> O+O	

Acetylated unit (A <sub>n</sub> )	Percent abundance of each distribution region (%)							
	DP2	DP3	DP4	DP5	DP6	DP7	DP8	DP9
A <sub>0</sub>	85	86	78	67	52	36	8	-
A <sub>1</sub>	15	14	22	33	40	54	75	100
A <sub>2</sub>	-	-	-	-	8	10	17	-

Note: “n” = number of acetylated units in each fragment of chitooligosaccharide.

## References

Zhou, W., DeLisio, J. B., Li, X., Liu, L., & Zachariah, M. R. (2015). Persulfate salt as an oxidizer for biocidal energetic nano-thermites. *Journal of Materials Chemistry A*, 3(22), 11838-11846.

# Facile preparation of chitooligosaccharides by degradation of chitosan powder dispersed in dilute salt solutions via electrical discharge plasma and their cytotoxicity evaluation against cancer cell lines and normal cells

*Chayanaphat Chokradjaroen<sup>a</sup>, Sewan Theeramunkong<sup>b</sup>, Hiroharu Yui<sup>c</sup>,  
Nagahiro Saito<sup>d</sup> and Ratana Rujiravanit<sup>a,e\*</sup>*

*<sup>a</sup>The Petroleum and Petrochemical College, Chulalongkorn University, Bangkok 10330, Thailand*

*<sup>b</sup>Faculty of Pharmacy, Thammasat University, Pathumthani 12120, Thailand*

*<sup>c</sup>Department of Chemistry, Tokyo University of Science, Tokyo 162-8601, Japan*

*<sup>d</sup>Department of Chemical Systems Engineering, Graduate School of Engineering, Nagoya University, Nagoya 464-8603, Japan*

*<sup>e</sup>Center of Excellence on Petrochemical and Materials Technology, Chulalongkorn University, Bangkok 10330, Thailand*

KEYWORDS: chitosan, degradation, electrical discharge plasma, chitooligosaccharides, cancer cells

**ABSTRACT:** Chitooligosaccharides, which obtain from degradation of chitosan, possess some interesting molecular weight-dependent biological properties, especially anticancer activity. Therefore, the conversion of chitosan to chitooligosaccharides with specific molecular weight has been continuously investigated in order to find effective strategies that can achieve both economic feasibility and environmental concerns. In this study, a novel process was developed to heterogeneously degrade chitosan powder by highly active species generated by electrical discharge plasma in a dilute salt solution (0.02 M) without the addition of other chemicals. The degradation rate obtained from the proposed process was comparable to that obtained from some other methods with the addition of acids and oxidizing agents. Separation of the water-soluble degraded products containing chitooligosaccharides from the reaction solution was simply done by filtration. The obtained chitooligosaccharides were further evaluated for an influence of their molecular weights on cytotoxicity against cancer cells and the selectivity toward cancer and normal cells.

## **Introduction**

Chitooligosaccharides (COS), which have received much attention owing to their inherently biological properties, can be produced from degradation of chitosan.<sup>1,2</sup> Chitosan is a polysaccharide derived from chitin that is the second most abundant natural polymer next to cellulose.<sup>3</sup> Chitosan is obtained by a partial deacetylation of chitin, which can be found in exoskeletons of crustaceans; for instance, squid pen, crab and shrimp shells.<sup>4-6</sup> Chitosan is a copolymer of randomly distributed  $\beta$ -(1 $\rightarrow$ 4)-linked 2-acetamido-2-deoxy-D-glucose and 2-amino-2-deoxy-D-glucose. The presence of the amino/acetamido groups at the C2 position in the pyranose ring of chitosan cause its positively charged character which is responsible for its versatile properties including flocculation, metal chelation and outstanding biological properties.<sup>7,8</sup> However, native chitosan has a high molecular weight which results in its

insolubility in water and when it can be dissolved in suitable acidic solutions, a high viscous solution is obtained.<sup>7</sup> Therefore, several studies in the field of chitosan have focused on preparation of a water-soluble form of the degraded chitosan, especially COS.<sup>9-11</sup> COS have not only the improved water solubility, but also the better biological properties, compared with intact chitosan. Biological properties of chitosan and COS reported in the literature have been summarized in the supporting information (Table S1). According to the studies in the past, COS have been reported on their potential as an alternative choice for cancer treatments.<sup>12,13</sup>

Degradation of chitosan can be generally accomplished by three main distinct methods that are chemical,<sup>14,15</sup> enzymatic<sup>1,16</sup> and physical degradation.<sup>17-19</sup> Nowadays, due to an increase in environmental concerns, alternative technologies have been developed and adopted to degradation of chitosan. Physical degradation by applying different types of energy such as microwave, gamma radiation, ultraviolet, and sonication have recently been of interest, because they have been found to reduce the chemical use in the degradation process, leading to a low risk of chemical contamination in degraded products.<sup>20,21</sup> Another emerging technology that can lead to an environmentally friendly process for a preparation of low-molecular-weight polymer products is plasma technology.

Plasma, in physics, is a state of matter comprising a collection of charged particles, both positive and negative, radicals and free electron that behave in a collective way because of attractive and repelling electric forces. Examples of plasma found in nature are lightening and aurora. Plasma can be artificially created by adding energy like an electric field to a pair of electrodes. And then electrons, that come out from the electrode by electrical potential, collide to the nearby molecules, resulting in the formation of various reactive species, *e.g.* negatively charged and positively charged particles, radicals and free electrons that would be useful in chemical reactions. Recently, the electrical discharge plasma in a liquid phase

generated by using a bipolar-pulsed power supply has been developed and used in various applications including polymer degradation.<sup>22,23</sup> Owing to the operation of bipolar-pulsed power supply, the plasma can be continuously generated at atmospheric pressure and ambient temperature. When the electricity flows to the tips of electrodes which are immersed in a solution, some molecules nearby the electrodes are continuously collided by the electrons, leading to the formation of highly active species (*e.g.*  $\text{H}_2\text{O} \rightarrow \bullet\text{H}, \bullet\text{O}, \bullet\text{OH}, \text{H}^-, \text{and } \text{O}^-$ ).<sup>24</sup> These highly active species have played an important role in the green synthesis of noble metal and bimetallic nanoparticles without the addition of any reducing agents,<sup>25-27</sup> the synthesis of carbon nanoparticles,<sup>28,29</sup> and the deposition of metal nanoparticles on supporting materials.<sup>30,31</sup> In addition, the highly active species generated by the electrical discharge plasma in a solution have been reported to be a powerful tool for degradation of various compounds, such as organic dyes,<sup>24</sup> synthetic<sup>32</sup> and natural polymers including cellulose,<sup>33</sup> alginate,<sup>34</sup> and chitosan.<sup>2,22,35,36</sup>

Since COS are high-value products possessing the potential of anticancer activity, the production of COS from chitosan, which involves not only degradation but also separation and purification processes, has received much attention in aiming at a large-scale production of COS. Normally, chitosan is dissolved in an acetic acid solution in order to obtain chitosan solution before going ahead with the degradation. Even in the studies of using the physical degradation methods such as microwave, sonication and plasma processes, chitosan solutions were used to prepare the low-molecular-weight products or COS.<sup>20,22,37,38</sup> The degradation of chitosan solution is generally followed by the troublesome separation processes in order to separate COS from the remaining high-molecular-weight chitosan because chitosan and COS are dissolved together in the same solution. Owing to the use of acetic acid solution for dissolving chitosan, the further neutralization by NaOH is required to neutralize the reaction solution and also precipitate the remaining high-molecular-weight chitosan from the COS.



Moreover, the purification step is necessary in order to obtain COS without any contaminants.<sup>37,39</sup> In this study, chitosan powder was degraded to produce COS by using the plasma treatment in the absence of hazardous chemicals at ambient temperature and atmospheric pressure. Chitosan flakes were firstly pulverized to powder by using a ball mill and then chitosan powder dispersed in an aqueous solution containing an inorganic salt, *e.g.* Na<sub>2</sub>SO<sub>4</sub>, NaCl and NaNO<sub>3</sub>, at a very dilute concentration (0.02 M) prior to the degradation by the electrical discharge plasma in the suspension of chitosan powder using a bipolar-pulsed power supply. It has been reported that ball milling process could lead to a considerable reduction in particle size and crystallinity of a polysaccharide, which should result in a significant increase in efficiency of degradation.<sup>40,41</sup> In addition, the presence of inorganic salts could interrupt the hydrogen-bonding networks inside the polymer chains and enhance the degradation of a polysaccharide such as cellulose.<sup>42</sup> Therefore, it had been expected that the plasma treatment can be used to degrade chitosan powder dispersed in dilute inorganic salt solutions and effectively produce COS products. Furthermore, only simple separation and purification processes could be performed in order to obtain COS, because of the use of heterogeneous reaction in the degradation process. Regarding the test on the biological properties of the COS products, the cytotoxicity of COS against both cancer and normal cells was examined in order to study the effects of COS concentrations and molecular weights of COS. In this study, a method for the simple production of COS by applying plasma technology in heterogeneous degradation of chitosan powder without the use of hazardous chemicals has been proposed. This may encourage further exploration of scaling up to an industrial production of COS for being used as an alternative for the cancer treatment or other medical uses.

## Experimental section

### Experimental setup and production procedure

The details on all chemicals used in this work were described in the supporting information. Chitosan powder was dispersed in 50-ml dilute salt solutions, *i.e.* NaCl, NaI, NaNO<sub>3</sub>, Na<sub>2</sub>SO<sub>4</sub>, CaCl<sub>2</sub>, MnCl<sub>2</sub> and CeCl<sub>3</sub>, at a concentration of 0.02 M containing in a plasma reactor with vigorously stirring by a magnetic stirrer for 5 min at room temperature. The plasma reactor was adapted from a 100-ml glass beaker equipped with two 1-mm-diameter tungsten electrodes; purity 99.9%; Nilaco Corp., Japan (Scheme 1). The plasma was discharged in the solution at the gap between the tips of tungsten electrodes by using a high frequency bipolar pulsed power supply (Kurita-Nagoya MPS-06K06C). The distance between the tips of electrodes was 0.75 mm. The operating pulse width, frequency and voltage were fixed at 2  $\mu$ s, 20 kHz and 1.92 kV, respectively. During the plasma treatment, the suspension was constantly stirred by a magnetic stirrer to maintain the uniformity of the suspension and the reaction temperature is approximately 70 °C.

After the plasma treatment, the solid residue of water-insoluble chitosan was removed by simple filtration using filter papers and then the filtrate was fractionated by using a centrifugal ultrafiltration. The molecular weight cut-off (MWCO) of membranes in the centrifugal ultrafilter units (Amicon® Ultra 4ml) were  $3 \times 10^3$  and  $10 \times 10^3$  Da, respectively. The water-soluble degraded product that did not pass through the membrane having MWCO of  $10 \times 10^3$  Da was assigned as COS1. The water-soluble degraded product that pass through the membrane having MWCO of  $10 \times 10^3$  Da but did not pass out through the membrane having MWCO of  $3 \times 10^3$  Da was assigned as COS2. The water-soluble degraded product that passed through the membrane having MWCO of  $3 \times 10^3$  Da was assigned as COS3. All fractions were freeze-dried and kept in a desiccator for further uses.

## Characterization

The changes of the number-average molecular weight ( $M_n$ ), weight-average molecular weight ( $M_w$ ) and polydispersity index (PDI) of the water-soluble degraded products of chitosan obtained after the plasma treatment were determined by gel permeation chromatography (GPC; Shimadzu CTO-10A). The GPC instrument which was equipped with a refractive index (RI) detector, was connected to the ultra-hydrogel linear column (Water 600E), with molecular weight resolving range of  $1.0 \times 10^3$ – $2.0 \times 10^7$  Da. The mobile phase was an acetate buffer solution consisting of 0.5 M acetic acid and 0.5 M sodium acetate at pH 4.5. The degraded products at a concentration of 3 mg/ml in the acetate buffer solution were filtrated through a syringe filter containing nylon 66 membrane with a pore size of 0.45  $\mu$ m. Then 40- $\mu$ l of the filtrated solution was injected with the operating flow rate at 0.6 ml/min and the temperature at 40 °C. Pullulans with  $M_w$  in the range of  $1.32 \times 10^3$ – $8.05 \times 10^5$  Da were used as standard samples. The changes of chemical structure of chitosan before and after the plasma treatment were detected by Fourier-transform infrared spectroscopy (FT-IR; Nicolet NEXUS 670) using 64 scans with a correction for atmospheric carbon dioxide (CO<sub>2</sub>). Samples for FTIR analysis were prepared as KBr pellets. A 500-MHz nuclear magnetic resonance spectroscopy (NMR; Bruker AVANCE III) was also used for characterization of COS fractions. The COS samples were dissolved in D<sub>2</sub>O and CD<sub>3</sub>COOD/D<sub>2</sub>O at a concentration in the range of 10–30 mg/ml. The crystalline structures of original chitosan powder as well as the degraded products were investigated by using X-ray diffraction (XRD; Rigaku Smartlab) with Cu K $\alpha$  radiation. Particle size of chitosan powder before and after the plasma treatment was examined by using a particle size analyzer (Malvern MasterSizer 3000). A volume mean diameter (D[4,3]) was then determined. Morphology of the original chitosan powder and the degraded chitosan products were examined by using field emission scanning electron microscope (FE-SEM; JEOL JSM-7610F). Electrospray ionization mass

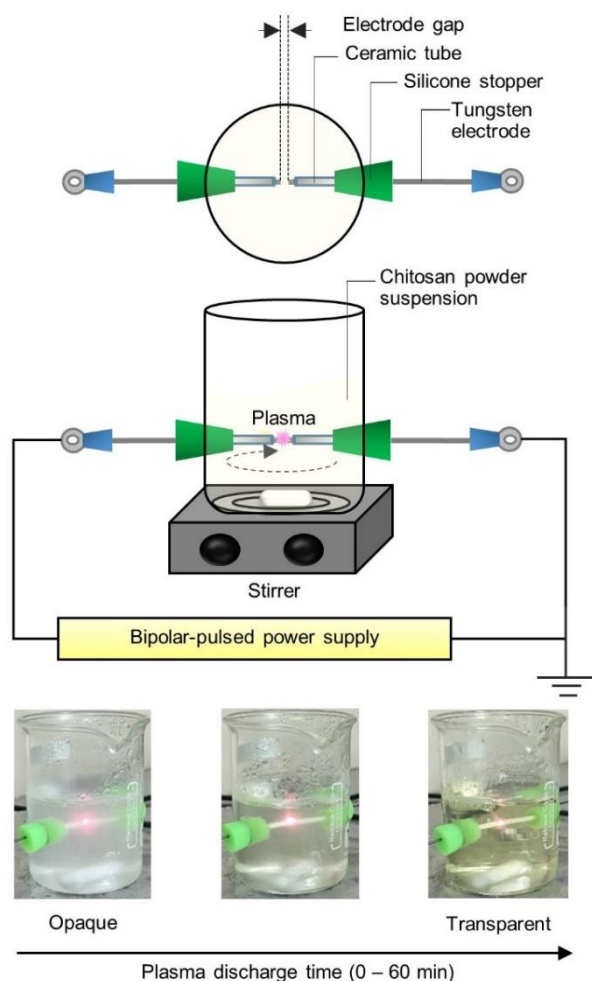
spectrometry (ESI-MS; Exactive Orbitrap), was used to analyze the masses of the COS fractions. 100  $\mu$ l of the 1 mg/ml sample solution was diluted with 800  $\mu$ l water and then mixed with 200  $\mu$ l of methanol before infusing directly into the ESI source with a flow rate of approximately 10  $\mu$ l/min. Sheath, auxiliary and sweep gases were N<sub>2</sub> gas set at 10, 1, and 1 psi, respectively. Spray voltage was 4.2 kV. Capillary temperature and voltage were set at 200 °C and 10 V, respectively. Tube lens voltage was 180–250 V. Skimmer voltage was 13 V. The emission spectra from the electrical discharge plasma in the suspension were analyzed by using an optical emission spectrometer according to Banno, et al.<sup>43</sup>

### **Cytotoxicity test**

For the tested cell culture, human uterine cervix cancer cell line (HeLa cells), human breast adenocarcinoma cell line (MCF-7 cells), human lung cancer cell line (H460 cells) and Medical Research Council cell strain 5 (MRC-5 cells) were used in cytotoxicity test of the COS samples. The procedure for the cell culture was explained in the supporting information. For the cytotoxicity test, MTT assay was used. Firstly, cells were seeded into 96-well plates at approximately 10<sup>4</sup> cells per well and grown for 24 h. Then, different concentrations of COS samples were added. After 24 h of the treatment with COS samples, all supernatant was discarded and MTT (3-(4,5-Dimethylthiazol-2-yl)-2,5-Diphenyltetrazolium Bromide) solution (0.5 mg/ml) was added, followed by incubation at 37 °C for 3 h. Subsequently, the supernatant was completely removed and DMSO was added to dissolve the formazan crystals. The absorbance (A) of each well was measured at 570 nm in a microplate reader (Varioskan™ Flash Multimode Reader). Doxorubicin was used as positive control. All experiments were performed in triplicate and repeated for three experiments (n = 3). The relative cell viability was expressed as a percentage relative to the untreated control cells and calculated by the following equation:

$$\text{Cell viability (\%)} = 100 \times |(A_{\text{treated}} - A_{\text{blank}})/(A_{\text{untreated}} - A_{\text{blank}})| \quad (1)$$

After the percentage of cell viability was calculated and plotted, a half maximal inhibitory concentration (IC<sub>50</sub>) value was determined. The induction of apoptosis in a cancer cell line by the COS products obtained in this work was also examined by FITC-Annexin V/propidium iodide (PI) double staining. At the beginning, the treated cells were harvested and washed with a cold phosphate buffer saline (PBS) solution twice. The cells were then stained with FITC-annexin V and PI by following the manufacturer's instructions (FITC Annexin V Apoptosis Detection Kit; BD Pharmingen) and analyzed in a flow cytometer (BD FACS Verse™). The data were collected with BD FACSuite™ software for 10<sup>4</sup> cells in each sample.



**Scheme 1** Experimental setup of the plasma equipment and the change in turbidity of the suspension containing chitosan powder dispersed in the dilute salt solution as a function of plasma treatment time.

## Results and discussion

### Degradation of chitosan

The heterogeneous degradation of chitosan powder dispersed in the dilute salt solutions (*i.e.* NaCl, NaI, NaNO<sub>3</sub>, Na<sub>2</sub>SO<sub>4</sub>, CaCl<sub>2</sub>, MnCl<sub>2</sub> and CeCl<sub>3</sub>) by applying the plasma treatment was conducted in comparison with the homogeneous degradation of chitosan solution, prepared by dissolving chitosan in 0.5% acetic acid solution, under the corresponding plasma operating condition. The chitosan powder could disperse well in the inorganic salt solutions

during the degradation reaction by simple stirring using a magnetic stirrer. The turbidity of chitosan suspension before the degradation and the transparency of the degraded chitosan solution after the plasma treatment for 60 min could be observed (Scheme 1). According to the GPC measurement,  $M_w$  and PDI of the degraded products of both chitosan powder and chitosan solution after the plasma treatment dramatically decreased (Table 1). The degradation of chitosan powder dispersed in the various salt solutions by applying the plasma treatment for 60 min could dramatically reduce the  $M_w$  of chitosan by approximately 95–98%. On the other hand, the  $M_w$  of chitosan solution was reduced by approximately 96%. It might be concluded that molecular weight reduction of chitosan powder dispersed in the dilute salt solutions by the plasma treatment was comparable to that of chitosan solution obtained under the corresponding plasma operating condition. Furthermore, this evidence suggested that the plasma treatment is an effective tool for facilitating the heterogeneous degradation of chitosan powder, even in the absence of the hazardous chemicals such as acids and oxidizing agents. Moreover, the production of COS from the heterogeneous degradation of chitosan powder dispersed in the dilute salt solutions was more facile, less time-consuming and less chemical wastes than that obtained from the homogeneous degradation of chitosan solution as demonstrated in the flowcharts in supporting information (Figure S1).

**Table 1**  $M_w$  and PDI of the degraded products of chitosan obtained after the plasma treatment of 0.2% (w/v) chitosan solution dissolved in 0.5% (v/v) acetic acid solution and 0.2% (w/v) chitosan powder dispersed in various salt solutions having a concentration of 0.02 M at different plasma treatment time intervals

Plasma treatment time (min)	$M_w$ (kDa) {PDI}							
	Chitosan solution	Chitosan powder						
		NaCl	NaI	NaNO <sub>3</sub>	Na <sub>2</sub> SO <sub>4</sub>	CaCl <sub>2</sub>	MnCl <sub>2</sub>	CeCl <sub>3</sub>
0	1200.0	800.0	800.0	800.0	800.0	800.0	800.0	800.0
	{2.4}	{3.3}	{3.3}	{3.3}	{3.3}	{3.3}	{3.3}	{3.3}
10	159.8	201.6	218.1	188.6	98.3	167.0	405.0	788.0
	{3.3}	{4.7}	{5.3}	{4.9}	{21.8}	{5.5}	{5.0}	{7.9}
20		69.6	142.5	67.9	40.7	78.8	200.0	663.8
		{5.5}	{5.6}	{5.6}	{11.4}	{6.3}	{5.8}	{6.6}
30	106.6	41.8	122.8	36.8	25.0	49.7	115.2	400.3
	{4.2}	{5.8}	{6.1}	{5.9}	{7.6}	{5.7}	{9.0}	{5.7}
45		26.2	79.5	25.4	5.2	26.5	69.0	143.3
		{7.6}	{5.4}	{6.9}	{3.1}	{6.4}	{10.1}	{4.9}
60	44.5	5.0	75.3	5.7	3.4	16.9	33.4	37.5
	{2.7}	{2.8}	{6.9}	{3.2}	{2.5}	{4.8}	{8.4}	{11.1}

The changes in  $M_w$  of the degraded chitosan obtained from the degradation of chitosan powder and chitosan solution by the plasma treatment were measured as a function of plasma treatment time (Table 1). At the beginning of the degradation reaction (0–10 min), the  $M_w$  of chitosan dramatically decreased and then kept on gradually decreasing with the increasing of plasma treatment time, until reached at 60 min. This phenomenon could be explained by the evidence from XRD analysis (Figure 1). The XRD result of the chitosan powder before the plasma treatment indicated that the original chitosan powder contained both amorphous and crystalline structures. The characteristic peaks, at  $2\theta = 10^\circ$  and  $21^\circ$ , of the degraded chitosan at 10 min of the plasma treatment became sharper than that obtained from the original chitosan powder, suggesting the former degradation of the amorphous region. However, at the longer plasma treatment time, the peaks became smaller and eventually almost disappeared, indicating the subsequent degradation of the remaining crystalline region.



According to the previous studies,<sup>39,44</sup> an amorphous region in semicrystalline polymers is more sensitive to degradation than a crystalline region. Therefore, the amorphous region was firstly degraded and dissolved in the reaction medium, while the crystalline region was gradually degraded and took longer time to completely dissolve. To further investigate, the morphology of the chitosan powder during the degradation by the plasma treatment was determined by using FE-SEM (Figure 1). According to the FE-SEM images, the original chitosan powder was a dense chunk. After the plasma treatment for 10 min, the FE-SEM image of the chitosan powder obviously revealed some layers which might belong to crystalline region of chitosan. The layers started to peel off from each other as increasing the plasma treatment time and this could lead to the expansion of particle sizes of chitosan powder. Finally, the layers were completely separated from each other and eventually a ribbon-like structure was observed after 60 min of the plasma treatment. The particle sizes of chitosan powder before and after the plasma treatment were also determined by using a particle size analyzer (Figure 1). The volume mean diameter ( $D[4,3]$ ) of the original chitosan powder was 154  $\mu\text{m}$  and increased to 168.3  $\mu\text{m}$  and 175.3  $\mu\text{m}$  after the plasma treatment for 10 min and 30 min, respectively.

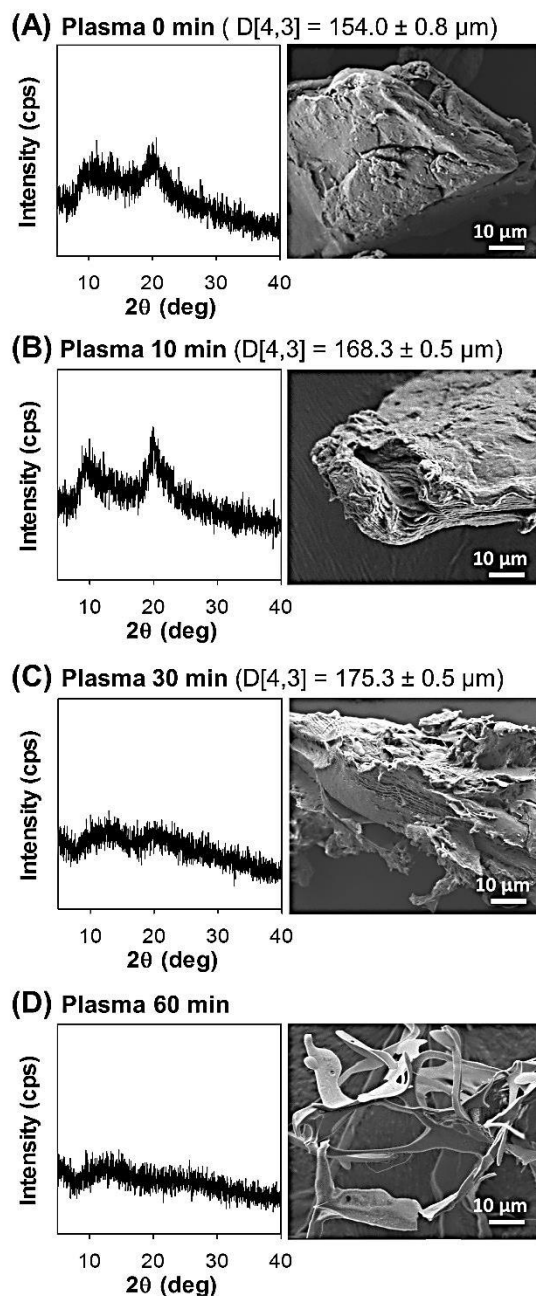


**Figure 1** XRD patterns, FE-SEM images and volume mean diameter ( $D[4,3]$ ) of (A) the original chitosan powder and the degraded products of chitosan obtained after the degradation of 0.2% (w/v) chitosan powder dispersed in 0.02 M NaCl solution at the plasma treatment time of (B) 10 min, (C) 30 min and (D) 60 min.

The changes in the  $M_w$  and PDI of chitosan as a function of the reaction time by the plasma treatment with the addition of different inorganic salts were also investigated (Table

1). The result suggested that the degradation of chitosan powder by the plasma treatment was affected by the presence of inorganic salts in the reaction solutions. It might be explained that the different types of inorganic salts led to the different dissociated ions in the solution. According to the  $M_w$  reduction, the presence of NaI,  $MnCl_2$  and  $CeCl_3$  in the reaction solutions resulted in the insufficient degradation of chitosan powder comparing to the others. The presence of NaI in the reaction solution was found to induce purple colour to the chitosan residues, as shown in the supporting information (Figure S2). Iodide ion ( $I^-$ ) was generated by the dissociation of NaI in the solution and could be oxidized to form iodine molecules.<sup>45</sup> Then, iodine molecules can form a charge-transfer complex with an amino group of chitosan and are responsible for the purple coloring of the complexes.<sup>46-48</sup> It might be a side reaction that could lower the degradation efficiency. In the cases of  $MnCl_2$  and  $CeCl_3$ , since they are a transition metal and a lanthanide, respectively, they have several oxidation states and can cause some redox reactions. These redox reactions could probably compete with the degradation reaction, leading to the lowering of the degradation efficiency.

The degradation kinetics were also determined by a linear relationship between the reversed  $M_w$  of chitosan and reaction time at the initial stage of the degradation (0–30 min) and the plots of graphs are shown in the supporting information (Figure S3). The rate constants of the degradation reactions were calculated by the following equation:

$$1/M_t = 1/M_0 + kt/m = 1/M_0 + k't \quad (2)$$

where  $M_t$  is the  $M_w$  of the chitosan sample at reaction time ( $t$ ),  $M_0$  is the initial  $M_w$  of the chitosan sample,  $t$  is the reaction time and  $m$  is the molecular weight of the monomer of chitosan.  $k$  ( $\text{min}^{-1}$ ) or  $k'$  ( $\text{mol}/(\text{g min})$ ) is the rate constant of the degradation reaction.<sup>49</sup> The obtained  $k$  values of the degradation reactions of chitosan powder dispersed in different salt solutions by the plasma treatment were determined and summarized in the supporting information (Table S2). With the addition of  $NaNO_3$ ,  $NaCl$  and  $CaCl_2$ , the  $k$  values were 1.25

$\times 10^{-4}$ ,  $1.12 \times 10^{-4}$ , and  $0.96 \times 10^{-4} \text{ min}^{-1}$ , respectively, while the addition of  $\text{Na}_2\text{SO}_4$  showed the relatively much higher  $k$  value of  $1.98 \times 10^{-4} \text{ min}^{-1}$ . On the other hand,  $\text{NaI}$  and  $\text{MnCl}_2$  exhibited relatively low  $k$  values at  $0.41 \times 10^{-4}$  and  $0.34 \times 10^{-4} \text{ min}^{-1}$ , respectively. Furthermore, the degradation of chitosan by the plasma treatment in the presence of  $\text{CeCl}_3$  showed the lowest  $k$  value which equaled to  $0.05 \times 10^{-4} \text{ min}^{-1}$ . Most of the  $k$  values obtained in this work were comparable to those reported in the literature using other degradation methods as reported in the supporting information (Table S2).

The chemical structures of the chitosan samples before and after the degradation by the plasma treatment in different salt solutions were confirmed by using FT-IR spectroscopy (Figure 2). In general, the characteristic peaks of the original chitosan powder are assigned to the  $-\text{OH}$  stretching at  $3450 \text{ cm}^{-1}$  and amide I at  $1655 \text{ cm}^{-1}$ .<sup>50-52</sup> The peak at the wavenumber of  $1375 \text{ cm}^{-1}$  is attributed to methyl group.<sup>42</sup> The peaks at the wavenumbers of  $1070 \text{ cm}^{-1}$  can be referred to  $\text{C}-\text{O}-\text{C}$  stretching.<sup>7</sup> All the degraded chitosan samples had the FT-IR spectra similar to that of the original chitosan powder. Degree of deacetylation (DD) of chitosan before and after the degradation was calculated by following the study of Baxter et al.,<sup>53</sup>  $\text{DD} = 100 - [115 \times (\text{A}_{1655}/\text{A}_{3450})]$  where A corresponds to the absorbance. The DD of original chitosan powder was calculated to be 65.5%, while the degraded chitosan obtained from the plasma treatment performing in the solutions containing various salts, *i.e.*  $\text{Na}_2\text{SO}_4$ ,  $\text{NaNO}_3$ ,  $\text{NaCl}$ ,  $\text{NaI}$ ,  $\text{CaCl}_2$ ,  $\text{MnCl}_2$  and  $\text{CeCl}_3$ , had the similar value of DD at approximately 65%. The results suggested that the plasma treatment could degrade chitosan powder dispersed in various inorganic salt solutions and caused a low impact to the chemical structure, including the acetamido and amino groups, of chitosan.

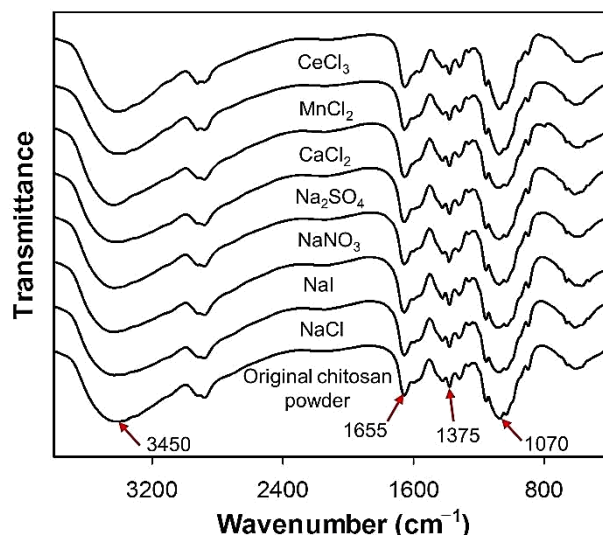


**Figure 2** FTIR spectra of the original chitosan powder and the degraded products obtained from the degradation of 0.2% (w/v) chitosan powder dispersed in different salt solutions at a concentration of 0.02 M by the plasma treatment for 30 min.

A possible mechanism of degradation of the chitosan powder dispersed in a dilute salt solution by applying the plasma treatment was proposed in this work (Figure 3). The preparation of chitosan powder by using a ball mill led to the reduction of both particle size and crystallinity of chitosan. When the chitosan powder was dispersed in a salt solution containing dissociated cations and anions, some hydrogen bonding networks existing inside the molecular chains of chitosan could be interrupted by the ionic species from salts according to the previous study.<sup>42</sup> The deterioration of hydrogen bonding networks in the chitosan powder would allow the penetration of free radicals, which were generated during plasma discharge, into the inner structure of chitosan powder which may subsequently facilitate the degradation of chitosan. In the suspension of chitosan powder, there were plenty of H<sub>2</sub>O molecules that can interact with reactive species generated during the discharge of plasma. As the result of the discharge of plasma in the solution, ionization and excitation of H<sub>2</sub>O molecules could occur and produce hydroxyl radicals (OH•) and hydrogen radicals (H•), which were detected by optical emission spectroscopy (OES) measurement (Figure 4).

Hydroxyl radicals have been reported as a significant free radical for the degradation of chitosan.<sup>3,39</sup> An hydroxyl radical possibly subtracted a hydrogen radical from the structure of chitosan, resulting in the eventually breaking down of the chitosan chain at  $\beta$ -1,4 glycosidic linkage, leading to the reduction of  $M_w$  of chitosan, as reported in the previous study.<sup>44</sup> The amorphous regions of chitosan were firstly degraded and dissolved into the solution, while the remaining crystalline regions of chitosan powder would swell and became separated into layers, followed by peeling off from each other as small fragments. With the prolonged reaction time, the small fragments of chitosan continuously underwent further degradation to attain shorter chains of chitosan and eventually dissolved into the solution. In addition, molecular chains of chitosan could possibly be interacted by free electrons generated from the discharge of plasma, causing the degradation of chitosan as well.

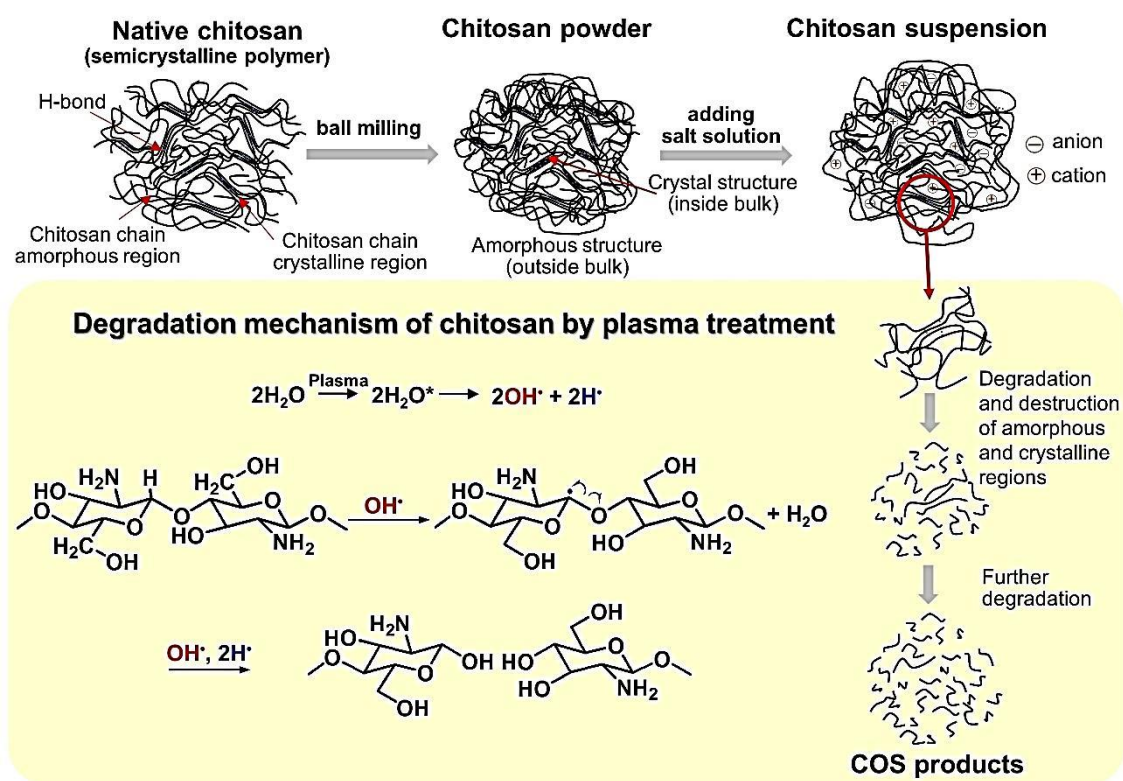


**Figure 3** Illustration of a possible degradation mechanism of chitosan powder dispersed in salt solutions by hydroxyl radicals generated by the electrical discharge plasma.

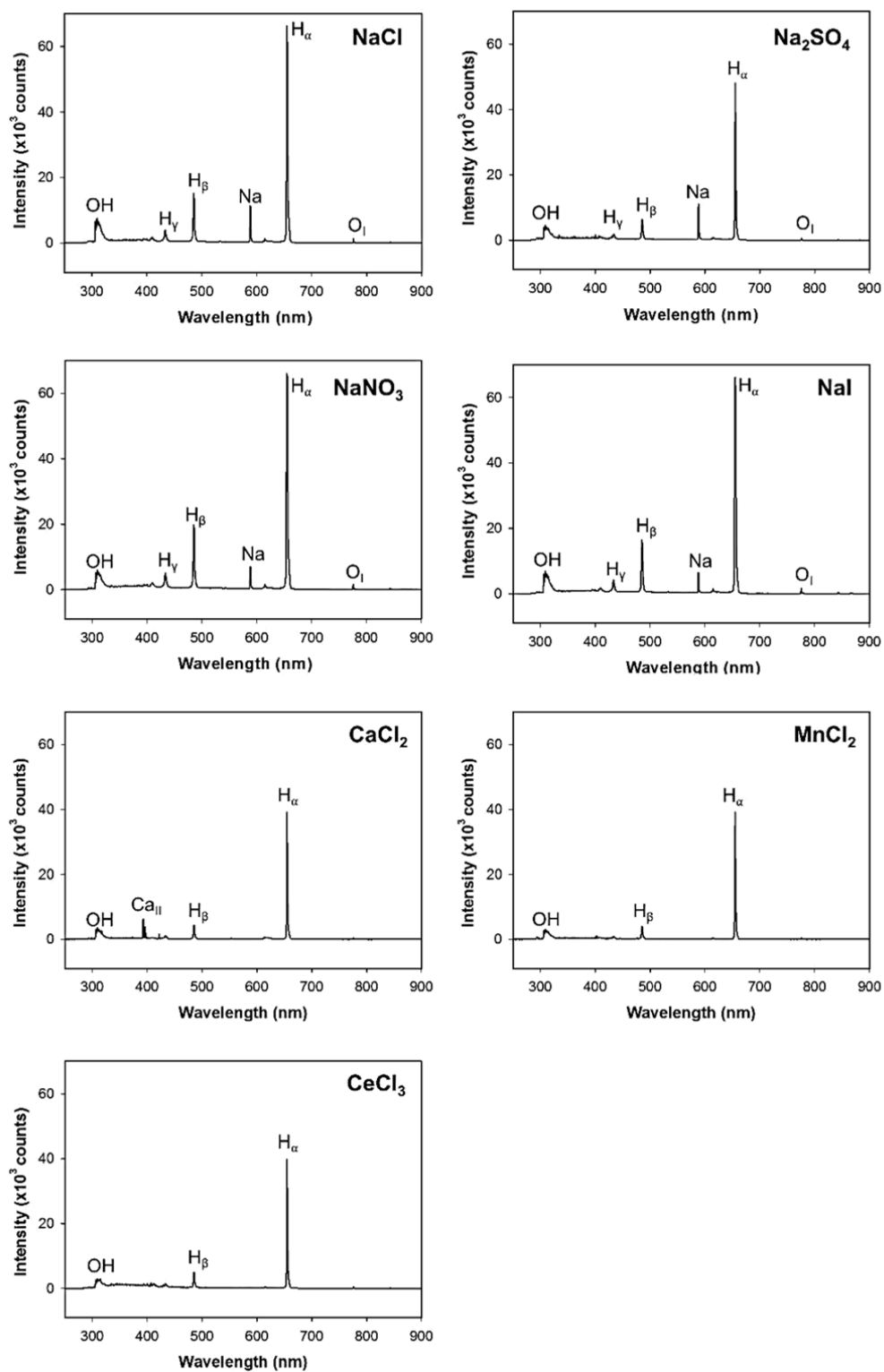


**Figure 4** Emission spectra from the electrical discharge plasma occurring in the solutions containing different inorganic salts at a concentration of 0.02 M.

## Characterization and cytotoxicity test of the COS products

By considering production efficiency and cost, NaCl seems to be the most suitable salt for the production of COS by degradation of chitosan powder dispersed in the dilute salt solution with the aid of the plasma treatment. After the plasma treatment in the presence of NaCl, the chitosan residue containing water-insoluble fraction was filtrated, and the filtrate containing water-soluble products of chitosan was further fractionated into three fractions, *i.e.* COS1, COS2 and COS3, by using centrifugal ultrafiltration membranes having MWCO equal to  $3 \times 10^3$  and  $10 \times 10^3$  Da. The COS products were freeze-dried prior to the determination of their production yields (Table 2). The total production yield was approximately 80% which included COS1 having  $M_w$  of  $11.2 \times 10^3$  Da (32.5%), COS2 having  $M_w$  of  $2.8 \times 10^3$  Da (35.3%), and COS3 having  $M_w$  of  $1.3 \times 10^3$  Da (14%). The chemical structures of the COS products were investigated by  $^1\text{H-NMR}$ , as shown in the supporting information (Figure S4 (A)–(D)). Chemical structures of COS1 and COS2 showed no major change from that of the original chitosan after the degradation and fractionation processes, while the COS3 had some changes in the chemical structure due to the ring-opening reaction of its constituent monomeric units.<sup>54</sup> Besides, degrees of deacetylation (DD) of the COS1, COS2, and COS3 were calculated to be 65%, 67% and 70%, respectively. COS2 and COS3, which had  $M_w$  less than 5000 Da and had narrow PDI, could be further characterized by ESI-MS in order to identify their degree of polymerization (DP), as shown in the supporting information (Figure S4 (E)–(F)). COS2 had DP ranging from 1 to 6, being composed of not only fully deacetylated sequences but also mono-, di-, tri-, tetra-, penta-, and fully acetylated COS. The major oligosaccharides in COS2 fraction were oligosaccharides containing mono- and di-acetylated units. DP of COS3 was found to be 2 to 5 with mono-acetylated COS as the major composition.



**Table 2**  $M_n$ ,  $M_w$ , PDI, production yields, water solubility and DD of the fractionated COS products.

Fractions	$M_n$ ( $\times 10^3$ Da)	$M_w$ ( $\times 10^3$ Da)	PDI	Yield (%)	DD* (%)
COS1	$2.82 \pm 0.03$	$11.22 \pm 0.56$	$3.10 \pm 0.68$	$32.5 \pm 4.2$	65
COS2	$1.51 \pm 0.06$	$2.83 \pm 0.11$	$1.30 \pm 0.11$	$35.3 \pm 5.6$	67
COS3	$0.96 \pm 0.01$	$1.32 \pm 0.06$	$1.10 \pm 0.24$	$14.0 \pm 7.3$	70

\*The values of DD were determined by  $^1\text{H-NMR}$  as shown in supporting information (Figure S4).

The obtained COS products were evaluated for their cytotoxicity on cancer cells (Figure 5). The percentages of cell viability were measured by comparing the cells treated and untreated with the COS products. The influence of the  $M_w$  of COS products was firstly investigated by treating HeLa cells with the COS samples at different concentrations ranging 0.1–5 mg/ml. Both COS2 and COS3, which had the lower  $M_w$  than COS1, could significantly inhibit the cell growth compared to COS1 (Figure 5(A)). The result was in good agreement with the previous study reporting that COS with the lower  $M_w$  could effectively inhibit the growth cancer cells such as PC3 (prostate cancer cell), A549 (lung cancer cell), and HepG2 (hepatoma cell) than COS with the high  $M_w$ .<sup>55</sup> According to the obtained results, COS2 should be the best choice for the further investigation for its cytotoxicity on other cancer cells including MCF-7 and H460 cells, doing in comparison with that of a normal cell, MRC-5 (Figure 5(B)). The cytotoxicity of the COS products on all cancer cells exhibited a concentration-dependent inhibition of cell growth. The morphological changes of both cancer and normal cells after being treated with the COS2 sample having the concentration of 5 mg/ml were observed (Figure 5(C)). Nevertheless, the apoptotic cell death induced by COS2 was confirmed by using flow cytometric analysis of MCF-7 cells which were stained with

both FITC Annexin V and PI (Figure 5(D) and (E)). The results obviously revealed the efficient induction of apoptotic cell death in MCF-7 cells by COS2. Furthermore, the concentration of COS2 that inhibited the growth of each cell for 50% ( $IC_{50}$ ) was also determined in this work. The  $IC_{50}$  of COS2 against cancer cells including HeLa, MCF-7 and H460 cells were approximately 2.3, 2.0 and 4.1 mg/ml, respectively. On the other hand, the  $IC_{50}$  of COS2 against the normal cell, MRC-5, was 4.3 mg/ml. A selectivity index (SI), which is the ratio of the  $IC_{50}$  of a compound tested against cancer cells and normal cells, was also calculated. SI refers to the differential cytotoxic activity of the tested compound against cancer and normal cells.<sup>56</sup> SI values of COS2 were approximately 1.8, 2.15 and 1.0 for HeLa, MCF-7 and H460 cells, respectively. This evidence indicated that COS2 had a slightly higher selectivity for cytotoxic activity against cancer cells. Even though the SI values of COS2 were not high compared with synthetic drugs used in cancer treatment, the COS2 may be considered as a starting material for further developed bio-based anticancer agent that is more specific to cancer cells by conducting chemical modification aiming for a higher value of selectivity for cancer cells. For example, introduction of sulfate groups to the amino or hydroxyl groups of chitosan which may result in a better selectivity to cancer cells over normal cells comparing to the original COS.<sup>13</sup>

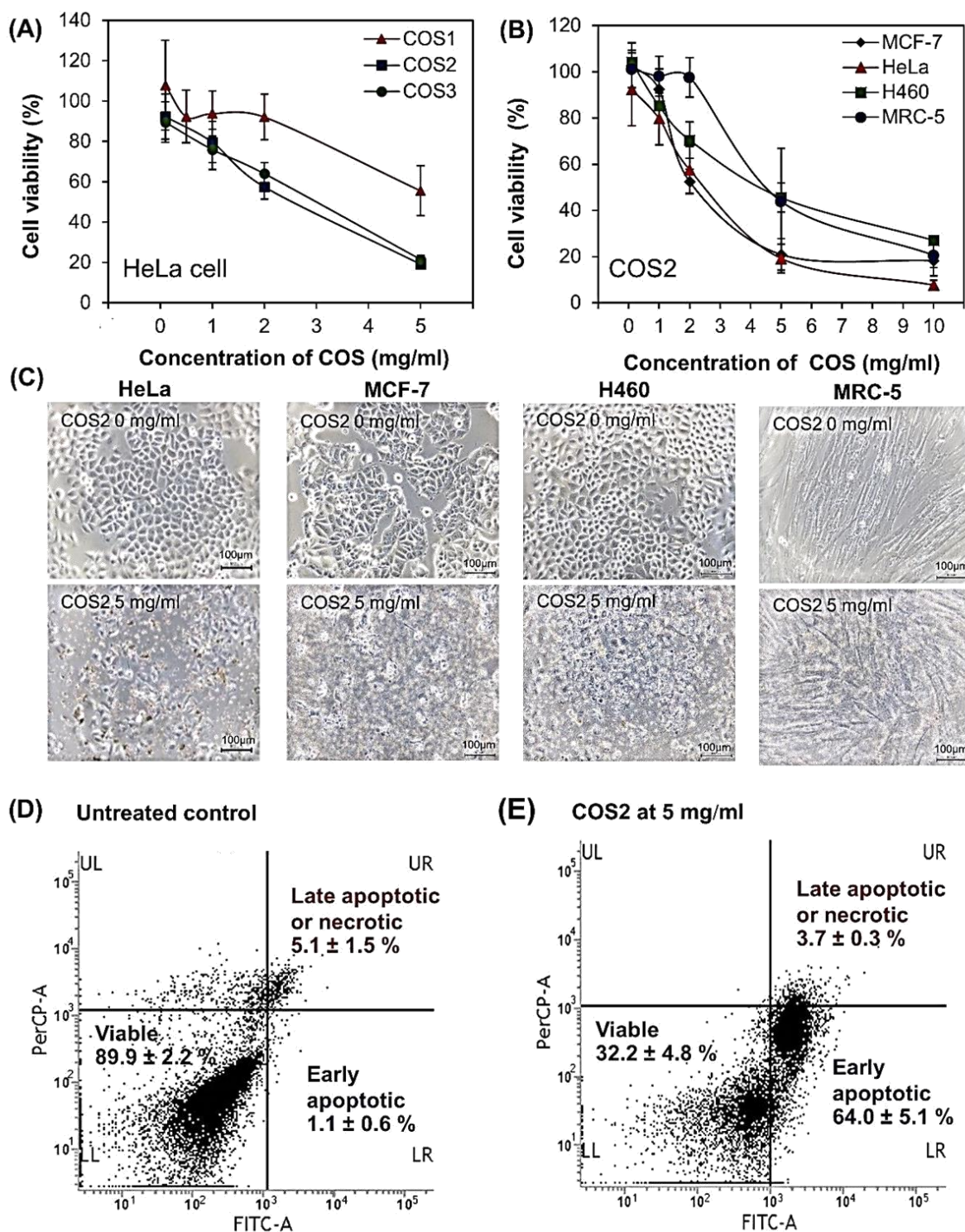


**Figure 5** (A) Cytotoxicity of COS1, COS2 and COS3 against HeLa cells and (B) cytotoxicity of COS2 against HeLa, MCF-7, H460 and MRC-5 cells, determined by MTT assay. (C) Microscopic images (×20) of cancer cells before and after the treatment with COS2 at a concentration of 5 mg/ml for 24 h. Flow cytometric analysis of FITC-annexinV and PI-

stained MCF-7 cells (D) untreated and (E) treated with COS2 at a concentration of 5 mg/ml for 24 h (Note:  $\pm$  presents mean average.).

## Conclusions

A novel method for the facile preparation of chitooligosaccharides (COS) has been proposed. The electrical discharge plasma in a liquid phase was adopted to achieve the heterogeneous degradation of chitosan powder dispersed in a dilute salt solution without the addition of any other hazardous chemicals. Because only chitosan powder and the inorganic salt existed in the reaction solution, separation and purification processes could be performed simply by membrane filtration in order to obtain the COS products having a specific range of molecular weight. The inorganic salts such as  $\text{Na}_2\text{SO}_4$  and  $\text{NaCl}$  played an important role in not only promoting the stable plasma formation but also disruption of compact structure of chitosan powder. Accordingly, depending on the type of inorganic salts existing in the suspension of chitosan powder, chitosan powder could be degraded at a comparable or even higher rate compared to that of chitosan dissolved in an acetic acid solution under a corresponding plasma condition. Since anticancer activity is one of the interesting biological properties of COS, the cytotoxic effects of the obtained COS on the cancer cell lines, *i.e.* HeLa, MCF-7 and H460, were evaluated in comparison with that of the normal cell, *i.e.* MRC-5. The results from the MTT assay revealed that the obtained COS had the higher selectivity to inhibit the growth of cancer cells than the normal cells. Regarding the mechanism of cytotoxic effect of the obtained COS investigated by the flow cytometric analysis, it was found that the obtained COS products (COS2) caused apoptotic cell death in MCF-7 cancer cells. From the evidences in this work, the electrical discharge plasma in a liquid phase is an emerging green technology that can be applied to degradation of not only

chitosan but probably also other natural polymers. The plasma technology may lead to a large scale production of COS for being used as biomedicine in the future.

## ASSOCIATED CONTENT

### Supporting Information

Summary of various methods of degradation of chitosan to produce chitooligosaccharides (COS) and biological properties of the degraded products; chemicals and materials; cell culture; comparison of experimental procedures for the homogeneous degradation of chitosan solution containing acetic acid and the heterogeneous degradation of chitosan powder dispersed in the dilute salt solutions by applying the plasma treatment; digital photographs of chitosan powder dispersed in NaCl and NaI solution at concentration of 0.02 M during the plasma treatment; plots of reversed weight-average molecular weight ( $1/M_t$ ) and reaction time ( $t$ ) at the initial stage (0–30 min) of the degradation of chitosan powder under the plasma treatment, including 0.2% (w/v) chitosan powder dispersed in 0.02 M solutions of sodium salts and metal chlorides; comparison of rate constants obtained in this study and some previous works;  $^1\text{H}$ -NMR and ESI-MS spectra of native chitosan and the obtained COS products; assigned ion composition found in COS fractions determined by ESI-MS.

## AUTHOR INFORMATION

### Corresponding Author

\* E-mail: ratana.r@chula.ac.th

### Acknowledgements

The authors would like to acknowledge the financial supports from the Thailand Research Fund (TRF) under the contract number BRG5480008 and from JST/CREST under the grant

number GJPMJCR12L1. CC would like to thank the Thailand Research Fund (TRF) for providing her a Royal Golden Jubilee Ph.D. Scholarship under the grant number PHD/0179/2556. The authors really appreciate Surapon Foods Public Co., Ltd. (Thailand) for providing the shrimp shells and the NU-PPC Plasma Chemical Technology Laboratory at Chulalongkorn University (Thailand) for providing the plasma equipment and chemicals. All facilities for biological tests supported by Drug Discovery and Development Center, Office of Advanced Science and Technology, Thammasat University (Thailand).

## References

1. Cabrera, J. C.; Van Cutsem, P., Preparation of chitooligosaccharides with degree of polymerization higher than 6 by acid or enzymatic degradation of chitosan. *Biochemical Engineering Journal* **2005**, 25, 165-172.
2. Prasertsung, I.; Damrongsakkul, S.; Terashima, C.; Saito, N.; Takai, O., Preparation of low molecular weight chitosan using solution plasma system. *Carbohydrate Polymers* **2012**, 87, 2745-2749.
3. Qin, C.; Du, Y.; Xiao, L., Effect of hydrogen peroxide treatment on the molecular weight and structure of chitosan. *Polymer Degradation and Stability* **2002**, 76, 211-218.
4. Jayakumar, R.; Prabakaran, M.; Nair, S. V.; Tamura, H., Novel chitin and chitosan nanofibers in biomedical applications. *Biotechnology Advances* **2010**, 28, 142-150.
5. Kim, S.-K., In *Chitin, chitosan, oligosaccharides and their derivatives: biological activities and applications*. CRC Press: Boca Raton, FL, 2010;p 11.
6. Xia, W.; Liu, P.; Zhang, J.; Chen, J., Biological activities of chitosan and chitooligosaccharides. *Food Hydrocolloids* **2011**, 25, 170-179.
7. Mourya, V. K.; Inamdar, N. N.; Choudhari, Y. M., Chitooligosaccharides: Synthesis, characterization and applications. *Polym. Sci. Ser. A* **2011**, 53, 583-612.
8. Yen, M.-T.; Yang, J.-H.; Mau, J.-L., Physicochemical characterization of chitin and chitosan from crab shells. *Carbohydrate Polymers* **2009**, 75, 15-21.
9. Feng, T.; Du, Y.; Li, J.; Hu, Y.; Kennedy, J. F., Enhancement of antioxidant activity of chitosan by irradiation. *Carbohydrate Polymers* **2008**, 73, 126-132.

10. Jung, W.-K.; Moon, S.-H.; Kim, S.-K., Effect of chitooligosaccharides on calcium bioavailability and bone strength in ovariectomized rats. *Life Sciences* **2006**, 78, 970-976.
11. Kim, E.-K.; Je, J.-Y.; Lee, S.-J.; Kim, Y.-S.; Hwang, J.-W.; Sung, S.-H.; Moon, S.-H.; Jeon, B.-T.; Kim, S.-K.; Jeon, Y.-J.; Park, P.-J., Chitooligosaccharides induce apoptosis in human myeloid leukemia HL-60 cells. *Bioorganic & Medicinal Chemistry Letters* **2012**, 22, 6136-6138.
12. Gibot, L.; Chabaud, S.; Bouhout, S.; Bolduc, S.; Auger, F. A.; Moulin, V. J., Anticancer properties of chitosan on human melanoma are cell line dependent. *International Journal of Biological Macromolecules* **2015**, 72, 370-379.
13. Huang, R.; Mendis, E.; Rajapakse, N.; Kim, S.-K., Strong electronic charge as an important factor for anticancer activity of chitooligosaccharides (COS). *Life Sciences* **2006**, 78, 2399-2408.
14. Mao, S.; Shuai, X.; Unger, F.; Simon, M.; Bi, D.; Kissel, T., The depolymerization of chitosan: effects on physicochemical and biological properties. *International Journal of Pharmaceutics* **2004**, 281, 45-54.
15. Vårum, K. M.; Ottøy, M. H.; Smidsrød, O., Acid hydrolysis of chitosans. *Carbohydrate Polymers* **2001**, 46, 89-98.
16. Kumar, A. V.; Tharanathan, R., A comparative study on depolymerization of chitosan by proteolytic enzymes. *Carbohydrate Polymers* **2004**, 58, 275-283.
17. Li, K.; Xing, R.; Liu, S.; Qin, Y.; Meng, X.; Li, P., Microwave-assisted degradation of chitosan for a possible use in inhibiting crop pathogenic fungi. *International Journal of Biological Macromolecules* **2012**, 51, 767-773.
18. Choi, W.-S.; Ahn, K.-J.; Lee, D.-W.; Byun, M.-W.; Park, H.-J., Preparation of chitosan oligomers by irradiation. *Polymer Degradation and Stability* **2002**, 78, 533-538.
19. Wang, S.-M.; Huang, Q.-Z.; Wang, Q.-S., Study on the synergetic degradation of chitosan with ultraviolet light and hydrogen peroxide. *Carbohydrate Research* **2005**, 340, 1143-1147.
20. Wasikiewicz, J. M.; Yeates, S. G., "Green" molecular weight degradation of chitosan using microwave irradiation. *Polymer Degradation and Stability* **2013**, 98, 863-867.
21. Wasikiewicz, J. M.; Yoshii, F.; Nagasawa, N.; Wach, R. A.; Mitomo, H., Degradation of chitosan and sodium alginate by gamma radiation, sonochemical and ultraviolet methods. *Radiation Physics and Chemistry* **2005**, 73, 287-295.

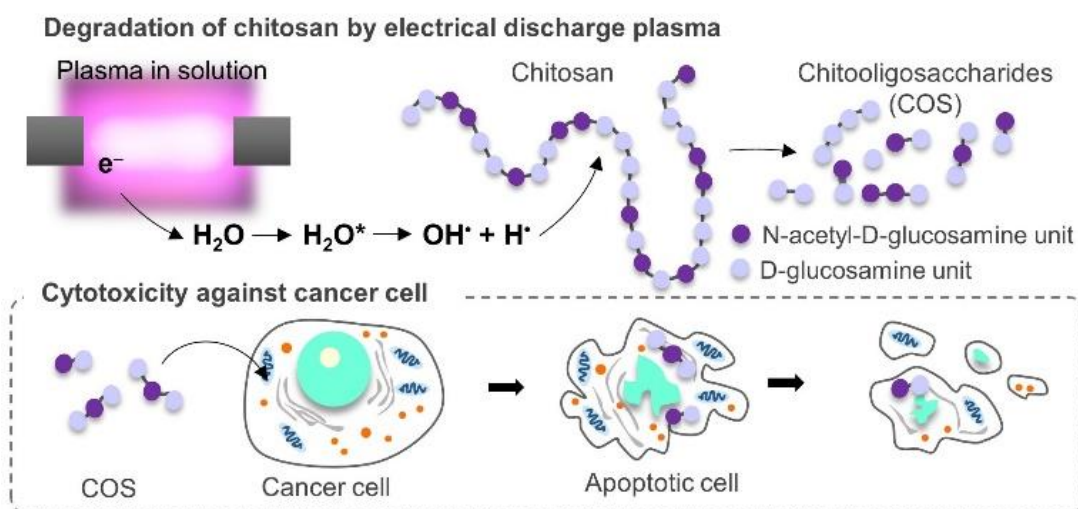
22. Pornsunthorntawe, O.; Katepetch, C.; Vanichvattanadecha, C.; Saito, N.; Rujiravanit, R., Depolymerization of chitosan–metal complexes via a solution plasma technique. *Carbohydrate Polymers* **2014**, *102*, 504-512.
23. Takai, O., Solution plasma processing (SPP). *Pure and Applied Chemistry* **2008**, *80*, 2003-2011.
24. Baroch, P.; Anita, V.; Saito, N.; Takai, O., Bipolar pulsed electrical discharge for decomposition of organic compounds in water. *Journal of Electrostatics* **2008**, *66*, 294-299.
25. Hieda, J.; Saito, N.; Takai, O., Exotic shapes of gold nanoparticles synthesized using plasma in aqueous solution. *Journal of Vacuum Science & Technology A* **2008**, *26*, 854-856.
26. Hu, X.; Shen, X.; Takai, O.; Saito, N., Facile fabrication of PtAu alloy clusters using solution plasma sputtering and their electrocatalytic activity. *Journal of Alloys and Compounds* **2013**, *552*, 351-355.
27. Watthanaphanit, A.; Panomsuwan, G.; Saito, N., A novel one-step synthesis of gold nanoparticles in an alginate gel matrix by solution plasma sputtering. *RSC Advances* **2014**, *4*, 1622-1629.
28. Kang, J.; Li, O. L.; Saito, N., Synthesis of structure-controlled carbon nano spheres by solution plasma process. *Carbon* **2013**, *60*, 292-298.
29. Panomsuwan, G.; Saito, N.; Ishizaki, T., Electrocatalytic oxygen reduction activity of boron-doped carbon nanoparticles synthesized via solution plasma process. *Electrochemistry Communications* **2015**, *59*, 81-85.
30. Davoodbasha, M.; Lee, S.-Y.; Kim, S.-C.; Kim, J.-W., One-step synthesis of cellulose/silver nanobiocomposites using a solution plasma process and characterization of their broad spectrum antimicrobial efficacy. *RSC Advances* **2015**, *5*, 35052-35060.
31. Nemoto, S.; Watthanaphanit, A.; Saito, N., Direct Deposition of Gold Nanoparticles on Cellulose Fiber by Solution Plasma Process. *MRS Online Proceedings Library* **2015**, 1723.
32. Pootawang, P.; Saito, N.; Takai, O., Solution plasma for template removal in mesoporous silica: pH and discharge time varying characteristics. *Thin Solid Films* **2011**, *519*, 7030-7035.
33. Prasertsung, I.; Chutinate, P.; Watthanaphanit, A.; Saito, N.; Damrongsakkul, S., Conversion of cellulose into reducing sugar by solution plasma process (SPP). *Carbohydrate Polymers* **2017**, *172*, 230-236.



34. Watthanaphanit, A.; Saito, N., Effect of polymer concentration on the depolymerization of sodium alginate by the solution plasma process. *Polymer Degradation and Stability* **2013**, 98, 1072-1080.
35. Ma, F.; Li, P.; Zhang, B.; Zhao, X.; Fu, Q.; Wang, Z.; Gu, C., Effect of solution plasma process with bubbling gas on physicochemical properties of chitosan. *International Journal of Biological Macromolecules* **2017**, 98, 201-207.
36. Prasertsung, I.; Damrongsakkul, S.; Saito, N., Degradation of  $\beta$ -chitosan by solution plasma process (SPP). *Polymer Degradation and Stability* **2013**, 98, 2089-2093.
37. Chokradjaroen, C.; Rujiravanit, R.; Watthanaphanit, A.; Theeramunkong, S.; Saito, N.; Yamashita, K.; Arakawa, R., Enhanced degradation of chitosan by applying plasma treatment in combination with oxidizing agents for potential use as an anticancer agent. *Carbohydrate Polymers* **2017**, 167, 1-11.
38. Wu, T.; Wu, C.; Xiang, Y.; Huang, J.; Luan, L.; Chen, S.; Hu, Y., Kinetics and mechanism of degradation of chitosan by combining sonolysis with H<sub>2</sub>O<sub>2</sub>/ascorbic acid. *RSC Advances* **2016**, 6, 76280-76287.
39. Kang, B.; Dai, Y.-d.; Zhang, H.-q.; Chen, D., Synergetic degradation of chitosan with gamma radiation and hydrogen peroxide. *Polymer Degradation and Stability* **2007**, 92, 359-362.
40. Nemoto, S.; Ueno, T.; Watthanaphanit, A.; Hieda, J.; Saito, N., Crystallinity and surface state of cellulose in wet ball-milling process. *Journal of Applied Polymer Science* **2017**, 134, DOI: 10.1002/APP.44903.
41. Zhang, W.; Zhang, J.; Xia, W., Effect of Ball-Milling Treatment on Physicochemical and Structural Properties of Chitosan. *International Journal of Food Properties* **2013**, 17, 26-37.
42. vom Stein, T.; Grande, P.; Sibilla, F.; Commandeur, U.; Fischer, R.; Leitner, W.; de María, P. D., Salt-assisted organic-acid-catalyzed depolymerization of cellulose. *Green Chemistry* **2010**, 12, 1844-1849.
43. Banno, M.; Kanno, K.; Yui, H., Development of direct gas injection system for atmospheric-pressure in-solution discharge plasma for plasma degradation and material syntheses. *RSC Advances* **2016**, 6, 16030-16036.
44. Tian, F.; Liu, Y.; Hu, K.; Zhao, B., Study of the depolymerization behavior of chitosan by hydrogen peroxide. *Carbohydrate Polymers* **2004**, 57, 31-37.
45. Cadle, R. D.; Huff, H., The The Oxidation of Iodide to Iodine by Dilute Solutions of Organic Peroxides. *The Journal of Physical and Colloid Chemistry* **1950**, 54, 1191-1195.

46. Mudarisova, P. K.; Murzagildina, A.; Kulish, E.; Kolesov, S.; Zaikov, G., Violet complex formation by the interaction of chitosan with iodine. *Journal of Information, Intelligence and Knowledge* **2013**, 5, 45.
47. Shigeno, Y.; Kondo, K.; Takemoto, K., Functional monomers and polymers. LXX. On the adsorption of iodine onto chitosan. *Journal of Applied Polymer Science* **1980**, 25, 731-738.
48. Yajima, H.; Morita, M.; Hashimoto, M.; Sashiwa, H.; Kikuchi, T.; Ishii, T., Complex Formation of Chitosan with Iodine and Its Structure and Spectroscopic Properties--Molecular Assembly and Thermal Hysteresis Behavior. *International Journal of Thermophysics* **2001**, 22, 1265-1283.
49. Chang, K. L. B.; Tai, M.-C.; Cheng, F.-H., Kinetics and Products of the Degradation of Chitosan by Hydrogen Peroxide. *Journal of Agricultural and Food Chemistry* **2001**, 49, 4845-4851.
50. Savitri, E.; Juliastuti, S. R.; Handaratri, A.; Sumarno; Roesyadi, A., Degradation of chitosan by sonication in very-low-concentration acetic acid. *Polymer Degradation and Stability* **2014**, 110, 344-352.
51. Brugnerotto, J.; Lizardi, J.; Goycoolea, F.; Argüelles-Monal, W.; Desbrieres, J.; Rinaudo, M., An infrared investigation in relation with chitin and chitosan characterization. *Polymer* **2001**, 42, 3569-3580.
52. Qin, C.; Du, Y.; Xiao, L.; Li, Z.; Gao, X., Enzymic preparation of water-soluble chitosan and their antitumor activity. *International Journal of Biological Macromolecules* **2002**, 31, 111-117.
53. Baxter, A.; Dillon, M.; Anthony Taylor, K. D.; Roberts, G. A. F., Improved method for i.r. determination of the degree of N-acetylation of chitosan. *International Journal of Biological Macromolecules* **1992**, 14, 166-169.
54. Pestov, A.; Nazirov, A.; Modin, E.; Mironenko, A.; Bratskaya, S., Mechanism of Au(III) reduction by chitosan: Comprehensive study with  $^{13}\text{C}$  and  $^1\text{H}$  NMR analysis of chitosan degradation products. *Carbohydrate Polymers* **2015**, 117, 70-77.
55. Park, J. K.; Chung, M. J.; Choi, H. N.; Park, Y. I., Effects of the molecular weight and the degree of deacetylation of chitosan oligosaccharides on antitumor activity. *International journal of molecular sciences* **2011**, 12, 266-277.
56. Badisa, R. B.; Darling-Reed, S. F.; Joseph, P.; Cooperwood, J. S.; Latinwo, L. M.; Goodman, C. B., Selective cytotoxic activities of two novel synthetic drugs on human breast carcinoma MCF-7 cells. *Anticancer research* **2009**, 29, 2993-2996.

## TABLE OF CONTENTS



Facile preparation of chitooligosaccharides by  
degradation of chitosan powder dispersed in dilute  
salt solutions via electrical discharge plasma and  
their cytotoxicity evaluation against cancer cell  
lines and normal cells

*Chayanaphat Chokradjaroen<sup>a</sup>, Sewan Theeramunkong<sup>b</sup>, Hiroharu Yui<sup>c</sup>,  
Nagahiro Saito<sup>d</sup> and Ratana Rujiravanit<sup>a,e\*</sup>*

*<sup>a</sup>The Petroleum and Petrochemical College, Chulalongkorn University, Bangkok 10330,  
Thailand*

*<sup>b</sup>Faculty of Pharmacy, Thammasat University, Pathumthani 12120, Thailand*

*<sup>c</sup>Department of Chemistry, Tokyo University of Science, Tokyo 162-8601, Japan*

*<sup>d</sup>Department of Chemical Systems Engineering, Graduate School of Engineering, Nagoya  
University, Nagoya 464-8603, Japan*

*<sup>e</sup>Center of Excellence on Petrochemical and Materials Technology, Chulalongkorn  
University, Bangkok 10330, Thailand*

*\*ratana.r@chula.ac.th*

## Introduction

**Table S1** Various methods of degradation of chitosan to produce chitooligosaccharides (COS) and biological properties of the degraded products (Note: MW refers to molecular weight.)

Degradation methods	MW (kDa)	Biological properties	Ref.
Using nitrous acid	2.2, 9.3	Antibacterial activity	1
Using enzyme	< 5	Antibacterial activity	2
Using enzyme	0.5–1	Antibacterial activity	3
Using enzyme	< 5	Calcium bioavailability	4
Using enzyme	1–3	Free radical scavenging activity	5
Using enzyme	5–10	Anti-inflammatory activity	6
Using potassium persulfate	~37	Inhibition of tumor-induced angiogenesis	7
Using enzyme	0.16–0.8	Anticancer activity	8
Using enzyme	1	Anticancer activity	9
Plasma	1.3	Anticancer activity	10

## Experimental section

### Chemicals and materials

Glacial acetic acid ( $\text{CH}_3\text{COOH}$ , 99.9%) and hydrochloric acid ( $\text{HCl}$ , 37.0%) were purchased from RCI Labscan. Sodium hydroxide ( $\text{NaOH}$ , 97.0%) pellets, sodium chloride ( $\text{NaCl}$ , 99.9%) and calcium chloride dihydrate ( $\text{CaCl}_2 \cdot 2\text{H}_2\text{O}$ , 99.0%) were brought from Ajax Finechem. A 50%  $\text{NaOH}$  solution was supplied by the Chemical Enterprise. Cerium chloride

heptahydrate ( $\text{CeCl}_3 \cdot 7\text{H}_2\text{O}$ ,  $\geq 98.0\%$ ) and sodium iodide ( $\text{NaI}$ , 98.0%) were ordered from Sigma-Aldrich. Sodium sulfate ( $\text{Na}_2\text{SO}_4$ , 99.5%) was purchased from Fisher Scientific. Sodium nitrate ( $\text{NaNO}_3$ , 99.0%) and manganese chloride tetrahydrate ( $\text{MnCl}_2 \cdot 4\text{H}_2\text{O}$ , 98.0%) were provided by Labo chimie. Sodium borohydride ( $\text{NaBH}_4$ ) and potassium bromide ( $\text{KBr}$ ) were obtained from Carlo Erba and Wako, respectively. Chitosan was prepared from *Metapenaeus dobsoni* shrimp shells by a protocol following Pornsunthorntawe et al.<sup>11</sup> Then, chitosan flakes were pulverized by a high-speed planetary ball mill (Fritsch Pulverisette) to get fine powder of chitosan. The rotational speed was 350 rpm. The chitosan powder was further screened through a sieve with a nominal mesh size of 180.

### **Cell culture**

For a cell culture, human uterine cervix cancer cell line (HeLa cells) and human breast adenocarcinoma cell line (MCF-7 cells) were grown by using high-glucose Dulbecco's Modified Eagle's medium (DMEM) with L-glutamine and sodium pyruvate (Biowest). Meanwhile, human lung cancer cell Line (H460 cells) was grown by using Roswell Park Memorial Institute (RPMI) 1640 media (Biowest). Medical Research Council cell strain 5 (MRC-5 cells) is fibroblast-like cells derived from normal lung tissue. Eagle's Minimum Essential Medium (EMEM) with 1.5 g/l sodium bicarbonate, non-essential amino acids, L-glutamine, and sodium pyruvate cell (Corning) was used as a cell culture medium for MRC-5 cells. All culture medium were mixed with 10% fetal bovine serum (Biowest) and 1% Penicillin-Streptomycin (10,000 U/ml ; Life Technologies) before use. All cells were cultured in a humidified incubator (37 °C, 5%  $\text{CO}_2$ ).

## Results and discussion

A comparison on the experimental procedures for the homogeneous degradation of chitosan solution (A) and the heterogeneous degradation of chitosan powder (B) by using the plasma discharging in a liquid phase was demonstrated in supporting data (Figure S1). Under an acidic environment,  $\text{NH}_2$  groups in the structure of chitosan are protonated by protons coming from the dissociation of acetic acid; therefore, chitosan becomes soluble leading to the homogeneous reaction in the degradation system. On the other hand, in the dilute salt solution that had a neutral pH, chitosan powder cannot be protonated due to the absence of protons in the system and still remained in a solid form before chitosan powder was degraded during the plasma treatment and eventually dissolved in the salt solutions at a prolonged reaction time. Accordingly, the water-soluble degraded products containing COS, that were produced by the plasma treatment of the chitosan powder dispersed in the dilute salt solutions, could be readily separated from the remaining solid residue of chitosan powder by using simple filtration. The remaining solid residue of chitosan powder was referred to the water-insoluble degraded products of chitosan which was chitosan having relatively high molecular weight and could not dissolve in a neutral pH solution. After filtration, the filtrated solution containing the water-soluble degraded products of chitosan was further fractionated by simple ultrafiltration using filter membranes having different MWCO in order to obtain the fractions of COS with narrow molecular weight distribution. For the chitosan solution, the plasma-treated chitosan solution that contained acetic acid as a solvent required the further neutralization by NaOH. After neutralization, the high-molecular-weight degraded products of chitosan were precipitated out from the reaction solution because of the poor solubility at a neutral pH. After that, the water-soluble degraded products of chitosan were obtained by the addition of a non-solvent such as ethanol in order to precipitate the water-soluble degraded products of chitosan from the reaction solution.

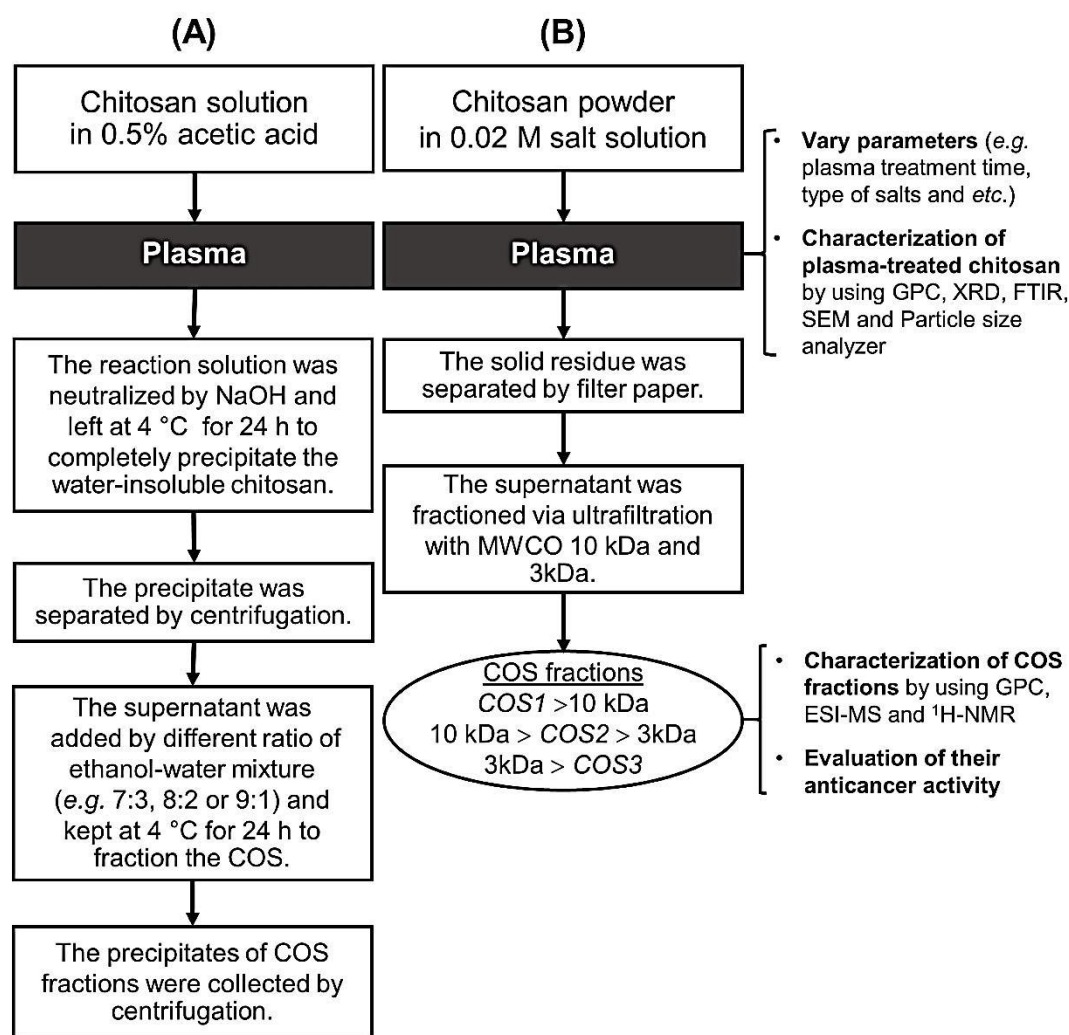


**Figure S1** Comparison of experimental procedures for (A) the homogeneous degradation of chitosan solution containing acetic acid<sup>11</sup> and (B) the heterogeneous degradation of chitosan powder dispersed in the dilute salt solutions by applying the plasma treatment.



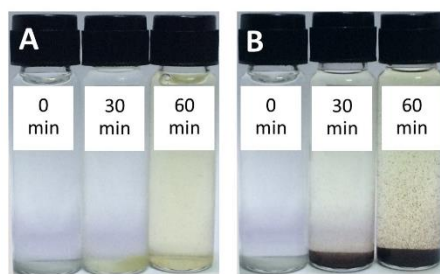


**Figure S2** Digital photographs of chitosan powder dispersed in (A) NaCl and (B) NaI solutions at a concentration of 0.02 M during the plasma treatment.

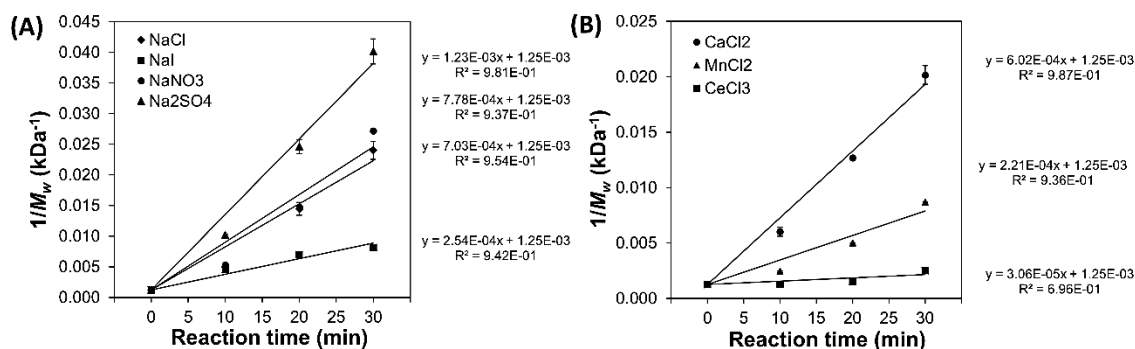


**Figure S3** Plots of reversed weight-average molecular weight ( $1/M_t$ ) and reaction time ( $t$ ) at the initial stage (0–30 min) of the degradation of chitosan powder under the plasma treatment, including 0.2% (w/v) chitosan powder dispersed in 0.02 M solutions of (A) sodium salts and (B) metal chlorides.

**Table S2** Comparison of rate constants obtained in this study and some previous works

Methods	[CS], %(w/v)	Solutions		$k$ , $\times 10^{-4} \text{ min}^{-1}$	Ref.
		Chemicals	Concentration		
SP	0.2	NaI	0.02 M	0.41	This work
		NaNO <sub>3</sub>		1.25	
		Na <sub>2</sub> SO <sub>4</sub>		1.98	
		CaCl <sub>2</sub>		0.96	
		MnCl <sub>2</sub>		0.34	
		CeCl <sub>3</sub>		0.05	
		NaCl		1.12	
SP	0.2	Acetic acid	0.5%	0.43	This work
Sonochemical degradation	0.1	Acetic acid	0.1 M	1.4	<sup>12</sup>
Microwave	3.0	Acetic acid	2%	$\approx 6.24$	<sup>13</sup>
Oxidative degradation	0.5–2	Acetic acid	2%	4.2–7.1	<sup>14</sup>
		H <sub>2</sub> O <sub>2</sub>	0.5–3.5%		
Oxidative degradation	1.5	Acetic acid	2%	$\approx 1.80$	<sup>15</sup>
		K <sub>2</sub> S <sub>2</sub> O <sub>8</sub>	0.1%		
and heating at 70°C					
Electrochemical degradation	0.3	Acetic acid	0.2 M	0.18–1.20	<sup>16</sup>
		Sodium acetate	0.3 M		
Enzymatic degradation	0.5	Sodium acetate buffer	0.2 M	$\approx 0.27$	<sup>17</sup>

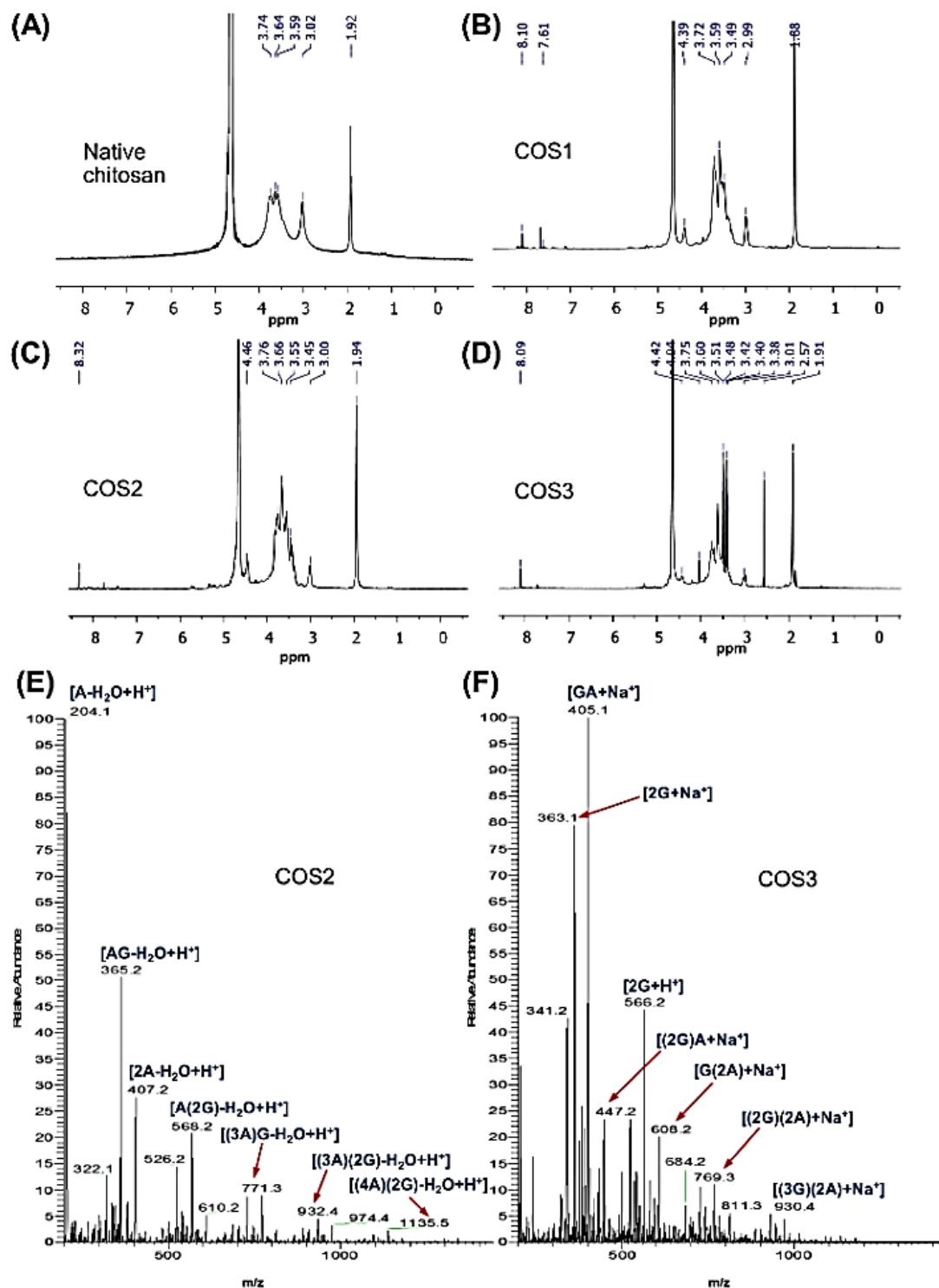


**Figure S4**  $^1\text{H}$ -NMR spectra of (A) native chitosan and the obtained COS products including (B) COS1, (C) COS2 and (D) COS3 and ESI-MS spectra of (E) COS2 and (G) COS3. (Note:

“G” refers to D-glucosamine unit ( $m = 161.06$  Da) and “A” refers to N-acetyl-D-glucosamine unit ( $m = 203.07$  Da.).

**Table S3** Assigned ion composition found in COS2 fraction determined by ESI-MS. “G” refers to D-glucosamine unit ( $m = 161.06$ ) and “A” refers to N-acetyl-D-glucosamine unit ( $m = 203.07$ )

<i>m/z</i>	Adduct ion	Attribution	(end)
204.09	H <sup>+</sup>	A-H <sub>2</sub>	(H <sub>2</sub> O)
233.08	H <sup>+</sup>	A-H+NO	
251.09	H <sup>+</sup>	A-H+NO+H <sub>2</sub> O	
269.11	H <sup>+</sup>	2G-4H <sub>2</sub> O	(H <sub>2</sub> O)
306.12	H <sup>+</sup>	2G-H <sub>2</sub> O-NH <sub>3</sub>	
322.11	H <sup>+</sup>	2G-H <sub>2</sub> -NH <sub>3</sub>	
323.15	H <sup>+</sup>	2G-H <sub>2</sub> O	
337.13	H <sup>+</sup>	2G-2H <sub>2</sub>	
341.16	H <sup>+</sup>	2G	
347.15	H <sup>+</sup>	AG-2H <sub>2</sub> O	
353.12	H <sup>+</sup>	2G-2H <sub>2</sub> +O	
364.13	H <sup>+</sup>	AG-H <sub>2</sub> -NH <sub>3</sub>	
365.16	H <sup>+</sup>	AG-H <sub>2</sub> O	
379.14	H <sup>+</sup>	AG-2H <sub>2</sub>	
383.17	H <sup>+</sup>	AG	
395.13	H <sup>+</sup>	AG-2H <sub>2</sub> +O	
407.17	H <sup>+</sup>	2A-H <sub>2</sub> O	
423.16	H <sup>+</sup>	2A-H <sub>2</sub>	
425.18	H <sup>+</sup>	2A	
436.16	H <sup>+</sup>	2A-2H <sub>2</sub> +NH	
484.22	H <sup>+</sup>	3G-H <sub>2</sub> O	(H <sub>2</sub> O)
502.23	H <sup>+</sup>	3G	
526.23	H <sup>+</sup>	A(2G)-H <sub>2</sub> O	
540.21	H <sup>+</sup>	A(2G)-2H <sub>2</sub>	
568.24	H <sup>+</sup>	(2A)G-H <sub>2</sub> O	
586.25	H <sup>+</sup>	(2A)G	
610.25	H <sup>+</sup>	3A-H <sub>2</sub> O	
663.30	H <sup>+</sup>	4G	(H <sub>2</sub> O)
687.30	H <sup>+</sup>	A(3G)-H <sub>2</sub> O	

701.28	H <sup>+</sup>	A(3G)-2H <sub>2</sub>	
<i>m/z</i>	Adduct ion	Attribution	(end)
705.31	H <sup>+</sup>	A(3G)	
729.31	H <sup>+</sup>	(2A)(2G)-H <sub>2</sub> O	
743.29	H <sup>+</sup>	(2A)(2G)-2H <sub>2</sub>	
771.32	H <sup>+</sup>	(3A)G-H <sub>2</sub> O	
813.33	H <sup>+</sup>	4A-H <sub>2</sub> O	
866.38	H <sup>+</sup>	A(4G)	(H <sub>2</sub> O)
890.38	H <sup>+</sup>	(2A)(3G)-H <sub>2</sub> O	
904.36	H <sup>+</sup>	(2A)(3G)-2H <sub>2</sub>	
908.39	H <sup>+</sup>	(2A)(3G)	
932.39	H <sup>+</sup>	(3A)(2G)-H <sub>2</sub> O	
950.40	H <sup>+</sup>	(3A)(2G)	
974.40	H <sup>+</sup>	(4A)G-H <sub>2</sub> O	
1016.41	H <sup>+</sup>	5A-H <sub>2</sub> O	
1069.46	H <sup>+</sup>	(2A)(4G)	(H <sub>2</sub> O)
1093.46	H <sup>+</sup>	(3A)(3G)-H <sub>2</sub> O	
1107.44	H <sup>+</sup>	(3A)(3G)-2H <sub>2</sub>	
1111.47	H <sup>+</sup>	(3A)(3G)	
1135.47	H <sup>+</sup>	(4A)(2G)-H <sub>2</sub> O	
1177.48	H <sup>+</sup>	(5A)G-H <sub>2</sub> O	
1254.52	H <sup>+</sup>	(3A)(4G)-H <sub>2</sub> O	(H <sub>2</sub> O)
1268.50	H <sup>+</sup>	(3A)(4G)-2H <sub>2</sub>	
1296.54	H <sup>+</sup>	(4A)(3G)-H <sub>2</sub> O	
1310.51	H <sup>+</sup>	(4A)(3G)-2H <sub>2</sub>	
1338.55	H <sup>+</sup>	(5A)(2G)-H <sub>2</sub> O	
1380.56	H <sup>+</sup>	(6A)G-H <sub>2</sub> O	

* G=Glucosamin unit	C <sub>6</sub> H <sub>11</sub> O <sub>4</sub> N
**A=Acetylglucosamine unit	C <sub>8</sub> H <sub>13</sub> O <sub>5</sub> N

**Table S4** Assigned ion composition found in COS3 fraction determined by ESI-MS. “G” refers to D-glucosamine unit (m = 161.06) and “A” refers to N-acetyl-D-glucosamine unit (m = 203.07)

<i>m/z</i>	Adduct ion	Attribution	(end)
323.15	H <sup>+</sup>	2G-H <sub>2</sub> O	(H <sub>2</sub> O)
337.13	H <sup>+</sup>	2G-2H <sub>2</sub>	
341.16	H <sup>+</sup>	2G	
362.11	Na <sup>+</sup>	2G-NH <sub>3</sub> +O	
363.14	H <sup>+</sup>	2G	
365.16	H <sup>+</sup>	AG-H <sub>2</sub> O	
369.15	H <sup>+</sup>	AG-CH <sub>2</sub>	
377.12	Na <sup>+</sup>	2G-H <sub>2</sub> +O	
383.17	H <sup>+</sup>	AG	
387.14	Na <sup>+</sup>	AG-H <sub>2</sub> O	
391.13	Na <sup>+</sup>	2G+CO	
404.12	Na <sup>+</sup>	AG-NH <sub>3</sub> +O	
405.15	Na <sup>+</sup>	AG	
419.13	Na <sup>+</sup>	AG-H <sub>2</sub> +O	
421.14	Na <sup>+</sup>	AG+O	
433.14	Na <sup>+</sup>	AG+CO	
447.16	Na <sup>+</sup>	2A	
451.16	Na <sup>+</sup>	AG+CH <sub>2</sub> +2O	
463.16	Na <sup>+</sup>	2A+O	
465.17	Na <sup>+</sup>	2A+H <sub>2</sub> O	
476.15	Na <sup>+</sup>	2A-H+NO	
502.23	H <sup>+</sup>	3G	(H <sub>2</sub> O)
524.21	H <sup>+</sup>	A(2G)-H <sub>2</sub> O-H <sub>2</sub>	
685.28	H <sup>+</sup>	A(3G)-H <sub>2</sub> O-H <sub>2</sub>	(H <sub>2</sub> O)
699.26	Na <sup>+</sup>	4G-H <sub>2</sub> +O	
705.31	H <sup>+</sup>	A(3G)	
727.29	Na <sup>+</sup>	A(3G)	
769.30	Na <sup>+</sup>	(2A)(2G)	
797.30	Na <sup>+</sup>	(2A)(2G)-H <sub>2</sub> +NO	
811.31	Na <sup>+</sup>	(3A)G	
888.33	Na <sup>+</sup>	A(4G)	(H <sub>2</sub> O)
930.37	Na <sup>+</sup>	(2A)(3G)	
972.38	Na <sup>+</sup>	(3A)(2G)	
1014.39	Na <sup>+</sup>	(4A)G	
1091.44	Na <sup>+</sup>	(2A)(4G)	(H <sub>2</sub> O)
1133.45	Na <sup>+</sup>	(3A)(3G)	
1147.43	Na <sup>+</sup>	(3A)(3G)+O-H <sub>2</sub>	
* G=Glucosamin unit		C <sub>6</sub> H <sub>11</sub> O <sub>4</sub> N	
**A=Acetylglucosamine unit		C <sub>8</sub> H <sub>13</sub> O <sub>5</sub> N	
<i>m/z</i>	Adduct ion	Attribution	(end)
538.19	Na <sup>+</sup>	3G-H <sub>2</sub> +O	
544.24	H <sup>+</sup>	A(2G)	
566.22	Na <sup>+</sup>	A(2G)	
594.21	Na <sup>+</sup>	A(2G)+CO	
608.23	Na <sup>+</sup>	(2A)G	
636.23	Na <sup>+</sup>	(2A)G-H <sub>2</sub> +NO	
650.24	Na <sup>+</sup>	3A	
654.24	Na <sup>+</sup>	(2A)G+CH <sub>2</sub> +2O	
666.24	Na <sup>+</sup>	3A+O	

## References

1. Tokura, S.; Ueno, K.; Miyazaki, S.; Nishi, N. In *New Macromolecular Architecture and Functions*, Kamachi, M.; Nakamura, A., Eds. Springer Berlin Heidelberg: New York, NY 1996; pp 199-207.
2. Zheng, L.-Y.; Zhu, J.-F., Study on antimicrobial activity of chitosan with different molecular weights. *Carbohydrate Polymers* **2003**, *54*, 527-530.
3. Jeon, Y.-J.; Kim, S.-K., Production of chitooligosaccharides using an ultrafiltration membrane reactor and their antibacterial activity. *Carbohydrate Polymers* **2000**, *41*, 133-141.
4. Jung, W.-K.; Moon, S.-H.; Kim, S.-K., Effect of chitooligosaccharides on calcium bioavailability and bone strength in ovariectomized rats. *Life Sciences* **2006**, *78*, 970-976.
5. Park, P.-J.; Je, J.-Y.; Kim, S.-K., Free radical scavenging activity of chitooligosaccharides by electron spin resonance spectrometry. *Journal of Agricultural and Food Chemistry* **2003**, *51*, 4624-4627.
6. Lee, S.-H.; Senevirathne, M.; Ahn, C.-B.; Kim, S.-K.; Je, J.-Y., Factors affecting anti-inflammatory effect of chitooligosaccharides in lipopolysaccharides-induced RAW264.7 macrophage cells. *Bioorganic & Medicinal Chemistry Letters* **2009**, *19*, 6655-6658.
7. Harish Prashanth, K. V.; Tharanathan, R. N., Depolymerized products of chitosan as potent inhibitors of tumor-induced angiogenesis. *Biochimica et Biophysica Acta (BBA) - General Subjects* **2005**, *1722*, 22-29.
8. de Assis, C. F.; Costa, L. S.; Melo-Silveira, R. F.; Oliveira, R. M.; Pagnoncelli, M. G. B.; Rocha, H. A. O.; de Macedo, G. R.; Santos, E. S. d., Chitooligosaccharides antagonize the cytotoxic effect of glucosamine. *World Journal of Microbiology and Biotechnology* **2012**, *28*, 1097-1105.

9. Kim, E.-K.; Je, J.-Y.; Lee, S.-J.; Kim, Y.-S.; Hwang, J.-W.; Sung, S.-H.; Moon, S.-H.; Jeon, B.-T.; Kim, S.-K.; Jeon, Y.-J.; Park, P.-J., Chitooligosaccharides induce apoptosis in human myeloid leukemia HL-60 cells. *Bioorganic & Medicinal Chemistry Letters* **2012**, *22*, 6136-6138.
10. Chokradjaroen, C.; Rujiravanit, R.; Watthanaphanit, A.; Theeramunkong, S.; Saito, N.; Yamashita, K.; Arakawa, R., Enhanced degradation of chitosan by applying plasma treatment in combination with oxidizing agents for potential use as an anticancer agent. *Carbohydrate Polymers* **2017**, *167*, 1-11.
11. Pornsunthorntawe, O.; Katepetch, C.; Vanichvattanadecha, C.; Saito, N.; Rujiravanit, R., Depolymerization of chitosan–metal complexes via a solution plasma technique. *Carbohydrate Polymers* **2014**, *102*, 504-512.
12. Wasikiewicz, J. M.; Yoshii, F.; Nagasawa, N.; Wach, R. A.; Mitomo, H., Degradation of chitosan and sodium alginate by gamma radiation, sonochemical and ultraviolet methods. *Radiation Physics and Chemistry* **2005**, *73*, 287-295.
13. Li, K.; Xing, R.; Liu, S.; Qin, Y.; Meng, X.; Li, P., Microwave-assisted degradation of chitosan for a possible use in inhibiting crop pathogenic fungi. *International Journal of Biological Macromolecules* **2012**, *51*, 767-773.
14. Chang, K. L. B.; Tai, M.-C.; Cheng, F.-H., Kinetics and Products of the Degradation of Chitosan by Hydrogen Peroxide. *Journal of Agricultural and Food Chemistry* **2001**, *49*, 4845-4851.
15. Hsu, S.-C.; Don, T.-M.; Chiu, W.-Y., Free radical degradation of chitosan with potassium persulfate. *Polymer Degradation and Stability* **2002**, *75*, 73-83.
16. Cai, Q.; Gu, Z.; Fu, T.; Liu, Y.; Song, H.; Li, F., Kinetic study of chitosan degradation by an electrochemical process. *Polym. Bull.* **2011**, *67*, 571-582.

17. Ilyina, A. V.; Tikhonov, V. E.; Albulov, A. I.; Varlamov, V. P., Enzymic preparation of acid-free-water-soluble chitosan. *Process Biochemistry* **2000**, *35*, 563-568.



## **Appendix A**

Orathai Pornsunthorntawee, Chaiyapruk Katepetch, Chutima Vanichvattanadecha, Nagahiro Saito, and Ratana Rujiravanit (2014) “Depolymerization of chitosan-metal complexes via a solution plasma technique”, Carbohydrate Polymers, 102, 504-512.  
Impact factor 4.811 (JCR year 2016)

## **Appendix B**

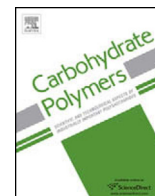
Chayanaphat Chokradjaroen, Ratana Rujiravanit, Anyarat Watthanaphanit, Sewan Theeramunkong, Nagahiro Saito, Kazuko Yamashita, Ryuichi Arakawa (2017) “Enhanced degradation of chitosan by applying plasma treatment in combination with oxidizing agents for potential use as an anticancer agent”, Carbohydrate Polymers, 167, 1-11.

Impact factor 4.811 (JCR year 2016)

## **Appendix C**

Chayanaphat Chokradjaroen, Ratana Rujiravanit, Sewan Theeramunkong and Nagahiro Saito (2018) “Degradation of chitosan hydrogel dispersed in dilute carboxylic acids by solution plasma and evaluation of anticancer activity of degraded products”, Japanese Journal of Applied Physics, 57(1), Article Number: 0102B5. DOI: 10.7567/JJAP.57.0102B5.

Impact factor 1.384 (JCR year 2016)



# Depolymerization of chitosan–metal complexes via a solution plasma technique



Orathai Pornsunthorntawe<sup>a</sup>, Chaipayruk Katepetch<sup>a</sup>, Chutima Vanichvattanadecha<sup>a</sup>,  
Nagahiro Saito<sup>b</sup>, Ratana Rujiravanit<sup>a,c,\*</sup>

<sup>a</sup> The Petroleum and Petrochemical College, Chulalongkorn University, Bangkok 10330, Thailand

<sup>b</sup> Department of Materials, Physics and Energy Engineering, Graduate School of Engineering, Nagoya University, Nagoya 464-8603, Japan

<sup>c</sup> Center of Excellence on Petrochemical and Materials Technology, Chulalongkorn University, Bangkok 10330, Thailand

## ARTICLE INFO

### Article history:

Received 27 July 2013

Received in revised form

17 November 2013

Accepted 19 November 2013

Available online 28 November 2013

### Keywords:

Chitosan

Solution plasma

Metal complexation

Chitosan oligomers

## ABSTRACT

Chitosan–metal complexes were depolymerized under acidic conditions using a solution plasma system. Four different types of metal ions, including  $\text{Ag}^+$ ,  $\text{Zn}^{2+}$ ,  $\text{Cu}^{2+}$ , and  $\text{Fe}^{3+}$  ions, were added to the chitosan solution at a metal-to-chitosan molar ratio of 1:8. The depolymerization rate was affected by the types of metal ions that form complexes with chitosan. The complexation of chitosan with  $\text{Cu}^{2+}$  or  $\text{Fe}^{3+}$  ions strongly promoted the depolymerization rate of chitosan using a solution plasma treatment. However, chitosan– $\text{Ag}^+$  and chitosan– $\text{Zn}^{2+}$  complexes exhibited no change in the depolymerization rate compared to chitosan. After plasma treatment of the chitosan–metal complexes, the depolymerized chitosan products were separated into water-insoluble and water-soluble fractions. The water-soluble fraction containing low-molecular-weight chitosan was obtained in a yield of less than 57% for the depolymerization of chitosan– $\text{Fe}^{3+}$  complex with the plasma treatment time of 180 min.

© 2013 Elsevier Ltd. All rights reserved.

## 1. Introduction

For chitin and chitosan, several studies have already been performed to prepare low-molecular-weight chitosan and their oligomers, which possess good biological activities, such as antitumor, antifungal, and antibacterial activities (Fernandes et al., 2008; Jeon, Park, & Kim, 2001; Kendra & Hadwiger, 1984; Liang et al., 2007; Muzzarelli, 2010; Qin et al., 2004; Toda et al., 1987) as well as the inhibition of metalloproteinase enzyme production, which can heal wounds and prevent wrinkle formation (Muzzarelli, 2009). In general, there are three widely used techniques for the depolymerization of chitin/chitosan, including chemical depolymerization, physical depolymerization, and enzymatic depolymerization. Among these three techniques, enzymatic methods have received more attention in recent years because they allow regioselective depolymerization of chitin/chitosan under the mildest conditions (Harish, Prashanth, & Tharanathan, 2007; Muzzarelli, Stanic, & Ramos, 1999). However, the important drawbacks of this technique are that the enzyme reaction progresses slowly and a low product yield is obtained (Choi et al., 2002).

Most commercial enzymes, especially those with a high purity, are also expensive (Klaikherd et al., 2004). For chemical methods, various strong chemical reagents are used for the acid hydrolysis of chitin/chitosan leading to difficulty with handling. The generated wastes from these harmful chemicals may cause environmental pollution. Therefore, the development of new methods for the depolymerization of chitin/chitosan is of great interest.

Plasma in the liquid phase, which is known as “solution plasma”, has recently been proposed to be one of the most effective strategies for the depolymerization of biopolymers, such as chitosan (Prasertsung et al., 2012) and sodium alginate (Wattanaphanit & Saito, 2013). However, most of the early research has been focused on the use of solution plasma, a glow discharge in the liquid phase, to synthesize metal nanoparticles with a narrow particle size distribution without adding reducing agents to the reaction system (Saito, Hieda, & Takai, 2009). Currently, the detailed structure of the solution plasma is still unclear but it is believed that the emission center of the plasma is located in the gas phase surrounded by a liquid phase, and an ion sheath is formed near the gas/liquid interface. This solution plasma capable of providing extremely rapid reactions due to the presence of activated chemical species and radicals under high pressure (Saito, Hieda, & Takai, 2009). Because the solution plasma is generated under mild conditions (i.e., the reaction proceeds at room temperature and without the use of strong chemical reagents) and is applicable to industrial material

\* Corresponding author at: The Petroleum and Petrochemical College, Chulalongkorn University, Bangkok 10330, Thailand. Tel.: +66 2 218 4132; fax: +66 2 215 4459.

E-mail address: [ratana.r@chula.ac.th](mailto:ratana.r@chula.ac.th) (R. Rujiravanit).

processing, this technique is very attractive for the depolymerization of biopolymers.

In the current study, the solution plasma was used for the depolymerization of an acidic chitosan solution. Various types of metal ions including the silver ion ( $\text{Ag}^+$ ), zinc ion ( $\text{Zn}^{2+}$ ), copper (II) ion ( $\text{Cu}^{2+}$ ), and ferric ion ( $\text{Fe}^{3+}$ ) were added to the chitosan solution to form chitosan–metal complexes because both hydroxyl groups ( $-\text{OH}$ ) and amine ( $-\text{NH}_2$ ) groups on the chitosan skeleton are good ligands for coordination with the metal ions. Coordination with the metal ions should result in weakening of the covalent bonds near the coordinating site resulting in weak points on the chitosan chain promoting the depolymerization reaction. A viscometric method and liquid chromatography were used to investigate the depolymerization process of chitosan. Any changes in the chemical structures and crystallinity of the depolymerized products were characterized by Fourier transform infrared (FTIR) spectroscopy and wide angle X-ray diffraction (WAXD) analysis, respectively. The molecular mass and degree of polymerization (DP) of the depolymerized chitosan were determined using mass spectrometry (MS).

## 2. Experimental

### 2.1. Materials

Chitosan was prepared from the shells of *Metapenaeus dobsoni* shrimp, which were provided by Surapon Foods Public Co., Ltd. (Thailand). Acetonitrile ( $\text{CH}_3\text{CN}$ ), glacial acetic acid ( $\text{CH}_3\text{COOH}$ ), hydrochloric acid ( $\text{HCl}$ ), and sodium hydroxide ( $\text{NaOH}$ ) pellets were purchased from RCI Labscan Limited (Thailand). A 50% (w/v)  $\text{NaOH}$  solution was supplied by the Chemical Enterprise Co., Ltd. (Thailand). Silver nitrate ( $\text{AgNO}_3$ ) was purchased from Fisher Scientific (UK). Zinc nitrate hexahydrate ( $\text{Zn}(\text{NO}_3)_2 \cdot 6\text{H}_2\text{O}$ ) and copper (II) sulfate pentahydrate ( $\text{CuSO}_4 \cdot 5\text{H}_2\text{O}$ ) were provided by Ajax Finechem Pty Ltd. (Australia). Ferric chloride hexahydrate ( $\text{FeCl}_3 \cdot 6\text{H}_2\text{O}$ ) and D-glucosamine hydrochloride ( $\text{GlcN} \cdot \text{HCl}$ ), which were used as a standard in the high performance liquid chromatography (HPLC), as well as high-purity distilled water, which was used as a solvent in the MS analysis, were supplied by Sigma–Aldrich (USA). Sodium borohydride ( $\text{NaBH}_4$ ) was obtained from Carlo Erba Reagenti (Italy).

### 2.2. Preparation of chitosan from shrimp shells

*M. dobsoni* shrimp shells were cleaned and dried under sunlight prior to grinding them into small pieces. The ground shrimp shells were immersed in a 1 M  $\text{HCl}$  solution for 2 days with occasional stirring and were washed with distilled water until neutral. The demineralized shrimp shell chips were soaked in a 4% (w/v)  $\text{NaOH}$  solution at  $80^\circ\text{C}$  for 4 h, followed by excessive washing with distilled water. The deproteinized product, or chitin, was subsequently deacetylated by heating in a 50% (w/v)  $\text{NaOH}$  solution containing 0.5 wt.%  $\text{NaBH}_4$  in an autoclave at  $110^\circ\text{C}$  for 75 min. After deacetylation, the chitosan flakes were washed with distilled water until neutral and were dried at  $60^\circ\text{C}$ . The deacetylation step was performed twice to obtain chitosan with a high degree of deacetylation (%DD) (i.e., 90%), as determined by the FTIR technique reported by Baxter, Zivanovic, & Weiss (2005). A solid-to-liquid ratio used in the decalcification, the deproteinization, and the deacetylation steps was maintained at 1:10.

### 2.3. Solution plasma experiment

An aqueous solution of chitosan used in the solution plasma experiment was prepared by dissolving chitosan platelets in a 1% (w/v)  $\text{CH}_3\text{COOH}$  solution at a chitosan concentration of 0.5%

(w/v). For the solution plasma experiment with metal complexation,  $\text{AgNO}_3$ ,  $\text{Zn}(\text{NO}_3)_2$ ,  $\text{Cu}(\text{SO}_4)$ , or  $\text{FeCl}_3$  was dissolved in a 1% (w/v) acetic acid solution prior to dropwise addition to the chitosan solution with constant stirring at a metal-to-chitosan molar ratio of 1:8 and a final chitosan concentration of 0.5% (w/v). The solution mixture was maintained at room temperature ( $30^\circ\text{C}$ ) for 5 h with constant stirring. Next, the chitosan solution either with or without complexation with metal ions was poured into the reaction vessel, which was a 100 mL beaker connected to two tungsten electrodes with a diameter of 1 mm. The solution plasma system used in this study has been described by Saito, Hieda, & Takai, 2009, Pootawang, Saito, & Takai (2011a), and Prasertsung et al. (2012). The operation parameters were maintained at an applied voltage of 1.44 kV, a pulse frequency of 15 Hz, a pulse width of 2.0  $\mu\text{s}$ , and a gap distance of 1 mm. The reaction temperature during plasma treatment was approximately  $80^\circ\text{C}$ . To determine the efficiency of the solution plasma technique for the depolymerization of chitosan, the acid hydrolysis of an aqueous chitosan solution in a 1% (w/v)  $\text{CH}_3\text{COOH}$  solution either with or without metal complexation at a reaction temperature of  $80^\circ\text{C}$  served as a control.

### 2.4. Separation and purification of depolymerized products

An aqueous solution of chitosan sample after the depolymerization via both acid hydrolysis and solution plasma treatment either with or without metal complexation at different reaction times was collected prior to adjusting the solution pH to approximately 7 using a 5 M  $\text{NaOH}$  solution. The neutralized chitosan solution was maintained overnight at  $4^\circ\text{C}$  for complete precipitation of the water-insoluble chitosan fraction (Choi et al., 2002). Then, the precipitate was removed by centrifugation at 8500 rpm at  $4^\circ\text{C}$  for 20 min. The obtained supernatant was further mixed with an equal volume of acetone to yield a second precipitate, which is the water-soluble chitosan fraction (Choi et al., 2002; Prasertsung et al., 2012). The solution mixture was maintained overnight at  $4^\circ\text{C}$ , and the second precipitate was collected by centrifugation at 8500 rpm at  $4^\circ\text{C}$  for 20 min. After drying at  $40^\circ\text{C}$  overnight, the water-insoluble and water-soluble chitosan fractions were weighed and used to calculate the percentage of water-insoluble and water-soluble chitosan fractions as well as the total yield percentage as follows:

$$\text{Water-insoluble chitosan (\%)} = \frac{W_i}{W_o} \times 100 \quad (1)$$

$$\text{Water-soluble chitosan (\%)} = \frac{W_s}{W_o} \times 100 \quad (2)$$

$$\text{Total yield (\%)} = \frac{W_i + W_s}{W_o} \times 100 \quad (3)$$

where  $W_i$  is the mass of the water-insoluble chitosan fraction after depolymerization,  $W_s$  is the mass of the water-soluble chitosan fraction after depolymerization, and  $W_o$  is the initial mass of chitosan in the acetic acid solution.

### 2.5. Analytical methods and measurements

As a preliminary study of the depolymerization of chitosan, the viscosity of the chitosan solution was measured as a function of the reaction time with a Cannon–Ubbelohde viscometer (Cannon Instrument Co., J758). The viscometer was filled with a test sample and then equilibrated in a water bath at  $25^\circ\text{C}$ . Then, the test solution was passed through the capillary once before measuring the running times at least in triplicate for each test sample. The running times of the solvent (i.e., a 1%, w/v,  $\text{CH}_3\text{COOH}$  solution) and the

sample solution were used to calculate the relative viscosity ( $\eta_{rel}$ ) from the following equation:

$$\eta_{rel} = \frac{t}{t_0} \quad (4)$$

where  $t$  is the running time of the sample solution,  $t_0$  is the running time of the solvent.

Next, the viscosity reduction percentage was calculated from the following equation to determine the depolymerization of chitosan via acid hydrolysis or the solution plasma technique with and without metal complexation.

$$\text{Viscosity reduction (\%)} = \frac{V_t}{V_0} \times 100 \quad (5)$$

where  $V_0$  is the viscosity of the initial chitosan solution and  $V_t$  is the viscosity of the depolymerized chitosan solution at reaction time  $t$ .

FTIR spectroscopy (Thermo Nicolet Nexus, 670) was used to detect any changes in the chemical structure of the chitosan sample after depolymerization via either acid hydrolysis or the solution plasma technique. All of the ATR-FTIR spectra were collected using 64 scans in the range of 4000–400  $\text{cm}^{-1}$  at a resolution of 4  $\text{cm}^{-1}$  with a correction for atmospheric carbon dioxide ( $\text{CO}_2$ ).

The crystalline structure of chitosan both before and after depolymerization was characterized using an X-ray diffractometer (Bruker AXS, D8 advance) operated with a  $\text{Cu K}\alpha$  X-ray source. The WAXD analysis was performed in a continuous mode with a scan rate of  $1^\circ \text{min}^{-1}$  covering a scanning angle ( $2\theta$ ) of  $5$ – $80^\circ$ .

Gel permeation chromatography (GPC) was used to determine any changes in the average molecular weight of the chitosan samples at different reaction times. The chitosan sample was filtered through a nylon 66 membrane with a pore size of  $0.45 \mu\text{m}$  (Millipore, USA) prior to injection into the GPC instrument (Waters, Water 600E) equipped with an refractive index (RI) detector using an ultrahydrogel linear column (molecular weight resolving range of  $1.0 \times 10^3$ – $2.0 \times 10^7$  Da). The eluent used in the GPC analysis was an acetate buffer at pH 4.0 (a mixture of 0.5 M  $\text{CH}_3\text{COOH}$  and 0.5 M sodium acetate,  $\text{CH}_3\text{COONa}$ ). The sample injection volume was  $20 \mu\text{L}$ , and the flow rate of the mobile phase was maintained at  $0.6 \text{ mL min}^{-1}$ . The GPC analysis was performed at a chitosan concentration of  $2 \text{ mg mL}^{-1}$  at  $30^\circ\text{C}$ . Pullulans with a molecular weight in the range of  $5.90 \times 10^3$ – $7.08 \times 10^5$  Da were used as standard samples.

The main components in the water-soluble depolymerized chitosan product were further analyzed using a high performance liquid chromatograph (HPLC) (an Alltech 580 autosampler, an Alltech 626 HPLC pump, and a LiChrospher® 100  $\text{NH}_2$  column) with an evaporative light scattering detector (ELSD) (Alltech, 2000ES). The mobile phase solution was an isocratic system containing 70%  $\text{CH}_3\text{CN}$  and 30% deionized water. The flow rate of the mobile phase was maintained at  $0.8 \text{ mL min}^{-1}$ , and the sample injection volume was  $50 \mu\text{L}$ . The ELSD drift tube temperature was  $90^\circ\text{C}$ , and the nebulizer flow rate was  $2.2 \text{ L min}^{-1}$ .

Both the molecular mass and degree of polymerization (DP) of the extracted water-soluble depolymerized chitosan products (the second precipitate discussed in Section 2.4) was measured using an electrospray ionization-mass spectrometer (ESI-MS) (Bruker, microTOF II) operated in the positive mode. The test sample was prepared by re-dissolving the extracted water-soluble chitosan fraction in highly purified distilled water at a concentration of  $1 \text{ mg mL}^{-1}$  prior to dilution to  $10^4$  times. The diluted sample solution was injected into the ESI-MS equipment using a syringe at an injection flow rate of  $0.8 \mu\text{L mL}^{-1}$ . The analysis conditions were maintained at a drying gas temperature of  $180^\circ\text{C}$ , a drying gas flow rate of  $4.0 \text{ L min}^{-1}$ , a nebulizer gas pressure of 0.2 bar, a capillary voltage of 4.5 kV, and a skimmer voltage of 30 V. The molecular mass of the test sample was scanned in a mass-to-charge ratio ( $m/z$ )

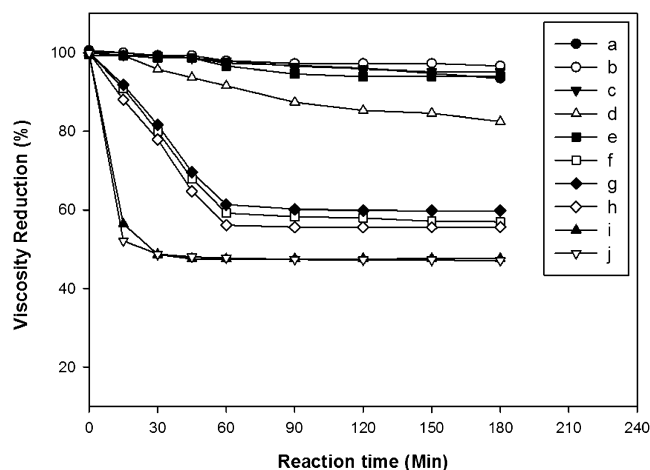


**Fig. 1.** Changes in the relative viscosity of chitosan samples after depolymerization via acid hydrolysis (a) without metal complexation, with complexation with (b)  $\text{Ag}^+$ , (c)  $\text{Zn}^{2+}$ , (d)  $\text{Cu}^{2+}$ , and (e)  $\text{Fe}^{3+}$  and (f) via a solution plasma technique without metal complexation and with complexation with (g)  $\text{Ag}^+$ , (h)  $\text{Zn}^{2+}$ , (i)  $\text{Cu}^{2+}$ , and (j)  $\text{Fe}^{3+}$  in a 1% (w/v)  $\text{CH}_3\text{COOH}$  solution either with or without the solution plasma technique at a metal-to-chitosan molar ratio of 1:8 as a function of reaction time.

range of 50–5000. All of the equipment used in the ESI-MS sample preparation was cleaned with  $\text{CH}_3\text{CN}$  prior to use.

To quantify the amount of remaining metal ions in the water-soluble depolymerized chitosan fraction, atomic absorption spectrophotometry (AAS) (Varian, AA280FS) was performed. The remaining metal percentage was calculated using the following equation:

$$\text{Remaining metal (\%)} = \frac{\text{remaining metal concentration}}{\text{initial metal concentration}} \times 100. \quad (6)$$

### 3. Results and discussion

As a preliminary investigation of the depolymerization process of the chitosan sample, the viscosity of the chitosan solution at a concentration of  $0.1 \text{ mg mL}^{-1}$  was measured as a function of reaction time. As shown in Fig. 1, the solution viscosity slightly decreased as the reaction time increased for the acid hydrolysis of chitosan with and without metal complexation in a 1% (w/v)  $\text{CH}_3\text{COOH}$  solution. When the corresponding chitosan solution was plasma-treated, the solution viscosity rapidly decreased as the reaction time increased from 0 min to 90 min before beginning to level off at reaction times longer than 90 min. These results implied that the depolymerization process was enhanced with the solution plasma treatment. In addition, the complexation between chitosan and various types of metal ions affected the depolymerization process. The addition of either  $\text{Ag}^+$  or  $\text{Zn}^{2+}$  to the chitosan solution exhibited a negligible effect on the viscosity reduction because the viscosity reduction profiles of the chitosan solution after complexation with these two metal ions were similar to that in the absence of metal ions. Meanwhile, the viscosity of the chitosan solution substantially decreased after complexation with  $\text{Cu}^{2+}$  or  $\text{Fe}^{3+}$ . From Fig. 1, the viscosity reduction percentage of the chitosan solution after the addition of  $\text{Cu}^{2+}$  for acid hydrolysis without plasma treatment decreased more than that with the other metal ions and without metal complexation and either  $\text{Cu}^{2+}$  or  $\text{Fe}^{3+}$  under plasma treatment dramatically decreased as the reaction time increased from 0 min to 45 min before remaining constant at reaction times longer than 45 min. These results suggested that, regardless of the depolymerization methods (i.e., acid hydrolysis and solution

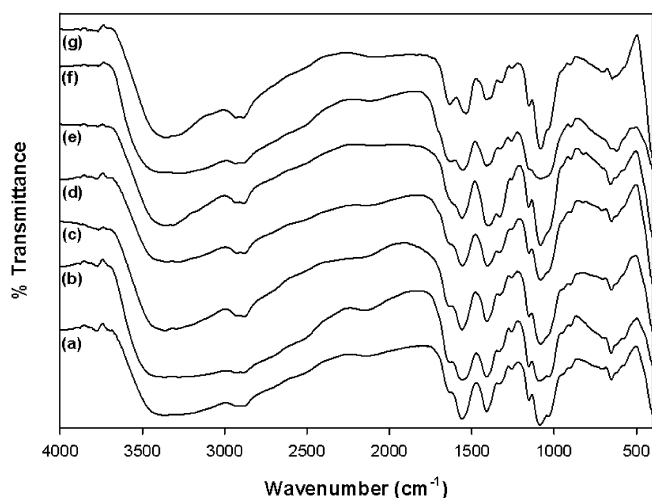


**Fig. 2.** FTIR spectra of the chitosan sample (a) before and after depolymerization via (b) acid hydrolysis and solution plasma technique (c) without metal complexation and with complexation with (d)  $\text{Ag}^+$ , (e)  $\text{Zn}^{2+}$ , (f)  $\text{Cu}^{2+}$ , and (g)  $\text{Fe}^{3+}$  at a metal-to-chitosan molar ratio of 1:8 and a reaction time of 2 h.

plasma treatment), the types of added metal ions play an important role in the depolymerization reaction of chitosan, which may be due to a difference in the affinities of chitosan toward different types of metal ions. The results suggested that the chitosan sample should form a stronger complex with  $\text{Cu}^{2+}$  and  $\text{Fe}^{3+}$  than  $\text{Zn}^{2+}$  and  $\text{Ag}^+$  (Varma, Deshpande, & Kennedy, 2004), resulting in a larger decrease in the molecular weight.

Due to the negligible effect of the viscosity reduction due to acid hydrolysis and acid hydrolysis with metal complexation, this study will focus on the depolymerization of chitosan–metal complexes via plasma solution to obtain low molecular weight chitosan products and/or chitosan oligomers compared to the chitosan products obtained from acid hydrolysis and solution plasma treatment without metal complexation.

Changes in the color of the chitosan solution during acid hydrolysis and solution plasma treatment either with or without metal complexation were also visually observed. The chitosan solution remained colorless and transparent during acid hydrolysis in a 1% (w/v)  $\text{CH}_3\text{COOH}$  solution over the studied reaction time. When the chitosan solution was plasma-treated either in the presence or absence of metal ions, the color of the chitosan solution changed from colorless to pale yellow and then to brown or dark brown as the reaction time increased from 0 min to 180 min. In addition, the color of the metal ions could interfere with the color of the chitosan solution. For examples, the addition of  $\text{Cu}^{2+}$  provided a pale bluish green color to the initial chitosan solution while the addition of  $\text{Fe}^{3+}$  resulted in an orange chitosan solution. A dark yellow to brown chitosan solution was obtained during the solution plasma treatment after complexation with  $\text{Ag}^+$ . Because  $\text{Ag}^+$  can be easily reduced after plasma discharge to form Ag particles (Pootawang, Saito, & Takai, 2011b), the Ag particles generated in the system may be responsible for the color of the plasma-treated chitosan solution being the darkest among those obtained under other conditions.

FTIR spectroscopy was used to investigate the changes in the chemical structure of the chitosan sample after the depolymerization process. As shown in Fig. 2a, the FTIR spectrum of the initial chitosan exhibited characteristic peaks located at approximately  $3450\text{ cm}^{-1}$ ,  $1650\text{ cm}^{-1}$ , and  $1550\text{ cm}^{-1}$ , which correspond to the stretching vibrations of the hydroxyl group ( $-\text{OH}$ ), amide I ( $-\text{NH}_2$ ), and amide II ( $-\text{NH}$ ), respectively, in the chemical structure of chitosan (Chen, Wu, & Zeng, 2005; Wang, Du, & Liu, 2004). After depolymerization via acid hydrolysis or solution plasma treatment both with and without metal complexation, these three

characteristic peaks remained in the FTIR spectra of the depolymerized products (see Fig. 2b–g). Because no additional characteristic peak were observed in the FTIR spectra of the depolymerized products, the studied depolymerization techniques (i.e., both acid hydrolysis and solution plasma treatment either with or without metal complexation) did not chemically modify the chitosan structure during the depolymerization process. However, in the presence of metal ions, the three characteristic peaks in the FTIR spectra of the depolymerized products gradually shifted to lower wavenumbers, which indicates that both  $-\text{OH}$  and  $-\text{NH}_2$  groups in the chemical structure of chitosan may be involved in metal complexation (see Fig. 2d–g). Fig. 3 shows the possible interactions between chitosan and the metal ions as well as the proposed depolymerization mechanism of chitosan via metal complexation. Chitosan was able to form a stable complex with the added metal ions via interactions with the  $-\text{OH}$  and  $-\text{NH}_2$  groups in the chitosan structure (Wang, Du, & Liu, 2004). As shown in Fig. 3, the hydroxyl radicals generated by the plasma reacted with the  $-\text{NH}_2$  groups of chitosan leading to the breakage of the  $\beta$ -1,4-glycosidic linkage (Prasertsung et al., 2012). The polymeric chain scissions at the  $\beta$ -1,4-glycosidic linkage decreased the molecular weight of chitosan (Chang, Tai, & Cheng, 2001).

It has been proposed that the formation of the chitosan–metal complex via the interaction of the  $-\text{OH}$  and  $-\text{NH}_2$  groups on the chitosan skeleton may lead to a weakened bond near the coordinating site, consequently providing weak points on the chitosan chain for the depolymerization (Yin et al., 2004). Because the polymeric chitosan chain in the complex was broken easier than that of chitosan itself, the depolymerization of chitosan could be enhanced after metal complexation (Yin et al., 2004). Furthermore, the added metal ions were capable of affecting the reaction during the depolymerization of chitosan, especially in the oxidative depolymerization. Yin et al. (2004) suggested that  $\text{Cu}^{2+}$  in the chitosan solution formed a complex with chitosan and catalyzed the decomposition of hydrogen peroxide ( $\text{H}_2\text{O}_2$ ) in the system, which acted as an initiator for the depolymerization reaction. In addition, the chitosan–metal complex exhibited a lower crystallinity than the chitosan itself, resulting in better accessibility to the reactants and better reactivity (Yin et al., 2004).

Fig. 4 shows the WAXD patterns of chitosan and the depolymerized chitosan products after acid hydrolysis and solution plasma treatment either with or without metal complexation. Prior to the depolymerization process (see Fig. 4a), the WAXD pattern exhibited two major characteristic diffraction peaks at a  $2\theta$  of  $10^\circ$  and  $20^\circ$ , which correspond to the semi-crystalline structure of chitosan (Kisku & Swain, 2012; Kumar & Koh, 2012; Wang, Du, & Liu, 2004; Yue, Yao, & Wei, 2009). After depolymerization via acid hydrolysis or the solution plasma technique, the diffraction peak located at a  $2\theta$  of  $10^\circ$  disappeared while the peak located at a  $2\theta$  of  $20^\circ$  became broader (see Fig. 4b and c), suggesting that the crystalline region of the chitosan sample was disrupted during the depolymerization. When the solution plasma treatment was applied in combination with metal complexation, the diffraction peak at  $2\theta$  equal to  $10^\circ$  in the WAXD patterns of the depolymerized chitosan products still disappeared but the peak at a  $2\theta$  of  $20^\circ$  was much broader with a much lower peak intensity, especially for those after complexation with  $\text{Cu}^{2+}$  and  $\text{Fe}^{3+}$  (see Fig. 4d–f). The results indicated that the solution plasma treatment of the chitosan–metal complexes could disrupt the crystalline structure of the chitosan sample more than acid hydrolysis and the solution plasma treatment without metal complexation. Interestingly, it was also observed that, after the chitosan– $\text{Ag}^+$  complex was plasma-treated, the WAXD patterns of the depolymerized product exhibited sharp and intense characteristic diffraction peaks of Ag particles at  $2\theta$  of approximately  $40^\circ$ ,  $45^\circ$ ,  $65^\circ$ , and  $78^\circ$  corresponding to the (1 1 1), (2 0 0), (2 2 0), and (3 1 1) planes of the Ag crystals, respectively (Mandal et al., 2005;



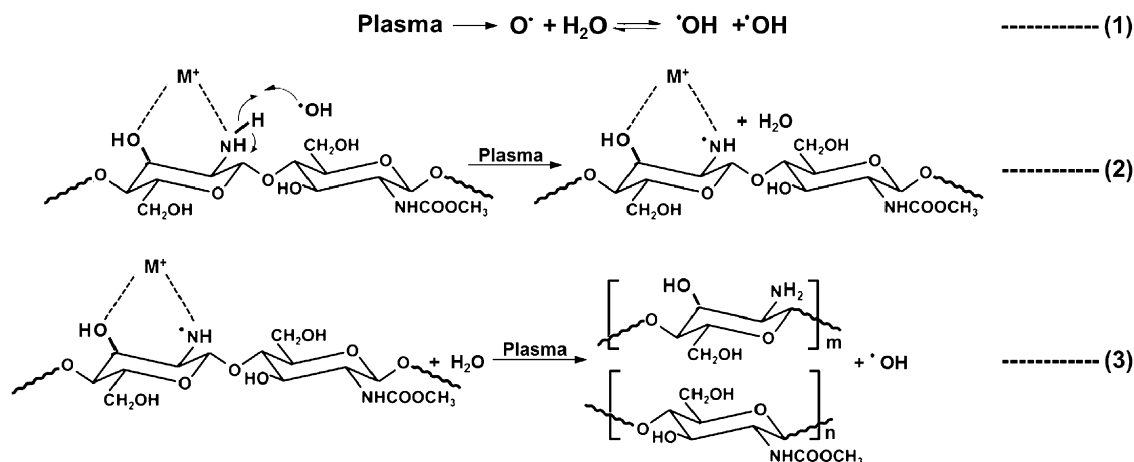


Fig. 3. Possible interactions between metal ions and chitosan during the formation of the chitosan–metal complex and proposed depolymerization mechanism.

Pootawang, Saito, & Takai, 2011b; Shameli et al., 2012). Therefore, the results of the WAXD analysis also confirmed the formation of Ag particles in the system during the solution plasma treatment of the chitosan solution after complexation with  $Ag^+$ .

Table 1 shows the changes in the weight average molecular weight ( $\bar{M}_w$ ) and polydispersity index (PDI) of the chitosan sample during depolymerization via acid hydrolysis and solution plasma treatment either with or without metal complexation as a function of the reaction time. From the GPC analysis, the molecular weight of the initial chitosan was determined to be in the range of  $10^5$ – $10^6$  Da. As shown in Table 1, after acid hydrolysis in a 1% (w/v)  $CH_3COOH$  solution for 180 min, the molecular weight of the chitosan sample slightly decreased from its initial value to  $10^4$ – $10^5$  Da. However, when the solution plasma treatment was employed for depolymerization, the molecular weight of chitosan substantially decreased to approximately  $10^3$ – $10^4$  Da. Therefore, the depolymerized products obtained from the solution plasma treatment could be identified as LMWC (molecular weight in the range of 5–20 kDa)

(Harish, Prashanth, & Tharanathan, 2007). Our results are consistent with those reported by Prasertsung et al. (2012), who found that the solution plasma technique was a potential method for the preparation of LMWC via the depolymerization of chitosan.

The results of the GPC analysis further revealed that the addition of either  $Ag^+$  or  $Zn^{2+}$  to the chitosan solution slightly affected the depolymerization reaction because the molecular weight of the obtained products did not significantly vary from that obtained from the solution plasma treatment without metal complexation (see Table 1). As the  $Cu^{2+}$  or  $Fe^{3+}$  was added to the chitosan solution, the depolymerization reaction was dramatically enhanced. As shown in Table 1, the weight average molecular weight of the depolymerized chitosan products was measured to be approximately  $10^3$  Da for the chitosan– $Cu^{2+}$  complex, which was considered to be in the range of chitosan oligomers (molecular weight less than 5 kDa) (Harish, Prashanth, & Tharanathan, 2007). A stronger promoting effect from the addition of  $Cu^{2+}$  or  $Fe^{3+}$  on the depolymerization reaction of chitosan may be due to the greater affinity of chitosan for these two metal ions and the catalytic activities of both ions for the decomposition of  $H_2O_2$  (i.e., Fenton reaction) (Chang, Tai, & Cheng, 2001; Tanioka et al., 1996) generated in the system during the plasma discharge (Bláha et al., 2011; Pootawang et al., 2011b; Prasertsung et al., 2012; Yin et al., 2004). Therefore, a catalyzed decomposition reaction of  $H_2O_2$  may also be responsible for the decrease in the molecular weight of the depolymerized products.

The depolymerization kinetics were analyzed based on the relationship between  $\bar{M}_w$  of the chitosan sample and the reaction time as follows:

$$\frac{1}{M_t} = \frac{1}{M_0} + \frac{kt}{M} = \frac{1}{M_0} + k't \quad (7)$$

where  $M_t$  is  $\bar{M}_w$  of the chitosan sample at reaction time ( $t$ ),  $M_0$  is the initial  $\bar{M}_w$  of the chitosan sample,  $M$  is the molecular weight of the chitosan monomer,  $k$  ( $\text{min}^{-1}$ ) or  $k'$  ( $\text{mol g}^{-1} \text{min}^{-1}$ ) is the depolymerization rate constant, and  $t$  is the reaction time (Chang, Tai, & Cheng, 2001). Fig. 5 shows a linear relationship between the inverse of the chitosan molecular weight and reaction time for the initial stage of depolymerization (reaction time between 0 min to 60 min). The  $k$  value of the depolymerization of chitosan via the acid hydrolysis route was determined to be  $2.42 \times 10^{-3} \text{ min}^{-1}$  while that obtained for the solution plasma treatment without metal complexation was one order of magnitude higher (or approximately  $2.42 \times 10^{-2} \text{ min}^{-1}$ ). After complexation with  $Ag^+$ ,  $Zn^{2+}$ ,  $Cu^{2+}$ , and  $Fe^{3+}$ , the  $k$  values were calculated to be  $2.47 \times 10^{-2} \text{ min}^{-1}$ ,  $4.83 \times 10^{-2} \text{ min}^{-1}$ ,  $1.10 \times 10^{-1} \text{ min}^{-1}$ , and  $8.83 \times 10^{-2} \text{ min}^{-1}$ ,

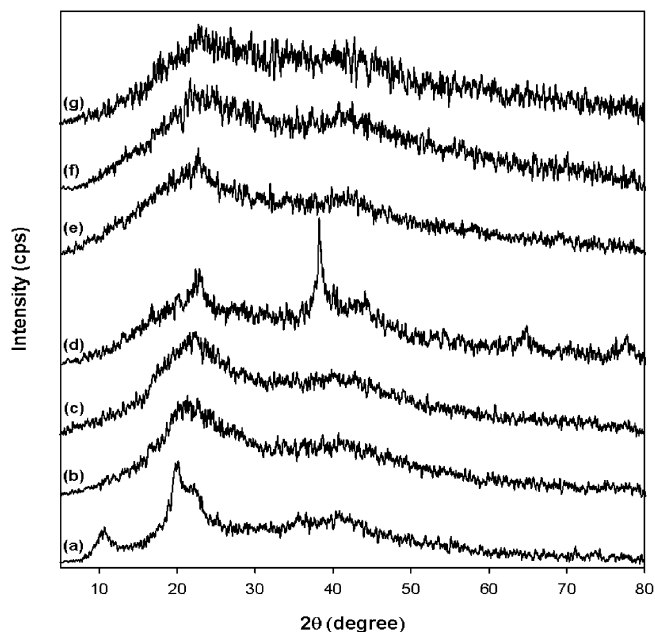


Fig. 4. WAXD patterns of the chitosan sample (a) before and after depolymerization via (b) acid hydrolysis and solution plasma technique (c) without metal complexation and with complexation with (d)  $Ag^+$ , (e)  $Zn^{2+}$ , (f)  $Cu^{2+}$ , and (g)  $Fe^{3+}$  at a metal-to-chitosan molar ratio of 1:8 and a reaction time of 2 h.



**Table 1**

Weight average molecular weight ( $\bar{M}_w$ ) and polydispersity index (PDI) of a chitosan sample after depolymerization via acid hydrolysis and solution plasma technique in a 1% (w/v)  $\text{CH}_3\text{COOH}$  solution without metal complexation and with complexation with  $\text{Ag}^+$ ,  $\text{Zn}^{2+}$ ,  $\text{Cu}^{2+}$ , and  $\text{Fe}^{3+}$  at a metal-to-chitosan molar ratio of 1:8 and different reaction time intervals.

Reaction time (min)	Molecular weight (Da)/PDI					
	Acid hydrolysis	Solution plasma	Solution plasma with metal complexation			
			$\text{Ag}^+$	$\text{Zn}^{2+}$	$\text{Cu}^{2+}$	$\text{Fe}^{3+}$
0	$1.1 \times 10^6$ <sup>a</sup> (4.1) <sup>b</sup>	$1.1 \times 10^6$ (4.1)	$1.1 \times 10^6$ (4.1)	$1.1 \times 10^6$ (4.1)	$1.1 \times 10^6$ (4.1)	$1.1 \times 10^6$ (4.1)
15	$8.3 \times 10^5$ (5.0)	$4.3 \times 10^5$ (5.4)	$7.1 \times 10^5$ (5.3)	$2.0 \times 10^5$ (3.3)	$1.3 \times 10^5$ (3.2)	$1.5 \times 10^5$ (4.1)
30	$7.9 \times 10^5$ (4.3)	$2.0 \times 10^5$ (5.3)	$1.8 \times 10^5$ (4.9)	$7.0 \times 10^4$ (3.3)	$7.0 \times 10^4$ (3.0)	$6.4 \times 10^4$ (4.1)
60	$5.5 \times 10^5$ (6.2)	$1.0 \times 10^5$ (4.4)	$9.5 \times 10^4$ (4.1)	$6.0 \times 10^4$ (3.6)	$2.2 \times 10^4$ (2.1)	$2.9 \times 10^4$ (3.6)
120	$6.4 \times 10^5$ (5.0)	$4.8 \times 10^4$ (5.7)	$1.6 \times 10^5$ (10.5)	$2.6 \times 10^4$ (3.9)	$6.2 \times 10^3$ (2.4)	$1.4 \times 10^4$ (2.9)
180	$2.3 \times 10^5$ (2.6)	$1.8 \times 10^4$ (3.7)	$1.4 \times 10^4$ (3.2)	$1.0 \times 10^4$ (2.7)	$1.9 \times 10^3$ (1.4)	$3.6 \times 10^4$ (21.8)

<sup>a</sup> Reported values are  $\bar{M}_w$  of the chitosan sample after depolymerization.

<sup>b</sup> Reported values in parentheses indicate the PDI of the chitosan sample after depolymerization.

respectively. Based on the calculated  $k$ , the order of the depolymerization reactions of chitosan sample was determined to be  $\text{Cu}^{2+}$  ( $1.10 \times 10^{-1} \text{ min}^{-1}$ )  $\sim$   $\text{Fe}^{3+}$  ( $8.83 \times 10^{-2} \text{ min}^{-1}$ )  $\gg$   $\text{Zn}^{2+}$  ( $4.83 \times 10^{-2} \text{ min}^{-1}$ )  $\sim$   $\text{Ag}^+$  ( $2.47 \times 10^{-2} \text{ min}^{-1}$ )  $\sim$  solution plasma without metal complexation ( $2.42 \times 10^{-2} \text{ min}^{-1}$ )  $\gg$  acid hydrolysis ( $2.42 \times 10^{-3} \text{ min}^{-1}$ )  $\sim$  acid hydrolysis with metal complexation (data not shown). Therefore, our results indicate that the solution plasma treatment with metal complexation, especially with  $\text{Cu}^{2+}$  and  $\text{Fe}^{3+}$ , is an effective method for the depolymerization of chitosan. In addition, the calculated  $k$  of the chitosan depolymerization via the solution plasma treatment with metal complexation in this study was much higher than those previously reported in the literature. For example, based on the work of Ilyina et al. (2000), the  $k$  value of the enzymatic depolymerization of chitosan was in the range of  $10^{-5}$ – $10^{-4} \text{ min}^{-1}$  (i.e., approximately 2–3 orders of magnitude lower than that of our results). In another study (Chang, Tai, & Cheng, 2001), the  $k$  value of the chitosan depolymerization in the presence of  $\text{H}_2\text{O}_2$  was reported to be in the range of  $4.2 \times 10^{-4} \text{ min}^{-1}$ – $7.1 \times 10^{-4} \text{ min}^{-1}$ .

To further investigate the potential use of the solution plasma treatment for the depolymerization of chitosan, the depolymerized products (i.e., the water-insoluble or water-soluble products) were subsequently separated from the chitosan solution at different reaction times. Fig. 6 shows the percentage of the water-insoluble

and water-soluble fractions as well as the total yield percentages as a function of reaction time. At each of the studied reaction times, a majority of the depolymerized chitosan product obtained from the conventional acid hydrolysis route was water-insoluble. This result indicated that the acid-depolymerized chitosan products still possessed a molecular weight that was too high to be dissolved in an aqueous solution at neutral pH. However, the depolymerized chitosan products obtained from the solution plasma treatment either with or without metal complexation contained both water-insoluble and water-soluble fractions as the reaction time increased beyond 120 min. As shown in Fig. 6, the highest water-soluble chitosan fraction was 57%, which was obtained with the solution plasma treatment in combination with  $\text{Fe}^{3+}$  complexation was used for the depolymerization with a reaction time of 180 min (which was comparable to that obtained from the solution plasma treatment in combination with  $\text{Cu}^{2+}$  complexation at the same reaction time (i.e., approximately 51%). The addition of  $\text{Ag}^+$  and  $\text{Zn}^{2+}$  to the chitosan solution slightly enhanced the depolymerization process because the percentages of water-insoluble and water-soluble depolymerized chitosan fractions were similar to those obtained from the solution plasma treatment in the absence of metal complexation. Therefore, the order of the efficiency of the depolymerization of the chitosan sample was determined to be  $\text{Cu}^{2+} \sim \text{Fe}^{3+} \gg \text{Zn}^{2+} \sim \text{Ag}^+ \sim$  solution plasma without metal complexation  $\gg$  acid hydrolysis. This result is also consistent with the calculated rate constant of the depolymerization reaction of the chitosan sample. According to the literature (Choi et al., 2002; Prasertsung et al., 2012), the water-soluble depolymerized chitosan fraction was expected to be the chitosan oligomers.

The HPLC-ELSD technique was subsequently used to analyze the components in the water-soluble depolymerized chitosan products. Obviously, the HPLC-ELSD chromatogram (figure not shown) of commercial GlcN exhibited a main peak at a retention time of approximately 6.9 min. This GlcN peak at the same retention time was also observed in the HPLC-ELSD chromatograms of all of the testes water-soluble depolymerized chitosan products. However, another peak was observed in the HPLC-ELSD chromatograms of the water-soluble fractions at a longer retention time of approximately 7.9 min, which mostly likely corresponds to the presence of chitosan oligomers in the test samples.

To verify the presence of chitosan oligomers in the water-soluble depolymerized chitosan products, ESI-MS analysis was performed. In the current study, because the MS analysis was operated in the positive ESI mode, positively charged molecules were observed. Fig. 7 shows the ESI-MS spectra of the water-soluble depolymerized chitosan products obtained from the solution plasma treatment either without or with metal complexation. All

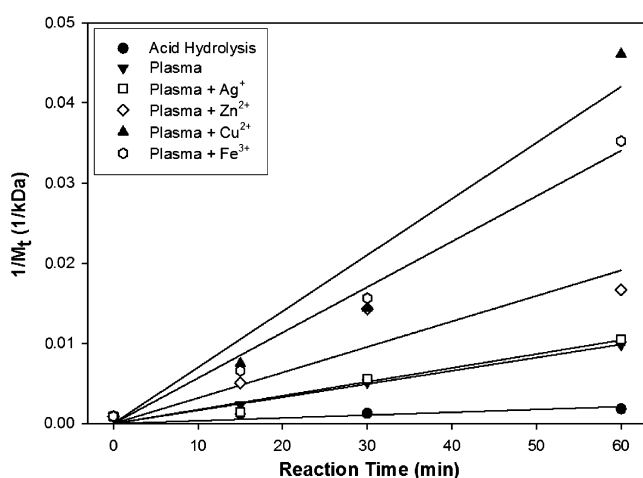


**Fig. 5.** Linear relationship between the inverse of the molecular weight ( $1/M_t$ ) and the degradation time ( $t$ ) for the initial stage of depolymerization of the chitosan sample after acid hydrolysis and solution plasma treatment either without metal complexation or with complexation with  $\text{Ag}^+$ ,  $\text{Zn}^{2+}$ ,  $\text{Cu}^{2+}$ , and  $\text{Fe}^{3+}$  at a metal-to-chitosan molar ratio of 1:8 and different reaction time intervals.

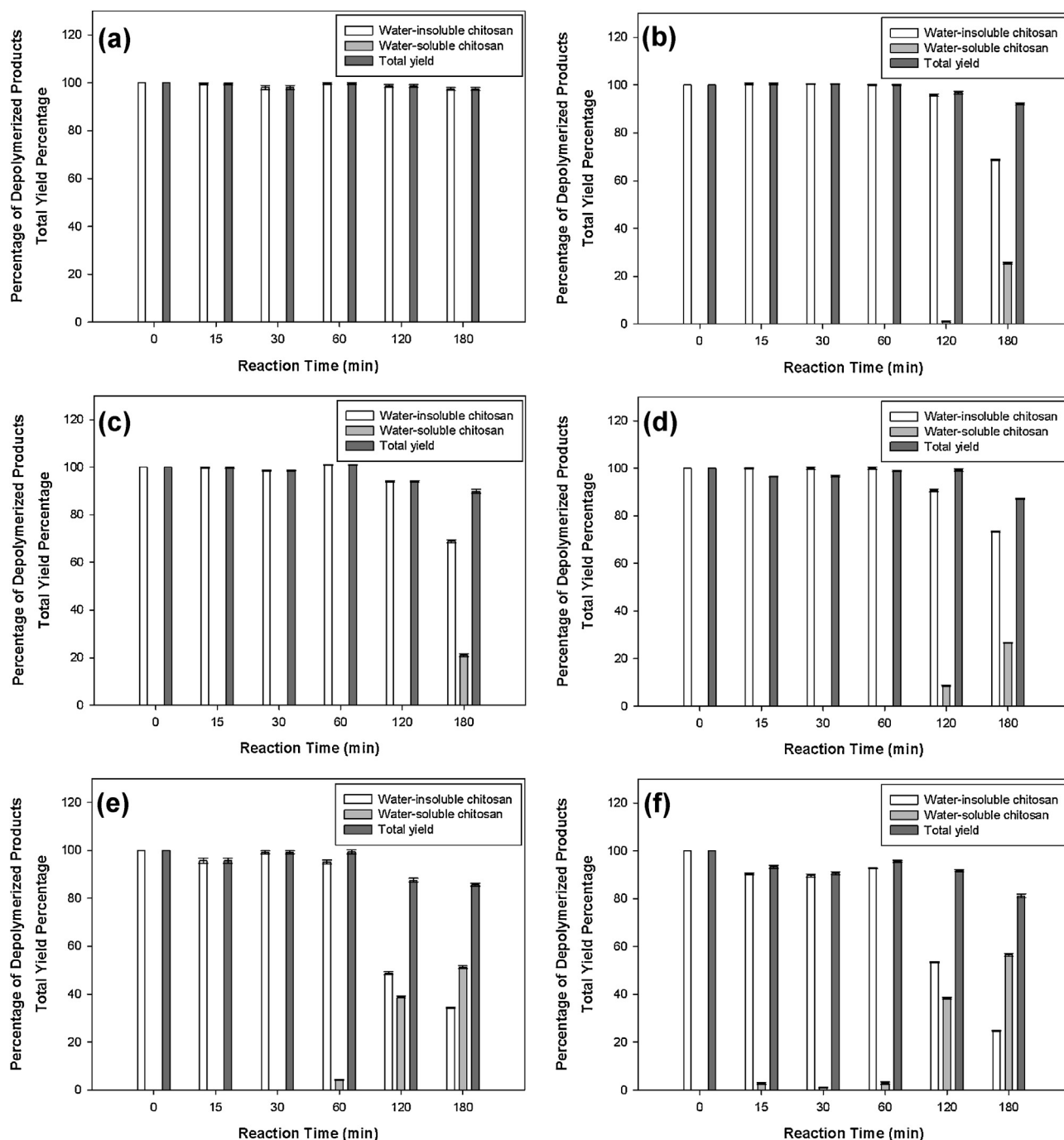


**Fig. 6.** Percentage of water-insoluble chitosan, water-soluble chitosan, and total yield of depolymerized products obtained from (a) acid hydrolysis and solution plasma treatment of chitosan in a 1% (w/v)  $\text{CH}_3\text{COOH}$  solution (c) without metal complexation and with complexation with (d)  $\text{Ag}^+$ , (e)  $\text{Zn}^{2+}$ , (f)  $\text{Cu}^{2+}$ , and (g)  $\text{Fe}^{3+}$  at a metal-to-chitosan molar ratio of 1:8 and different reaction time intervals.

of the ESI-MS spectra exhibited three dominant peaks located at an  $m/z$  ratio of approximately 381, 425, and 543, which are most likely due to the cluster ions of the GlcN monomer  $[2(\text{GlcN})+\text{Na}^+]$ , the  $\text{CH}_3\text{CN}$  adduct of the dimer containing one GlcN unit and one GlcNAc unit  $[\text{GlcN}-\text{GlcNAc}+\text{CH}_3\text{CN}+\text{H}^+]$ , and the proton adduct of the trimer containing two GlcN units and one GlcNAc unit  $[2(\text{GlcN})-\text{GlcNAc}+\text{H}^+]$ . Therefore, the ESI-MS results indicated that the water-soluble depolymerized chitosan products were composed of GlcN monomers as well as chitosan oligomers with DP in the range of 2–3.

AAS analysis was performed to quantify the amount of the added metals remaining in the water-soluble depolymerized chitosan fraction because the remaining metals could potentially affect the end-use of the chitosan oligomer products. The AAS results indicated that all of the added metals remaining in the water-soluble depolymerized chitosan products obtained from the solution plasma treatment after complexation with  $\text{Ag}^+$ ,  $\text{Zn}^{2+}$ ,  $\text{Cu}^{2+}$ , and  $\text{Fe}^{3+}$  were very low (i.e.,  $6.87 \pm 0.03$  ppm ( $1.16 \pm 0.01\%$ ),  $38.99 \pm 0.25$  ppm ( $3.75 \pm 0.02\%$ ),  $8.07 \pm 0.03$  ppm ( $0.93 \pm 0.00\%$ ) and  $0.35 \pm 0.01$  ppm ( $0.04 \pm 0.00\%$ ), respectively) indicating that

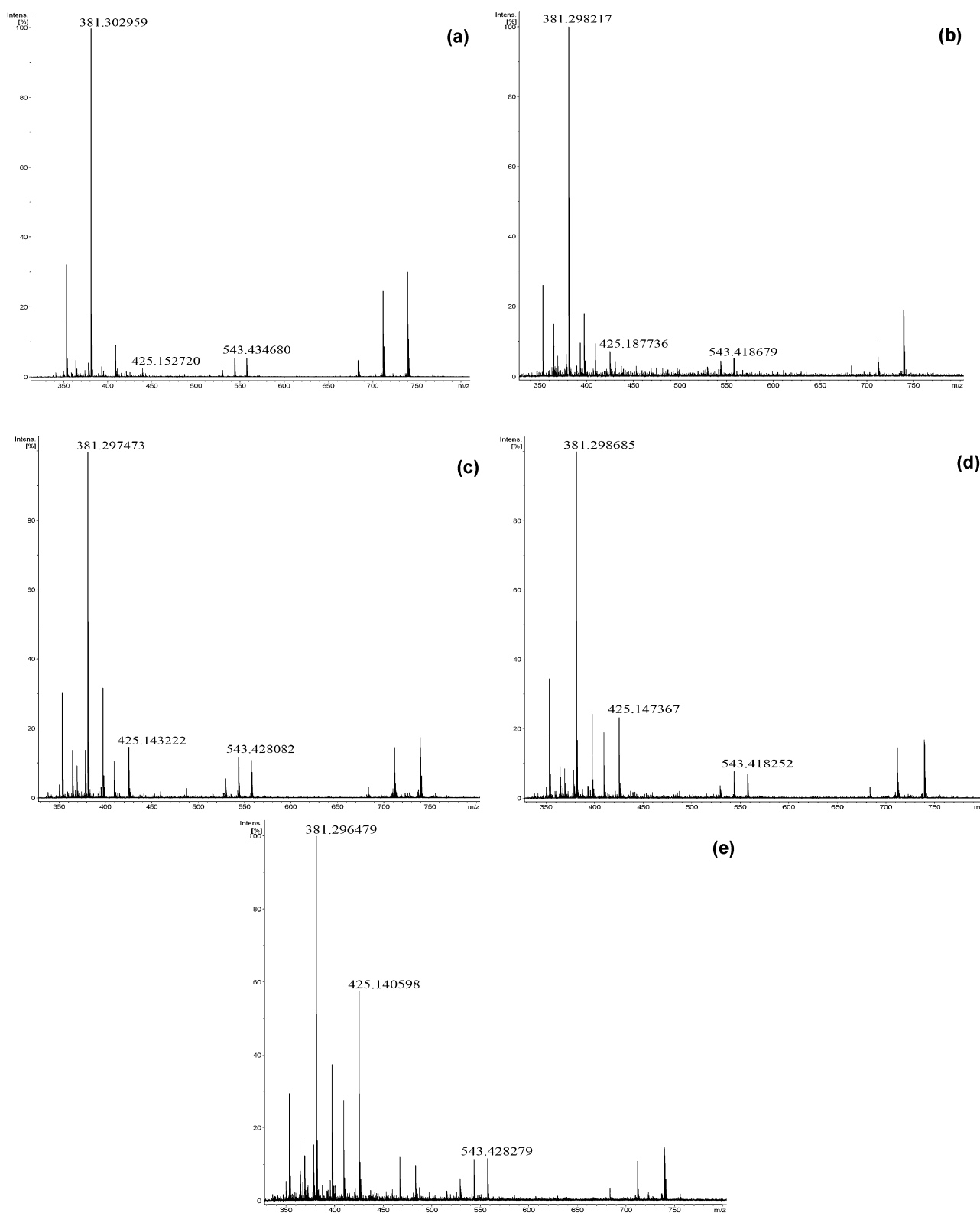


**Fig. 7.** ESI-MS spectra of the water-soluble depolymerized chitosan products obtained from the solution plasma technique (a) without metal complexation and with complexation with (b)  $\text{Ag}^+$ , (c)  $\text{Zn}^{2+}$ , (d)  $\text{Cu}^{2+}$ , and (e)  $\text{Fe}^{3+}$  at a metal-to-chitosan molar ratio of 1:8 and a reaction time of 180 min. All of the spectra exhibited three main peaks at an  $m/z$  of approximately 381 [ $2(\text{GlcN})+\text{Na}^+$ ], 425 [ $\text{GlcN-GlcNAc}+\text{CH}_3\text{CN}+\text{H}^+$ ] and 543 [ $2(\text{GlcN})-\text{GlcNAc}+\text{H}^+$ ].

most of the added metals were removed during the separation and purification step.

#### 4. Conclusions

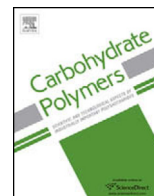
In comparison to conventional acid hydrolysis, chitosan was more effectively depolymerized by a solution plasma treatment. The depolymerization of chitosan via the solution plasma technique was further enhanced after the complexation of chitosan with metal ions. However, the types of metal ions added to the chitosan solution also played a crucial role in the depolymerization process due to a difference in the affinities of chitosan for the different metal ions. Glucosamine and low-molecular-weight depolymerized chitosan products (i.e., approximately  $10^3$  Da), which is in the range of chitosan oligomers, were obtained when the solution plasma was applied in combination with complexation with either  $\text{Cu}^{2+}$  or  $\text{Fe}^{3+}$ . In summary, the solution plasma technique in combination with chitosan–metal complexation has the potential for use in large-scale production of both LMWC and chitosan oligomers with high polymerization rates and yields of water-soluble depolymerized products.

#### Acknowledgments

OP and CV wish to thank the Ratchadapiseksomphot Endowment Fund, Chulalongkorn University for providing postdoctoral fellowships. CK wishes to thank Chulalongkorn University for the Dutsadi Phiphat Ph.D. Scholarship. This work was financially supported by the Thailand Research Fund (TRF) from contract number BRG5480008. The authors wish to thank Surapon Foods Public Co., Ltd. (Thailand) for providing the shrimp shells used in the preparation of chitosan.

#### References

- Baxter, S., Zivanovic, S., & Weiss, J. (2005). Molecular weight and degree of acetylation of high-intensity ultrasonicated chitosan. *Food Hydrocolloids*, 19, 821–830.
- Bláha, M., Riesová, M., Zedník, J., Anžlovar, A., Žigon, M., & Vohlídal, J. (2011). Polyaniline synthesis with iron(III) chloride–hydrogen peroxide catalyst system: Reaction course and polymer structure study. *Synthetic Metals*, 161, 1217–1225.
- Chang, K. L. B., Tai, M. C., & Cheng, F. H. (2001). Kinetics and products of the degradation of chitosan by hydrogen peroxide. *Journal of Agricultural and Food Chemistry*, 49, 4845–4851.
- Chen, S., Wu, G., & Zeng, H. (2005). Preparation of high antimicrobial activity thiourea chitosan– $\text{Ag}^+$  complex. *Carbohydrate Polymers*, 60, 33–38.
- Choi, W. S., Ahn, K. J., Lee, D. W., Byun, M. W., & Park, H. J. (2002). Preparation of chitosan oligomers by irradiation. *Polymer Degradation and Stability*, 78, 533–538.
- Fernandes, J. C., Tavará, F. K., Soares, J. C., Ramos, O. S., Monteiro, M. J., Pintado, M. E., et al. (2008). Antimicrobial effects of chitosans and chitoooligosaccharides, upon *Staphylococcus aureus* and *Escherichia coli*, in food model systems. *Food Microbiology*, 25, 922–928.
- Harish Prashanth, K. V., & Tharanathan, R. N. (2007). Chitin/chitosan: Modifications and their unlimited application potential – An overview. *Trends in Food Science & Technology*, 18, 117–131.
- Ilyina, A. V., Tikhonov, V. E., Albulov, A. I., & Varlamov, V. P. (2000). Enzymic preparation of acid-free-water-soluble chitosan. *Process Biochemistry*, 35, 563–568.
- Jeon, Y.-J., Park, P.-J., & Kim, S.-K. (2001). Antimicrobial effect of chitoooligosaccharides produced by bioreactor. *Carbohydrate Polymers*, 44, 71–76.
- Kendra, D. F., & Hadwiger, L. A. (1984). Characterization of the smallest chitosan oligomer that is maximally antifungal to *Fusarium solani* and elicits pisatin formation in *Pisum sativum*. *Experimental Mycology*, 8, 276–281.
- Kisku, S. K., & Swain, S. K. (2012). Synthesis and characterization of chitosan/boron nitride composites. *Journal of the American Ceramic Society*, 95, 2753–2757.
- Klaikherd, A., Jayanta, M. L. S., Boonjawat, J., Aiba, S., & Sukwattanasinitt, M. (2004). Depolymerization of  $\beta$ -chitin to mono- and disaccharides by the serum fraction from the para rubber tree, *Hevea brasiliensis*. *Carbohydrate Research*, 339, 2799–2804.
- Kumar, S., & Koh, J. (2012). Physicochemical, optical and biological activity of chitosan–chromone derivative for biomedical applications. *International Journal of Molecular Sciences*, 13, 6102–6116.
- Liang, T.-W., Chen, Y.-J., Yen, Y.-H., & Wang, S.-L. (2007). The antitumor activity of the hydrolysates of chitinous materials hydrolyzed by crude enzyme from *Bacillus amyloliquefaciens* V656. *Process Biochemistry*, 42, 527–534.
- Mandal, S., Arumugam, S. K., Pasricha, R., & Sastry, M. (2005). Silver nanoparticles of variable morphology synthesized in aqueous foams as novel template. *Bulletin of Materials Science*, 28, 503–510.
- Muzzarelli, R. A. A. (2009). Chitins and chitosans for the repair of wounded skin, nerve, cartilage and bone. *Carbohydrate Polymers*, 76, 167–182.
- Muzzarelli, R. A. A. (2010). Enhanced biochemical efficacy of oligomeric and partially depolymerized chitosans. In F. Columbus (Ed.), *Chitosan: Manufacture, properties and usages*. Hauppauge, NY, USA: Nova Publ.
- Muzzarelli, R. A. A., Stanic, V., & Ramos, V. (1999). Enzymatic depolymerization of chitins and chitosans. In C. Bucke (Ed.), *Methods in biotechnology: Carbohydrate biotechnology protocols*. Totowa: Humana Press.
- Pootawang, P., Saito, N., & Takai, O. (2011a). Solution plasma for template removal in mesoporous silica: pH and discharge time varying characteristics. *Thin Solid Films*, 519, 7030–7035.
- Pootawang, P., Saito, N., & Takai, O. (2011b). Ag nanoparticles incorporation in mesoporous silica synthesized by solution plasma and their catalysis for oleic acid hydrogenation. *Materials Letters*, 65, 1037–1040.
- Prasertsung, I., Damrongsakkul, S., Terashima, C., Saito, N., & Takai, O. (2012). Preparation of low molecular weight of chitosan using solution plasma system. *Carbohydrate Polymers*, 87, 2745–2749.
- Qin, C., Zhou, B., Zeng, L., Zhang, Z., Liu, Y., Du, Y., & Xiao, L. (2004). The physicochemical properties and antitumor activity of cellulase-treated chitosan. *Food Chemistry*, 84, 107–115.
- Saito, N., Hieda, J., & Takai, O. (2009). Synthesis process of gold nanoparticles in solution plasma. *Thin Solid Films*, 518, 912–917.
- Shameli, K., Ahmad, M. B., Jazayeri, S. D., Sedaghat, S., Shabanzadeh, P., Jahangirian, H., & Abdollahi, Y. (2012). Synthesis and characterization of polyethylene glycol mediated silver nanoparticles by the green method. *International Journal of Molecular Sciences*, 13, 6639–6650.
- Tanioka, S., Matsui, Y., Irie, T., Tanigawa, T., Tanaka, Y., Shibata, H., & Kono, Y. (1996). Oxidative depolymerization of chitosan by hydroxyl radical. *Bioscience, Biotechnology and Biochemistry*, 60, 2001–2004.
- Toda, M., Shimoji, K., & Sasaki, J. (1987). Preparation of glucosamine derivatives as immunostimulants and antitumor agents. Eur Pat 226,381(1987). *Chemical Abstracts*, 107, 237216.
- Varma, A. J., Deshpande, S. V., & Kennedy, J. F. (2004). Metal complexation by chitosan and its derivatives: A review. *Carbohydrate Polymers*, 55, 77–93.
- Wang, X., Du, Y., & Liu, H. (2004). Preparation, characterization, and antimicrobial activity of chitosan–Zn complex. *Carbohydrate Polymers*, 56, 21–26.
- Wattananaphanit, A., & Saito, N. (2013). Effect of polymer concentration on the depolymerization of sodium alginate by the solution plasma process. *Polymer Degradation and Stability*, 98, 1072–1080.
- Yin, X., Zhang, X., Lin, Q., Feng, Y., Yu, X., & Zhang, Q. (2004). Metal-coordinating controlled oxidative degradation of chitosan and antioxidant activity of chitosan–metal complex. *ARKIVOC*, ix, 66–78.
- Yue, W., Yao, P., & Wei, Y. (2009). Influence of ultraviolet-irradiated oxygen on depolymerization of chitosan. *Polymer Degradation and Stability*, 94, 851–858.



# Enhanced degradation of chitosan by applying plasma treatment in combination with oxidizing agents for potential use as an anticancer agent

Chayanaphat Chokradjaroen<sup>a</sup>, Ratana Rujiravanit<sup>a,b,c,\*</sup>, Anyarat Watthanaphanit<sup>d</sup>, Sewan Theeramunkong<sup>e</sup>, Nagahiro Saito<sup>f</sup>, Kazuko Yamashita<sup>g</sup>, Ryuichi Arakawa<sup>g</sup>

<sup>a</sup> The Petroleum and Petrochemical College, Chulalongkorn University, Bangkok 10330, Thailand

<sup>b</sup> Center of Excellence on Petrochemical and Materials Technology, Chulalongkorn University, Bangkok 10330, Thailand

<sup>c</sup> NU-PPC Plasma Chemical Technology Laboratory, Chulalongkorn University, Bangkok 10330, Thailand

<sup>d</sup> Department of Chemistry, Faculty of Science, Mahidol University, Bangkok 10400, Thailand

<sup>e</sup> Faculty of Pharmacy, Thammasat University, Pathumthani 12120, Thailand

<sup>f</sup> Department of Materials, Physics and Energy Engineering, Graduate School of Engineering, Nagoya University, Nagoya 464-8603, Japan

<sup>g</sup> Department of Chemistry and Materials Engineering, Faculty of Chemistry, Materials and Bioengineering, Kansai University, Osaka 564-8680, Japan

## ARTICLE INFO

### Article history:

Received 9 December 2016

Received in revised form 2 March 2017

Accepted 2 March 2017

Available online 6 March 2017

### Keywords:

Chitosan

Degradation

Plasma treatment

Oxidizing agent

Chitoooligosaccharide

## ABSTRACT

Solution plasma (SP) treatment in combination with oxidizing agents, i.e., hydrogen peroxide ( $H_2O_2$ ), potassium persulfate ( $K_2S_2O_8$ ) and sodium nitrite ( $NaNO_2$ ) were adopted to chitosan degradation in order to achieve fast degradation rate, low chemicals used and high yield of low-molecular-weight chitosan and chitoooligosaccharide (COS). Among the studied oxidizing agents,  $H_2O_2$  was found to be the best choice in terms of appreciable molecular weight reduction without major change in chemical structure of the degraded products of chitosan. By the combination with SP treatment, dilute solution of  $H_2O_2$  (4–60 mM) was required for effective degradation of chitosan. The combination of SP treatment and dilute solution of  $H_2O_2$  (60 mM) resulted in the great reduction of molecular weight of chitosan and water-soluble chitosan was obtained as a major product. The resulting water-soluble chitosan was precipitated to obtain COS. An inhibitory effect against cervical cancer cell line (HeLa cells) of COS was also examined.

© 2017 Elsevier Ltd. All rights reserved.

## 1. Introduction

Chitosan is a deacetylated form of chitin which can be found in some crustaceans such as shrimp and crab. Chitosan consists of 2-deoxy-2-amino-D-glucopyranose (GlcN) and 2-deoxy-2-acetamido-D-glucopyranose (GlcNAc) units that are linked together with  $\beta$ -(1,4) glycosidic bonds. A native chitosan usually has a high molecular weight with ubiquitous hydrogen bonds leading to low solubility of chitosan powder and high viscosity of chitosan solution. Degradation of chitosan to obtain low-molecular-weight chitosan (LMWC) and chitoooligosaccharide (COS) can solve the problems originated from its high molecular weight. Moreover, LMWC and COS exhibit some incredible biological functions, especially antitumor and anticancer

activities (Harish Prashanth & Tharanathan, 2005; Zheng & Zhu, 2003). Harish Prashanth and Tharanathan (2005) have reported that COS with the molecular weight of 0.4–1.2 kDa showed *in vitro* and *in vivo* inhibitory effect on human hepatocellular carcinoma cells (HepG2 cells) proliferation and lung cancer metastasis. Shen et al. (2009) also evaluated and suggested about a potential anti-tumor growth and anti-metastatic potency of COS with molecular weight of 23.99 kDa against HepG2 cells and Lewis lung carcinoma cells (LLC cells). COS having degree of polymerization (DP) from 3 to 9 or molecular weight of 0.5–1.5 kDa was found to induce an apoptosis in human hepatocellular carcinoma cells (SMMC-7721 cells) (Xu et al., 2008).

Degradation of chitosan by using strong acids for preparing LMWC and COS is widely used in both industries and research works due to the cost effectiveness and simple processing (Vårum, Ottøy & Smidsrød, 2001). However, the hazardous chemical usage may lead to chemical contamination in the final products and cause environmental pollution. Alternatively, enzymatic methods have received more attention in recent years because of the

\* Corresponding author at: The Petroleum and Petrochemical College, Chulalongkorn University, Bangkok 10330, Thailand.

E-mail addresses: [ratana.r@chula.ac.th](mailto:ratana.r@chula.ac.th), [ratana.chula@gmail.com](mailto:ratana.chula@gmail.com) (R. Rujiravanit).



potential of region-selective degradation of chitin and chitosan under mild conditions (Cabrera & Van Cutsem, 2005; Harish Prashanth & Tharanathan, 2007). Although, enzymatic method gives a good yield of oligomers being composed of 2–8 monomers, it exhibits slow progress in molecular weight reduction (Mourya, Inamdar & Choudhari, 2011). In addition, production of LMWC and COS can also be achieved by the oxidative degradation using oxidizing agents, such as  $O_3$ ,  $HNO_2$  and  $H_2O_2$  (Allan & Peyron, 1995; Chang, Tai & Cheng, 2001; Yue, Yao & Wei, 2009). In general, oxidizing agents are attractive for not only chemical decomposition of organic compounds (De Laat & Gallard, 1999; Venkatadri & Peters, 1993), but also chemical degradation of polymers (Liu et al., 2014; Moad et al., 2015) including chitosan. Most oxidizing agents can generate highly reactive species which are capable of attacking many organic compounds and polymers with high rate constants (Chang, Tai & Cheng, 2001; Méndez-Díaz et al., 2010; Tian et al., 2004). Moreover, using oxidizing agents in polymer degradation is highly versatile, since other physical methods can be applied together with an oxidizing agent in order to enhance effectiveness of the reactions.

Chitosan degradation by applying physical methods using energy impact such as microwave (Li et al., 2012), ultraviolet (Yue, Yao & Wei, 2009), ultra-sonication (Savitri et al., 2014), gamma-ray (Wasikiewicz et al., 2005) and plasma has been widely reported. These methods have been considered as effective tools for the degradation reaction because of the ability to provide a rapid reaction with less chemicals used. However, the studies in the past have shown that degradation of chitosan by employing energy impact alone is less effective than that using energy impact in combination with other methods. Some researchers investigated the combination of energy impact method with oxidative degradation aiming to increase radical intensity in the systems. For example,  $^{60}Co$   $\gamma$ -rays together with  $H_2O_2$  was applied to degrade chitosan (El-Sawy et al., 2010; Kang et al., 2007). Microwave irradiation in combination with  $H_2O_2$  was another example used for the degradation of chitosan (Li et al., 2012). Accordingly, it has been suggested that the combined methods are more effective than the individual methods for effective degradation of chitosan (El-Sawy et al., 2010; Kang et al., 2007). Although, there were numerous degradation methods studied in the past, the attempt to acquire novel effective methods is still a challenge focusing on for better production of LMWC and COS together with an environmental concern.

Solution plasma (SP), one of the newly invented non-thermal plasma, is a plasma discharge generated between two electrodes immersed under a liquid phase by providing high voltage electricity to the electrodes. When plasma is generated, molecules surrounding the electrodes are collided by electrons coming out from the electrodes, resulting in the formation of highly active species (e.g.  $\cdot H$ ,  $\cdot O$ ,  $\cdot OH$ ,  $H^-$ , and  $O^-$ ), high energy electrons and UV radiation (Baroch et al., 2008; Bratescu et al., 2011). Therefore, SP is a powerful tool to provide extremely rapid reactions (Potocký, Saito & Takai, 2009). The previous researches have focused on using SP for the synthesis of noble metal nanoparticles (Bratescu et al., 2011; Jin et al., 2014; Saito, Hieda & Takai, 2009), the decomposition of some organic compounds in waste water (Baroch et al., 2008) and the removal of polymeric template in mesoporous silica (Pootawang, Saito & Takai, 2011). In recent years, several studies have adopted the use of SP for synthesis and modification of carbon nanoparticles (Ishizaki et al., 2014; Panomsuwan, Saito & Ishizaki, 2016). The SP technology also has potential as an alternative method for biopolymer degradation, because SP generates radicals such as  $\cdot OH$  that can promote the degradation of polymer chains such as chitosan (Prasertsung, Damrongsakul & Saito, 2013; Prasertsung et al., 2012) and sodium alginate (Wattanaphanit & Saito, 2013). Even though, the SP treatment alone could facilitate the degradation of chitosan, the improvement of degradation rate

and production yield of LMWC and COS by applying the SP treatment is still of great challenge. It has been expected that when the SP treatment has been used together with oxidizing agents, highly active species will be intensively produced by the both systems, resulting in synergetic effect on degradation of chitosan.

In this study, the degradation of chitosan by the combination of the SP treatment and oxidizing agents including  $H_2O_2$ ,  $NaNO_2$  and  $K_2S_2O_8$  at very low concentrations of oxidizing agents (4–60 mM) were carried out. The effects of plasma treatment time, initial concentrations of chitosan and oxidizing agents on molecular weight reduction of chitosan were evaluated. In addition, anticancer activity against HeLa cells of the obtained COS was also examined in comparison with normal cells.

## 2. Experimental

### 2.1. Materials

Shells of *Metapenaeus dobsoni* shrimp, provided by Surapon Foods Public Co., Ltd. (Thailand), were used to prepare chitosan by following a procedure described by Pornsunthorntawe et al. (2014). A 50% (w/v) NaOH solution was purchased from the Chemical Enterprise Co., Ltd. (Thailand). Glacial acetic acid ( $CH_3COOH$ , 99.9%), hydrochloric acid (HCl, 37.0%), hydrogen peroxide ( $H_2O_2$ , >30.0%) and sodium hydroxide (NaOH, 97.0%) pellets were obtained from RCI Labscan Ltd. (Thailand). Potassium persulfate ( $K_2S_2O_8$ , 99.5%) and sodium nitrite ( $NaNO_2$ , 99.0%) were supplied by Sigma–Aldrich (USA). Sodium borohydride ( $NaBH_4$ ) was obtained from Carlo Erba Reagenti (Italy). All chemicals were reagent grade and used without further purification.

### 2.2. Degradation of chitosan

Chitosan solution was prepared in 40 mL of 0.1 M acetic acid. The solution of each oxidizing agent was separately prepared to achieve a desired concentration in 40 mL of 0.1 M acetic acid solution. Then, the two solutions were poured into a 100 mL SP glass reactor equipped with 1 mm-diameter tungsten electrodes (purity 99.9%, Nilaco Corp., Japan) and mixed by stirring for 5 min prior to the discharge of plasma. A schematic of the experimental set-up of the SP reactor is shown in Fig. 1. The plasma discharge occurred at the tip of the tungsten electrodes that were connecting to a high-frequency bipolar pulsed DC power supply (Kurita-Nagoya MPS-06K06C, Kurita Co. Ltd., Japan). The electrodes were submerged in the reaction solution and the distance between the electrodes was adjusted to be 0.5 mm. The operating condition of SP treatment was fixed at the frequency, voltage and pulse width of 15 kHz, 1.6 kV and 2  $\mu s$ , respectively. A magnetic stirrer was used in order to provide the uniformity of the solution inside the reactor.

### 2.3. Separation and purification of plasma-treated chitosan

The plasma-treated chitosan solution was neutralized by the addition of 2 M NaOH solution and kept at 4 °C overnight for complete precipitation (Pornsunthorntawe et al., 2014). After that, the precipitate was collected as a water-insoluble fraction. The supernatant was concentrated by a rotary evaporator under vacuum to a final volume of 10 mL (8 times concentrated). The concentrated solution was then added to a twice-volume acetone, followed by keeping at 4 °C overnight and the precipitate was collected as a water-soluble fraction. Each fractions was collected by centrifugation at 10,000 rpm for 30 min and washed twice with the same ratio of acetone–water mixture. Finally, the precipitated products were dried in a vacuum oven at ambient temperature for 4 h. The

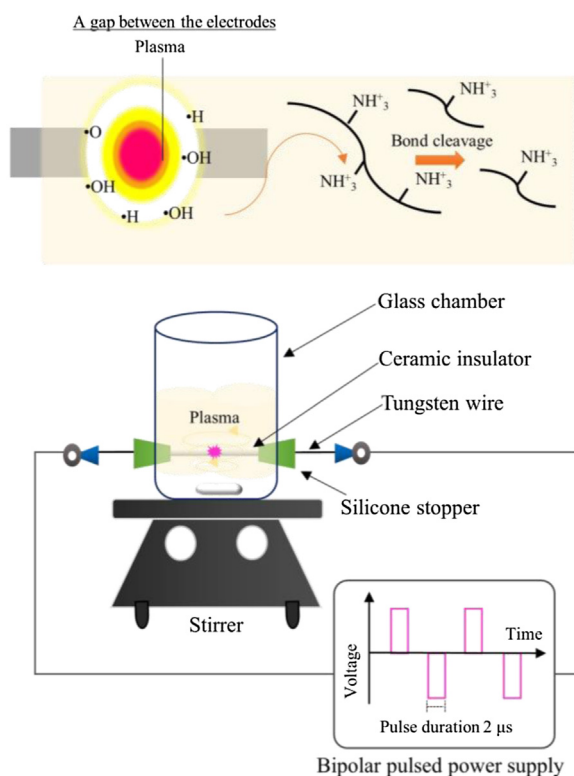


Fig. 1. Experimental set-up of solution plasma equipment.

water-insoluble and water-soluble fractions were weighed and calculated by the following equations:

$$\text{Percentage of insoluble-chitosan fraction} = 100 \times W_i/W_0 \quad (1)$$

$$\text{Percentage of soluble-chitosan fraction} = 100 \times W_s/W_0 \quad (2)$$

$$\text{Percentage of total yield} = 100 \times (W_i + W_s)/W_0 \quad (3)$$

where  $W_0$  is the initial dry weight of chitosan and  $W_i$  and  $W_s$  are the dry weight of water-insoluble fraction and water-soluble fraction, respectively.

#### 2.4. Fractionation of chitoooligosaccharides by adding water-ethanol mixture solution

This method was modified from the previous works (Cabrera & Van Cutsem, 2005; Lin & Lin, 2003). After neutralization and removal of water-insoluble chitosan, ethanol, which had a volume equal to a concentrated solution of water-soluble chitosan, was gradually poured into the solution. The first precipitate, labeled as 1:1 (volumetric ratio of sample solution to the added ethanol) fraction, was then collected by centrifugation. After that, the additional ethanol was added into a supernatant, which left from the above process, to obtain 1:3 fraction and the second precipitate was collected. The same procedure was repeated to prepare the 1:5 fraction. After adding ethanol, all samples were kept at 4 °C overnight for complete precipitation. The precipitates were washed with their corresponding water-ethanol mixture solution for three times and then dissolved in deionized water prior to freeze drying. Finally, freeze-dried products were kept in dehumidifier for further characterization.

#### 2.5. Characterization

The change in viscosity of chitosan solution as a function of the plasma treatment time was measured by Cannon-Ubbelohde

viscometer (J758, Cannon Instrument Co., USA). A 0.1 M  $\text{CH}_3\text{COOH}$  solution was used as a solvent for measuring the running time of the solvent ( $t_0$ ). A sample of the plasma-treated chitosan solution was poured into the viscometer immersed in a water bath at a controlled temperature of 25 °C and the running time of the sample ( $t_s$ ) was measured repeatedly for at least three times. Then, the relative viscosity ( $\eta_r$ ) was calculated according to the following Eq. (4):

$$\eta_r = t_s/t_0 \quad (4)$$

And the percentage of the relative viscosity reduction,  $\eta_r$  (%), was further calculated by using the following equation:

$$\eta_r (\%) = 100 \times (\eta_{r,t}/\eta_{r,0}) \quad (5)$$

where  $\eta_{r,0}$  is the viscosity of the chitosan solution before plasma treatment and  $\eta_{r,t}$  is the viscosity of the plasma-treated chitosan solution at reaction time  $t$ .

The weight-average molecular weight ( $M_w$ ) and polydispersity index (PDI) of chitosan during the degradation by applying SP treatment were determined by GPC (CTO-10A, Shimadzu, Japan) was equipped with a refractive index (RI) detector. The ultra-hydrogel linear column (Water 600E, Waters, USA) was connected with the guard column in series. An acetate buffer at pH 4.0 which consists of 0.5 N  $\text{CH}_3\text{COOH}$  and 0.5 N sodium acetate ( $\text{CH}_3\text{COONa}$ ) was used as mobile phase. A 40  $\mu\text{L}$  of chitosan solution in the acetate buffer was filtrated through a syringe filter containing a 0.45  $\mu\text{m}$ -pore sized nylon 66 membrane (Vertical Chromatography Co., Ltd., Thailand) before injection. The operating flow rate and temperature were set at 0.6  $\text{mL min}^{-1}$  and 40 °C, respectively. Pullulans with the molecular weight range of  $1.32 \times 10^3$ – $8.05 \times 10^5$  Da were used as standard samples.

The change of chemical structure was investigated by FT-IR (Nicolet iS5, Thermo Fisher Scientific, USA) using 64 scans in the range of 4000–600  $\text{cm}^{-1}$  at a resolution of 4  $\text{cm}^{-1}$  with a correction for atmospheric carbon dioxide ( $\text{CO}_2$ ). A 500-MHz NMR (AVANCE III, Bruker, Bruker Corp., Germany) was also used. Samples were dissolved in  $\text{CD}_3\text{COOD/D}_2\text{O}$  at a concentration of 10–30  $\text{mg mL}^{-1}$ . Degree of deacetylation (DD) is calculated by Eqs. (6) and (7) according to previously reported methods (Kasaai et al., 1999; Sabnis & Block, 1997).

For FT-IR,

$$\text{DD} = 97.67 - \{26.486 \times (A_{1655}/A_{3450})\} \quad (6)$$

where  $A$  corresponds to the absorbance of the respective bands.

For  $^1\text{H}$  NMR,

$$\text{DD} = 100 \times \{1 - (I_{\text{at2 ppm}}/3)/I_{\text{at3 ppm}}\} \quad (7)$$

where  $I$  corresponds to the integral of the respective bands.

The crystalline structure of chitosan before and after degradation was observed by using an XRD (SmartLab, Rigaku, Japan) with  $\text{Cu K}\alpha$  radiation in a continuous mode with a scan rate of 5°  $\text{min}^{-1}$ .

An ESI(+)-MS (Exactive Orbitrap, Thermo Fisher Scientific, USA) was employed in an infusion mode with a flow rate of approximately 10  $\mu\text{L min}^{-1}$  for mass spectrometry analysis of the COS product. Sheath, auxiliary and sweep gases were  $\text{N}_2$  gas set at 10, 1, and 1 psi, respectively. Spray voltage was 4.2 kV. Capillary temperature and voltage were 200 °C and 10 V. Tube lens voltage was 180–250 V. Skimmer voltage was 13 V.

#### 2.6. Biological assay

##### 2.6.1. Cell culture

HeLa cells (Human uterine cervix cancer cell line) and MRC-5 cells (Homo sapiens lung normal cell line) were cultured by using Dulbecco's Modified Eagle Medium (DMEM) high glucose with  $L$ -glutamine and sodium pyruvate (Biowest, France), and Eagle's

Minimum Essential Medium (EMEM) with sodium bicarbonate, non-essential amino acids, *L*-glutamine, and sodium pyruvate (Corning Inc., USA), respectively. Both media were supplemented with 10% fetal bovine serum (Biowest, France), 100 U mL<sup>-1</sup> Penicillin and 100 µg mL<sup>-1</sup> Streptomycin (Gibco, Life Technologies Inc., USA) prior to culturing in a humidified incubator (37 °C, 5% CO<sub>2</sub>).

### 2.6.2. Cytotoxicity assay

The chitosan samples were tested *in vitro* by using MTT assay. Cells were seeded into 96-well microliter plates (1 × 10<sup>4</sup> cells/well). After 24 h, cells were treated with different concentrations of 1.44-kDa COS sample, diluted with sterile water to make the desired final concentration (0.1–40 mg mL<sup>-1</sup>). Then, the COS-treated cells were incubated in an incubator at 37 °C and 5% CO<sub>2</sub> for 24 h. After incubation, medium was replaced with PBS (phosphate buffer saline) solution containing 0.05% w/v of MTT (3-(4,5-dimethylthiazol-2-yl)-2,5-diphenyltetrazolium bromide) solution and further incubated for 3 h. The solution were then discarded and DMSO was added to dissolve the formed formazan crystals and the absorbance (A) of each well was measured at 570 nm using a microplate reader (Varioskan™ Flash Multimode Reader, Thermo Fisher Scientific, USA). Doxorubicin was used as positive control. All experiments were performed in triplicate and repeated for five experiments. The cell viability was expressed as a percentage relative to the untreated control cells as following:

$$\text{Cell viability (\%)} = 100 \times [(A_{\text{treated}} - A_{\text{blank}}) / (A_{\text{untreated}} - A_{\text{blank}})] \quad (8)$$

After the percentage of cell viability was calculated and plotted, then the mean growth-inhibitory concentration (IC<sub>50</sub>) value was determined.

## 3. Results and discussion

### 3.1. Degradation of chitosan by applying SP treatment in combination with different oxidizing agents

As shown in Fig. 2A, the change in viscosity of the chitosan solution was measured as a function of reaction time as a preliminary study on the degradation of chitosan. The chitosan solution with the addition of each oxidizing agent at a concentration of 4 mM was subjected to either SP treatment or conventional heat treatment at a temperature of 75 °C which was the maximum temperature of the chitosan solutions measured during the SP treatment. The viscosity of chitosan solution slightly decreased during the heat treatment at 75 °C for 60 min. On the contrary, SP treatment resulted in dramatically decreasing of viscosity of the chitosan solution under the corresponding condition. The reduction of viscosity of chitosan solution reflected the cleavage of chitosan chains (Choi et al., 2002). This evidence indicated that the SP treatment could greatly promote the degradation of chitosan and possibly lead to the production of COS (Pornsunthorntawee et al., 2014). The viscosity of chitosan solution dramatically decreased within the first 30 min of the SP treatment, followed by gradually reducing until the SP treatment time of 60 min. This might be explained in terms of crystalline structure of chitosan which could be investigated by the XRD. The XRD result was shown in supplementary data (see Fig. A1). Chitosan is a semicrystalline polymer containing both amorphous and crystalline regions. In general, amorphous structure is more susceptible to degradation than crystalline structure (Tian et al., 2004). At the beginning of the SP treatment, the amorphous region was firstly degraded and would eventually dissolve in the reaction medium, whereas the crystalline region still remained intact. However, the crystalline region in the chitosan was subsequently destroyed with

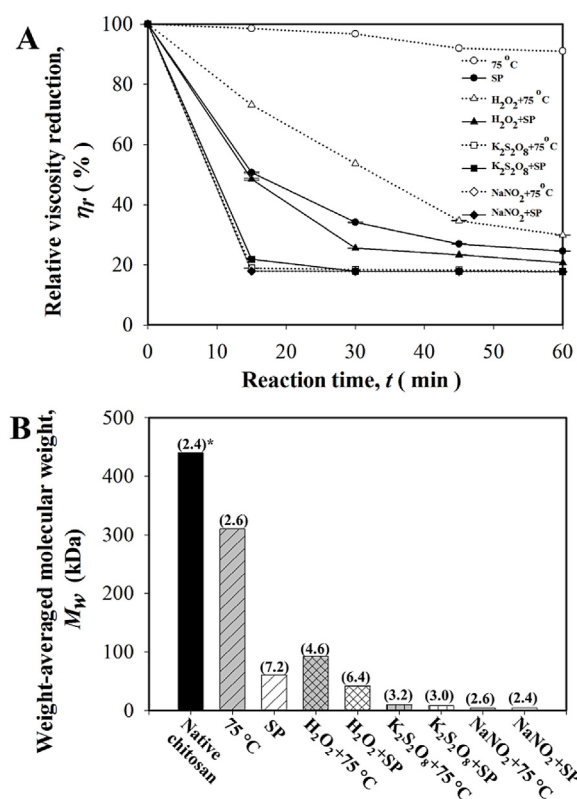


**Fig. 2.** (A) Reduction of relative viscosity as a function of the reaction time and (B)  $M_w$  and PDI of chitosan solutions containing 0.5% chitosan in 0.1 M CH<sub>3</sub>COOH after 60 min of degradation via either the conventional heat treatment at 75 °C or SP treatment with and without oxidizing agents at a concentration of 4 mM (Note: \* refers to PDI).

further degradation and turned into amorphous structure before peeling off to the reaction medium (Kang et al., 2007; Tian et al., 2004). Accordingly, the presence of crystalline structure of chitosan was a plausible cause that retards the decrement of viscosity of chitosan solution (Prasertsung et al., 2012). Besides, it was found that the addition of the oxidizing agents enhanced the degradation reaction of chitosan in all studied conditions. After the SP treatment, the viscosity of chitosan solution with the addition of either K<sub>2</sub>S<sub>2</sub>O<sub>8</sub> or NaNO<sub>2</sub> sharply decreased over 80%, while viscosity of chitosan solution obtained from the corresponding condition with the addition of H<sub>2</sub>O<sub>2</sub> reduced by 70%. The addition of either K<sub>2</sub>S<sub>2</sub>O<sub>8</sub> or NaNO<sub>2</sub> resulted in the similar viscosity reduction profiles regardless of the degradation methods. Degradation of chitosan by the SP treatment in the presence of H<sub>2</sub>O<sub>2</sub> led to more rapid reduction in viscosity of chitosan solution than that obtained under the corresponding condition using heat treatment.

A comparison on  $M_w$  of the degraded chitosan obtained by the heat treatment and the SP treatment at the reaction time of 60 min with and without the addition of oxidizing agents at the concentration of 4 mM is shown in Fig. 2B. The tendency on the reduction of  $M_w$  of chitosan after degradation by heat treatment and SP treatment was in good agreement with the result that was determined by the viscosity measurement of chitosan solution that is shown in Fig. 2A. Without the addition of oxidizing agent, the SP treatment could reduce  $M_w$  of chitosan more effective than the heat treatment at the same temperature. Moreover, it was found that the use of oxidizing agents in combination with heat treatment and SP treatment could enhance the degradation reaction of chitosan. Nevertheless, in case of NaNO<sub>2</sub>, the SP treatment and the heat treatment gave the degraded products having about the same  $M_w$ . It has been reported that in an acid-nitrite system, nitrosating species could be formed



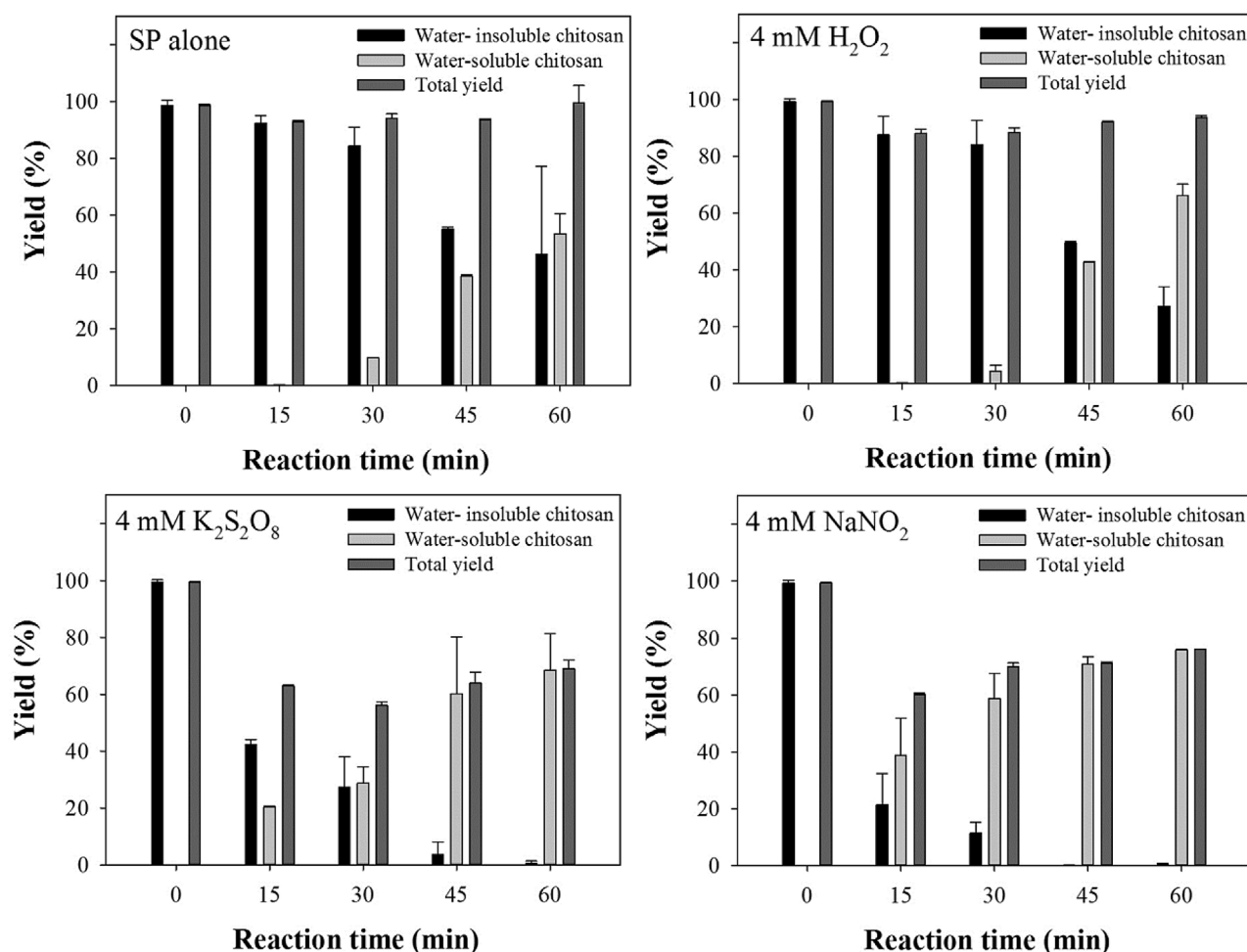


**Fig. 3.** Percentages of water-insoluble and water-soluble fractions, and total yield of degraded chitosan using the SP treatment alone and the SP treatment in combination with oxidizing agents at a concentration of 4 mM.

at the room temperature or even lower, resulting in degradation of chitosan (Mao et al., 2004). In case of K<sub>2</sub>S<sub>2</sub>O<sub>8</sub>, the SP treatment had a slightly higher performance than the heat treatment in the aspect of giving lower *M<sub>w</sub>* of the degraded chitosan. According to the literature, K<sub>2</sub>S<sub>2</sub>O<sub>8</sub> was thermally dissociated at 75 °C to form anionic radicals which would further attack chitosan chains, resulting in cleavage of β-1,4 glycosidic bond and eventually chitosan degradation (Harish Prashanth & Tharanathan, 2005; Hsu, Don & Chiu, 2002).

Fig. 3 shows the percentages of water-insoluble and water-soluble fraction as well as the percentage of total yield of the degraded chitosan as a function of reaction time. Water-soluble chitosan was referred to chitosan having molecular weight less than 10 kDa (Lee et al., 2001). The results in all studied conditions revealed that the longer reaction time proceeded, the higher amount of water-soluble chitosan was obtained. According to the percentages of the total yield, loss of chitosan sample after the degradation by the SP treatment alone was relatively low, while the SP treatment in combination with oxidizing agents led to more loss of chitosan sample. The SP treatment with the addition of H<sub>2</sub>O<sub>2</sub> resulted in losing 4.5% of chitosan sample. Degradation of chitosan by the SP treatment in the presence of either NaNO<sub>2</sub> or K<sub>2</sub>S<sub>2</sub>O<sub>8</sub> led to much more loss of the chitosan, that were 24% and 32%, respectively. The severe reaction occurring by the addition of NaNO<sub>2</sub> and K<sub>2</sub>S<sub>2</sub>O<sub>8</sub> may cause the formation of by-products, which were unable to recover by the collecting method in this work, such as 2,5-anhydro-D-mannitol and 5-hydroxymethylfurfural (HMF)

(Tømmeraa et al., 2001). However, the addition of each oxidizing agent could lead to the increasing of the amount of water-soluble chitosan after the SP treatment, compared to that obtained from using the SP treatment alone. At the plasma treatment time of 60 min, the addition of either K<sub>2</sub>S<sub>2</sub>O<sub>8</sub> or NaNO<sub>2</sub> achieved approximately 70% of the water-soluble chitosan, while the water-soluble chitosan obtained from the corresponding condition with the addition of H<sub>2</sub>O<sub>2</sub> was 66% and the SP treatment alone gave 50%. This result is consistent with the viscosity reduction of the plasma-treated chitosan solution in the presence of oxidizing agents.

FT-IR analysis was carried out to evaluate degree of deacetylation (DD) and chemical structures of native chitosan and the degraded chitosan. The results are shown in Fig. 4A. The characteristic peaks of native chitosan and the degraded chitosan obtained by the SP treatment with and without oxidizing agents appeared at the wavenumbers of 3450, 1650, 1550 and 1074 cm<sup>-1</sup> corresponding to –OH stretching, amide I C=O bending, amide II N–H bending and C–O–C, respectively (Ifuku et al., 2012; Kang et al., 2007; Ostrowska-Czubenko & Gierszewska-Drużyńska, 2009; Qin et al., 2006). The native chitosan had the DD of 91.5%, whereas the degraded chitosan obtained from the SP treatment alone had the DD of 87.8%. The DD of degraded chitosan obtained from the combination of the SP treatment with H<sub>2</sub>O<sub>2</sub>, K<sub>2</sub>S<sub>2</sub>O<sub>8</sub> and NaNO<sub>2</sub> were 87.5%, 85.6% and 77.2%, respectively. The results suggested that the SP treatment with and without oxidizing agents could induce scission of some side chains at the amino group of chitosan resulting in the reduction of DD of the degraded chitosan.

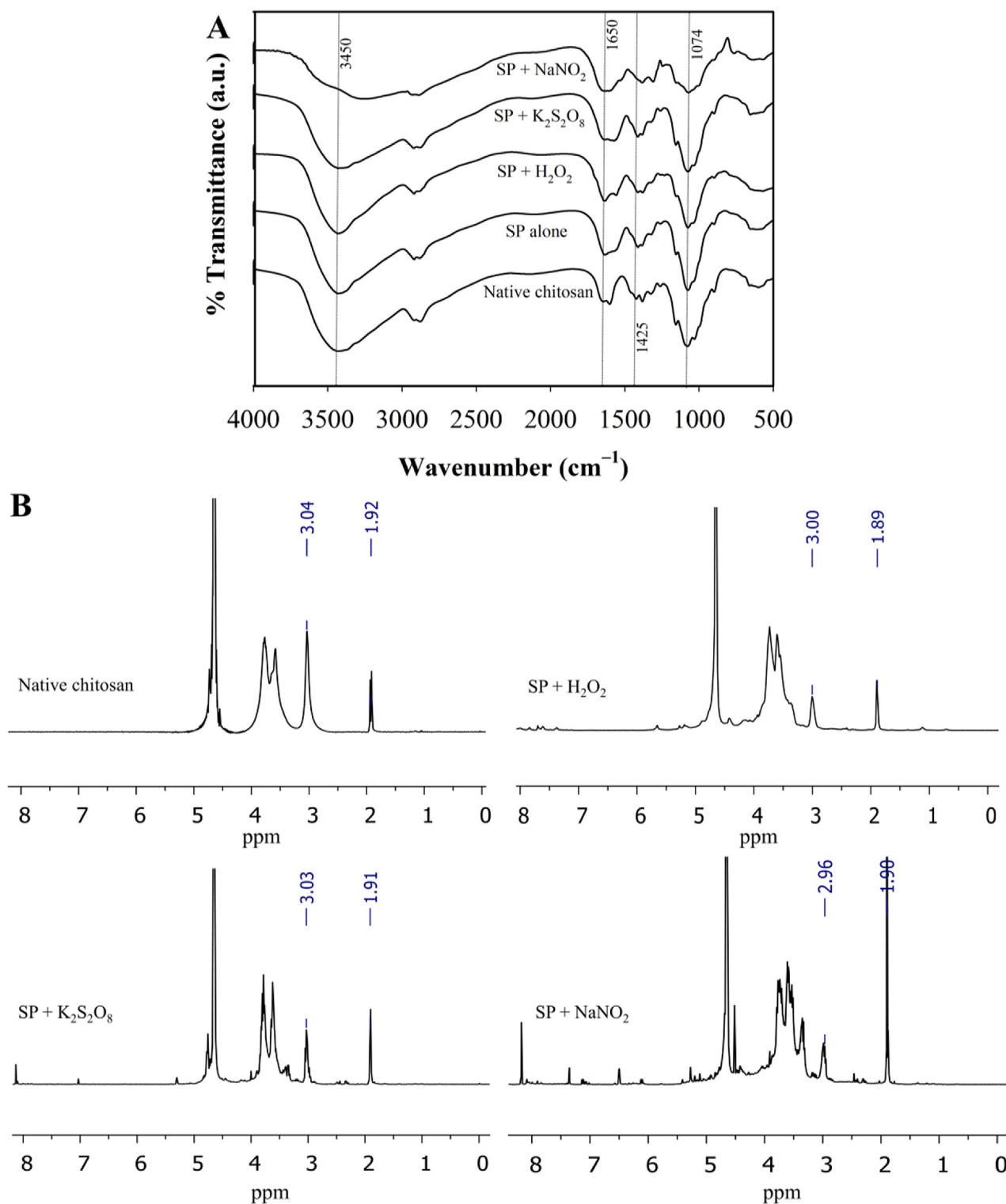


**Fig. 4.** (A) FT-IR spectra and (B)  $^1\text{H}$  NMR spectra of the native chitosan and degraded chitosan obtained by degradation of chitosan at a concentration of 0.5% by the SP treatment in combination with  $\text{H}_2\text{O}_2$ ,  $\text{K}_2\text{S}_2\text{O}_8$  and  $\text{NaNO}_2$  at a concentration of 4 mM for 60 min.

The chemical structures of chitosan before and after degradation by applying the SP treatment in combination with different oxidizing agents were further investigated by  $^1\text{H}$  NMR as shown in Fig. 4B. Native chitosan showed a singlet at 3.0 ppm and multiplets at 3.2–4.3 ppm, corresponding to the ring methane protons, together with a singlet at approximately 1.90 ppm, which refers to N-acetyl glucosamine units (Tian et al., 2004). Regardless of

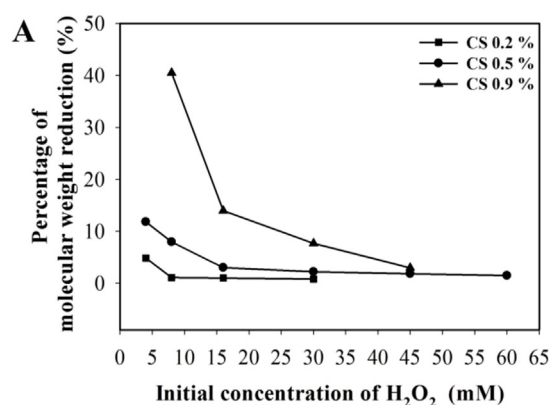
type of oxidizing agents, the  $^1\text{H}$  NMR spectra of the degraded chitosan had similar pattern to that of native chitosan. The DD was also calculated from the NMR results. The DD of the native chitosan was equal to 92%, while the DD of the degraded chitosan obtained by the SP treatment in combination with  $\text{H}_2\text{O}_2$ ,  $\text{K}_2\text{S}_2\text{O}_8$  and  $\text{NaNO}_2$  were equal to 80%, 83% and 74%, respectively. Moreover, the NMR spectrum of the degraded chitosan obtained from

the SP treatment in combination with  $\text{NaNO}_2$  had minimal signals appearing at 4.5, 6.5 and 7.3 ppm which could be assigned to HMF (Vigier et al., 2012). According to the literature, the severe degradation of chitosan by using nitrous acid could lead to the change of the chemical structure of chitosan to 2,5-anhydro-D-mannitol and 5-hydroxymethylfurfural (HMF) (Sánchez et al., 2017; Tømmeraaas et al., 2001).

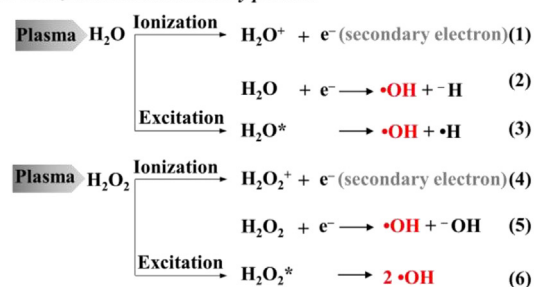
Even though  $\text{H}_2\text{O}_2$  may not be as powerful oxidizing agent as  $\text{K}_2\text{S}_2\text{O}_8$  and  $\text{NaNO}_2$ , the yield of the water-soluble chitosan and the total yield of degraded chitosan were acceptable and the loss of degraded chitosan in case of  $\text{H}_2\text{O}_2$  was less than that obtained from the addition of either  $\text{K}_2\text{S}_2\text{O}_8$  or  $\text{NaNO}_2$ .  $\text{H}_2\text{O}_2$  was easy to handle, cheap and environmentally friendly oxidant (Qin et al., 2002; Shen et al., 2010). Moreover,  $\text{H}_2\text{O}_2$  could degrade chitosan with less side reaction than  $\text{K}_2\text{S}_2\text{O}_8$  and  $\text{NaNO}_2$ . As mentioned, the severe degradation of chitosan by the addition of  $\text{NaNO}_2$  could result in the change of the chemical structure of chitosan to 2, 5-anhydro-D-mannitol or HMF. In case of degradation of chitosan by using  $\text{K}_2\text{S}_2\text{O}_8$ , it has been reported that anionic persulfate free radicals which generated from  $\text{K}_2\text{S}_2\text{O}_8$  could attack at the cationic amino group of chitosan and form crosslinking via electrostatic attraction (Prashanth & Tharanathan, 2006). Therefore,  $\text{H}_2\text{O}_2$  was considered as a good choice of oxidizing agent for enhancing the degradation of chitosan by using the SP treatment.

The factors influencing the degradation of chitosan by the combination of SP treatment and  $\text{H}_2\text{O}_2$ , such as the initial concentration of chitosan and  $\text{H}_2\text{O}_2$ , were investigated. Fig. 5A depicts the effect of the initial concentrations of chitosan and  $\text{H}_2\text{O}_2$  on the changes in the  $M_w$  of chitosan after the degradation by SP treatment for 60 min. This evidence implied that the susceptibility to degradation of chitosan was correlated to the initial concentration of the polymer. According to the literature, chitosan chains normally expand in an acidic aqueous solution, because of the protonation reaction of amino group at the C2 position that lead to an electrostatic repulsion (Mao et al., 2004). Therefore, at low concentration, the chitosan chains are in the expanded conformation and can freely move in the solution, causing an easy access of the free radicals such as  $\bullet\text{OH}$  to the polymer chains. On the contrary, the increment of initial concentration of chitosan solution leads to a progressive entanglement between the polymer chains. As a result of less mobility, some intermolecular interactions between polymer chains become stronger and the accessible chain segments may be limited while the distribution of  $\bullet\text{OH}$  in solution can be obstructed, leading to the reduction of the degradability of the polymer chains. On the other hand, the increment of the amount of  $\text{H}_2\text{O}_2$  could increase the chitosan degradation, because of the production of more  $\bullet\text{OH}$ . The increasing of  $\bullet\text{OH}$  content in the system would increase an opportunity of  $\bullet\text{OH}$  to react with the chitosan chains.

The degradation mechanism of chitosan by applying the SP treatment in combination with  $\text{H}_2\text{O}_2$  was proposed (Fig. 5B). In the reaction solution, there were four types of molecules including  $\text{H}_2\text{O}$ ,  $\text{H}_2\text{O}_2$ ,  $\text{CH}_3\text{COOH}$  and chitosan. The major component in the system was  $\text{H}_2\text{O}$  molecules. When the plasma was discharged in the solution, excitation and ionization of  $\text{H}_2\text{O}$  molecules occurred. Electrons, that were emitted as a result of ionization (secondary electrons) (Fig. 5B (1)), collided with the surrounding  $\text{H}_2\text{O}$  molecules. The ionization and excitation of  $\text{H}_2\text{O}$  molecules can further produce more  $\bullet\text{OH}$  (Fig. 5B (2, 3)) which is important for the degradation of chitosan (Kang et al., 2007; Qin, Du & Xiao, 2002). The addition of  $\text{H}_2\text{O}_2$  could promote the chitosan degradation because  $\text{H}_2\text{O}_2$  itself dissociates to form  $\bullet\text{OH}$  as shown in Fig. 5B (4–6) (Chang, Tai & Cheng, 2001). This phenomenon helps to increase the  $\bullet\text{OH}$  concentration in the system. The possible mechanism for the degradation of chitosan in the presence of  $\bullet\text{OH}$  has been proposed. In general, amino groups of chitosan are protonated by  $\text{H}^+$  dissociated from  $\text{CH}_3\text{COOH}$  in water. The structure of chitosan



#### B Ionization and excitation by plasma:



#### Degradation of chitosan in acidic solution:

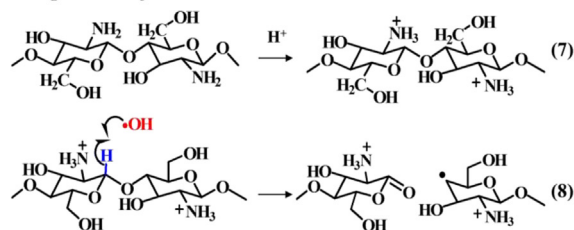


Fig. 5. (A)  $M_w$  of chitosan measured by GPC after 60 min of the SP treatment with the addition of various  $\text{H}_2\text{O}_2$  concentrations as a function of initial chitosan concentrations of 0.2%, 0.5% and 0.9% in 0.1 M  $\text{CH}_3\text{COOH}$ . (B) Possible mechanism for the degradation of chitosan by applying the combination of the SP treatment and  $\text{H}_2\text{O}_2$ .

in  $\text{CH}_3\text{COOH}$  solution carries positive charge as displayed in Fig. 5B (7). The  $\bullet\text{OH}$  attacks at the C-1 carbon and transferred the radical to the C-1 carbon by subtracting the hydrogen from it, resulting in the breaking down of the chitosan chain at  $\beta$ -1,4 glycosidic linkage (Chang, Tai & Cheng, 2001; Tian et al., 2004). The scission of the  $\beta$ -1,4 glycosidic linkage causes the reduction of chitosan molecular weight (Kang et al., 2007). Besides, chitosan molecule itself can also possibly be collided by electron generated by the SP treatment, leading to the scission at  $\beta$ -1,4 glycosidic linkages.

The kinetics of degradation reaction were evaluated by a linear relationship of reversed molecular weight ( $1/M_w$ ) as a function of reaction time ( $t$ ), according to the previous reports (Chang, Tai & Cheng, 2001; Pornsunthorntawee et al., 2014; Wasikiewicz et al., 2005). The rate constant ( $k$ ) was calculated by the following equation:

$$1/M_t = (1/M_0) + (kt/M) = (1/M_0) + k't \quad (9)$$

where  $M_t$  is  $M_w$  of the sample at reaction time  $t$ ,  $M_0$  is the initial  $M_w$  of the sample,  $M$  is the molecular weight of the monomer,  $k$  ( $\text{min}^{-1}$ ) or  $k'$  ( $\text{mol g}^{-1} \text{min}^{-1}$ ) is the rate constant, and  $t$  is the reaction time (min). The  $k$  values of chitosan degradation by the combination of SP treatment and  $\text{H}_2\text{O}_2$  were calculated and compared to other methods that have been reported in some previous works, as shown in Table 1. To the best of our knowledge it was found that according

**Table 1**

Comparison of rate constants obtained in this study with some previous works.

Methods	[chitosan], %(w/v)	[H <sub>2</sub> O <sub>2</sub> ], mM	k × 10 <sup>-2</sup> , min <sup>-1</sup>	Ref.
SP	0.2	4	7.20	This study
	0.5	4	2.46	
	0.9	4	0.54	
	0.5	8	3.70	
	0.5	16	8.05	
	0.5	30	14.49	
	0.5	45	19.64	
	0.5	60	19.96	
SP	1.0	–	4.83	Prasertsung et al. (2012)
SP + Fe <sup>3+</sup> complex	0.5	–	8.83	Pornsunthorntawee et al. (2014)
Heating at 80 °C	0.5	447	0.71	Chang et al. (2001)
γ-irradiation	5.0	420	7.95	Hien et al. (2012)

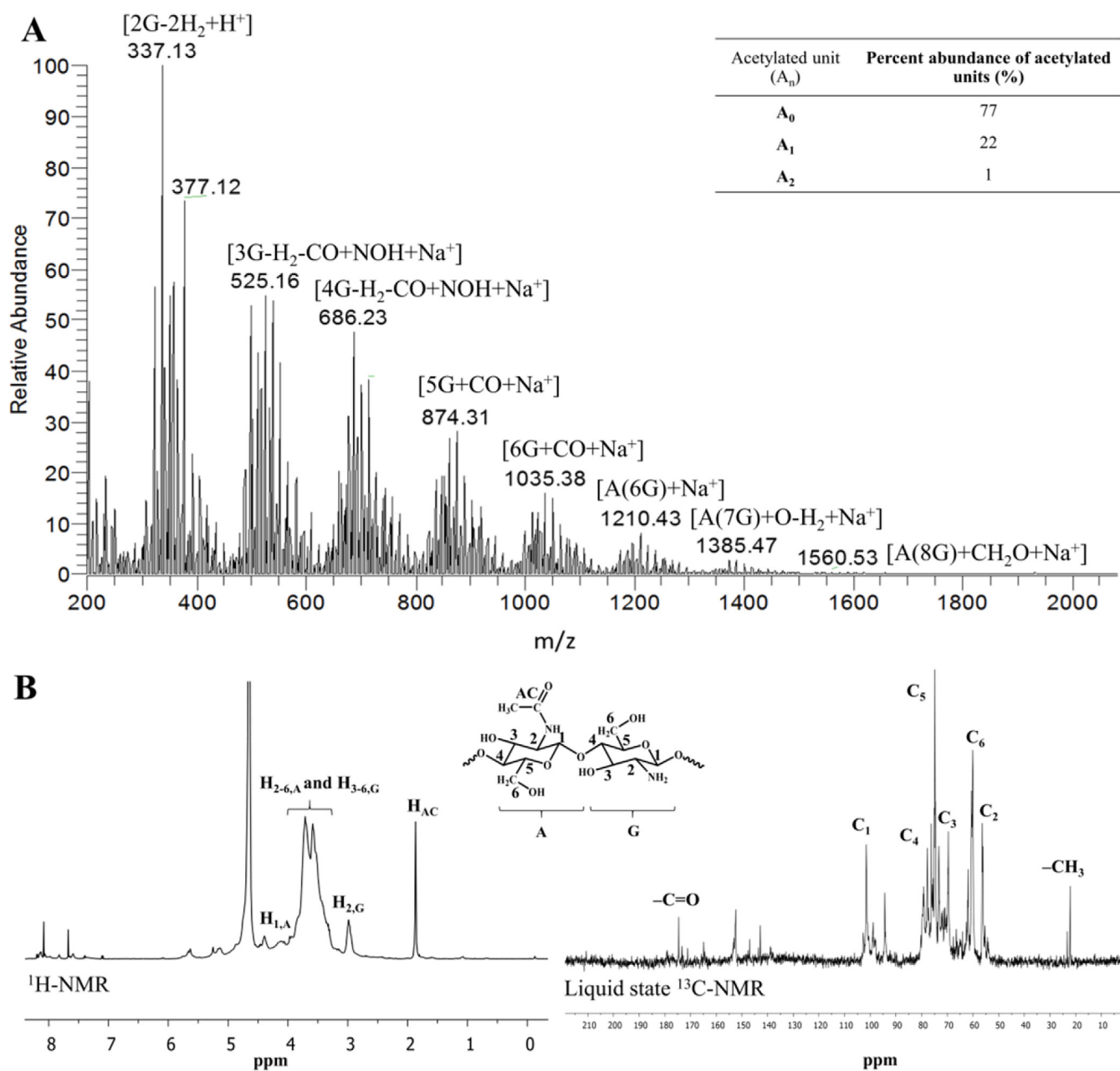


**Fig. 6.** (A) ESI-MS spectrum of 1.44-kDa chitosan fraction (COS3). “G” refers to D-glucosamine unit ( $m = 161.06$  Da), “A” refers to N-acetyl-D-glucosamine unit ( $m = 203.07$  Da) and “n” refers to the number of acetylated unit found in COS3. (B) <sup>1</sup>H NMR and liquid-state <sup>13</sup>C NMR spectra of 1.44-kDa chitosan fraction (COS3) obtained by precipitation using water-ethanol mixture solution at the ratio of water-to-ethanol of 1:5.



to the rate constants, the degradation rate of chitosan by the SP treatment in combination with the dilute concentration of  $\text{H}_2\text{O}_2$  at 60 mM was found to be faster than the degradation rate of chitosan by most physical methods reported in the literature.

The relationships between initial concentration of chitosan ( $c_0$ ) and  $k$  were also evaluated for the determination of the order of reaction,  $n$ . The relationship of  $k$  and  $c_0$  can be described as  $k \propto c_0^{-1}$ . For zeroth-order reaction ( $n=0$ ),  $k$  is proportional to  $c_0^{-1}$ . For a first-order reaction ( $n=1$ ),  $k$  is independent of  $c_0$ . For a second-order reaction ( $n=2$ ),  $k$  is proportional to  $c_0$  (Cai et al., 2011; Tayal, Kelly & Khan, 1999). The obtained  $k$  values were plotted against  $c_0$  and the initial concentration of  $\text{H}_2\text{O}_2$  as shown in supplementary data Fig. A3. The  $k$  values were inversely proportional to  $c_0$ , which implied the zeroth-order reaction. The result indicated that the increasing of chitosan concentration did not increase the number of bond cleavages in the polymer chains under the investigated condition. Similar kinetic behavior was observed for the degradation of chitosan by an electrochemical process (Cai et al., 2011). Furthermore, the  $k$  values were found to be proportional to the concentration of  $\text{H}_2\text{O}_2$ . The result suggested that the higher concentration of  $\text{H}_2\text{O}_2$  led to the better degradation of chitosan under the studied condition.

### 3.2. Fractionation of chitoooligosaccharides by adding ethanol/water mixture solution

The degraded chitosan was separated into various fractions having different molecular weights by precipitation using water–ethanol mixture solution. A degraded chitosan fraction with  $M_w$  of 12.03 kDa, which was assigned as COS1, could be precipitated by the mixture solution at the water-to-ethanol ratio of 1:1. The lower- $M_w$  degraded chitosan fraction with  $M_w$  of 4.92 kDa and 1.44 kDa, which were assigned as COS2 and COS3, were precipitated by the mixture solution having water-to-ethanol ratios of 1:3 and 1:5, respectively. The precipitated products were freeze-dried to determine the production yield and re-dissolved to evaluate their solubility in water. The production yield of COS1, which could rarely dissolve in water, was found to be 5% whereas those of COS2 and COS3 were 32% and 23%, respectively. COS2 could mostly dissolve in water, while COS3 was able to completely dissolve in water. More details were given in supplementary data (Table A1).

In this study, the completely water-soluble chitosan fraction, COS3, was used for evaluation of anticancer activity. Therefore, the mass of COS3 was further characterized by ESI-MS as shown in Fig. 6A. The COS3 having the degree of polymerization (DP) ranging from 2 to 9 was composed of fully deacetylated sequences as well as mono- and di-acetylated COS. The details on the assigned ion composition of ESI-MS spectra of COS exhibit in the supplementary data (see Fig. A4 and Table A2). The fully deacetylated sequences were dominant with percent abundance equal to 77%, while mono- and di-acetylated COS possessed percent abundance equal to 22% and 1%, respectively. The chemical structure of the COS3 product was also evaluated by  $^1\text{H}$  NMR and liquid-state  $^{13}\text{C}$  NMR as shown in Fig. 6B. Chemical structures of the monomeric units in COS3 were not altered from those of chitosan during the degradation and fractionation processes. In addition, the DD of COS3 was calculated to be 80%.

### 3.3. Evaluation of anticancer activity

To evaluate the inhibitory effect of COS3 having  $M_w$  of 1.44 kDa on the cell proliferation of HeLa cells, different concentrations of the COS3 ranging from 1 to 40  $\text{mg mL}^{-1}$  were added to the wells containing the cancer cells. Fig. 7A shows the morphology of HeLa cells before and after being treated with different concentrations of COS3. HeLa cells normally have rhomboid–tetrahedral shape as

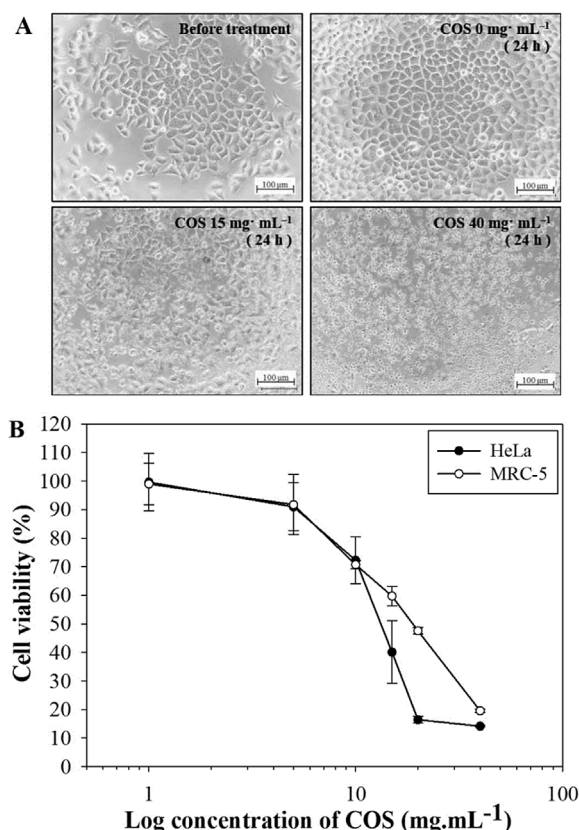


**Fig. 7.** (A) Microscopic images ( $\times 20$ ) of HeLa cells before and after the treatment with COS3 having molecular weight of 1.44 kDa for 24 h and (B) the effect of concentrations of COS3 on cell viability of cancer cells (HeLa cells) and normal cells (MRC-5 cells), determined by the MTT assay. Values are mean  $\pm$  SD of 15 determinations from 5 separated experiments ( $n=3$  for each experiment).

reported by Martínez-Ramos et al. (2005). After 24 h of the treatment, the wells without the addition of the COS3 exhibited the rapid increasing of the number of cells, while the cells that were treated with the COS3 at a concentration of 15  $\text{mg mL}^{-1}$  grew in a slower manner. The morphology of HeLa cells gradually changed with the increasing of COS3 concentrations and completely changed to abnormal shapes when the concentration of the COS3 reached 40  $\text{mg mL}^{-1}$ . Furthermore, the percentage of cell viability was measured by comparing the values of absorbance at  $\lambda = 570$  nm of the COS3-treated cells and the control. As shown in Fig. 7B, the number of survival cells gradually decreased as the increasing of the loaded amounts of COS3. The COS3 concentration that inhibited 50% of the cell proliferation ( $IC_{50}$ ) was approximately 13.5  $\text{mg mL}^{-1}$ . Moreover, the cell viability of normal cells (MRC-5 cells) was also examined by the corresponding concentration of COS3.  $IC_{50}$  for MRC-5 was approximately 20.7  $\text{mg mL}^{-1}$ . A selectivity index ( $SI$ ), which is determined by the  $IC_{50}$  ratio of a compound tested against cancer cells and normal cells, refers to the differential cytotoxic activity of the tested compound against cancer and normal cells (Badisa et al., 2009). The  $SI$  of COS3 in this study was approximately 1.5 which indicated a slightly higher selectivity for cytotoxic activity against HeLa cells than MRC-5 cells. As a result, COS3, that was the chitoooligosaccharide with the  $M_w$  of 1.44 kDa and DD of 80%, showed a potential to be an anticancer agent, even though the  $SI$  was not significantly higher than that of normal cell. Nevertheless, COS3 can be used as a starting material for further modification aiming for higher degree of cytotoxic selectivity for cancer cells. As one possible strategy, COS may be chemically modified by etherification with glycidyl trimethylammonium chloride (GTMAC) in order to obtain quaternized COS which become a stronger

positively charged molecule and may exhibit a better selectivity to cancer cells over normal cells comparing to native COS (Huang et al., 2006). Therefore, the further chemical modification of COS3 is another step to acquire a potent anticancer agent with higher selectivity to cancer cells.

#### 4. Conclusion

The SP treatment alone could effectively reduce  $M_w$  of chitosan and could achieve as high as 86% of molecular weight reduction which was higher than that obtained by the conventional heat treatment for approximately 3 times under the corresponding condition. The combination of the SP treatment and  $H_2O_2$  resulted in much more reduction of molecular weight of chitosan without causing any changes to the chemical structure of the degraded products of chitosan. The SP treatment of chitosan solution in presence of a very low concentration of  $H_2O_2$  (60 mM) produced a high yield of the water-soluble chitosan that consisted of LMWC and COS. After fractionation of the degraded products of chitosan, the COS having DP up to 9 could be produced with relatively high production yield of approximately 23% within 1 h. Moreover, the obtained COS showed the inhibitory effect on the proliferation of HeLa cancer cells. It might be concluded that the SP treatment is an effective tool for the production of water-soluble chitosan via the degradation reaction. Especially, when the SP treatment was used together with a small amount of the oxidizing agent like  $H_2O_2$ , a considerable yield of COS with DP up to 9 was generated at a comparable fast reaction rate. The combination of the SP treatment and  $H_2O_2$  is a promising green technology for a mass production of COS.

#### Acknowledgements

CC would like to acknowledge the Thailand Research Fund (TRF) for providing her a Royal Golden Jubilee Ph.D. Scholarship (RGJ-Ph.D.: Grant number PHD/0179/2556). This work was financially supported by the Thailand Research Fund (TRF) under the contract number BRG5480008. The authors thank Surapon Foods Public Co., Ltd. (Thailand) for providing the shrimp shells and the NU-PPC Plasma Chemical Technology Laboratory at Chulalongkorn University (Thailand) for providing the use of solution plasma equipment. All facilities for biological tests were supported by Drug Discovery and Development center at Thammasat University (Thailand).

#### Appendix A. Supplementary data

Supplementary data associated with this article can be found, in the online version, at <http://dx.doi.org/10.1016/j.carbpol.2017.03.006>.

#### References

- Allan, G. G., & Peyron, M. (1995). Molecular weight manipulation of chitosan I: Kinetics of depolymerization by nitrous acid. *Carbohydrate Research*, 277(2), 257–272.
- Badisa, R. B., Darling-Reed, S. F., Joseph, P., Cooperwood, J. S., Latinwo, L. M., & Goodman, C. B. (2009). Selective cytotoxic activities of two novel synthetic drugs on human breast carcinoma MCF-7 cells. *Anticancer Research*, 29(8), 2993–2996.
- Baroch, P., Anita, V., Saito, N., & Takai, O. (2008). Bipolar pulsed electrical discharge for decomposition of organic compounds in water. *Journal of Electrostatics*, 66(5–6), 294–299.
- Bratescu, M. A., Cho, S.-P., Takai, O., & Saito, N. (2011). Size-controlled gold nanoparticles synthesized in solution plasma. *The Journal of Physical Chemistry C*, 115(50), 24569–24576.
- Cabrera, J. C., & Van Cutsem, P. (2005). Preparation of chitooligosaccharides with degree of polymerization higher than 6 by acid or enzymatic degradation of chitosan. *Biochemical Engineering Journal*, 25(2), 165–172.
- Cai, Q., Gu, Z., Fu, T., Liu, Y., Song, H., & Li, F. (2011). Kinetic study of chitosan degradation by an electrochemical process. *Polymer Bulletin*, 67(4), 571–582.
- Chang, K. L. B., Tai, M.-C., & Cheng, F.-H. (2001). Kinetics and products of the degradation of chitosan by hydrogen peroxide. *Journal of Agricultural and Food Chemistry*, 49(10), 4845–4851.
- Choi, W.-S., Ahn, K.-J., Lee, D.-W., Byun, M.-W., & Park, H.-J. (2002). Preparation of chitosan oligomers by irradiation. *Polymer Degradation and Stability*, 78(3), 533–538.
- De Laat, J., & Gallard, H. (1999). Catalytic decomposition of hydrogen peroxide by Fe (III) in homogeneous aqueous solution: Mechanism and kinetic modeling. *Environmental Science & Technology*, 33(16), 2726–2732.
- El-Sawy, N. M., Abd El-Rehim, H. A., Elbarbary, A. M., & Hegazy, E.-S. A. (2010). Radiation-induced degradation of chitosan for possible use as a growth promoter in agricultural purposes. *Carbohydrate Polymers*, 79(3), 555–562.
- Harish Prashanth, K. V., & Tharanathan, R. N. (2005). Depolymerized products of chitosan as potent inhibitors of tumor-induced angiogenesis. *Biochimica et Biophysica Acta (BBA) – General Subjects*, 1722(1), 22–29.
- Harish Prashanth, K. V., & Tharanathan, R. N. (2007). Chitin/chitosan: Modifications and their unlimited application potential—An overview. *Trends in Food Science & Technology*, 18(3), 117–131.
- Hien, N. Q., Phu, D. V., Duy, N. N., & Lan, N. T. K. (2012). Degradation of chitosan in solution by gamma irradiation in the presence of hydrogen peroxide. *Carbohydrate Polymers*, 87(1), 935–938.
- Hsu, S.-C., Don, T.-M., & Chiu, W.-Y. (2002). Free radical degradation of chitosan with potassium persulfate. *Polymer Degradation and Stability*, 75(1), 73–83.
- Huang, R., Mendis, E., Rajapakse, N., & Kim, S.-K. (2006). Strong electronic charge as an important factor for anticancer activity of chitooligosaccharides (COS). *Life Sciences*, 78(20), 2399–2408.
- Ifuku, S., Wada, M., Morimoto, M., & Saimoto, H. (2012). A short synthesis of highly soluble chemoselective chitosan derivatives via click chemistry. *Carbohydrate Polymers*, 90(2), 1182–1186.
- Ishizaki, T., Chiba, S., Kaneko, Y., & Panomsuwan, G. (2014). Electrocatalytic activity for the oxygen reduction reaction of oxygen-containing nanocarbon synthesized by solution plasma. *Journal of Materials Chemistry A*, 2(27), 10589–10598.
- Jin, S.-H., Kim, S.-M., Lee, S.-Y., & Kim, J.-W. (2014). Synthesis and characterization of silver nanoparticles using a solution plasma process. *Journal of Nanoscience and Nanotechnology*, 14(10), 8094–8097.
- Kang, B., Dai, Y.-D., Zhang, H.-Q., & Chen, D. (2007). Synergetic degradation of chitosan with gamma radiation and hydrogen peroxide. *Polymer Degradation and Stability*, 92(3), 359–362.
- Kasaai, M. R., Arul, J., Chin, S. L., & Charlet, G. (1999). The use of intense femtosecond laser pulses for the fragmentation of chitosan. *Journal of Photochemistry and Photobiology A: Chemistry*, 120(3), 201–205.
- Lee, M., Nah, J.-W., Kwon, Y., Koh, J. J., Ko, K. S., & Kim, S. W. (2001). Water-soluble and low molecular weight chitosan-based plasmid DNA delivery. *Pharmaceutical Research*, 18(4), 427–431.
- Li, K., Xing, R., Liu, S., Qin, Y., Meng, X., & Li, P. (2012). Microwave-assisted degradation of chitosan for a possible use in inhibiting crop pathogenic fungi. *International Journal of Biological Macromolecules*, 51(5), 767–773.
- Lin, C.-W., & Lin, J.-C. (2003). Characterization and blood coagulation evaluation of the water-soluble chitooligosaccharides prepared by a facile fractionation method. *Biomacromolecules*, 4(6), 1691–1697.
- Liu, X., Jiang, Y., He, H., & Ping, W. (2014). Hydrogen peroxide-induced degradation of type I collagen fibers of tilapia skin. *Food Structure*, 2(1–2), 41–48.
- Méndez-Díaz, J., Sánchez-Polo, M., Rivera-Utrilla, J., Canonica, S., & von Gunten, U. (2010). Advanced oxidation of the surfactant SDBS by means of hydroxyl and sulphate radicals. *Chemical Engineering Journal*, 163(3), 300–306.
- Mao, S., Shuai, X., Unger, F., Simon, M., Bi, D., & Kissel, T. (2004). The depolymerization of chitosan: Effects on physicochemical and biological properties. *International Journal of Pharmaceutics*, 281(1–2), 45–54.
- Martínez-Ramos, I., Maya-Mendoza, A., Gariglio, P., & Aranda-Anzaldo, A. (2005). A global but stable change in HeLa cell morphology induces reorganization of DNA structural loop domains within the cell nucleus. *Journal of Cellular Biochemistry*, 96(1), 79–88.
- Moad, G., Dagley, I. J., Habsuda, J., Garvey, C. J., Li, G., Nichols, L., et al. (2015). Aqueous hydrogen peroxide-induced degradation of polyolefins: A greener process for controlled-rheology polypropylene. *Polymer Degradation and Stability*, 117, 97–108.
- Mourya, V. K., Inamdar, N. N., & Choudhari, Y. M. (2011). Chitooligosaccharides: Synthesis, characterization and applications. *Polymer Science Series A*, 53(7), 583–612.
- Ostrowska-Czubenko, J., & Gierszewska-Drużyńska, M. (2009). Effect of ionic crosslinking on the water state in hydrogel chitosan membranes. *Carbohydrate Polymers*, 77(3), 590–598.
- Panomsuwan, G., Saito, N., & Ishizaki, T. (2016). Electrocatalytic oxygen reduction on nitrogen-doped carbon nanoparticles derived from cyano-aromatic molecules via solution plasma process. *Carbon*, 98, 411–420.
- Pootawang, P., Saito, N., & Takai, O. (2011). Solution plasma for template removal in mesoporous silica: pH and discharge time varying characteristics. *Thin Solid Films*, 519(20), 7030–7035.
- Pornsunthornawee, O., Katepetch, C., Vanichvattanadecha, C., Saito, N., & Rujiravanit, R. (2014). Depolymerization of chitosan–metal complexes via a solution plasma technique. *Carbohydrate Polymers*, 102, 504–512.
- Potocký, Š., Saito, N., & Takai, O. (2009). Needle electrode erosion in water plasma discharge. *Thin Solid Films*, 518(3), 918–923.

- Prasertsung, I., Damrongsakkul, S., Terashima, C., Saito, N., & Takai, O. (2012). Preparation of low molecular weight chitosan using solution plasma system. *Carbohydrate Polymers*, 87(4), 2745–2749.
- Prasertsung, I., Damrongsakkul, S., & Saito, N. (2013). Degradation of  $\beta$ -chitosan by solution plasma process (SPP). *Polymer Degradation and Stability*, 98(10), 2089–2093.
- Prashanth, K. V. H., & Tharanathan, R. N. (2006). Crosslinked chitosan—Preparation and characterization. *Carbohydrate Research*, 341(1), 169–173.
- Qin, C. Q., Du, Y. M., & Xiao, L. (2002). Effect of hydrogen peroxide treatment on the molecular weight and structure of chitosan. *Polymer Degradation and Stability*, 76(2), 211–218.
- Qin, C., Li, H., Xiao, Q., Liu, Y., Zhu, J., & Du, Y. (2006). Water-solubility of chitosan and its antimicrobial activity. *Carbohydrate Polymers*, 63(3), 367–374.
- Sánchez, Á., Mengibar, M., Rivera-Rodríguez, G., Moerschbacher, B., Acosta, N., & Heras, A. (2017). The effect of preparation processes on the physicochemical characteristics and antibacterial activity of chitooligosaccharides. *Carbohydrate Polymers*, 157, 251–257.
- Sabnis, S., & Block, L. H. (1997). Improved infrared spectroscopic method for the analysis of degree of N-deacetylation of chitosan. *Polymer Bulletin*, 39(1), 67–71.
- Saito, N., Hieda, J., & Takai, O. (2009). Synthesis process of gold nanoparticles in solution plasma. *Thin Solid Films*, 518(3), 912–917.
- Savitri, E., Juliastuti, S. R., Handaratri, A., & Sumarno Roesyadi, A. (2014). Degradation of chitosan by sonication in very-low-concentration acetic acid. *Polymer Degradation and Stability*, 110, 344–352.
- Shen, K.-T., Chen, M.-H., Chan, H.-Y., Jeng, J.-H., & Wang, Y.-J. (2009). Inhibitory effects of chitooligosaccharides on tumor growth and metastasis. *Food and Chemical Toxicology*, 47(8), 1864–1871.
- Shen, C., Song, S., Zang, L., Kang, X., Wen, Y., Liu, W., et al. (2010). Efficient removal of dyes in water using chitosan microsphere supported cobalt (II) tetrasulfophthalocyanine with  $H_2O_2$ . *Journal of Hazardous Materials*, 177(1–3), 560–566.
- Tømmeraas, K., Vårum, K. M., Christensen, B. E., & Smidsrød, O. (2001). Preparation and characterisation of oligosaccharides produced by nitrous acid depolymerisation of chitosans. *Carbohydrate Research*, 333(2), 137–144.
- Tayal, A., Kelly, R. M., & Khan, S. A. (1999). Rheology and molecular weight changes during enzymatic degradation of a water-soluble polymer. *Macromolecules*, 32(2), 294–300.
- Tian, F., Liu, Y., Hu, K., & Zhao, B. (2004). Study of the depolymerization behavior of chitosan by hydrogen peroxide. *Carbohydrate Polymers*, 57(1), 31–37.
- Vårum, K. M., Ottøy, M. H., & Smidsrød, O. (2001). Acid hydrolysis of chitosans. *Carbohydrate Polymers*, 46(1), 89–98.
- Venkatadri, R., & Peters, R. W. (1993). Chemical oxidation technologies: Ultraviolet light/hydrogen peroxide, Fenton's reagent, and titanium dioxide-assisted photocatalysis. *Hazardous Waste and Hazardous Materials*, 10(2), 107–149.
- Vigier, K. D. O., Benguerba, A., Barrault, J., & Jerome, F. (2012). Conversion of fructose and inulin to 5-hydroxymethylfurfural in sustainable betaine hydrochloride-based media. *Green Chemistry*, 14(2), 285–289.
- Wasikiewicz, J. M., Yoshii, F., Nagasawa, N., Wach, R. A., & Mitomo, H. (2005). Degradation of chitosan and sodium alginate by gamma radiation, sonochemical and ultraviolet methods. *Radiation Physics and Chemistry*, 73(5), 287–295.
- Wattthanaphanit, A., & Saito, N. (2013). Effect of polymer concentration on the depolymerization of sodium alginate by the solution plasma process. *Polymer Degradation and Stability*, 98(5), 1072–1080.
- Xu, Q., Dou, J., Wei, P., Tan, C., Yun, X., Wu, Y., et al. (2008). Chitooligosaccharides induce apoptosis of human hepatocellular carcinoma cells via up-regulation of Bax. *Carbohydrate Polymers*, 71(4), 509–514.
- Yue, W., Yao, P., & Wei, Y. (2009). Influence of ultraviolet-irradiated oxygen on depolymerization of chitosan. *Polymer Degradation and Stability*, 94(5), 851–858.
- Zheng, L.-Y., & Zhu, J.-F. (2003). Study on antimicrobial activity of chitosan with different molecular weights. *Carbohydrate Polymers*, 54(4), 527–530.

SELECTED TOPICS IN APPLIED PHYSICS

## Degradation of chitosan hydrogel dispersed in dilute carboxylic acids by solution plasma and evaluation of anticancer activity of degraded products

To cite this article: Chayanaphat Chokradjaroen *et al* 2018 *Jpn. J. Appl. Phys.* **57** 0102B5

View the [article online](#) for updates and enhancements.

### Related content

- [Structure and properties of polycaprolactone/chitosan nonwovens tailored by solvent systems](#)  
Olga Urbanek, Pawe Sajkiewicz, Filippo Pierini *et al.*
- [Sonophotocatalysis of Malonic Acid Solution: Possibility of a New Contribution to Organic Reactions](#)  
Yukio Naruke, Mika Goto, Hisashi Tanaka *et al.*
- [Versatile theranostics agents designed by coating ferrite nanoparticles with biocompatible polymers](#)  
M Zahraei, M Marciello, A Lazaro-Carrillo *et al.*





## Degradation of chitosan hydrogel dispersed in dilute carboxylic acids by solution plasma and evaluation of anticancer activity of degraded products

Chayanaphat Chokradjaroen<sup>1</sup>, Ratana Rujiravanit<sup>1,2\*</sup>, Sewan Theeramunkong<sup>3</sup>, and Nagahiro Saito<sup>4,5</sup>

<sup>1</sup>The Petroleum and Petrochemical College, Chulalongkorn University, Bangkok 10330, Thailand

<sup>2</sup>Center of Excellence on Petrochemical and Materials Technology, Chulalongkorn University, Bangkok 10330, Thailand

<sup>3</sup>Faculty of Pharmacy, Thammasat University, Pathumthani 12120, Thailand

<sup>4</sup>Department of Materials, Physics and Energy Engineering, Graduate School of Engineering, Nagoya University, Nagoya 464-8603, Japan

<sup>5</sup>Core Research for Evaluation Science and Technology (CREST), Japan Science and Technology Agency (JST), Kawaguchi, Saitama 333-0012, Japan

\*E-mail: ratana.r@chula.ac.th

Received June 15, 2017; accepted August 18, 2017; published online November 1, 2017

Chitosan is a polysaccharide that has been extensively studied in the field of biomedicine, especially its water-soluble degraded products called chitooligosaccharides (COS). In this study, COS were produced by the degradation of chitosan hydrogel dispersed in a dilute solution (i.e., 1.55 mM) of various kinds of carboxylic acids using a non-thermal plasma technology called solution plasma (SP). The degradation rates of chitosan were influenced by the type of carboxylic acids, depending on the interaction between chitosan and each carboxylic acid. After SP treatment, the water-soluble degraded products containing COS could be easily separated from the water-insoluble residue of chitosan hydrogel by centrifugation. The production yields of the COS were mostly higher than 55%. Furthermore, the obtained COS products were evaluated for their inhibitory effect as well as their selectivity against human lung cancer cells (H460) and human lung normal cells (MRC-5).  
© 2018 The Japan Society of Applied Physics

### 1. Introduction

Biopolymers are polymers produced by living organisms such as animals, plants, fungi, and bacteria.<sup>1,2)</sup> Biopolymers contain monomeric units that are covalently bonded together to form polymeric chain structures. For example, polysaccharides have monosaccharides as repeating units linked together through glycosidic bonds.<sup>3,4)</sup> Owing to their biocompatibility and biodegradability, their uses for eco-commodities, food supplements, cosmetics, and especially biomedical applications have been growing during the past decade.<sup>5)</sup>

Chitosan is one of the polysaccharides that has attracted much interest from both academic and industrial viewpoints. Chitosan is a derivative of chitin, which can be found as a structural component in shells of crustaceans, the cuticle of insects, and cell walls of fungi. Chitosan contains D-glucosamine as a major monomeric unit randomly connected with N-acetyl-D-glucosamine units by  $\beta$ -(1  $\rightarrow$  4) glycosidic linkages.<sup>6)</sup> Their chemical structures are shown in Fig. 1. Chitosan consists of reactive functional groups including hydroxyl groups at the C3 and C6 positions and an amino or acetamido group at the C2 position.<sup>7)</sup> The presence of amino groups that cause positively charged character of chitosan is the main reason that chitosan differs from other polysaccharides, which have a neutral or negatively charged character. The positively charged nature of chitosan correlates to its metal chelation, flocculation, as well as biological properties.<sup>7)</sup> Therefore, chitosan has been intensively investigated in several applications, especially in biomedical fields such as drug and gene delivery,<sup>8,9)</sup> tissue engineering,<sup>10)</sup> wound dressings,<sup>11,12)</sup> and biosensors.<sup>13)</sup>

Unfortunately, native chitosan generally has a high molecular weight together with intra- and intermolecular hydrogen bond networks due to the abundance of hydroxyl groups, resulting in its insolubility in water and poor solubility in most organic solvents.<sup>14)</sup> Therefore, many studies relating to chitosan have focused on a water-soluble form of chitosan, such as chitooligosaccharides (COS), which, moreover, broadens the biological applications of chitosan. The bio-

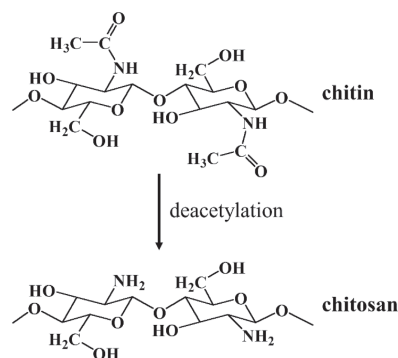


Fig. 1. Chemical structures of chitin and chitosan.

logical properties of both chitosan and COS according to previous studies are summarized in supplementary data (Table I).

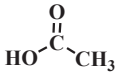
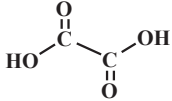
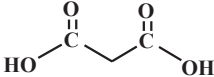
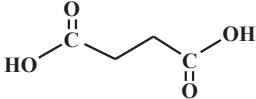
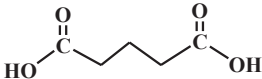
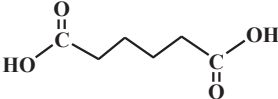
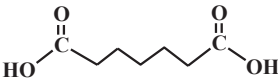
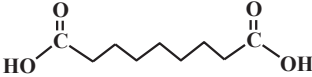
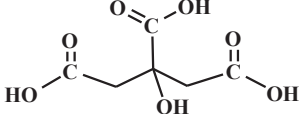
Cancer is one of the major causes of death worldwide.<sup>15)</sup> The current treatments for cancer, such as radiation therapy and chemotherapy, still cause high risks of harming normal cells and lead to long-term and short-term side effects in patients.<sup>16,17)</sup> Therefore, many researchers have attempted to find alternative ways of treating cancer minimizing negative effects on healthy cells, such as by using natural products. COS are natural products that have been widely studied and show potential as an alternative choice for the treatment of cancer.<sup>18–20)</sup> Some examples relating to the anticancer activity of COS are presented in supplementary data (Table II).

COS can be prepared by the degradation of chitosan. This degradation has been used to produce low-molecular-weight products of not only chitosan but also other polysaccharides, leading to the improvement of their water solubility and absorbability in order to exert their biological effects. In general, there are three main methods applied for the degradation of polysaccharides: chemical degradation,<sup>21–23)</sup> enzymatic degradation,<sup>24–26)</sup> and physical degradation.<sup>27,28)</sup> Degradation by using strong chemicals has been widely used on an industrial scale, but the use of a large amount of

**Table I.**  $M_w$  (Da) and PDI of chitosan solution at a concentration of 0.2% dissolved in 1 and 2 M acetic acid solutions and chitosan hydrogel at a solid content of 0.2% (dry weight) dispersed in 1.55 mM acetic acid solution after the degradation via conventional heat treatment and SP treatment for different reaction times in this study in comparison with the previous works.

SP treatment time (min)	$M_w$ (PDI)				
	Heat at 75 °C		SP		
	Chitosan hydrogel	Chitosan hydrogel	Chitosan solution	Chitosan solution <sup>29)</sup>	Chitosan solution <sup>40)</sup>
0	$4.8 \times 10^5$ (2.35)	$4.8 \times 10^5$ (2.35)	$4.8 \times 10^5$ (2.35)	$1.1 \times 10^6$ (4.10)	$2.1 \times 10^5$ (4.10)
15	—	$7.3 \times 10^4$ (4.20)	—	$4.3 \times 10^5$ (5.40)	—
30	$4.2 \times 10^5$ (4.35)	$2.2 \times 10^4$ (3.35)	$1.1 \times 10^5$ (5.21)	$2.0 \times 10^5$ (5.30)	$6.2 \times 10^4$ (2.70)
45	—	$1.1 \times 10^4$ (2.74)	—	—	—
60	$4.0 \times 10^5$ (4.24)	$6.6 \times 10^3$ (2.35)	$2.1 \times 10^4$ (5.42)	$1.0 \times 10^5$ (2.35)	$5.6 \times 10^4$ (2.70)

**Table II.** Chemical structures, acid dissociation constants, number of carboxylic groups, and number of methylene groups on the backbone of the carboxylic acids used in this study.

Acid	Chemical structure	$pK_a$ <sup>54)</sup>	Number of carboxylic groups	Number of –CH <sub>2</sub> – groups on backbone
Acetic acid		4.76	1	—
Oxalic acid		1.23, 4.19	2	0
Malonic acid		2.83, 5.76	2	1
Succinic acid		4.19, 5.48	2	2
Glutaric acid		4.34, 5.42	2	3
Adipic acid		4.42, 5.41	2	4
Pimelic acid		4.48, 5.42	2	5
Azelaic acid		4.55, 5.41	2	7
Citric acid		3.09, 4.75, 5.41	3	—

hazardous chemicals leads to difficulty in handling the generated waste and may cause environmental pollution.<sup>29)</sup> Using enzymes to degrade chitosan has drawn much attention because they were found to be able to region-selectively degrade chitosan under mild conditions.<sup>30)</sup> However, high-quality enzymes and the operating setup are expensive, while the production yield has been reported to be relatively low.<sup>6)</sup> Recently, physical methods, applying an energy, such as mi-

crowaves,<sup>31–34)</sup> ultraviolet,<sup>35)</sup> sonication,<sup>36,37)</sup> gamma rays,<sup>27)</sup> and plasma,<sup>38)</sup> have been extensively studied because they can enhance the degradation of chitosan with low chemical requirements.

Non-thermal plasma discharge under a liquid phase, called solution plasma (SP), is one of the energy-impact methods that has been recently utilized as a tool for the degradation of polysaccharides such as chitosan<sup>29,39,40)</sup> and alginate.<sup>41)</sup> The term SP was proposed by Takai.<sup>42)</sup> In early research, SP was used for the synthesis of noble-metal nanoparticles<sup>43,44)</sup> and the decomposition of organic compounds in water treatment.<sup>45)</sup> SP has the ability to produce highly active species such as hydroxyl radicals ( $\cdot\text{OH}$ ), hydroperoxyl radicals ( $\cdot\text{HO}_2$ ), free electrons ( $e^-$ ), superoxide anions ( $\text{O}_2^-$ ), and atomic oxygen anions ( $\text{O}^-$ ) under atmospheric pressure and room temperature.<sup>29,46)</sup> These radicals play a part in the enhancement of the degradation of polymers. For instance, in the degradation of chitosan to produce COS by SP treatment, it has been reported that the plasma-induced  $\cdot\text{OH}$  attacked the chitosan chain and caused scission at the glycosidic bonds.<sup>29)</sup>

Since COS are high-valued natural substances possessing potential anticancer activity, their production processes, including not only degradation but also separation and purification, are very important. Currently, the production of COS still uses a lot of chemicals and needs some complicated separation and purification systems. For example, it has been reported that the degradation of chitosan by 35% HCl was effectively conducted within 30 min to produce COS with a degree of polymerization (DP) of 8, but owing to the use of strong acid, further neutralization by NaOH as well as separation and purification to remove contaminants were required.<sup>25)</sup> Even though, methods such as microwave and SP treatment have been claimed to realize the green degradation of chitosan, chitosan still has to be dissolved in an acetic acid solution with a concentration of approximately 1–2 M in order to obtain chitosan solution prior to the degradation.<sup>19,29,32,39,40)</sup> The degradation of chitosan solution usually leads to some difficulty in separating COS from the high-molecular-weight chitosan. This is because they are dissolved together in the solution. Therefore, the heterogeneous degradation of chitosan in an undissolved form, such as chitosan hydrogel, will probably ease the separation of the COS products from the high-molecular-weight chitosan. A hydrogel is generally defined as a hydrophilic polymer capable of holding a large amount of water in its three-dimensional networks.<sup>47)</sup> In this study, COS were produced by applying plasma technology in order to reduce the use of chemicals in the degradation reaction. Furthermore, simple separation and purification processes to attain COS should be accomplished by conducting the heterogeneous degradation of chitosan hydrogel dispersed in dilute acid solution. Chitosan hydrogel was prepared by the reprecipitation method, which resulted in the reduction of the crystallinity of chitosan.<sup>48)</sup> Various carboxylic acids, such as di- and tricarboxylic acids, were added to the suspension of chitosan hydrogel in order to examine the influences of distinct carboxylic acids, other than acetic acid, which is a monocarboxylic acid, in relation to the degradation of chitosan. Finally, the obtained COS products were evaluated for their anticancer activity as well as their selectivity to cancer cells in comparison with normal cells.

## 2. Experimental methods

### 2.1 Materials

Chitosan was obtained from the deacetylation of chitin, which was prepared from the shells of *Metapenaeus dobsoni* shrimp, provided by Surapon Foods Public. Glacial acetic acid ( $\text{CH}_3\text{COOH}$ , 99.9%), hydrochloric acid (HCl, 37.0%), sodium chloride (NaCl, 99.0%), and sodium hydroxide (NaOH, 97.0%) pellets were purchased from RCI Labscan. A 50% (w/v) NaOH solution was supplied by the Chemical Enterprise. Oxalic acid dihydrate [ $(\text{COOH})_2 \cdot 2\text{H}_2\text{O}$ , 98.0%] and succinic acid [ $\text{C}_2\text{H}_4(\text{COOH})_2$ , 99.5%] were purchased from Ajax Finechem. Malonic acid [ $\text{CH}_2(\text{COOH})_2$ , 99.0%], glutaric acid [ $\text{C}_3\text{H}_6(\text{COOH})_2$ , 99.0%], adipic acid [ $\text{C}_4\text{H}_8(\text{COOH})_2$ , 99.0%], pimelic acid [ $\text{C}_5\text{H}_{10}(\text{COOH})_2$ , 98.0%], and azelaic acid [ $\text{C}_7\text{H}_{14}(\text{COOH})_2$ , 98.0%] were supplied by Sigma-Aldrich. Citric acid [ $\text{C}_3\text{H}_5\text{O}(\text{COOH})_3$ , 99.5–102.0%] was purchased from Loba Chemie. Sodium borohydride ( $\text{NaBH}_4$ ) and potassium bromide (KBr) were obtained from Carlo Erba Reagents and Wako, respectively.

### 2.2 Preparation of chitosan hydrogel from the shrimp shell

*M. dobsoni* shrimp shells were washed and dried under sunlight before grinding into small flakes. The flakes of dried shrimp shell were demineralized by soaking in a 1 M HCl solution for 24 h. The demineralization step to remove calcium carbonate in shrimp shells was repeated by adding a fresh 1 M HCl solution and soaking for another 24 h before the flakes were removed and washed with distilled water until neutral. Subsequently, the demineralized shrimp shell flakes were deproteinized by immersion in a 4% (w/v) NaOH solution at 80 °C with vigorous stirring for 4 h. The flakes were filtered and washed with distilled water until the eluent reached a pH of 7.0. Then, the deproteinized product, known as chitin, was obtained. A 50% (w/v) NaOH solution containing 0.5% (w/v)  $\text{NaBH}_4$  was added to the chitin flakes before the suspension was heated in an autoclave at 110 °C for 75 min. After filtration, the solid fraction from the deacetylation process was washed with distilled water until the pH became neutral. The deacetylation process was repeated twice to achieve the required degree of deacetylation (%DD) of chitosan (i.e., 90%), calculated by following an equation of Sabnis and Block.<sup>49)</sup> The solid-to-liquid ratio used in all processes was 1 : 10. After each process, water in the product was removed by drying in an oven at 60 °C before continuing further steps or use.

Chitosan solution was prepared by dissolving chitosan flakes (2 g) into 200 ml of 2% (v/v) acetic acid solution. The obtained chitosan solution was then poured dropwise into 400 ml of 5% (w/v) NaOH solution with vigorous stirring.<sup>48)</sup> The gel-like precipitate was dialyzed against distilled water in a dialysis tube with a molecular weight cutoff of 12,132 Da (Sigma-Aldrich) until neutral to attain chitosan hydrogel.

### 2.3 Degradation of chitosan hydrogel

A suspension of chitosan hydrogel for the degradation by the SP treatment was prepared by adding 6 g of chitosan hydrogel (having dry weight  $\sim 0.1$  g) to the SP reactor and then 50 ml of dilute acid solution was added to the suspension with an acid-to-chitosan mole ratio of 1 : 8 or equivalent to 1.55 mM. The suspension was stirred at room temperature (30 °C) for 5 min. The SP reactor was made of a glass beaker

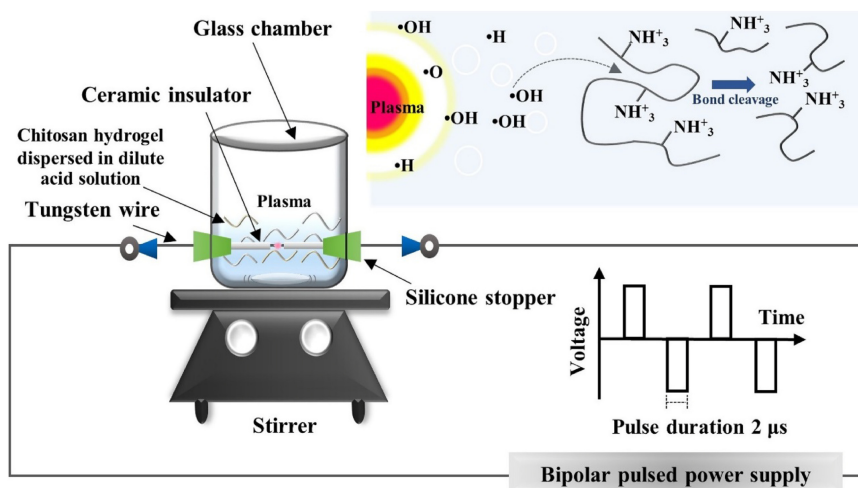


Fig. 2. (Color online) Schematic diagram of SP setup.

having two tungsten electrodes (purity 99.9%, Nilaco) with a diameter of 1 mm inserted in it. The SP system used in this study has been described in previous works<sup>40,42,46</sup> and is schematically shown in Fig. 2. The operation parameters of the typical voltage, pulse frequency, pulse width, and electrode distance were 1.6 kV, 23 kHz, 2  $\mu$ s, and 0.75 mm, respectively. The reaction temperature during the plasma operation was approximately 60–70 °C.

## 2.4 Separation of degraded chitosan product

After the degradation of chitosan hydrogel by the SP treatment, the suspension was centrifuged to collect the remaining solid residue assigned as the solid fraction, which was water-insoluble chitosan that was then dried in an oven at 60 °C. The supernatant was further freeze-dried and assigned as the solution fraction, which should contain water-soluble COS. All fractions were weighed and the percentage yield of each fraction was calculated using the following equation:

$$\text{Yield (\%)} = \frac{W_i}{W_0} \times 100, \quad (1)$$

where  $W_0$  is the initial dry weight of chitosan in the system and  $W_i$  is the dry weight of the degraded chitosan fraction, while  $i$  refers to either the solid fraction or solution fraction.

## 2.5 Characterization

The crystallinity of native chitosan and chitosan hydrogel before and after the SP treatment was characterized by using a wide-angle X-ray diffraction (WAXD) analyzer (Rigaku SmartLab) operated in a continuous mode with a scan speed of 5° min<sup>−1</sup> and a scattering angle ( $2\theta$ ) from 5 to 60° using Cu K $\alpha$  as an X-ray source.

The morphology of the chitosan flakes and dried chitosan hydrogel was examined by using field-emission scanning electron microscopy (FE-SEM; JEOL JSM-7610F).

The changes in the average molecular weight and the molecular weight distribution of chitosan during the degradation via the SP treatment were determined using gel permeation chromatography (GPC; Shimadzu CTO-10A) apparatus equipped with a refractive index (RI) detector. An ultra-hydrogel linear column (Waters 600E) for separation of the molecular weight in the range of  $1.0 \times 10^3$  to  $2.0 \times 10^7$  Da was connected in series with a guard column equipped in an oven at the operating temperature of 40 °C. The mobile phase

was a 0.5 M acetate buffer solution at pH 4.0 and the flow rate was set at 0.6 ml·min<sup>−1</sup>. The injection volume of a sample was 40  $\mu$ l, comprising 3 mg·ml<sup>−1</sup> chitosan in the acetate buffer solution. Pullulans with molecular weight in the range of  $2.17 \times 10^3$  to  $8.05 \times 10^5$  Da were used as standard samples.

The investigation of any changes in the chemical structures of chitosan after the degradation via the SP treatment was carried out by using Fourier transform infrared (FT-IR) spectrometry (Thermo Fisher Scientific Nicolet iS5). FT-IR spectra with wavenumbers from 4000 to 400 cm<sup>−1</sup> were taken on KBr pellets at a resolution of 4 cm<sup>−1</sup> using 64 scans with correction for atmospheric carbon dioxide (CO<sub>2</sub>).

## 2.6 Biological assay

**2.6.1 Cell culture.** H460 cells (human lung cancer cell line) and MRC-5 cells (human lung normal cell line) were cultured by using Roswell Park Memorial Institute (RPMI) 1640 Medium with L-glutamine (Biowest), and Eagle's Minimum Essential Medium (EMEM) with sodium bicarbonate, non-essential amino acids, L-glutamine, and sodium pyruvate (Corning). Before the cell cultivation, both media were supplemented with 10% fetal bovine serum (Biowest), 100 U·ml<sup>−1</sup> penicillin, and 100  $\mu$ g·ml<sup>−1</sup> streptomycin (Life Technologies Gibco). The cells were incubated in a 5% CO<sub>2</sub> humidified incubator at 37 °C.

**2.6.2 Cytotoxicity assay.** A test on the in vitro cytotoxicity of the chitosan sample was performed by MTT assay against both cancer and normal cells. Firstly, cells were seeded into 96-well microliter plates (10<sup>4</sup> cells/well) and incubated in a 5% CO<sub>2</sub> humidified incubator at 37 °C for 24 h. After that, different concentrations of chitosan samples, diluted with sterile water, were added into the wells to make the desired final concentration (0.1 to 5 mg·ml<sup>−1</sup>) and further incubated in an incubator at 37 °C and 5% CO<sub>2</sub>. After 24 h incubation, the medium was discarded and replaced with phosphate buffer saline solution (PBS) containing 0.05% (w/v) of 3-(4,5-dimethylthiazol-2-yl)-2,5-diphenyltetrazolium bromide (MTT) solution with further incubation for 3 h. Then, the solution was discarded and DMSO was added to dissolve the formed formazan crystals and the absorbance (A) of each well was measured at 570 nm using a microplate reader (Thermo Fisher Scientific Varioskan™ Flash Multi-



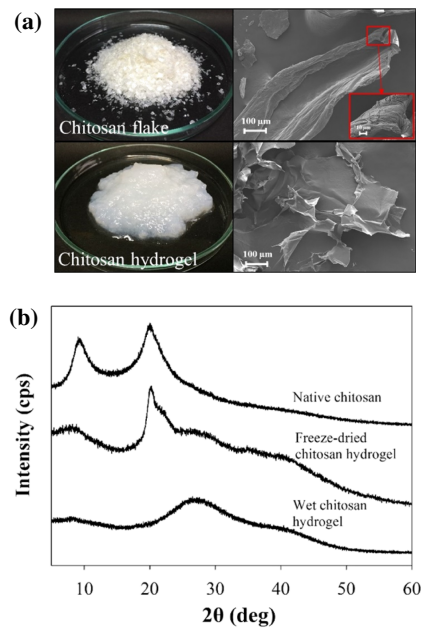


**Fig. 3.** (Color online) (a) FE-SEM images and (b) WAXD spectra of native chitosan, freeze-dried, and wet chitosan hydrogel samples.

mode Reader). The cell viability was calculated using the following equation:

$$\text{Cell viability (\%)} = 100 \times \frac{A_{\text{treated}} - A_{\text{blank}}}{A_{\text{untreated}} - A_{\text{blank}}}. \quad (2)$$

The percentage cell viability was plotted versus the concentration of the COS sample to determine the mean growth-inhibitory concentration ( $\text{IC}_{50}$ ) value. All experiments were repeated five times. Doxorubicin was used as a positive control.

### 3. Results and discussion

#### 3.1 Degradation of chitosan hydrogel

A comparison of the morphology of native chitosan flakes and freeze-dried chitosan hydrogel was performed by using FE-SEM, and the FE-SEM images are shown in Fig. 3(a). The FE-SEM image revealed that the chitosan flakes were composed of well-packed multilayered sheets. After dissolving chitosan flakes in the acetic acid solution, followed by reprecipitation in the NaOH solution to form chitosan hydrogel, intra- and intermolecular hydrogen bonding interactions within the structure of native chitosan were disrupted. The dissolution and regeneration of chitosan hydrogel resulted in the loss of the former well-packed multilayered structure, leading to a more amorphous region in chitosan hydrogel compared with native chitosan.<sup>50)</sup>

Moreover, the change in the crystalline structure of native chitosan and chitosan hydrogel was examined by WAXD analysis, as shown in Fig. 3(b). The WAXD spectrum of native chitosan showed that the main characteristic peaks of native chitosan appeared at  $2\theta = 9.8$  and  $19.9^\circ$ . As reported in the previous works,<sup>51,52)</sup> the reflection of  $2\theta$  around  $9\text{--}10.5^\circ$  indicated that chitosan had a hydrate polymorph. In the hydrate tendon crystal, the chain conformation appeared as a 2-fold helix stabilized by a hydrogen bond ( $\text{O3}\cdots\text{O5}$ ) with the orientation of O6. Hydrogen bonds also occurred between adjacent chains (via  $\text{N2}\cdots\text{O6}$ ) to form a sheet

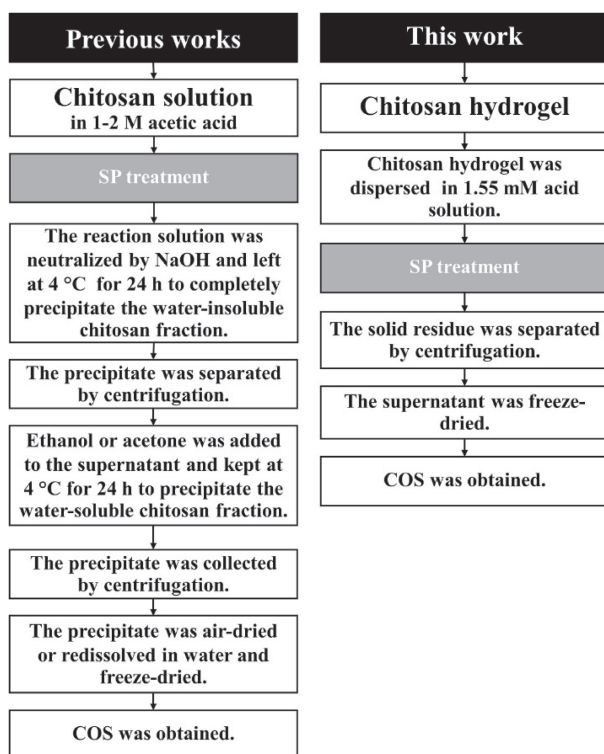
structure. These sheets stacked together in a parallel fashion and could be stabilized by water molecules that presented inside the chitosan structure.<sup>52)</sup> Upon the transformation of native chitosan to hydrogel, the crystalline structure in native chitosan was changed. The WAXD result of chitosan hydrogel exhibited clearly broader peaks at  $2\theta = 9.8^\circ$ . The characteristic peak at  $2\theta = 19.9^\circ$  disappeared, while two new broad peaks at  $2\theta = 28.1$  and  $35.0^\circ$  could be observed. The WAXD result suggested that the crystalline structure of native chitosan was destroyed. The peaks of  $2\theta$  at  $28.1$  and  $35.0^\circ$  indicated the formation of chitosan acetate salt as reported by Modrzejewska et al.<sup>53)</sup> According to this evidence, the chitosan hydrogel had lower crystallinity than native chitosan and should be more susceptible to degradation by the SP treatment.

The degradation of chitosan hydrogel dispersed in the dilute acetic acid by applying the SP treatment and the conventional heat treatment were conducted under the same condition. The chitosan hydrogel was found to disperse well in the dilute acetic acid solutions. It was found that the weight-average molecular weight ( $M_w$ ) of chitosan hydrogel after SP treatment dramatically decreased, while the slight reduction of  $M_w$  for chitosan hydrogel by the conventional heating treatment occurred, as shown in Table I. Furthermore, the degradation of chitosan hydrogel dispersed in the dilute acetic acid by the SP treatment was performed for comparison with the degradation of chitosan solution dissolved in 1 M acetic acid by SP treatment, which has been studied in some previous works.<sup>29,39,40)</sup> It was found that the  $M_w$  values of both types of chitosan samples were greatly reduced after the SP treatment. From GPC measurement, the degradation of chitosan hydrogel dispersed in the dilute acetic acid by applying the SP treatment for 60 min could reduce  $M_w$  for chitosan by approximately 98%. On the other hand,  $M_w$  for chitosan in the chitosan solution was decreased by 95% under the same condition. Therefore, it might be concluded that chitosan hydrogel dispersed in the dilute acetic acid was readily degraded by the SP treatment. Moreover, it also indicated that the SP treatment is an effective tool for promoting the degradation of chitosan to produce COS, even though only a dilute organic acid solution was present in the reaction.

Figure 4 shows flow charts giving a comparison of the experimental procedures for the degradation of chitosan solution and chitosan hydrogel to produce COS by SP treatment employed in this study and other previous works.<sup>19,29)</sup> At a high concentration of acetic acid ( $\text{pH} \approx 4.0$ ), chitosan can dissolve well because most  $\text{NH}_2$  groups at the C2 position in the structure of chitosan are protonated by protons from the dissociation of acetic acid and become soluble under an acidic environment.<sup>36)</sup> However, at a very low concentration ( $\text{pH} \approx 6.5$ ) of acetic acid, only a small number of  $\text{NH}_2$  groups in chitosan can be protonated due to the lack of protons and consequently, the chitosan hydrogel still remains as a suspension in the dilute acetic acid solution. Accordingly, the water-soluble degraded product of COS obtained from the SP treatment of the chitosan hydrogel dispersed in the dilute acetic acid could be easily separated from the remaining solid fractions by using simple centrifugation. The COS dissolving in the solution was collected as a supernatant, while the solid fraction that contained water-insoluble,

**Table III.**  $M_w$  (Da) and PDI of chitosan hydrogel at a solid content of 0.2% (dry weight) dispersed in various carboxylic acid solutions with a concentration of 1.55 mM after degradation via SP treatment for different reaction times.

SP treatment time (min)	$M_w$ (PDI)								
	Acetic acid	Oxalic acid	Malonic acid	Succinic acid	Glutaric acid	Adipic acid	Pimelic acid	Azelaic acid	Citric acid
0	$4.8 \times 10^5$ (2.35)	$4.8 \times 10^5$ (2.35)	$4.8 \times 10^5$ (2.35)	$4.8 \times 10^5$ (2.35)	$4.8 \times 10^5$ (2.35)	$4.8 \times 10^5$ (2.35)	$4.8 \times 10^5$ (2.35)	$4.8 \times 10^5$ (2.35)	$4.8 \times 10^5$ (2.35)
15	$7.1 \times 10^4$ (4.20)	$7.1 \times 10^4$ (4.95)	$1.0 \times 10^5$ (5.64)	$1.0 \times 10^5$ (4.97)	$8.9 \times 10^4$ (5.82)	$8.9 \times 10^4$ (4.20)	$1.2 \times 10^5$ (7.50)	$1.4 \times 10^5$ (6.06)	$1.8 \times 10^5$ (3.76)
30	$2.5 \times 10^4$ (3.35)	$2.6 \times 10^4$ (3.67)	$3.9 \times 10^4$ (4.55)	$4.1 \times 10^4$ (4.50)	$3.4 \times 10^4$ (4.92)	$2.7 \times 10^4$ (3.35)	$4.0 \times 10^4$ (5.34)	$5.8 \times 10^4$ (6.72)	$1.2 \times 10^5$ (5.48)
45	$1.0 \times 10^4$ (2.74)	$1.0 \times 10^3$ (2.59)	$1.7 \times 10^4$ (3.68)	$1.8 \times 10^4$ (3.46)	$1.2 \times 10^4$ (3.13)	$1.6 \times 10^4$ (2.74)	$2.0 \times 10^4$ (4.03)	$2.3 \times 10^4$ (4.73)	$5.7 \times 10^4$ (4.20)
60	$6.7 \times 10^3$ (2.35)	$5.8 \times 10^3$ (2.22)	$9.2 \times 10^3$ (3.00)	$8.7 \times 10^3$ (2.62)	$7.1 \times 10^3$ (2.65)	$7.8 \times 10^3$ (2.35)	$1.3 \times 10^4$ (3.58)	$1.7 \times 10^4$ (4.75)	$2.5 \times 10^4$ (3.68)

**Fig. 4.** Comparison of the experimental procedures for the degradation of chitosan solution and chitosan hydrogel to produce COS by SP treatment.

high-molecular-weight chitosan was separated as a precipitate after centrifugation. On the other hand, the degraded product from the degradation of the chitosan solution in the presence of a high concentration of acetic acid by the SP treatment required neutralization by using NaOH in order to separate the water-insoluble, high-molecular-weight chitosan from the water-soluble, low-molecular-weight product that contained COS. Furthermore, the addition of a non-solvent such as ethanol or acetone was necessary for separation of the COS products from the solution as a precipitate. According to the flow charts in Fig. 4, the production of COS from chitosan hydrogel was simpler and less time-consuming than that obtained from chitosan solution.

In addition to acetic acid, various types of other carboxylic acids were also used to disperse chitosan hydrogel in order to study their influence on the degradation of chitosan hydrogel

by applying the SP treatment. The various types of other carboxylic acids including chemical structures, acid dissociation constants,<sup>54)</sup> number of carboxylic groups, and number of methylene groups on the backbone are shown in Table II. According to GPC analysis, the results on molecular weight reduction as a function of the SP treatment time are shown in Table III.  $M_w$  for the original chitosan hydrogel before the SP treatment was  $4.8 \times 10^5$  Da.  $M_w$  was found to decrease for all types of carboxylic acids with increasing SP treatment time. For the addition of oxalic acid, the dramatic reduction of  $M_w$  was observed and the scale of molecular weight reduction was comparable to that obtained from acetic acid.  $M_w$  for the degraded products obtained from the systems containing acetic acid and oxalic acid was approximately  $6 \times 10^3$  Da after 60 min of SP treatment. It was expected that the degraded products would contain COS having  $M_w$  less than 5 kDa<sup>30)</sup> as a major component. In the systems with the addition of malonic acid, succinic acid, glutaric acid, and pimelic acid, the SP treatment could reduce  $M_w$  for the chitosan hydrogel from  $4.8 \times 10^5$  Da to the range of  $7.1 \times 10^3$ – $1.3 \times 10^4$  Da, while by the addition of azelaic acid and citric acid,  $M_w$  for the degraded chitosan was equal to approximately  $2 \times 10^4$  Da after the SP treatment for 60 min.

The rate constant of the degradation reaction of chitosan hydrogel was analyzed on the basis of the following linear relationship between inverse molecular weight ( $1/M_w$ ) and reaction time ( $t$ ) in previous reports:<sup>29,55)</sup>

$$\frac{1}{M_t} = \left( \frac{1}{M_0} \right) + \left( \frac{kt}{M} \right) = \left( \frac{1}{M_0} \right) + k't, \quad (3)$$

where  $M_t$  is  $M_w$  for the sample at the reaction time ( $t$ ),  $M_0$  is the initial  $M_w$  for the sample,  $M$  is the molecular weight of the monomer,  $k$  ( $\text{min}^{-1}$ ) or  $k'$  ( $\text{mol g}^{-1} \text{min}^{-1}$ ) is the rate constant, and  $t$  is the reaction time. The  $k$  values are shown in Table IV. The  $k$  value obtained by the system with the addition of oxalic acid was equal to  $3.67 \times 10^{-4} \text{ min}^{-1}$ , which was slightly higher than that for the addition of acetic acid ( $k = 3.48 \times 10^{-4} \text{ min}^{-1}$ ). Meanwhile, the addition of the other dicarboxylic acids led to lower  $k$  values than that obtained by the system with the addition of acetic acid. The obtained  $k$  values for the systems using dicarboxylic acids ranged from  $1.36 \times 10^{-4}$  to  $3.67 \times 10^{-4} \text{ min}^{-1}$ , which seemed to vary, depending on the number of methylene groups on the backbone. For the tricarboxylic acid, citric acid, the  $k$  value

**Table IV.** Rate constants ( $k$ ) of the degradation reactions of chitosan hydrogel at a solid content of 0.2% (dry weight) dispersed in 1.55 mM carboxylic acid solutions by SP treatment and production yield of water-soluble COS produced by the degradation of chitosan hydrogel dispersed in various carboxylic acids at a concentration of 1.55 mM by applying SP treatment as well as their  $M_w$ ,  $M_n$ , and PDI.

Acid	$k \times 10^{-4}$ ( $\text{min}^{-1}$ )	COS			
		Yield (%)	$M_n$ (Da)	$M_w$ (Da)	PDI
Acetic acid	$3.48 \pm 0.05$	$68.3 \pm 2.36$	1861	2969	1.59
Oxalic acid	$3.67 \pm 0.20$	$60.3 \pm 6.85$	1944	3344	1.72
Malonic acid	$2.37 \pm 0.26$	$53.3 \pm 7.17$	2053	3482	1.69
Succinic acid	$2.39 \pm 0.08$	$60.9 \pm 4.71$	2321	4484	1.93
Glutaric acid	$3.09 \pm 0.01$	$63.1 \pm 3.12$	2181	4033	1.84
Adipic acid	$2.75 \pm 0.02$	$60.3 \pm 3.54$	2008	3395	1.69
Pimelic acid	$1.80 \pm 0.04$	$64.1 \pm 6.56$	2216	4032	1.81
Azelaic acid	$1.36 \pm 0.03$	$40.0 \pm 2.04$	2133	4515	1.93
Citric acid	$0.75 \pm 0.02$	$2.5 \pm 0.21$	1538	2330	1.51

was the lowest among all the studied carboxylic acids. Nevertheless, the  $k$  values obtained in this study from the degradation of chitosan hydrogel dispersed in dilute carboxylic acids by applying the SP plasma treatment were comparable to those obtained from the degradation of chitosan solution by using concentrated  $\text{H}_2\text{O}_2$  or using various types of energy with the  $k$  values ranging from  $10^{-4}$  to  $10^{-2} \text{ min}^{-1}$ .<sup>32,39,55,56</sup>

For further investigation, the chemical structures of chitosan hydrogel before and after degradation by applying the SP treatment in the presence of various types of dilute carboxylic acids were examined by using FT-IR, and the FT-IR results are shown in Fig. 5. The absorption peaks of chitosan hydrogel before the SP treatment at the wavenumber of approximately  $3450 \text{ cm}^{-1}$  were assigned to the N–H and hydrogen bonded O–H stretching vibration and the peaks at the wavenumbers of  $1650$  and  $1600 \text{ cm}^{-1}$  were referred to the C=O stretching of the amide bond and the N–H bending vibrations of the secondary amide, respectively.<sup>6,15,57,58</sup> The peaks at around  $1420$  and  $1375 \text{ cm}^{-1}$  were attributed to  $-\text{CH}_2-$  bending with the orientation of the primary hydroxyl group in the polysaccharides and methyl group.<sup>59,60</sup> The peak at  $1070 \text{ cm}^{-1}$  was assigned to the stretching of C–O–C.<sup>6</sup> According to the FT-IR results, the overall chemical structures of the degraded chitosan hydrogel dispersed in various dilute carboxylic acids did not change after the SP treatment. For the degraded chitosan hydrogel obtained from the system with the addition of acetic acid, strong absorption at  $1650 \text{ cm}^{-1}$  was observed. This might indicate the ionic interaction between the protonated amino groups of chitosan and the carboxylate anion ( $-\text{COO}^-$ ) of the carboxylic acid.<sup>61</sup> Normally, protons ( $\text{H}^+$ ) from the dissociation of acetic acid ( $\text{CH}_3\text{COOH}$ ) can protonate amino groups ( $-\text{NH}_2$ ) of chitosan to form ammonium groups ( $-\text{NH}_3^+$ ).<sup>50</sup> Then, acetate anions ( $\text{CH}_3\text{COO}^-$ ), which have relatively small size and low steric hindrance, should be able to penetrate into the structure of chitosan and undergo ionic interaction with  $-\text{NH}_3^+$ . After that, these interactions could lead to an electrostatic repulsion between chitosan chains.<sup>19</sup> Consequently, the structure of chitosan may freely expand and distribute in the solution, as demonstrated later in Fig. 7(a), leading to an increasing probability that radicals generated by plasma discharge could

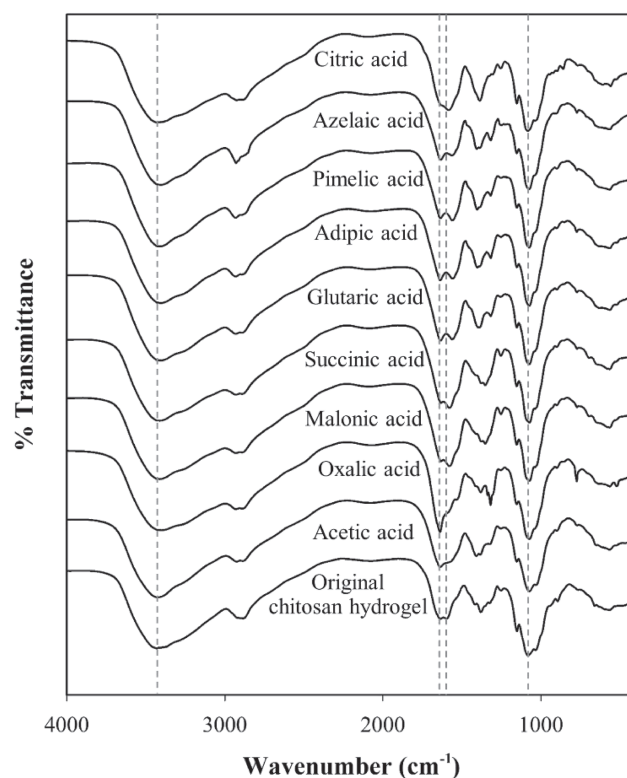


**Fig. 5.** FT-IR spectra of the chitosan hydrogel before the SP treatment and the degraded chitosan hydrogel dispersed in various carboxylic acid solutions at a concentration of 1.55 mM after applying the SP treatment for 60 min.

penetrate to the  $\beta$ -(1,4)-glycosidic linkages of chitosan and greatly promote the  $M_w$  reduction of chitosan hydrogel. For the addition of oxalic acid, the FT-IR spectra of the degraded product showed that the absorption at  $1650 \text{ cm}^{-1}$  became sharp and stronger than that of the degraded product obtained from the system with the addition of acetic acid. In the case of oxalic acid, which is a dicarboxylic acid with no methylene group, it was reported that its dissociation could be influenced by the phenomenon called the mesomeric effect.<sup>62</sup> The mesomeric effect might lead to intramolecular hydrogen bonding between the first dissociated carboxylic group and the OH part of the undissociated group in the oxalic acid, which bears a partial positive charge. Similar to acetic acid, oxalic acid could interact with chitosan, but the interaction might be slightly stronger, leading to a slightly higher rate of degradation than that of acetic acid. Meanwhile, the FT-IR spectra of the degraded product from the system with the addition of other dicarboxylic acids and the tricarboxylic acid exhibited the characteristic peak at  $1600 \text{ cm}^{-1}$ , which slightly shifted to lower wavenumbers, and the absorption at  $1650 \text{ cm}^{-1}$  became obvious but had lower intensity than that obtained by the addition of oxalic acid. According to the  $\text{p}K_a$  values in Table II, all dicarboxylic acids and the tricarboxylic acid are able to dissociate in the water and can lead to the protonation of  $-\text{NH}_2$  in chitosan, similar to acetic acid and oxalic acid. The result might indicate that there were ionic interactions between the  $-\text{NH}_3^+$  groups of chitosan and the  $-\text{COO}^-$  groups of the carboxylic acids. However, since dicarboxylic acid and tricarboxylic acid contain two and three groups of  $-\text{COO}^-$ , respectively, they could undergo ionic crosslinking or complexation with some adjacent chitosan chains, as reported in some previous



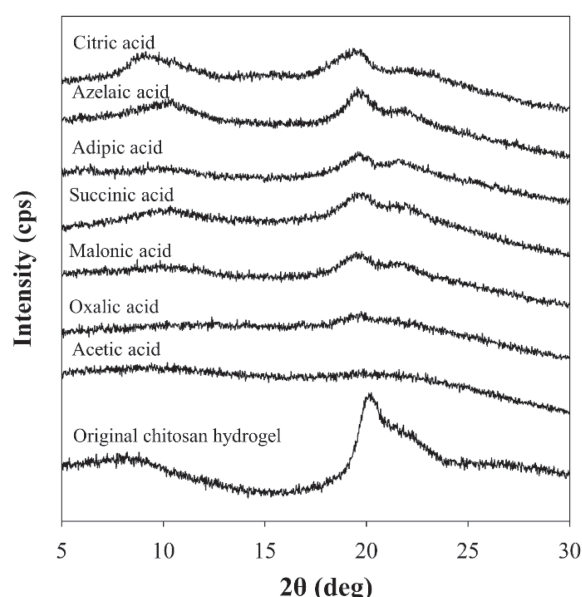


**Fig. 6.** WAXD spectra of the chitosan hydrogel before SP treatment and the degraded chitosan hydrogel dispersed in various carboxylic acid solutions at a concentration of 1.55 mM after applying SP treatment for 60 min.

studies.<sup>63–65</sup> These ionic crosslinking or complexation might be the reason for the slower  $M_w$  reduction of chitosan hydrogel. Moreover, the result showed that the rate of the degradation of chitosan depended on the number of methylene groups in the structures of dicarboxylic acid and tricarboxylic acid.

Figure 6 shows the WAXD patterns of chitosan hydrogel before the SP treatment and the degraded chitosan hydrogel

after applying the SP treatment in the presence of various types of carboxylic acid solutions at a concentration of 1.55 mM. The presence of acetic acid during the SP treatment resulted in a degraded product with an amorphous structure and, in the case of oxalic acid, very low intensity of the peaks at  $2\theta = 19.6$  and  $22.2^\circ$  was observed. This may imply that the destruction of the crystalline structure of chitosan was facilitated by the presence of acetic acid and oxalic acid during the SP treatment. Meanwhile, the addition of other dicarboxylic acids and the tricarboxylic acid gave peaks with relatively stronger intensity at  $2\theta = 19.6$  and  $22.2^\circ$ . According to a previous study, the broad peak at around  $2\theta = 19$  and  $23^\circ$  might be ascribed to the diffraction of the plane of the crystal region in the chitosan carboxylate.<sup>66</sup> The chitosan carboxylate was induced by the formation of ionic interactions between the  $-\text{NH}_3^+$  groups of chitosan and  $-\text{COO}^-$  groups of the carboxylic acid. In the case of the dicarboxylic acids and tricarboxylic acid, they could undergo ionic crosslinking or complexation with some adjacent chitosan chains, leading to stabilization of the crystal structure of chitosan and, consequently, these two peaks could be clearly observed. In particular, the relatively high crystallinity of the degraded chitosan products from the systems with the addition of azelaic acid and citric acid was evidence that indicated some extent of crosslinking within the structure of degraded chitosan. Therefore, the WAXD results were consistent with the FT-IR results and could also be used to explain the reason that different rates of degradation were obtained when the chitosan hydrogel dispersed in the different carboxylic acids was degraded by SP treatment.

A schematic drawing of a possible degradation mechanism of chitosan hydrogel dispersed in various carboxylic acid

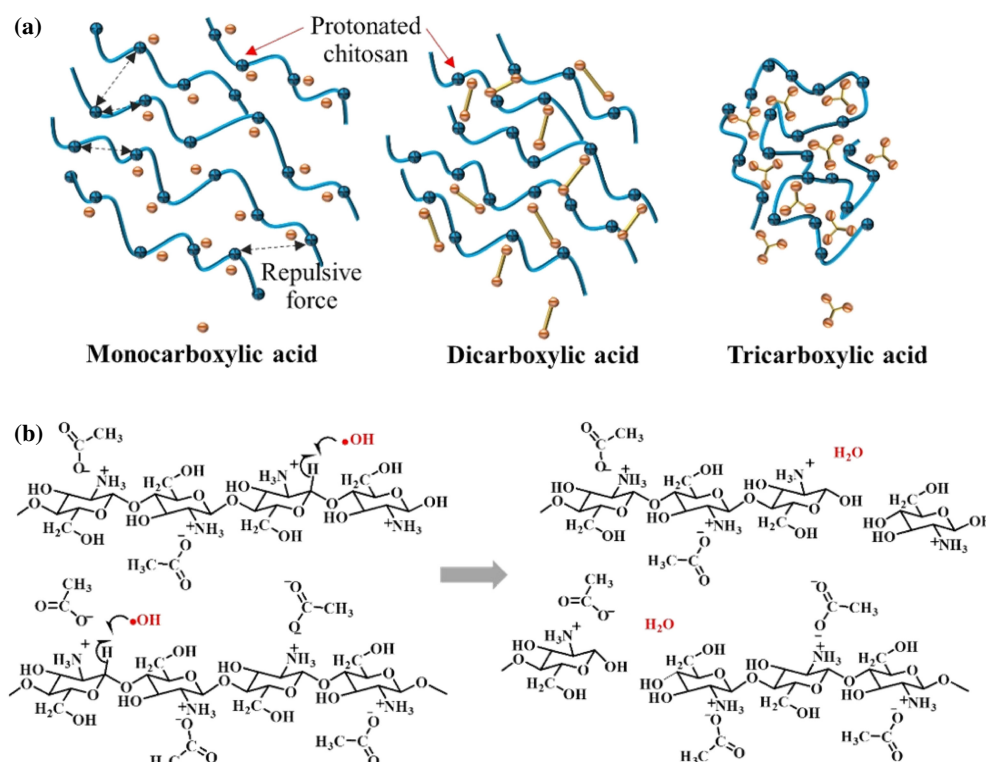


**Fig. 7.** (Color online) (a) Possible ionic interaction and ionic crosslink between chitosan hydrogel and different types of carboxylic acids including monocarboxylic, dicarboxylic, and tricarboxylic acids. (b) Possible degradation mechanism of chitosan hydrogel dispersed in dilute acid solution by SP treatment.



solutions by applying SP treatment is shown in Fig. 7(b). The reaction solution containing only molecules of  $\text{H}_2\text{O}$ , carboxylic acids, and chitosan was subjected to SP treatment. The major component in the system was  $\text{H}_2\text{O}$  molecules. The plasma discharge can result in the excitation and ionization of  $\text{H}_2\text{O}$  molecules.<sup>67)</sup> Electrons are emitted as a result of ionization (i.e.,  $\text{H}_2\text{O} \rightarrow \text{H}_2\text{O}^+ + \text{e}^-$ ) and then continuously collide with the surrounding  $\text{H}_2\text{O}$  molecules (i.e.,  $\text{e}^- + \text{H}_2\text{O} \rightarrow \cdot\text{OH} + \cdot\text{H}$ ) to produce radicals. In addition, the excitation of  $\text{H}_2\text{O}$  molecules also directly leads to the formation of radicals (i.e.,  $\text{H}_2\text{O}^* \rightarrow \cdot\text{OH} + \cdot\text{H}$ ). Both the ionization and excitation of  $\text{H}_2\text{O}$  molecules by SP treatment rapidly produce  $\cdot\text{OH}$ , which is necessary for the degradation of chitosan.<sup>60,68)</sup> The generated  $\cdot\text{OH}$  could lead to the chain scission of the chitosan at  $\beta$ -1,4-glycosidic linkage which have been reported in the previous studies.<sup>29,55,60)</sup> The breakdown of the  $\beta$ -1,4-glycosidic linkage leads to the reduction of the molecular weight of chitosan.<sup>60)</sup> Moreover, the electron from the plasma discharge can also directly collide with a chitosan molecule, leading to the chain scission.

The degraded chitosan hydrogel obtained by SP treatment in the presence of various dilute carboxylic acids for 60 min was centrifuged in order to separate the degraded products into water-soluble and water-insoluble degraded products. The solid fraction consisted of water-insoluble chitosan, while the liquid fraction contained the water-soluble COS. Further purification after the centrifugation was unnecessary because a very low concentration of carboxylic acids was used in the reaction. Moreover, carboxylic acids are generally found in many natural products and are safe for use in food and drug production.<sup>69)</sup> After centrifugation, in most cases of the studied carboxylic acids, the production yield of water-soluble COS was in the range of 50 to 70% with the exception of azelaic acid and citric acid, where the production yields of water-soluble COS were 40% and less than 5%, respectively. The production yield in this study was comparable to that obtained by different methods in other previous studies, as shown in supplementary data (Table III). For further investigation of the molecular weight reduction,  $M_w$ , number-average molecular weight ( $M_n$ ), and PDI of the water-soluble COS were determined by GPC, as shown in Table IV. On the basis of  $M_n$ , the major oligosaccharides in the water-soluble COS could be estimated for each carboxylic acid, as shown in Table V. Degradation of chitosan hydrogel dispersed in the dilute solution of citric acid could produce COS with the major oligosaccharide of 10-mers, while the addition of acetic acid, oxalic acid, and adipic acid resulted in the COS containing mainly oligosaccharides of 12-mers. The addition of malonic acid, glutaric acid, and azelaic acid could give the major oligosaccharides of 13-mers and the COS with the major oligosaccharide of 14-mers could be produced by the addition of succinic acid and pimelic acid. Therefore, it could be concluded that the degradation of chitosan hydrogel dispersed in the dilute solution of various carboxylic acids by applying SP treatment could produce COS with a DP ranging from 10 to 14, which are difficult to produce by enzymatic degradation.<sup>6)</sup> Besides, since the carboxylate anions still remained in the degraded products, they should undergo ionic interactions with the COS leading to the formation of COS-carboxylates.

**Table V.** Possible major oligosaccharides in the water-soluble COS-carboxylate samples with the evaluation of their anticancer activity.

COS sample	Possible major oligosaccharide	Evaluation of anticancer activity		
		IC <sub>50</sub> <sup>a)</sup> (mg·ml <sup>-1</sup> )		SI <sup>b)</sup>
		H460	MRC-5	
COS-acetate	12	2.9	5.0	1.72
COS-oxalate	12	2.6	3.7	1.42
COS-malonate	13	2.0	4.5	2.25
COS-succinate	14	1.6	5.0	3.13
COS-glutarate	13	2.2	4.0	1.81
COS-adipate	12	2.0	2.4	1.20
COS-pimelate	14	1.6	3.5	2.19
COS-azalate	13	2.4	3.7	1.54
COS-citrate	10	—	—	—
COS <sup>c)</sup>	13	5.0	6.5	1.30

a) IC<sub>50</sub> is the concentration required to kill 50% of the cell population.

b) SI is the selectivity index (SI = IC<sub>50</sub> of pure compound in a normal cell line/IC<sub>50</sub> of the same pure compound in a cancer cell line).<sup>70,71)</sup>

c) COS was obtained from the precipitation of the degraded chitosan solution in 1 M acetic acid after SP treatment under the corresponding condition.

### 3.2 Evaluation of anticancer activity

To evaluate the anticancer activity and to determine the concentrations of the COS-carboxylate samples that could kill 50% of the cell population (IC<sub>50</sub>), H460 and MRC-5 were used as representatives of the cancer cell line and the normal cell line, respectively. The COS-carboxylate samples were tested at final concentrations ranging from 1 to 5 mg·ml<sup>-1</sup>. IC<sub>50</sub> of the COS-carboxylate and the normal COS samples against cancer cells (H460) and normal cells (MRC-5) are shown in Table V. The morphology of H460 cells untreated and treated with the COS-carboxylate samples at a concentration of 5 mg·ml<sup>-1</sup> is also shown in the online supplementary data at <http://stacks.iop.org/JJAP/57/0102B5/mmedia> (Fig. S1). The normal COS was obtained by following the protocol as reported in a previous work,<sup>19)</sup> using SP treatment of chitosan solution. For comparing the COS-carboxylate and the COS, the result suggested that the presence of carboxylate in the structure of the COS could enhance the anticancer activity. Among the studied COS-carboxylate samples, it was found that the COS-carboxylate samples with the majority of 14-mers, which were obtained from the degradation of chitosan hydrogel dispersed in succinic acid and pimelic acid, exhibited the best inhibitory effect on the growth of H460 cells (IC<sub>50</sub> = 1.6 mg·ml<sup>-1</sup>). For cytotoxicity against MRC-5 cells, the COS-acetate and COS-succinate samples had the highest IC<sub>50</sub> value at 5 mg·ml<sup>-1</sup>. Moreover, the selectivity index (SI) of the COS-carboxylate and COS samples could be determined by the IC<sub>50</sub> ratio of a compound tested against cancer cells and normal cells. SI implies the difference in the cytotoxic activity of the tested sample against cancer and normal cells.<sup>70,71)</sup> Therefore, a high SI value indicates a higher selectivity for cytotoxic activity against H460 cells than MRC-5 cells. Among the studied COS-carboxylate samples, the SI of the COS-succinate had the highest value of 3.1. The COS-succinate was also found to have better selectivity to cancer cells than COS. Since the last decade, succinate has been extensively studied for the treatment of cancer, because it was found to be a key metabolic factor in the cancer-

**Table VI.** Anticancer activity of COS and COS derivatives prepared by different methods.

COS and COS derivatives	Preparation method	Cell lines	Cell viability (%)			SI <sup>a)</sup>	Ref.
			At ~0.5 mg·ml <sup>-1</sup>	At ~1.5 mg·ml <sup>-1</sup>	At ~15 mg·ml <sup>-1</sup>		
COS (DP1–5)	Enzymatic	HeLa	48	—	—	—	20
COS (DP3–9)	Enzymatic	SMMC-7721	80	65	—	—	76
COS (DP2–9)	SP	HeLa	—	95	45	1.5	19
		MRC-5 <sup>b)</sup>	—	100	70		
COS-succinate (DP~14)	SP	H460	80	50	—	3.1	This work
		MRC-5 <sup>b)</sup>	89	75	—		

a) SI is the selectivity index ( $SI = IC_{50}$  of pure compound in a normal cell line/ $IC_{50}$  of the same pure compound in a cancer cell line).<sup>70,71)</sup>

b) Normal cell line.

immune and may lead to cancer immunotherapies.<sup>72,73)</sup> Previous studies reported that vitamin E succinate showed an inhibitory effect on cancer cells and tumors.<sup>74,75)</sup> Therefore, the combination of COS and succinate, which exhibited better selectivity against cancer cells, could be recommended for further development as a potential anticancer agent. In addition, according to Table VI, the cell viability obtained for the COS-succinate was comparable to that of the COS prepared by enzymatic degradation. From this evidence, it was proved that SP treatment can be used to reduce the molecular weight of chitosan in order to obtain COS without changing the biological properties such as anticancer activity, which naturally belongs to COS.

#### 4. Conclusions

Chitosan hydrogel was found to be a suitable form of chitosan to produce water-soluble COS via a heterogeneous degradation reaction by using solution plasma treatment. As a result of the further disruption of the crystalline structure of chitosan hydrogel, the molecular weight reduction of chitosan hydrogel was enhanced by the presence of a small amount of carboxylic acids, especially acetic acid and oxalic acid, during the degradation of chitosan hydrogel under the discharge of plasma. Since a dilute concentration of carboxylic acids was used and chitosan hydrogel still remained as an undissolved hydrogel, the separation process to remove water-soluble degraded products containing COS from the remaining chitosan hydrogel could be simply achieved by centrifugation. Owing to the application of simple processes with less chemical use, the production cost of COS can be significantly reduced. Although the addition of carboxylic acids to the suspension of chitosan hydrogel results in the formation of COS-carboxylate products, the presence of succinate anions in COS could enhance the inhibitory effect towards cancer cells, resulting in a higher value of selectivity index. In this study, we proposed a novel, simple process to produce COS with anticancer activity. The proposed process not only gives a high production yield of COS but can also reduce the production cost of COS.

#### Acknowledgments

CC would like to express thank to the Thailand Research Fund (TRF) for financial support through a Royal Golden Jubilee Ph.D. program (RGJ-Ph.D.: Grant Number PHD/0179/2556). This work was financially supported by the Thailand Research Fund (TRF) under contract number BRG5480008, the National Research Funding from the

Government of Thailand given to Chulalongkorn University, and Japan Science and Technology Agency: Core Research for Evolutional Science and Technology (JST/CREST: Grant Number GJPMJCR12L1). Moreover, the authors would like to acknowledge Surapon Foods Public Co., Ltd. (Thailand) for providing the shrimp shells and Nagoya University (Japan) for providing solution plasma equipment. In addition, the authors would like to thank the Drug Discovery and Development Center at Thammasat University (Thailand) for providing all facilities that were used for the biological tests.

- 1) I. Armentano, N. Bitinis, E. Fortunati, S. Mattioli, N. Rescignano, R. Verdejo, M. A. Lopez-Manchado, and J. M. Kenny, *Prog. Polym. Sci.* **38**, 1720 (2013).
- 2) X. Tang, P. Kumar, S. Alavi, and K. Sandeep, *Crit. Rev. Food Sci. Nutr.* **52**, 426 (2012).
- 3) A. K. Mohanty, M. Misra, L. T. Drzal, S. E. Selke, B. R. Harte, and G. Hinrichsen, in *Natural Fibers, Biopolymers, and Biocomposites*, ed. A. K. Mohanty, M. Misra, and L. T. Drzal (CRC Press, Boca Raton, FL, 2005) Chap. 1.
- 4) M. A. Meyers, P.-Y. Chen, A. Y.-M. Lin, and Y. Seki, *Prog. Mater. Sci.* **53**, 1 (2008).
- 5) J. Liu, S. Willför, and C. Xu, *Bioact. Carbohydr. Dietary Fibre* **5**, 31 (2015).
- 6) V. K. Mourya, N. N. Inamdar, and Y. M. Choudhari, *Polym. Sci., Ser. A* **53**, 583 (2011).
- 7) W. Xia, P. Liu, J. Zhang, and J. Chen, *Food Hydrocolloids* **25**, 170 (2011).
- 8) S. A. Agnihotri, N. N. Mallikarjuna, and T. M. Aminabhavi, *J. Controlled Release* **100**, 5 (2004).
- 9) X. Zou, X. Zhao, and L. Ye, *RSC Adv.* **5**, 96230 (2015).
- 10) C. Tangsathakun, S. Kanokpanont, N. Sanchavanakit, R. Pichyangkura, T. Banaprasert, Y. Tabata, and S. Damrongsakkul, *J. Biomater. Sci., Polym. Ed.* **18**, 147 (2007).
- 11) F.-L. Mi, S.-S. Shyu, Y.-B. Wu, S.-T. Lee, J.-Y. Shyong, and R.-N. Huang, *Biomaterials* **22**, 165 (2001).
- 12) R. Jayakumar, M. Prabakaran, P. T. Sudheesh Kumar, S. V. Nair, and H. Tamura, *Biotechnol. Adv.* **29**, 322 (2011).
- 13) X.-L. Luo, J.-J. Xu, Y. Du, and H.-Y. Chen, *Anal. Biochem.* **334**, 284 (2004).
- 14) N. M. El-Sawy, H. A. Abd El-Rehim, A. M. Elbarbary, and E.-S. A. Hegazy, *Carbohydr. Polym.* **79**, 555 (2010).
- 15) R. L. Siegel, K. D. Miller, and A. Jemal, *CA Cancer J. Clin.* **66**, 7 (2016).
- 16) M. L. Tan, P. F. M. Choong, and C. R. Dass, *J. Pharm. Pharmacol.* **61**, 3 (2009).
- 17) C. E. DeSantis, C. C. Lin, A. B. Mariotto, R. L. Siegel, K. D. Stein, J. L. Kramer, R. Alteri, A. S. Robbins, and A. Jemal, *CA Cancer J. Clin.* **64**, 252 (2014).
- 18) C. Qin, Y. Du, L. Xiao, Z. Li, and X. Gao, *Int. J. Biol. Macromol.* **31**, 111 (2002).
- 19) C. Chokradjaroen, R. Rujiravanit, A. Watthanaphanit, S. Theeramunkong, N. Saito, K. Yamashita, and R. Arakawa, *Carbohydr. Polym.* **167**, 1 (2017).
- 20) C. F. de Assis, L. S. Costa, R. F. Melo-Silveira, R. M. Oliveira, M. G. B. Pagnoncelli, H. A. O. Rocha, G. R. de Macedo, and E. S. dos Santos, *World J. Microbiol. Biotechnol.* **28**, 1097 (2012).
- 21) A. Einbu, H. Grasdalen, and K. M. Vårum, *Carbohydr. Res.* **342**, 1055

- (2007).
- 22) K. M. Vårum, M. H. Ottøy, and O. Smidsrød, *Carbohydr. Polym.* **46**, 89 (2001).
  - 23) Y.-B. Huang and Y. Fu, *Green Chem.* **15**, 1095 (2013).
  - 24) S.-K. Kim and N. Rajapakse, *Carbohydr. Polym.* **62**, 357 (2005).
  - 25) J. C. Cabrera and P. Van Cutsem, *Biochem. Eng. J.* **25**, 165 (2005).
  - 26) G. Li, L. Qi, A. Li, R. Ding, and M. Zong, *Macromol. Symp.* **216**, 165 (2004).
  - 27) J. M. Wasikiewicz, F. Yoshii, N. Nagasawa, R. A. Wach, and H. Mitomo, *Radiat. Phys. Chem.* **73**, 287 (2005).
  - 28) J. Shao, Y. Yang, and Q. Zhong, *Polym. Degrad. Stabil.* **82**, 395 (2003).
  - 29) O. Pornsunthorntawe, C. Katepetch, C. Vanichvattanadecha, N. Saito, and R. Rujiravanit, *Carbohydr. Polym.* **102**, 504 (2014).
  - 30) K. V. Harish Prashanth and R. N. Tharanathan, *Trends Food Sci. Technol.* **18**, 117 (2007).
  - 31) J. M. Wasikiewicz and S. G. Yeates, *Polym. Degrad. Stabil.* **98**, 863 (2013).
  - 32) K. Li, R. Xing, S. Liu, Y. Qin, X. Meng, and P. Li, *Int. J. Biol. Macromol.* **51**, 767 (2012).
  - 33) M. Chhatbar, R. Meena, K. Prasad, and A. K. Siddhanta, *Carbohydr. Polym.* **76**, 650 (2009).
  - 34) V. L. Budarin, J. H. Clark, B. A. Lanigan, P. Shuttleworth, and D. J. Macquarrie, *Bioresour. Technol.* **101**, 3776 (2010).
  - 35) W. Yue, P. Yao, and Y. Wei, *Polym. Degrad. Stabil.* **94**, 851 (2009).
  - 36) E. Savitri, S. R. Juliastuti, A. Handaratri, S. Sumarno, and A. Roesyadi, *Polym. Degrad. Stabil.* **110**, 344 (2014).
  - 37) Q. Zou, Y. Pu, Z. Han, N. Fu, S. Li, M. Liu, L. Huang, A. Lu, J. Mo, and S. Chen, *Carbohydr. Polym.* **90**, 447 (2012).
  - 38) F. Ma, Z. Wang, H. Zhao, and S. Tian, *Int. J. Mol. Sci.* **13**, 7788 (2012).
  - 39) I. Prasertsung, S. Damrongsakkul, and N. Saito, *Polym. Degrad. Stabil.* **98**, 2089 (2013).
  - 40) I. Prasertsung, S. Damrongsakkul, C. Terashima, N. Saito, and O. Takai, *Carbohydr. Polym.* **87**, 2745 (2012).
  - 41) A. Watthanaphanit and N. Saito, *Polym. Degrad. Stabil.* **98**, 1072 (2013).
  - 42) O. Takai, *Pure Appl. Chem.* **80**, 2003 (2008).
  - 43) N. Saito, J. Hieda, and O. Takai, *Thin Solid Films* **518**, 912 (2009).
  - 44) M. A. Bratescu, S.-P. Cho, O. Takai, and N. Saito, *J. Phys. Chem. C* **115**, 24569 (2011).
  - 45) P. Baroch, V. Anita, N. Saito, and O. Takai, *J. Electrostatics* **66**, 294 (2008).
  - 46) P. Pootawang, N. Saito, and O. Takai, *Thin Solid Films* **519**, 7030 (2011).
  - 47) E. M. Ahmed, *J. Adv. Res.* **6**, 105 (2015).
  - 48) K. Okano, T. Minagawa, J. Yang, M. Shimojoh, and K. Kurita, *Polym. Bull.* **62**, 119 (2009).
  - 49) S. Sabnis and L. H. Block, *Polym. Bull.* **39**, 67 (1997).
  - 50) S. Lu, X. Song, D. Cao, Y. Chen, and K. Yao, *J. Appl. Polym. Sci.* **91**, 3497 (2004).
  - 51) K. V. Harish Prashanth, F. S. Kittur, and R. N. Tharanathan, *Carbohydr. Polym.* **50**, 27 (2002).
  - 52) K. Okuyama, K. Noguchi, T. Miyazawa, T. Yui, and K. Ogawa, *Macromolecules* **30**, 5849 (1997).
  - 53) Z. Modrzejewska, W. Maniukiewicz, and A. Wojtasz-Pajak, in *Progress on Chemistry of Chitin and Its Derivatives*, ed. M. M. Jaworska (Polish Chitin Society, Lodz, 2006) Monograph XI, Chap. 14.
  - 54) W. P. Jencks and J. Regenstein, in *Handbook of Biochemistry and Molecular Biology*, ed. R. L. Lundblad and F. Macdonald (CRC Press, Boca Raton, FL, 2010) p. 595.
  - 55) K. L. B. Chang, M.-C. Tai, and F.-H. Cheng, *J. Agric. Food Chem.* **49**, 4845 (2001).
  - 56) N. Q. Hien, D. V. Phu, N. N. Duy, and N. T. K. Lan, *Carbohydr. Polym.* **87**, 935 (2012).
  - 57) J. Brugnerotto, J. Lizardi, F. Goycoolea, W. Argüelles-Monal, J. Desbrieres, and M. Rinaudo, *Polymer* **42**, 3569 (2001).
  - 58) S. Sahoo, A. Sasmal, D. Sahoo, and P. Nayak, *J. Appl. Polym. Sci.* **118**, 3167 (2010).
  - 59) A. B. Vishu Kumar, M. C. Varadaraj, R. G. Lalitha, and R. N. Tharanathan, *Biochim. Biophys. Acta: Gen. Subj.* **1670**, 137 (2004).
  - 60) B. Kang, Y.-D. Dai, H.-Q. Zhang, and D. Chen, *Polym. Degrad. Stabil.* **92**, 359 (2007).
  - 61) T. Mitra, G. Sailakshmi, A. Gnanamani, and A. B. Mandal, *Mater. Res.* **16**, 755 (2013).
  - 62) F. A. Peter and P. Neta, *J. Phys. Chem.* **76**, 630 (1972).
  - 63) M. V. Shamov, S. Y. Bratskaya, and V. A. Avramenko, *J. Colloid Interface Sci.* **249**, 316 (2002).
  - 64) B. Martel, M. Weltrowski, D. Ruffin, and M. Morcellet, *J. Appl. Polym. Sci.* **83**, 1449 (2002).
  - 65) A. Watthanaphanit, P. Supaphol, T. Furuike, S. Tokura, H. Tamura, and R. Rujiravanit, *Biomacromolecules* **10**, 320 (2009).
  - 66) U. Ubaidulla, R. K. Khar, F. J. Ahmad, Y. Sultana, and A. K. Panda, *J. Pharm. Sci.* **96**, 3010 (2007).
  - 67) S. Le Caër, *Water* **3**, 235 (2011).
  - 68) C. Qin, Y. Du, and L. Xiao, *Polym. Degrad. Stabil.* **76**, 211 (2002).
  - 69) C. Skonberg, J. Olsen, K. G. Madsen, S. H. Hansen, and M. P. Grillo, *Expert Opin. Drug Metab. Toxicol.* **4**, 425 (2008).
  - 70) R. B. Badisa, S. F. Darling-Reed, P. Joseph, J. S. Cooperwood, L. M. Latinwo, and C. B. Goodman, *Anticancer Res.* **29**, 2993 (2009).
  - 71) R. B. Badisa, L. T. Ayuk-Takem, C. O. Ikediobi, and E. H. Walker, *Pharm. Biol.* **44**, 141 (2006).
  - 72) S. Jiang and W. Yan, *Cancer Lett.* **390**, 45 (2017).
  - 73) J. F. Wentzel, A. Lewies, A. J. Bronkhorst, E. van Dyk, L. H. du Plessis, and P. J. Pretorius, *Biochimie* **135**, 28 (2017).
  - 74) M. P. Malafa and L. T. Neitzel, *J. Surg. Res.* **93**, 163 (2000).
  - 75) K. T. Barnett, F. D. Fokum, and M. P. Malafa, *J. Surg. Res.* **106**, 292 (2002).
  - 76) Q. Xu, J. Dou, P. Wei, C. Tan, X. Yun, Y. Wu, X. Bai, X. Ma, and Y. Du, *Carbohydr. Polym.* **71**, 509 (2008).



**Chayanaphat Chokradjaroen** is a Ph.D. student at the faculty of polymer science at the Petroleum and Petrochemical College, Chulalongkorn University, Thailand. She holds the bachelor's degree in chemical engineering from the Sirindhorn International Institute of Technology, Thammasat University, Thailand. For her further study, she continued and completed her master's degree at Kanazawa University, Japan. Currently, her research focuses on the degradation and the modification of chitin and chitosan, and the evaluation of biological activities of the obtained products.



**Sewan Theeramunkong** is a lecture of faculty of pharmacy at Thammasat University, one of high ranked universities in Thailand. She holds the bachelor's degree in pharmacy, a master's degree in pharmaceutical chemistry from Thailand and a Ph.D. in medicinal chemistry from Italy. Prior to studying master's degree she had over 8 years of industrial quality control experience in Bangkok. During her Ph.D. period, she got internship in CEA-Saclay in France. Currently, her research focuses on the synthesis of novel anticancer agents and find out the mechanism of them.



**Nagahiro Saito** is the research director for "Deepening of the Precise Reaction Field in Solution Plasma and Development of Advanced Carbon Catalyst" in JST/CREST research area; Establish of Molecular Technology towards the Creation of New Functions by Research Supervisor, Hisashi Yamamoto, Ph.D. The author is venturing into the novel and new organic reactions through solution plasma.



**Ratana Rujiravanit** is an associate professor of the Polymer Science Program at the Petroleum and Petrochemical College, Chulalongkorn University, Bangkok, Thailand. She received her master's and doctorate degrees from Hokkaido University, Japan. After that she earned post-doctoral fellowship at Japan Advanced Institute of Science and Technology (JAIST). Ratana's main research interest is the development of biopolymer-derived functionalized materials. Her published research works have been cited more than 2,000 times with the h-index of 27. One of her publication in Carbohydrate Polymers became one of the Top Ten Cited Articles in the year 2008–2010. In addition, her invention on bio-cellulose composite wound dressing received the Gold Medal Award from the 45th International Exhibition of Inventions, Geneva, Switzerland.